

**NATIONAL UNIVERSITY OF IRELAND, GALWAY**

**A toolkit for assessing unsaturated soil time  
lag with respect to Water Framework  
Directive deadlines**

Sara E. Vero, M.Sc.

Research Supervisors:

Dr. Mark G. Healy, Civil Engineering, NUI Galway

Dr. Tiernan Henry, Earth & Ocean Sciences, NUI Galway

Dr. Owen Fenton, Teagasc, Johnstown Castle, Wexford

Thesis submitted in fulfilment of the requirements for the degree of Doctor of  
Philosophy

November 2015

The National University of Ireland requires the signatures of all persons using or photocopying this thesis. Please sign below, and give the address and date.

‘The larger the searchlight, the greater the circumference of the unknown’

*The Tesseract – Alex Garland*

‘The Lord God took the man and put him in the Garden of Eden, to work it and take care of it.’

*Genesis 3:15*

‘You may say to yourself, “My power and the strength of my hands have produced this wealth for me.” But remember the Lord your God, for it is He who gives you the ability to produce wealth, and so confirms His covenant, which He swore to your forefathers, as it is today.’

*Deuteronomy 8:17-18*

## Abstract

The European Union Water Framework Directive (EU-WFD) requires member states to achieve ‘good status’ ground- and surface-water quality by specified reporting deadlines (2015, 2021 and 2027). To attain these goals, the Irish agricultural sector has implemented a robust Programme of Measures (POM) i.e. the Nitrates Directive. At present 98.5% of Irish groundwater and 71.5% of surface-water meet the prescribed standards. National plans for sustainable agricultural intensification post-abolition of the milk quota (2015) necessitate derogation to Nitrates Directive fertiliser application rates. However, failure to maintain at least ‘good-status’ places the continued implementation of this derogation at risk. It is generally accepted that the 2015 deadline is unattainable, and it is therefore, critical that future water quality trends be anticipated. The efficacy of POM cannot be assessed without determining the inherent delay or ‘time-lag’ of nutrients lost from the soil surface and transported to a receptor *via* various pathways. The vertical pathway, by which leached Nitrate travel through the soil profile to the groundwater, is challenging to quantify, due to the heterogeneity of soil hydraulic properties and the unsaturated nature of the soil profile. Hence, unsaturated time lag ( $t_u$ ) is frequently overlooked or simplified. The aim of this thesis was to develop a toolkit by which  $t_u$  ranges in agricultural catchments may be estimated, with a particular focus on assessing trends in water quality.

A literature review was conducted in which the controlling factors on  $t_u$  were identified, and various approaches to simulating water and solute transport using unsaturated zone numerical models were examined. Subsequently, an investigation was conducted to determine the consequences for  $t_u$  estimates made using a popular model (Hydrus 1D) depending on whether low-complexity (texture and bulk density) or high-complexity (the soil water characteristic curve (SWCC)) soil input data are used. It was found that high-complexity data improved model performance, but for trend assessment, low-complexity data suffice. The position of the nutrient source relative to the receptor was found to influence model requirements, with high-complexity data becoming more critical in locations where source and receptor are close.

Having identified the utility of low- and high-complexity input data, the impact of four common soil textural analysis (low-complexity data) methods were assessed. It was found that there were only minor differences in  $t_u$  estimates (<0.03 yrs), irrespective of whether laser diffraction, hydrometer, or pipette methods were used. The hand texturing method performed poorest, indicating superior performance of any of the three laboratory methods. Regarding high-complexity input data, the impact of various temporal rules concerning the time to hydraulic equilibrium when constructing an SWCC using the centrifuge method was statistically assessed. This simple but novel approach allows the impact of experimental duration on SWCCs of specific soils to be determined. A methodological toolkit to estimate  $t_u$  was developed using soil data available from the Irish Soil Information System. Using this toolkit,  $t_u$  was estimated for a grassland and an arable catchment. In both catchments,  $t_u$  estimates frequently exceeded three years, and were almost 10 years for the deepest soils, indicating that the targets of the EU-WFD may not be achievable until the second reporting period. Trend estimates were verified using potassium bromide (KBr<sup>-</sup>) tracer tests in each catchment. The toolkit approach satisfactorily indicated trend ranges for most scenarios when compared to the *in situ* tracer study.

This toolkit may be employed specifically in catchments exhibiting poor or declining water quality in order to anticipate future improvements, and on a national scale, to aid in the design of judicious policies and effective monitoring campaigns.

## **Declaration**

This dissertation is the result of my own work, except where explicit reference is made to the work of others, and has not been submitted for another qualification to this or any other university.

Sara E. Vero

## Acknowledgements

The list of people who have helped me over the past three years could likely fill an entire thesis chapter, but I will do my best to remember everyone. Thanks firstly to my supervisors for giving me this wonderful opportunity and for their advice and guidance throughout: Owen Fenton – a patient teacher and my daily first port of call with every question, problem and request; Mark Healy – a wonderful editor and an enthusiastic support; Tiernan Henry – whose knowledge of hydrology I can only aspire to; Karl Richards – who frequently provided critical expertise, especially regarding the tracer experiment; and Rachel Creamer – who taught me so much about soil and helped me to persevere when the going was tough. Thanks to my co-authors and collaborators; Per-Erik Mellander, Gaelene Kramers, Diana Selbie, Brian Reidy, Daire O’Huallachain, Paul Murphy, Eoin McAleer, Jim Grant and Patrick Forristal; these people were invaluable. Thanks also to Stan Lalor and Diogenes Antille, who were so encouraging in the early days of this project. I am grateful to the Teagasc Walsh Fellowship Scheme for funding this research.

Without the assistance of the laboratory and farm staff at Johnstown Castle, literally none of this work would have been possible; thank you Anna Fenelon, Pat Sills, Denis Brennan, Paddy Hayes, Brendan Connick, Pat Donnelly, Donal Doyle, Cathal Somers, Teresa Cowman, Carmel Lynch, and Linda Moloney Finn. Thanks also to everyone who worked around my centrifuge schedule!

I am deeply grateful to all the members of the Agricultural Catchments Program; Simon Leach patiently prepared the maps in this thesis, Eddie Burgess and Dermot Leahy took care of my field sites and particularly, the land-owners James Masterson and D.J. Hurley. Their generosity never ceases to amaze me.

Several associations have supplied bursaries and awards which allowed me to attend major conferences in the United States. I am so grateful to the Irish Grassland Association, International Association of Hydrogeologists, Irish Geological Association, Soil Science Society of America, Chartered Institution of Water and Environmental Management, British Council, and to the family of Robert Luxmoore.

I never expected to travel to such an extent so early in my career; it has been an excellent adventure, and would never have been possible without these groups.

Numerous other people have assisted me; Sarah Knight and Martina Prendergast, who do such a wonderful job getting research into the public discourse; Jirka Šimůnek, who I'm sure must have got tired of my endless questions about Hydrus, but was always a fount of information; Susan Chapman and Emily Fuger, who helped me get involved with the Tri-Societies and provided so many opportunities; Nancy Miragoglio and Ofelia Chernock, my friends at Elsevier, and Ann-Marie Clarke, who was such a pleasure to deal with.

Thanks to all the staff and students at Johnstown Castle. The past and present members of WMBSoc should know I am truly so glad for their friendship and for all the laughter, coffee and cake over the past three years; Dominika Krol, Orlaith Ni Choncubhair, Mairead Shore, Mary Harty, Leanne Roche (who literally saved the day during installation of my monitoring arrays), and Noeleen McDonald (who provided me with endless help and advice, and is responsible for introducing me to the X-Files (thanks to Mulder and Scully for being a welcome break during preparation of this thesis!)). One of the biggest thanks of all is due to Sophie Sherriff; who helped with my experiments, took me meals when I was up to my eyes, co-authored a paper, fed my chickens, proof-read drafts, and generally had my back every step of the way. No-one could ask for better friends than those I have been blessed with.

My grandparents Eamon and Francis Dunn; thank you for all your love and unwavering support. All my love and deepest gratitude to my parents Ken and Lisa Vero, and my siblings Hannah, Peter, Cosima and Martin. Nothing I have ever done has been without your help, and I have not forgotten. I love you dearly. You are the best part of every week.

The Lord God Almighty has poured blessings upon me, beyond anything I could have imagined. Let me never forget His graciousness, which is beyond measure. Let everything that has breath praise the Lord.

## Abbreviations

### **Abbreviations**

1D/2D/3D – One-dimensional/Two-dimensional/Three-dimensional

$\alpha$  – Alpha Parameter

$\gamma_s$  – Performance Index

$\theta/\theta_r/\theta_s$  - Volumetric Water Content/Residual Water Content/Saturated Water Content

$\rho$  – Density of Pore Fluid

$\rho_b$  – Bulk Density

$\rho_s$  – Particle Density

$\Psi$  – Matric Potential

$\mu\text{m}$  – Micrometers

$\omega$  – Angular Velocity

-Sol = Total Solute

A – Cross-sectional Area of Flow

ACP – Agricultural Catchments Program

AECOM – Architecture, Engineering, Construction, Operations and Management

ASA – Agronomy Society of America

ASTM – American Society for Testing and Materials

BGL – Below Ground Level

BSI – British Standard Instrument

$^{\circ}\text{C}$  – Degrees Celcius

CIWEM – The Chartered Institution of Water and Environmental Management

cm – Centimetres

$C_{\text{max}}$  – Maximum Permissible Courant Number

## Abbreviations

CMT – Catchment Management Tool

COM – Centre of Mass

$C_r$  – Courant Number (dimensionless)

CSA – Critical Source Area

CSSA – Crops Science Society of America

$c_{Top}$  = Solute Concentration at the Upper Boundary Condition

$d$  – depth (m)

DAFM – Dept. of Agriculture, Food and the Marine (Ireland)

DEFRA – Dept. for the Environment, Food and the Marine (UK)

DELG – Dept. of the Environment and Local Government (Ireland)

DEM – Digital Elevation Model

ds/m – Decisiemens per metre

EC – European Commission

$EC$  – Electrical Conductivity (ds/m)

EEA – European Environment Agency

EEB – European Environment Bureau

$E_e$  – Effective Hydraulic Equilibrium

$E_t$  – Total Hydraulic Equilibrium

EPA – Environmental Protection Agency

ER – Effective Rainfall

$E_t$  - Evapotranspiration

EU – European Union

EU-WFD – European Union Water Framework Directive

## Abbreviations

Exit – Exit of the solute/tracer from the soil profile/End of breakthrough curve

g - Grams

GIS – Geographic Information System

GPR – Ground Penetrating Radar

GSI – Geological Survey of Ireland

GUI – Graphical User Interface

*h* – Head

ha - Hectare

hr – Hour(s)

IAH – International Association of Hydrologists

IBT/Trend – Initial Breakthrough/Trend initiation

IGA<sub>1</sub> – Irish Grassland Association

IGA<sub>2</sub> – Irish Geological Association

IPSO – Integrated Particle Swarm Optimisation

KBr<sup>-</sup> - Potassium Bromide

kg - Kilograms

kPa – Kilopascals

kph – Kilometers per Hour

$K_s$  – Saturated Conductivity

*l* – Tortuosity

LSD – Least Significant Difference

m – Metres

MAC – Maximum Allowable Concentration

## Abbreviations

m asl – Metres above sea level

met. – Meteorological

ml - Millilitres

mm - Millimetres

mmol - Millimoles

msl – Metres above sea level

n – Fitting Parameter

N - Nitrogen

$n_e$  – Effective Porosity

NO<sub>3</sub> - Nitrate

NSS – National Soil Survey

NUIG – National University of Ireland, Galway

OECD - Organisation for Economic Co-operation and Development

P – Phosphorus

$P_e$  – Peclet Number (dimensionless)

Peak – Peak Solute Concentration (Breakthrough Curve)

PET – Potential Evapotranspiration

POM – Programmes of Measures

PTF – Pedotransfer Function

q – Specific Discharge

$R^2$  – Regression Coefficient

rad – Radians

RBMD – River Basin Management District

## Abbreviations

RBMP – River Basin Management Plan

$RO_{cum}$  = Cumulative Runoff

RPM – Revolutions per Minute

RSD – Relative Standard Deviation

S/SPQ – Soil Physical Quality and Index

SD – Standard Deviation

SI – Standard Instrument

SIS – Soil Information System

SMD – Soil Moisture Deficit

SOM – Soil Organic Matter

SSSA – Soil Science Society of America

SWCC – Soil Water Characteristic Curve

$t$  - Timestep

$t_r$  – Relative Time Lag

$t_s$  – Saturated/Groundwater Time Lag

$t_T$  – Total Time Lag

$t_u$  – Unsaturated/Vadose Zone Time Lag

TVBC – Time Variable Boundary Condition

$u$  – Magnitude of Velocity

VGM – Van Genuchten Mualem (equation or parameters)

$x$  - Length

yr – Year(s)

$z$  - Elevation

## Table of Contents

<b>Abstract</b>	I
<b>Declaration</b>	II
<b>Acknowledgements</b>	III
<b>Abbreviations</b>	V
<b>Table of Contents</b>	X
<b>List of Tables</b>	XVI
<b>List of Figures</b>	XVIII
<b>Chapter 1: Introduction</b>	1
1.1 Overview of Thesis	1
1.2 Objectives	3
1.3 Layout of Thesis	4
1.4 Peer Reviewed Publications	6
<b>Chapter 2: Literature Review</b>	9
Overview	9
2.1 The Water Framework Directive	9
2.2 Irish Agriculture and Water Quality	14
2.3 Time Lag	18
2.4 Landscape Position	22
2.5 Unsaturated Flow Equations	23
2.6 Numerical Modelling	25
2.7 Model Inputs	29

## Table of Contents

2.7.1 <i>Direct Approach – The Soil Water Characteristic Curve</i>	30
2.7.2 <i>Indirect Approach – Pedotransfer Functions</i>	34
2.7.3 <i>Meteorological Input Data</i>	35
2.8 Conclusions and Knowledge Gaps	38
<b>Chapter 3: Consequences of varied soil hydraulic and meteorological data complexity on unsaturated zone time lag estimates</b>	39
Overview	39
3.1 Introduction	39
3.2 Hypotheses and Objectives	40
3.3 Materials and Methods	42
3.3.1 <i>Model Simulations</i>	42
3.3.2 <i>Landscape Position</i>	48
3.4 Results	48
3.4.1 <i>Meteorological Data Resolution</i>	48
3.4.2 <i>Soil Hydraulic Properties</i>	52
3.4.3 <i>Solute Breakthrough</i>	55
3.4.4 <i>Landscape Position</i>	58
3.5 Discussion	58
3.5.1 <i>Meteorological Data Resolution</i>	58
3.5.2 <i>Soil Hydraulic Properties</i>	64
3.5.3 <i>Solute Breakthrough</i>	65
3.5.3.1 <i>Validity of Hydrus Simulations</i>	65
3.5.3.2 <i>Comparison of Simple to Complex Input Data</i>	69

## Table of Contents

3.5.4 <i>Landscape Position</i>	70
3.6 Conclusions	71
Summary	72
<b>Chapter 4: Low-complexity approach – Consequences of soil texture evaluation methodologies on hydraulic properties, unsaturated time lag and soil physical quality estimates</b>	73
Overview	73
4.1 Introduction	73
4.2 Materials and Methods	75
4.2.1 <i>Site Description</i>	75
4.2.2 <i>Soil Textural Analysis</i>	76
4.2.3 <i>Applications of Soil Hydraulic Parameters</i>	78
4.2.3.1 Unsaturated Time Lag	78
4.2.3.2 Soil Physical Quality	79
4.2.3.3 Data Analysis	79
4.3 Results and Discussion	80
4.3.1 <i>Soil Texture</i>	80
4.3.2 <i>Soil Hydraulic Parameters</i>	81
4.3.3 <i>Time Lag Estimates</i>	84
4.3.4 <i>Soil Physical Quality</i>	87
4.4 Conclusions	87
Summary	88
<b>Chapter 5: High-complexity approach - Consequences of truncated dewatering on soil water characteristic curves measured via</b>	89

## Table of Contents

### **centrifugation**

Overview	89
5.1 Introduction	89
5.2 Materials and Methods	92
<i>5.2.1 Centrifuge Method Setup</i>	92
<i>5.2.2 Initial Testing</i>	94
<i>5.2.3 Experimental Design and Data Analysis</i>	95
5.3 Results and Discussion	96
5.4 Conclusions	100
Summary	101
<b>Chapter 6: Indicating Trends in Response to Programmes of Measures in Two Agricultural Catchments</b>	102
Overview	102
6.1 Introduction	102
6.2 Materials and Methods	105
<i>6.2.1 Toolkit Description and Data Sources</i>	105
<i>6.2.2 Description of Study Sites</i>	112
<i>6.2.3 Data Sources for the Study Sites</i>	117
6.2.3.1 Meteorological Data	117
6.2.3.2 Soil Data	119
6.2.3.3 Boundary Data	121
6.3 Results	121
<i>6.3.1 Catchment Mapping</i>	121

## Table of Contents

6.3.2. <i>Soil Hydraulic Parameters – Modal Profile Approach</i>	122
6.3.3 <i>Time Lag Estimates – 2012 Implementation</i>	126
6.3.3.1 Modal Profile Approach	126
6.3.3.2 Time Lag Estimates – Long-term Simulations	128
6.4 Discussion	128
6.4.1 <i>Catchment Mapping</i>	128
6.4.2 <i>Modal Profiles – 2012 Implementation</i>	130
6.4.3 <i>Long-term Time Lag Estimates</i>	130
6.4.4 <i>Comparison of Textural vs. Modal Profile Approaches</i>	131
6.4.5 <i>Implications for Policy and Monitoring</i>	133
6.5 Conclusions	134
Summary	137
<b>Chapter 7: Validation of time lag estimates using field tracer tests</b>	138
Overview	138
7.1 Introduction	138
7.2 Materials and Methods	139
7.2.1 <i>Tracer Study</i>	139
7.2.1.1 Profile Instrumentation	140
7.2.1.2 Tracer Application and Monitoring	144
7.2.2 <i>Model Simulations</i>	149
7.3 Results	156
7.3.1 <i>Tracer Results – Pore Water Samples</i>	156

## Table of Contents

7.3.2 <i>Tracer Results – Electrical Conductivity</i>	158
7.3.3 <i>Model Simulation Results</i>	159
7.4 Discussion	163
7.4.1 <i>General Discussion</i>	163
7.4.2 <i>Tracer Study</i>	168
7.5 Conclusions	169
Summary	169
<b>Chapter 8: Conclusions and Recommendations</b>	170
Overview	170
8.1 Synopsis of Main Research Findings	170
8.2 Recommendations for Further Research	173
8.3 Concluding Remarks	175
<b>Bibliography</b>	176
<b>Appendices</b>	213
Appendix A: List of publications and presentations	
Appendix B: Published journal papers	
Appendix C: Soil profile descriptions and hydraulic parameters for all soil profiles appearing in Chapter 3.	
Appendix D: Effect of duration of centrifugation on soil hydraulic parameters, unsaturated zone time lag estimates and soil physical quality assessment.	
Appendix E: Datasheets for the Modal Soil Profiles employed in Chapter 6.	

## List of Tables

<b>Table 1.1:</b> Summary of data sources used in the experimental chapters (Chapters 3-7).	8
<b>Table 2.1:</b> Key dates and deadlines relating to the EU-WFD.	11
<b>Table 3.1:</b> Summary of NSS (Waterford) soils (Diamond and Sills, 2011).	45
<b>Table 3.2:</b> Daily vs. hourly estimates of IBT/Trend, Peak, COM and Exit for the 12 textural classes during a wet and a dry year respectively.	51
<b>Table 3.3:</b> Physical properties of Profile No. 1 (Ballymacart) (Diamond and Sills, 2011).	53
<b>Table 3.4:</b> Hydraulic properties of Profile No. 1 (Ballymacart) determined from the textural menu, ROSETTA and by fitting of the full and low pressure SWCC.	54
<b>Table 3.5:</b> Importance of $t_u$ relative to total time lag ( $t_T$ ) in % ( $t_r$ ) across data complexity range, when the saturated time lag ( $t_s$ ) varies (0.5, 5 and 10 years).	60
<b>Table 3.6:</b> Summary results of Kramers <i>et al.</i> (2012) lysimeter study.	67
<b>Table 4.1:</b> Soil physical quality index (Dexter, 2004a, b, c).	74
<b>Table 4.2:</b> Field soil profile description. The soil is classified as a Typic Cambisol using the World Reference Base system.	77
<b>Table 4.3:</b> Profile A hydraulic parameters ( $\theta_r$ , $\theta_s$ , $\alpha$ , $n$ and $k_s$ ) and S value determined from sand-silt-clay percentage and default $\rho_b$ ( $1.2 \text{ g cm}^{-3}$ ) parameters using pipette, hydrometer or laser.	82
<b>Table 4.4:</b> Profile B hydraulic parameters ( $\theta_r$ , $\theta_s$ , $\alpha$ , $n$ and $k_s$ ) and S value determined from sand-silt-clay percentage and default $\rho_b$ ( $1.2 \text{ g cm}^{-3}$ ) parameters using pipette, hydrometer or laser.	83
<b>Table 4.5:</b> Soil hydraulic parameters and S value of the soil profile derived from texture as determined in the field using hand textured method.	83

<b>Table 5.1:</b> Summary of methodologies used in the literature to determine the SWCC.	91
<b>Table 5.2:</b> Summary of site and soil information.	94
<b>Table 5.3:</b> Estimated mean effective saturation (over all $\Psi$ ), according to treatment, for the grassland and arable sites.	96
<b>Table 6.1:</b> Summary of the grassland and arable catchments.	114
<b>Table 6.2:</b> Horizon-specific hydraulic parameters for soil series at the grassland site derived via the low-complexity modal profile approach, using PTFs. * indicates default mineral $\rho_d$ value of $1.20 \text{ g cm}^{-3}$ .	124
<b>Table 6.3:</b> Horizon-specific hydraulic parameters for soil series at the arable site derived via the low-complexity modal profile approach, using PTFs. * indicates default mineral $\rho_d$ value of $1.20 \text{ g cm}^{-3}$ .	125
<b>Table 6.4:</b> Results of modal profile simulations, subsequent to 2012 implementation, according to various profile depths indicative of slope position. X indicates failure to achieve that $t_u$ stage within the simulation period.	127
<b>Table 6.5:</b> Results of long-term modal profile simulations, using an average yearly meteorological dataset. Profile depths are indicative of various slope positions.	129

## List of Figures

<b>Fig. 1.1:</b> Flowchart showing thesis structure.	5
<b>Fig. 1.2:</b> Map of study sites and location of data sources used in this thesis.	6
<b>Fig. 2.1:</b> (A) Irish RBDs, and (B) catchment outlines (including both river and coastal catchments) (Fealy <i>et al.</i> , 2010).	12
<b>Fig. 2.2:</b> Trends in Irish groundwater quality, with respect to Nitrate. The threshold for 'good' quality is $<37.5 \text{ mg NO}_3\text{-N L}^{-1}$ , while non-impacted waters exhibit less than $10 \text{ mg L}^{-1}$ (EPA, 2013).	18
<b>Fig. 2.3:</b> Water flow paths to a surface receptor (river), over the soil surface and through subsurface ( $t_u$ and $t_s$ ) pathways (Ibrahim <i>et al.</i> , 2013b).	20
<b>Fig. 2.4:</b> Conceptual landscape diagram, indicating the varying distance of a potential contaminant source from a surface water receptor, and consequently, varying $t_u$ and $t_s$ .	21
<b>Fig. 2.5:</b> Example Soil Water Characteristic Curve (SWCC).	25
<b>Fig. 2.6:</b> Hysteresis in the SWCC, indicating water retention measured via wetting or drying processes.	31
<b>Fig. 2.7:</b> A schematic representative of centrifuge bucket adaptors used for retaining a soil sample during centrifugation.	33
<b>Fig. 2.8:</b> Mean annual precipitation across Ireland (Fealy <i>et al.</i> , 2010). A gradient is observed indicating increasing precipitation from East to West.	36
<b>Fig. 2.9:</b> (A) Synoptic stations (automatic and manual), and (B) rainfall recording stations operated by Met Éireann (Met., 2015a/b).	37
<b>Fig. 3.1:</b> Example of a solute breakthrough curve at the base of a soil profile generated using Hydrus. IBT/Trend, Peak, COM and Exit of the solute are indicated.	41
<b>Fig. 3.2:</b> Conceptual unsaturated numerical model diagram indicating input parameters, boundary conditions, horizon characteristics and model outputs.	44

<b>Fig. 3.3:</b> Outline map of Ireland; County Waterford (in which the soil series examined in this chapter are located) is highlighted.	47
<b>Fig. 3.4:</b> Low to high complexity soil characteristic data employed in Hydrus.	48
<b>Fig. 3.5:</b> Standard deviation (SD) in IBT/Trend, Peak, COM and Exit for each of the 9 NSS profiles, depending on data complexity.	55
<b>Fig. 3.6:</b> Top to bottom: (A) IBT/Trend, (B) Peak, (C) COM and (D) Exit for the NSS profiles using simple to complex input data.	57
<b>Fig. 3.7:</b> (A) Position of NSS profiles No. 1-9 relative to a surface receptor and $t_r$ ranges, (B) Position of various soil types relative to a surface receptor. Soils simulated in this paper (Podzol to Surface Water Gleys) highlighted. Adapted with permission from Ibrahim <i>et al.</i> (2013b).	61
<b>Fig. 4.1</b> Soil profile and sample grid location along a deep open drain at a permanent grassland site. C1=Profile A, F1=Profile B.	75
<b>Fig. 4.2:</b> Hydrus model setup for Pipette/Hydrometer/Laser (7 layered model) and Hand method (4 layered model). S/S/C% = Sand-Silt-Clay percentage. The four layered model represents the horizons identified by the soil scientist i.e. Ah, Bw1, Bw2, Bw3.	79
<b>Fig. 4.3:</b> (A) Initial Breakthrough at the base of the soil profiles, and (B) Centre of Mass at base of soil profiles, for 2004 and 2010, according to method of textural analysis.	85
<b>Fig. 5.1:</b> Sigma 6-16KS centrifuge used in this study.	92
<b>Fig. 5.2:</b> Adaptor components and centrifuge loaded with prepared adaptor units.	92
<b>Fig. 5.3:</b> Dewatering at -20 kPa, assessed on an hourly basis.	95
<b>Fig. 5.4:</b> Effective saturation relative to initial water contents for the grassland and arable sites, according to treatment.	99
<b>Fig. 5.5:</b> Methodological framework for experimental duration assessment,	100

and associated timeframes.

- Fig. 6.1:** Unsaturated zone time lag toolkit, including data-sources and outputs. Input data complexity within each step is increased by moving from left to right. 106
- Fig. 6.2:** SIS map interface, indicating a polygon and affiliated soil association, and soil series within that association. The lower image indicates a sample data-sheet for a modal profile associated with the Clonroche series – see Appendix E for a high resolution version of this data-sheet (SIS, 2015). 108
- Fig. 6.3:** Conceptual diagram of textural and modal profiles, as interpretations of a real soil profile. In the current study, simulations of  $t_u$  are ascertained for textural and modal profiles, subject to various hillslope positions. 109
- Fig. 6.4:** Diagram of the unsaturated and saturated zones. The depths of both the soil and unsaturated bedrock vary spatially, and the position of the watertable may fluctuate, both spatially and temporally. 111
- Fig. 6.5:** Locations of the grassland and arable catchments (Mellander *et al.*, 2014). 113
- Fig. 6.6:** Map of the grassland catchment, indicating soil association, synoptic station, monitoring wells, catchment outlet, profile sampling locations and elevation. 115
- Fig. 6.7:** Map of the arable catchment indicating soil association, synoptic station, monitoring wells, catchment outlet, profile sampling locations and elevation. 116
- Fig. 6.8:** Daily rainfall and evapotranspiration (ET) and cumulative rainfall for the grassland and arable sites, respectively, from 2012 to 2014 (ACP, Personal Communication). 117
- Fig. 6.9:** Daily and cumulative rainfall, and daily evapotranspiration at the Rosslare synoptic station (ACP, Personal Communication). 118
- Fig. 6.10:** Hierarchy, indicating soil association and affiliated soil series for 120

## List of Figures

the arable (top) and grassland (bottom) catchments.

- Fig. 6.11:** Validation (ground-truthing) of soil series in the grassland catchment via soil sampling. 120
- Fig. 6.12:** Relative area represented by each soil series within the grassland and arable catchments. 123
- Fig. 6.13:** Irish hydrological catchments (including both river and marine catchments). The grassland and arable sites used in this study are indicated (Fealy, 2010). 135
- Fig. 7.1:** Cross-section of the grassland and arable hillslopes, indicating position of the soil monitoring arrays, the surface water receptors, groundwater monitoring wells, bedrock and mean annual watertable depths. 140
- Fig. 7.2:** Instrumentation depths of the soil profiles (indicating pore water samplers, EC probes and matric potential sensors. Horizontal lines indicate horizon boundaries. 140
- Fig. 7.3: (A):** Rhizosphere Macrorhizon pore water sampler, including ceramic head, piping, and lauer-lock extraction point. **(B):** Ceramic sampling head which is inserted into the pit face. 140
- Fig. 7.4: (A)** 5TE soil moisture and *EC* probe and **(B)** MPS2 matric potential probe (Decagon, 2015). 141
- Fig. 7.5:** Installation of the instruments into the pit-face (grassland, midslope location), using guide holes and soil paste. 141
- Fig. 7.6: (A):** Instruments routed from pit-face to surface via piping, prior to backfilling of the excavation. Hammer indicates scale. **(B):** Lauer-lock syringes collecting pore water at the soil surface, subsequent to backfilling of the excavation. Colour coded tag indicates the depth of the pore water samplers. Both photographs obtained at the grassland, lowslope location. 144
- Fig. 7.7:** Schematic of EC response test in the laboratory; indicating volumetric water content ( $\theta$ ) of the soil and concentration of the KBr- solution. 145

## List of Figures

- Fig. 7.8:** Electrical conductivity response (ds/m) to various KBr- solute concentrations (0-5%) and soil volumetric water content (0-50%). 145
- Fig. 7.9: (A):** Data-logger and solar charged battery, inside waterproof loggerbox, affixed to steel support. **(B):** Downloading data using Loggernet™ software, at the grassland site. 147
- Fig. 7.10:** Damaged piping for pore water samplers, as a result of vandalism. 147
- Fig. 7.11:** Hourly rainfall and evapotranspiration (ET), and cumulative rainfall at the grassland (top) and arable (lower) sites, respectively, during the tracer study period (ACP, Personal Communication). 148
- Fig. 7.12:** Eisenhower box indicating data complexity/site specificity interactions, and appropriate end-users/stakeholders. Data complexity increases from left to right, while site-specificity increases from top to bottom. 151
- Fig. 7.13a:** Profile description of the lowslope installation at the grassland site. 152
- Fig. 7.13b:** Profile description of the midslope installation at the grassland site. 153
- Fig. 7.13c:** Profile description of the lowslope installation at the arable site. 154
- Fig. 7.13d:** Profile description of the midslope installation at the arable site. 155
- Fig. 7.14:** Bromide concentration from pore water samples at the grassland low-slope position. 156
- Fig. 7.15:** Bromide concentration from pore water samples at the grassland midslope position. 157
- Fig. 7.16:** Solute transport scenarios, where Scenario A indicates early stages of transport, with the bulk of the solute in the upper horizons, and Scenario B indicates later stage transport, where centre of mass is lower in the soil profile. 158
- Fig. 7.17:** Results of the modal and *in situ* (texture and SWCC) simulations, and the field tracer (as detected from *EC*), at the grassland, midslope location. Model simulations failed to anticipate Exit within the monitoring/simulation period. 161

List of Figures

**Fig. 7.18:** Results of the modal and *in situ* (texture and SWCC) simulations, and the field tracer (as detected from *EC*), at the arable, lowslope location. COM and Exit (and Peak at the shallowest sensor) were not observed from tracer test results within the monitoring period. 162

**Fig. 7.19:** Results of the modal and *in situ* (texture and SWCC) simulations, and the field tracer (as detected from *EC*), at the arable, midslope location. Exit of the solute was not observed in the simulations/tracer results, and COM was not detected from the tracer test. 163

**Fig. 7.20:** An example of a poor soil core, exhibiting both a large stone and an air space. This core is not suitable for SWCC assessment. 168

## Chapter 1

### Introduction

#### 1.1 Overview of thesis

Time lag is the delay between the implementation of water quality mitigation measures and observed effects on water quality. This delay arises as a result of the long hydrological/hydrogeological pathways between nutrient sources and water receptors (Fenton *et al.*, 2011; Sousa *et al.*, 2013). Although time lag is an intrinsic component of nutrient transport through the vertical pathway (through the unsaturated zone), which has been identified as a controlling factor on the response to programmes of mitigation measures (POM). However, it is not currently accounted for within the European Union Water Framework Directive (EU-WFD) (EC, 2000), nor is there any established and accepted method of time lag assessment or prediction within the Republic of Ireland. This represents not only a knowledge gap from a theoretical perspective, but also a major limitation for assessing the efficacy of current measures on water quality (Schulte *et al.*, 2006), ascertaining the implementation of legislative requirements (Wall *et al.*, 2012), and developing appropriate policies for future iterations of this directive (Schröder *et al.*, 2004; Bournaoui and Grizzetti, 2014). Although reporting periods within the EU-WFD are fixed at three- to six-year intervals (2012-2015, 2021 and 2027) (EC, 2000), time lag may frequently exceed these periods, leading to a perceived failure of either the POM or their implementation (Fenton *et al.*, 2011).

While broad estimates of time lag have been proposed in the literature (Fenton *et al.*, 2011), they lack the site specificity to be meaningful at given locations, and also assume simplifications which are not reflective of the hydrologic and meteorological complexities observed in reality (e.g. constant saturation of the soil). Such an approach may be useful as a rough guide for policymakers, but can oversimplify complex scenarios. Particularly challenging is the quantification of time lag in the unsaturated zone ( $t_u$ ), which is subject to spatial heterogeneity of soil and subsoil properties (Sonneveld and Bouma, 2003), and temporal fluctuations in water content (Schulte *et al.*, 2005). The relative importance of  $t_u$  must also be considered in light of the position within the landscape of the nutrient source and a receptor (Sousa *et al.*, 2013). Of particular interest to policymakers and monitoring agencies is the

‘trend’ response to POM; that is, when the effects of POM may first be observed in either surface- or groundwaters (Craig and Daly, 2010), as this aspect is critical for ascertaining POM performance within set reporting periods, and allows comparison of POM performance across diverse regions, independent of absolute concentrations and site specific conditions (OECD, 2008; van Grinseven *et al.*, 2012). Failure to ascertain the effects of  $t_u$  on trend response creates difficulties in disentangling the legacy effects of past and present management practices. A toolkit for  $t_u$  assessment on a catchment basis is therefore required, which both realistically encapsulates unsaturated soil behaviour, and addresses the heterogeneity of soil properties.

Numerical modelling of water and solute transport is a viable method to address these knowledge gaps (Cherry *et al.*, 2008). However, there is a requirement for input data and methodological frameworks (using a popular unsaturated zone software package - Hydrus 1D (Šimůnek *et al.*, 2013) as an example) in order to develop this approach. First, the effect of input data complexity on model outputs has not been addressed; with frequent reliance in the literature on data obtained *via* low-complexity pedotransfer functions (PTF) (Vereecken *et al.*, 2010). Further assessment is required in order to determine the capacity of such data to reflect various scenarios, and to determine in which instances increases in complexity are merited, e.g. depending on stage of  $t_u$  or the position of the source within the landscape. The scale of those differences in  $t_u$  estimates arising as a result of input-data complexity relative to reporting period duration will indicate the suitability of the low- or high-complexity approaches. Where high complexity data (i.e. measured Soil Water Characteristic Curves (SWCCs)) are optimum, they must first be measured; as such information is typically not available from soil maps. Given the limitations (slow, small sample size, measurement uncertainty) of the various SWCC apparatus traditionally used (Peck and Rabbidge, 1969; Campbell, 1988; Cresswell *et al.*, 2008; Bittelli and Flury, 2009), the centrifuge method has been proposed as a cost-effective and rapid means of assessment. Although use of the centrifuge method has been established in the literature (Nimmo *et al.*, 1987; Smagin *et al.*, 1998; Reatto *et al.*, 2008; Cropper *et al.*, 2011; Smagin, 2012), the confounding array of sample sizes and formats, and the non-linear nature of dewatering, have led to ambiguities regarding the experimental timescales required (Šimůnek and Nimmo,

2005) in its use. This issue must be resolved before such a method can be utilised to provide high-complexity input data.

When the issues relating to model input data complexity and assessment are resolved, data selection criteria must be structured into a toolkit by which  $t_u$  ranges may be determined at a catchment scale, with a particular focus on trend assessment. Addressing the issues delineated above would represent a useful advance in the field, and provide a valuable tool for monitoring bodies and policymakers.

## 1.2 Objectives

The objectives of this thesis are:

- to ascertain the effect of low- versus high-complexity soil physical data on hydraulic parameter assessment and  $t_u$  estimates;
- to ascertain the effect of landscape position on model input data requirements and  $t_u$  estimates;
- to determine  $t_u$  for a range of soil profiles (indicative of landscape position) for a sample county (Co. Waterford), from existing soil physical data (low- to high-complexity);
- to design a bucket adaptor by which a standard laboratory centrifuge can be used to measure the SWCC (high-complexity soil physical data), without alterations to the machine itself;
- to develop a methodological framework to determine the optimum duration of centrifugation at each pressure-step during SWCC construction using the centrifuge method and hence, to identify suitable temporal rules for specific soil samples;
- to develop and implement a toolkit for  $t_u$  assessment, incorporating the aspects described above, by which estimates of  $t_u$  for the major soil series present within specific agricultural catchments can be made;
- to evaluate the performance of the toolkit as a predictor of  $t_u$  compared to *in situ* field measurements of solute movement, and;
- to discuss how such a toolkit approach might be implemented, as a guide to both policymakers, monitoring agencies and catchment scientists as to the likely efficacy and timescales of POM.

### 1.3 Layout of Thesis

A flowchart indicating the structure of this thesis is given in Fig. 1.1. In **Chapter 2** time lag in response to POM in both the unsaturated zone and groundwater is defined, with a particular focus on the unsaturated zone component ( $t_u$ ) and evidence is presented for its occurrence across the EU. A review of the current EU water quality policies and of the POM implemented in Ireland subsidiary to those policies are also presented. The current status of Irish waterbodies is defined. Numerical modelling as a means to estimate solute transport is also discussed, as are the various methodologies for SWCC assessment, and areas needing further development in order to allow such methods to be incorporated in an assessment toolkit are identified. In **Chapter 3** the results of a numerical modelling exercise are presented, in which the effects of low- versus high-complexity soil hydraulic data on  $t_u$  estimates was examined. Estimates of  $t_u$  for nine soil profiles in Co. Waterford, which are exemplary of Irish agricultural soils exhibiting groundwater vulnerability through the vertical pathway, are provided, and the data requirements as influenced by proximity to a surface water receptor are assessed. Differences in low-complexity  $t_u$  estimates arising as a result of soil textural analysis methodology selection are assessed in **Chapter 4**. The effects of various temporal rules on dewatering in the centrifuge method on SWCCs, from which hydraulic parameters and  $t_u$  estimates are derived (high-complexity approach) are examined in **Chapter 5**. Case studies are presented in **Chapter 6**, in which  $t_u$  ranges are calculated for a grassland and an arable catchment, and a toolkit is presented by which such an assessment may be conducted at other locations. The toolkit details data requirements and sources, model settings and methodology. **Chapter 7** presents a field study in which the results of a surface applied potassium bromide ( $KBr^-$ ) tracers in two agricultural catchments (grassland and arable) is compared to both high- and low-complexity  $t_u$  estimates, to ascertain the suitability of such approaches. The same grassland and arable catchments are used throughout chapters 5, 6 and 7. Finally, the overall conclusions of these chapters are addressed in **Chapter 8**, with recommendations for further research and suggestions for incorporating these findings in a  $t_u$  assessment toolkit.

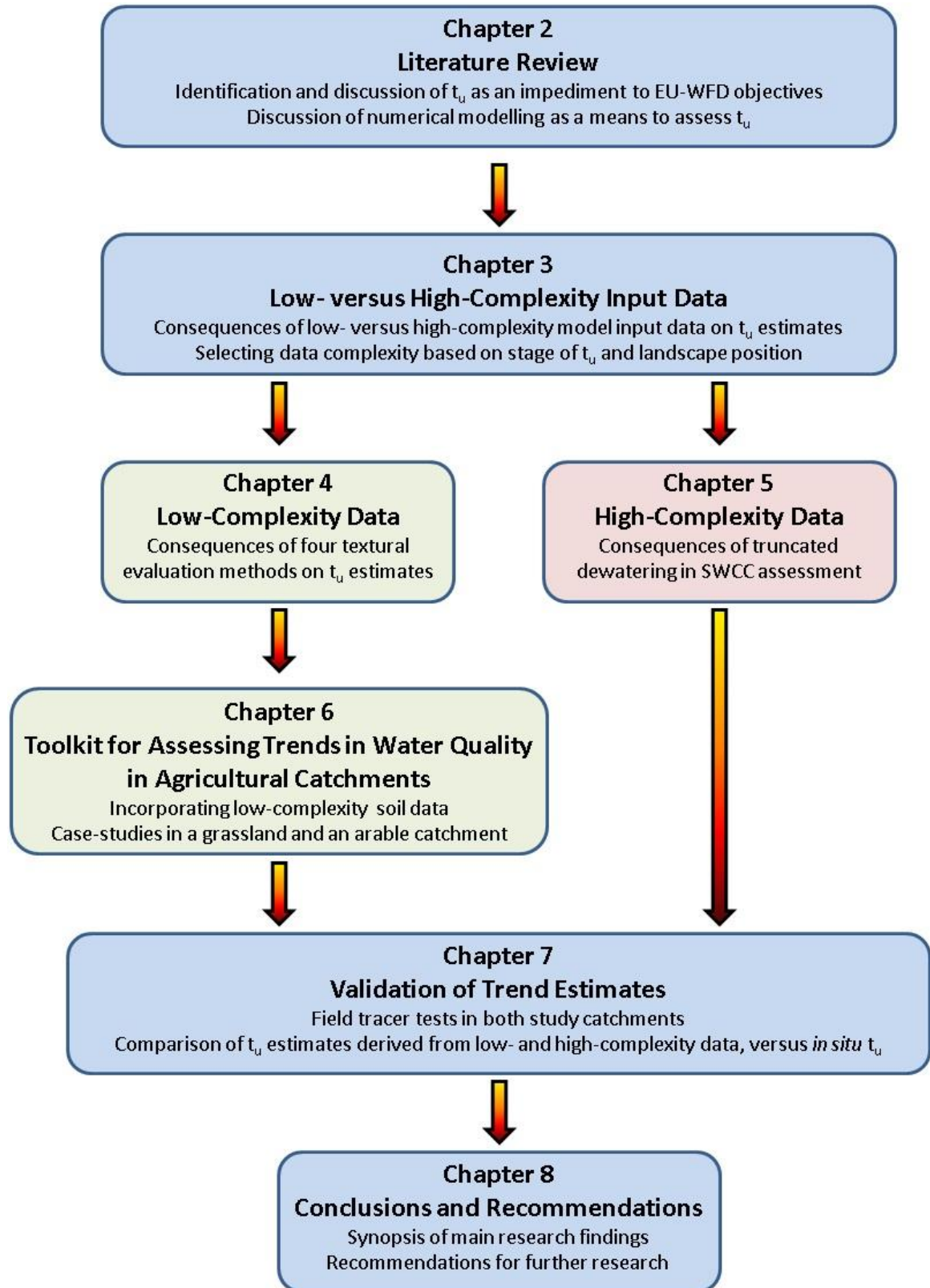


**Fig. 1.1:** Flowchart of thesis structure.

Several sites and catchments, and meteorological datasets are employed in the experimental chapters (3, 4, 5, 6 and 7) of the present thesis. A summary of the data used in each chapter is given in Table 1.1, and a map indicating the locations of these sources is provided in Fig. 1.2.

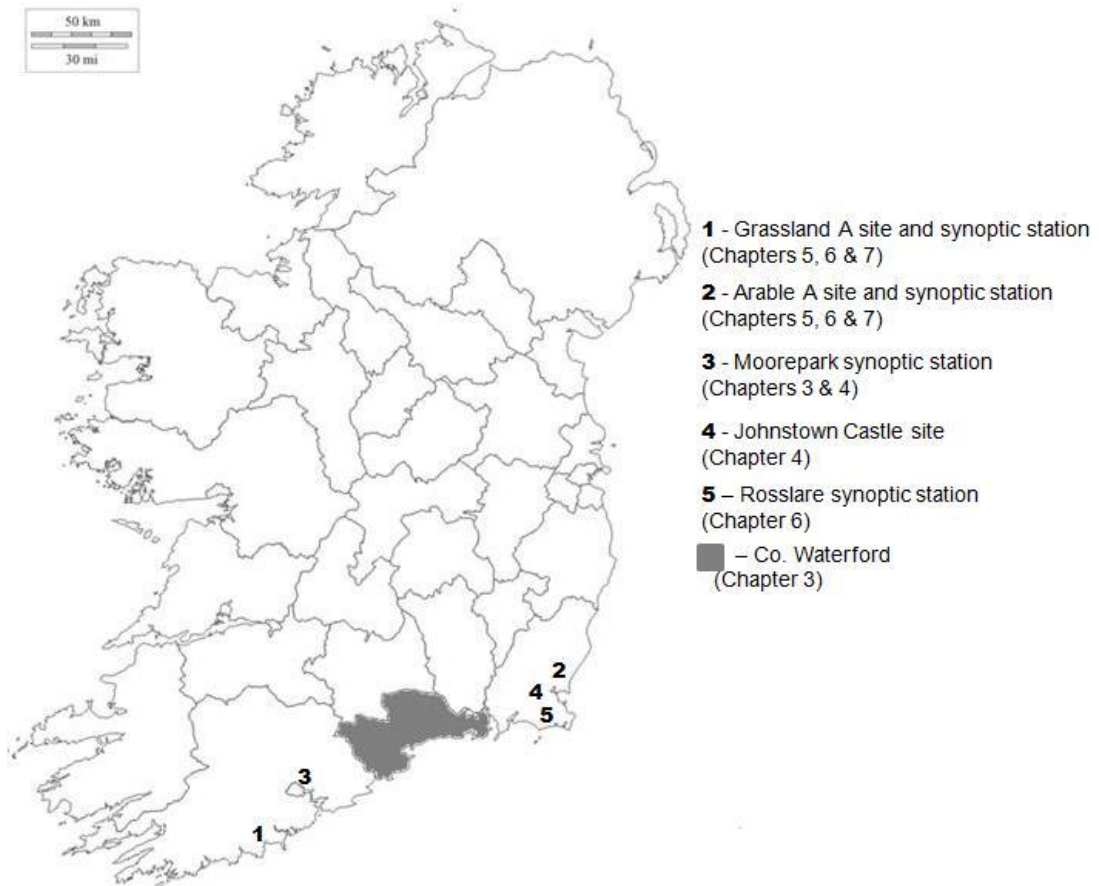


**Fig. 2.2:** Map of study sites and location of data sources used in this thesis.

#### 1.4 Peer Reviewed Publications

A full list of all peer-reviewed, conference and other dissemination outputs is provided in Appendix A. To date, two international peer-reviewed papers have been published, based on Chapters 3 and 4 of this thesis, respectively:

- **Vero, S.E.,** Ibrahim, T.G., Creamer, R.E., Grant, J., Healy, M.G., Henry, T., Kramers, G., Richards, K.G., Fenton, O., 2014. Consequences of varied soil hydraulic and meteorological complexity on unsaturated zone time lag estimates. *Journal of Contaminant Hydrology*, 170: 53-67

## Chapter 1 - Introduction

- Fenton, O., **Vero, S.E.**, Ibrahim, T.G., Murphy, P.N.C., Sherriff, S. and Ó'hUallachian, D. 2015. Consequences of using different soil texture determination methodologies for soil physical quality and unsaturated zone time lag estimates. *Journal of Contaminant Hydrology*. 182: 16-24
- A manuscript based on Chapter 5 is currently under review, and another based upon Chapter 6 is in the latter stages of preparation, and due for journal submission imminently.

**Table 2.1:** Summary of data sources used in the experimental chapters (Chapters 3-7).

	<b>Chapter Number</b>				
	<b>3</b>	<b>4</b>	<b>5</b>	<b>6</b>	<b>7</b>
<b>Site</b>	Co. Waterford	Johnstown Castle Environmental Research Centre, Co. Wexford	Grassland (Co. Wexford) and Arable (Co. Cork) Catchments		
<b>Soil Data- Source</b>	National Soil Survey	Site Sampling	Site Sampling	Site Sampling Irish Soil Information System Agricultural Catchments Program	
<b>Meteorological Data-Source</b>	Moorepark Synoptic Station (Co. Cork)	Moorepark Synoptic Station (Co. Cork)	n/a	Onsite Synoptic Stations Rosslare Synoptic Station (Co. Wexford)	Onsite Synoptic Stations
<b>Meteorological Data Years</b>	Wet Year -2004 Dry Year 2010	Wet Year -2004 Dry Year 2010	n/a	2012-2014 Sample Moderate Dataset	2014-2015

## Chapter 2

### Literature Review

#### Overview

In this chapter the EU-WFD, the Nitrates Directive, current Irish water quality status and the role of Irish agriculture as an influence on water quality are introduced, with a particular focus on nitrate ( $\text{NO}_3$ ) contamination of groundwater. The time lag between the implementation of POM and observed changes in water quality is discussed. A detailed review of the methodologies by which time lag may be appraised, with a particular focus on the unsaturated zone and numerical modelling, is presented. While it is acknowledged that some degree of solute dispersion and lateral flow occurs, it is herein assumed that flow through the unsaturated zone is predominantly vertical (1D).

#### 2.1 The Water Framework Directive

The EU-WFD was enacted in December 2000 (EC, 2000). Its primary aim is to achieve ‘good’ qualitative (chemical and ecological) and quantitative status in all waterbodies, within set reporting periods (EC, 2000), the first of which ends in 2015. Key dates within the EU-WFD are shown in Table 2.1. The qualitative objectives relate to fixed chemical thresholds, defined as maximum allowable concentrations (MAC), above which a waterbody may be considered in breach of the EU-WFD. For example, a MAC of  $11.3 \text{ mg L}^{-1}$  in drinking water and of  $37.5 \text{ mg L}^{-1}$  in groundwater is set for nitrogen (N). According to Article 3 of the Groundwater Directive (EC, 2006), each state within the EU is responsible for determining threshold concentrations for specific pollutants within their respective groundwaters to quantify ‘good status’ at local or national levels. Likewise, each country is empowered to ‘determine penalties applicable to breaches of the national provisions adopted pursuant to this Directive’ (EC, 2000). The EU-WFD further indicates that penalties imposed due to non-compliance should be ‘effective, proportionate and dissuasive,’ but the actual nature of these penalties is at member states’ discretion. While this allows some flexibility in recognition of national circumstances, it cannot account for the differences in local soil, geological, topographic and meteorological

conditions, which may influence water quality on a more local level (OECD, 2008; van Grinsven *et al.*, 2012).

The EU-WFD objectives are to be achieved by adopting and implementing POM (Fenton *et al.*, 2011). In Ireland, the primary POM in relation to agricultural impacts on water quality, is the Nitrates Directive (EC, 1991), which details controls on this prevalent agricultural contaminant which, along with phosphorus (P), may contribute to declining ecological quality of surface waters (Hamilton, 2012) due to eutrophication (Carpenter *et al.*, 1998; Azevedo *et al.*, 2015). The Nitrates Directive focusses on managing the application of agricultural fertilisers and manures, in order to prevent loss of NO<sub>3</sub> to waterbodies from the agricultural system (Goodchild, 1998), and increasing N use efficiency in Ireland (van Grinsven *et al.*, 2012). The Agricultural Catchments Program (ACP), run by Teagasc, is currently responsible for evaluating the environmental and economic effects of POM implemented under the Nitrates Directive (ACP, 2013).

The Nitrates Directive encompasses the storage of, and rates and timings of the application of agricultural fertilisers. Key POM designated within the Nitrates Directive includes:

- Regulations pertaining to the storage capacity for livestock slurry/manures, dairy washings, soiled water, and effluents (capacity must be sufficient to store manure for all housed livestock for 16 to 22 weeks, depending on region).
- Implementation of buffer strips (>3 m, depending on the nature of the waterbody) around surface waters, in which fertiliser application is prohibited at all times.
- Soil testing and nutrient budgeting.
- Closed periods for fertiliser application corresponding to seasonally high rainfall (and so N transport risk). These periods range between 15<sup>th</sup> September to 31<sup>st</sup> January for chemical fertilisers, and from 1<sup>st</sup> November to 31<sup>st</sup> January for livestock manures.
- A limit of 170 kg N ha<sup>-1</sup> from livestock manure, either from mechanical application (e.g. slurry spreading) or deposited by grazing livestock. The EU

Nitrates Committee approved a derogation which permits grassland production systems (farms consisting of >80% grass-based production) to exceed the prescribed rate, up to a maximum of 250 kg N ha<sup>-1</sup>, conditional on achievement of EU-WFD and Nitrates Directive objectives.

**Table 2.2:** Key dates and deadlines relating to the EU-WFD.

Year	Action
2000	EU-WFD enacted (18 <sup>th</sup> December)
2003	EU-WFD transposed into Irish legislation Identification of River Basin Management Districts (RBMDs) Appointment of implementation authorities
2004	Characterisation of RBMDs
2005	Establishment of groundwater quality chemical criteria Publication of RBD characterisation report (22 <sup>nd</sup> March)
2006	Establishment of water quality monitoring programmes Start of public consultation on water quality issues
2007	Publication of interim report on each RBMD
2009	Publication of River Basin Management Plan (RBMP)
2012	Deadline for implementation of POM
2015	End of first management cycle/reporting period Target deadline for achieving water quality objectives
2021	End of second management cycle/reporting period Extended deadline for achieving water quality objectives
2027	End of third management cycle/reporting period Final deadline for achieving water quality objectives

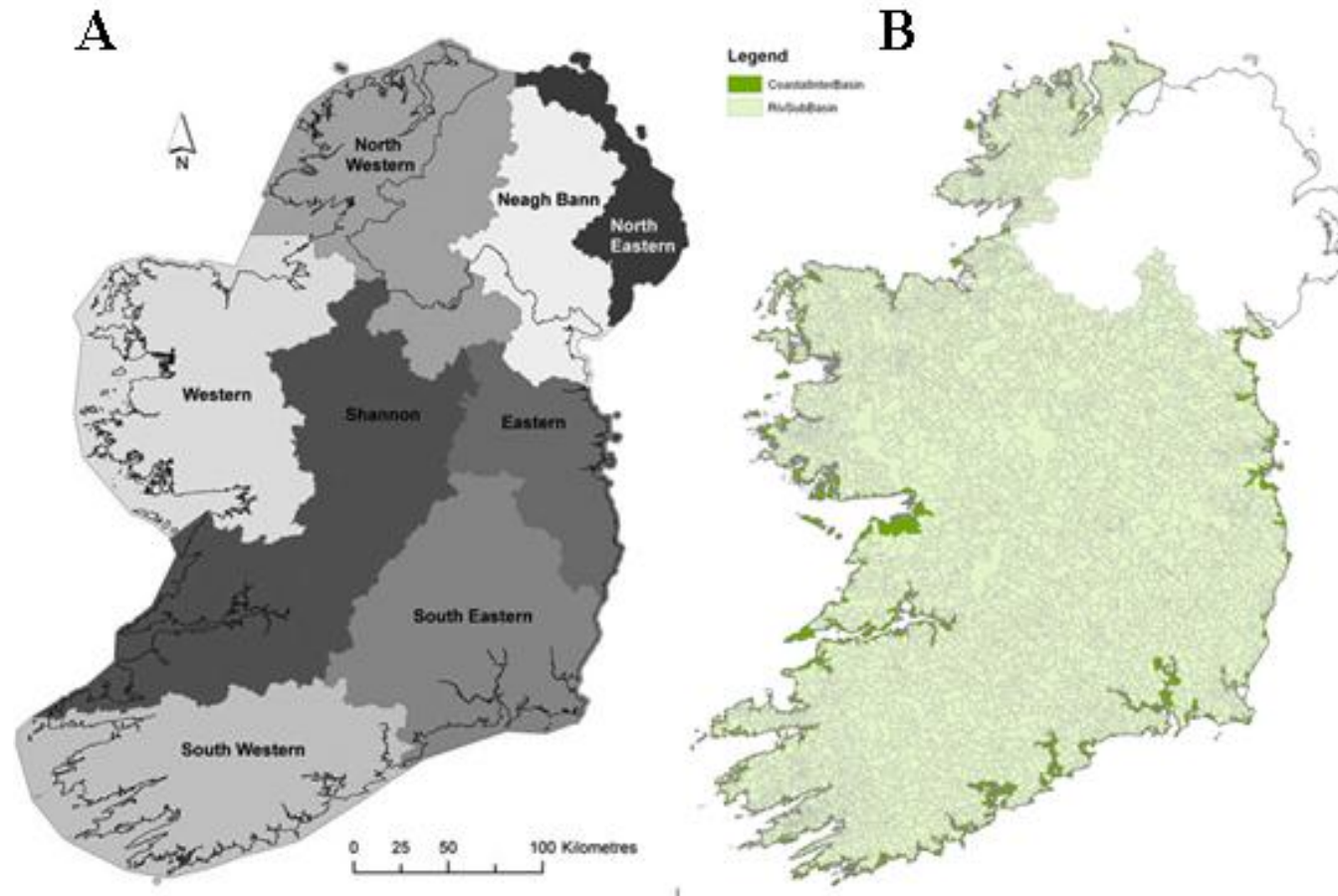


**Fig. 2.1:** (A) Irish RBDs, and (B) – catchment outlines (including both river and coastal catchments) (Fealy et al., 2010).

While EU member states had the option to implement Nitrates Directive POM in designated ‘vulnerable’ areas, Ireland was one of only six nations which decided to implement on a whole territory basis (Goodchild, 1998). This subjects all areas of the country to identical obligations, irrespective of regional differences in landscape, soil, geology or meteorology. Under Article 11 of the EU-WFD (EC, 2000), implementation of these POM on farms was required by 2012. However, as under the Nitrates Directive a robust and comprehensive suite of POM (entitled ‘Good Agricultural Practices’) were enacted in Ireland 2006 (EC, 2006; Statutory Instrument (SI) No. 378) (amended in 2009 (EC, 2009a; SI No. 101), 2010 (EC, 2010; SI No. 106) and 2014 (EC, 2014; SI No. 31)), it is to be expected that many of these POM will have been instituted well in advance of the 2012 deadline, and policymakers expect that some response in water quality should be observed. Goodchild (1998) considered only poor implementation as an impediment to anticipated improvements. Despite this assumption, time lag in both the unsaturated zone and groundwater is responsible for substantial delays (which will be discussed in detail in Section 2.3) and may make it difficult to disentangle POM effects from the legacy of past practices. A key requirement defined in the EU-WFD legislation is trend analysis (EC, 2000; EC, 2009b; Craig and Daly, 2010); that is, identification of sustained effects on water quality (either positive or negative) in response to anthropogenic activity such as land management practices and POM. It has been acknowledged that a limitation in the data available from environmental monitoring (from 2007 onwards) precludes reliable assessment of water quality trends in some locations, within the first management cycle/reporting period (Craig and Daly, 2010). Furthermore, groundwater sampled from an abstraction point represents the sum of contamination and dilution within its capture zone (Frind *et al.*, 2006). Hence, it cannot indicate the concentration of a nutrient arriving at the watertable at any single point within that capture zone – which is indicative of the trend effects of POM. This is particularly true in light of the low density of groundwater sampling points in Ireland (1 per 1,000 km<sup>2</sup>) compared to certain other member states (e.g. Belgium – 99 per 1,000 km<sup>2</sup> or Denmark – 34 per 1,000km<sup>2</sup>) (van Grinsven *et al.*, 2012). Furthermore, denitrification in groundwater ‘hotspots’ (Jahangir *et al.*, 2013a) means that abstracted groundwater samples may not reflect concentrations delivered through the soil to the watertable, either spatially or temporally.

Implementation of the EU-WFD is through River Basin Management Plans (RBMPs), which at the time this thesis was instigated, were operated by River Basin Management Districts (RBMDs). Eight RBMDs were initially established on the island of Ireland (Fig. 2.1A): four entirely in the Republic of Ireland, one entirely in Northern Ireland, and three shared RBMDs (Environmental Protection Agency (EPA), 2005). These designated administrative units were responsible for the implementation and enactment of the policies and measures under the EU-WFD. For the second management cycle/reporting period (2015-2021), those RBMDs which are wholly contained within the Republic of Ireland have been merged to form a single administrative unit (Anon, 2014). This unit shall be responsible for assessment and reporting, while implementation of POM will continue through regional authorities (Anon, 2014). While the EU-WFD deadlines and standards are consistent nationally, and implementation is at RBMD scale, monitoring occurs at a smaller, catchment scale (Fig. 2.1B), and application of measures are at farm-scale. Hence, understanding of catchment hydrology, which depends on the various soil types, landscapes, geology and other factors presenting within the area, is critical for correct interpretation of monitoring results, and design of effective policies and measures, reflective of those heterogeneities.

## **2.2 Irish Agriculture and Water Quality**

Agriculture presently accounts for 4.99 million ha (61%) of Irish land use (Dept. of Agriculture, Food and the Marine (DAFM), 2015), 160,000 jobs and in excess of €26 billion in gross output (DAFM, 2015). A review of Irish agriculture post-EU membership (Hennessy and Kinsella, 2013) depicted an industry which has undergone dramatic changes in structure, productivity, focus and demographics over the past 40 years. Hence, there is not only a physical legacy of past practices which may be observed in the present environmental status, but also a political and legislative climate which reflects that history. After two failed applications in the early 1960s, Ireland became a member state of the then European Economic Community (now EU) in 1973. Unprecedented intensification, particularly of the dairy sector, over the 1970s and 1980s led to surpluses (often colloquially referred to as ‘butter mountains’). In response, a quota system restraining production and laws including the Nitrates Directive, to address the associated environmental challenges, were introduced. The 1990s featured a suite of policy changes (the Mac Sharry

Reforms) placing further emphasis on environmental concerns, which continued throughout the 2000s. The priority areas in Irish agriculture have shifted, from primary production (1970s), through environmental concerns (1990s), and currently focus upon three pillars: smart/efficient production, environmental protection and industry growth (DAFM, 2010). As such, the Irish agricultural sector of 2016 is distinctly more intensive than it was when the Nitrates Directive was initially designed and implemented, and is likely to become more so over the coming decade. Primary production is projected to expand by 65% under the current national agricultural plan, Food Wise 2025 (DAFM, 2015). Agriculture is therefore a cornerstone of national industry and employment. Critical to attaining the Food Harvest 2020 and Food Wise 2025 goals is the derogation to the Nitrates Directive mentioned in Section 2.1 (Boyle *et al.*, 2013; Irish Cooperative Organisation Society, 2015), which permits higher rates of N application (up to 250 kg ha<sup>-1</sup>). This is particularly true in light of the declining number of small dairy farms nationally, and the increase in stocking rates (up to 2.94 cows ha<sup>-1</sup> under derogation) and plans for the sustainable intensification of production (Breathnach, 2000; OECD, 2008; Dillon *et al.*, 2014) post-abolition of the milk quota in 2015. Not only does this trend in farming practices lead to a higher N loading as a result of stocking rate, but also necessitates increased and efficient grass production to support livestock numbers (O'Donovan *et al.*, 2011). It should be noted that all EU member states, with the exception of France, negotiated derogations to the Nitrates Directive application limits (van Grinsven *et al.*, 2012). (France does not operate a system which legally defines application rates) This suggests a discrepancy between legislative stipulations and the requirements of the burgeoning agricultural sector, which affects all member states. This issue is particularly conspicuous in nations such as Ireland in which agriculture (specifically pasture-based) is a predominant nitrate source (>70% share), compared to other member states in which industry and environmental sources are more significant (van Grinsven *et al.*, 2012).

Specifically regarding dairy farming within Ireland, a 50% increase in output is targeted by 2020 under the Food Harvest 2020 plan (DAFM, 2010). As of Summer 2015, over 5,500 dairy farms utilize the derogation (Buckley *et al.*, 2015). In order to maintain the derogation, certain water quality goals must be met in accordance with the EU-WFD. These goals include:

- Prevention of deterioration of water quality status, and to maintain high or good quality status of all water-bodies;
- Restoration of good status of water-bodies currently exceeding threshold values;
- Achievement of good status by set deadlines (2015; or later, where extended deadlines are in place), and;
- Reversal of any upward trends in groundwater contamination.

Ireland currently faces the challenge of resolving the intensification and production goals outlined in Food Harvest 2020 (DAFM, 2010) and Food Wise 2025 (DAFM, 2015), and the water quality goals defined by the EU-WFD (Buckley and Carney, 2013; O’Donoghue and Hennessy, 2014). As the derogation is critical to achieving the targets outlined by the Irish agricultural plans (DAFM, 2010; DAFM, 2015); policymakers need a method by which the effects of POM and past practices with current and projected water quality can be correlated (Chyzheuskaya, 2015).

#### *Current Irish Water Quality Status*

##### *Groundwater*

The quality of groundwater is of particular importance, as it is both a vector for the transport of contaminants to surface waters, where they may impair ecological quality, and also as a source of drinking-water abstraction. Groundwater supplies 20-25% of drinking-water nationally, but in certain areas that contribution is greater (e.g. 86% in Roscommon and 60% in Offaly) (DELG/EPA/GSI, 1999). Unlike other waterbody-types, groundwater chemical quality status has only two designated quality statuses: good or poor. These statuses are determined according to the concentration of specified chemicals relative to fixed threshold values (e.g. good quality  $<37.5 \text{ mg NO}_3\text{-N L}^{-1}$ ). The EU-WFD regulations operate on a ‘one-out-all-out’ principle, in which failure to achieve the quality requirements for any one chemical indicates poor status, regardless of the concentration of any other potential contaminant. In the latest EPA water quality report covering the 2010 to 2012 period (EPA, 2015a), 98.5% of Irish groundwaters (by area) were of good chemical status. This is an improvement from the previous report (2007 to 2009), in which 86.4%

were of good status. The 11 groundwater bodies currently failing to meet good status were as a result of phosphate contribution to rivers (particularly in areas having karst geology, leading to point-source pollution (Mellander *et al.*, 2012a)) and contamination as a result of historic mining and industry. Regarding N, 96% of monitoring locations reported NO<sub>3</sub>-N concentrations below the threshold level of 37.5 mg L<sup>-1</sup> (mean concentration), with downward trends observed in 74% of locations, and stable concentrations at a further 21% (EPA, 2015a). The percentage of groundwaters by area of good and poor status from 1995 to 2012 is shown in Fig. 2.2 (EPA, 2013). Also shown is the % of groundwaters exhibiting mean NO<sub>3</sub> concentration of <10 mg L<sup>-1</sup>, which is indicative of minimal anthropogenic influence (EPA, 2008).

Elevated NO<sub>3</sub> concentrations were focussed in the South and South-East of Ireland – corresponding to the area of most intensive agriculture, particularly dairy production (Breathnach, 2000). The remaining 15% in which the trend is for increasing concentrations should be a cause for concern; this could be the legacy of past management practices, in which leached NO<sub>3</sub> is only now reaching the watertable as a result of prolonged time lag (Section 2.3). Analyses of these sites (EPA, 2015a) indicated that these trends were significant in two locations, and likely to increase mean N concentration above the threshold by 2021. Despite these exceptions, these results are largely in contrast to the majority of EU groundwater quality reports, which report NO<sub>3</sub> from agricultural sources as the most significant cause of poor groundwater status. The European Indicator Assessment (European Environment Agency (EEA), 2013) indicated poor chemical status of 25% (by area) of EU groundwaters. 16% of member states exhibit poor status in >10% of groundwater bodies, while Luxembourg, Belgium, Malta and the Czech Republic are failing in excess of 50% of their groundwaters (EEA, 2013). In light of this, Ireland's performance as regards groundwater quality should be regarded as highly successful.

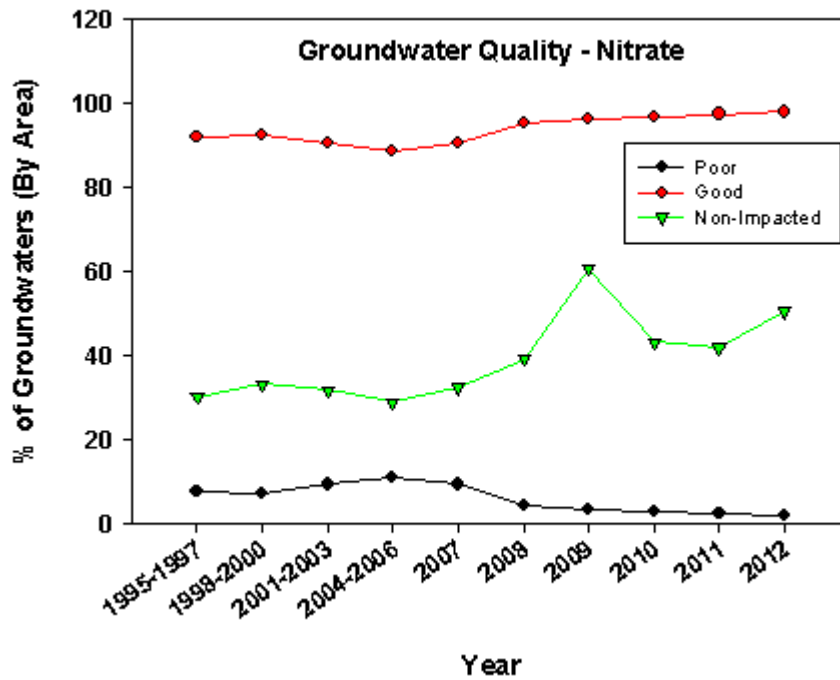


**Fig. 2.2:** Trends in Irish groundwater quality, with respect to Nitrate. The threshold for 'good' quality is  $<37.5 \text{ mg NO}_3\text{-N L}^{-1}$ , while non-impacted waters exhibit less than  $10 \text{ mg L}^{-1}$  (EPA, 2013).

### *Surface Waters*

Eutrophication as a result of nutrient loss from agricultural sources is a primary concern regarding the quality status of surface waters (Tunney *et al.*, 2007). However, the trend in surface water chemical quality is broadly positive; in 2007, 55% of monitored rivers had mean N concentrations of less than  $10 \text{ mg L}^{-1}$  (indicating negligible anthropogenic influence) (EEA, 2015). The 2010 to 2012 report indicated that this figure rose to 71.5%. Maintaining and furthering this trend necessitates prevention of  $\text{NO}_3$  transport to rivers through all pathways, including the groundwater pathway (Archbold *et al.*, 2010). For this reason, even if the  $\text{NO}_3$  load from baseflow is small, it may be sufficient to tip a receiving surface waterbody into a negative status when combined with loads *via* other pathways, such as overland flow and point-source pollution.

### **2.3 Time Lag**

The EU-WFD sets fixed reporting periods for attainment of its objectives; however, meeting these deadlines can be complicated by the behaviour of water in

the soil and bedrock (Fenton *et al.*, 2011). There is an inherent delay in nutrient transport from a source (such as fertiliser or slurry spread on the soil surface). This means that any changes in agricultural management practices may not be reflected in a waterbody (either surface or groundwater) for an extended period of time. This delay, which is referred to as ‘time lag’ ( $t_T$ ), and alternatively, as legacy effect, retardation factor, residence time, or memory effect (Cook *et al.*, 2003; Bechmann *et al.*, 2008; Fenton *et al.*, 2011; Tesoriero *et al.*, 2013). Time lag, may impair the ability of a catchment to attain water quality changes within arbitrarily defined time periods, even assuming full and timely compliance with POM (Cherry *et al.*, 2008).

Time lag is a function of the unique landscape, soil, subsoil, bedrock and meteorological conditions in a catchment (Schulte *et al.*, 2006; Fenton *et al.*, 2011; Sousa *et al.*, 2013). In their review of the Nitrates Directive in North Western Europe, van Grinsven *et al.* (2012) noted that this combination of influencing factors means that the exceedence of threshold values at groundwater is a poor indicator of the efficacy of POM. While ‘high-vulnerability’ (Misstear and Brown, 2008) catchments (in which short  $t_T$  renders waterbodies vulnerable to contamination within relatively short periods) display a rapid response to POMs (e.g. free draining soils underlain by high permeability karst bedrock (Huebsch *et al.*, 2013)), catchments with prolonged  $t_T$  (having lower soil and bedrock permeability (Wang *et al.* 2012)), display slower responses limiting the potential to assess POM efficacy within the same reporting periods. Lack of extensive temporal water quality data is also problematic (Wahlin and Grimvall, 2008): only a limited appraisal of the water quality is possible, as the natural seasonal and long-term fluctuations in water chemistry can be overlooked. Despite extensive peer-reviewed evidence for time lag in many EU member states (e.g. Behrendt *et al.*, 2000 (Germany); Granlund *et al.*, 2005 (Finland); Bechmann *et al.*, 2008 (Norway); Kronvang *et al.*, 2008 (Denmark); van Grinsven *et al.*, 2013 (throughout EU)), it has been largely dismissed as a ‘generic excuse’ (Scheure and Naus, 2010) to escape more stringent policy measures. Quantifying the effects of  $t_T$  on a catchment or sub-catchment basis allows assessment of the efficacy of current and past policies, and facilitates the design of future policies which better reflect the range of  $t_T$  observed as a result of diverse soil, landscape and meteorological scenarios (Sonneveld and Bouma, 2003; Jordan *et al.*, 2005; Meals *et al.*, 2010; Fenton *et al.*, 2011; Mellander *et al.*, 2012b), and is

therefore of vital importance to policymakers and monitoring agencies (Tedd *et al.*, 2014).

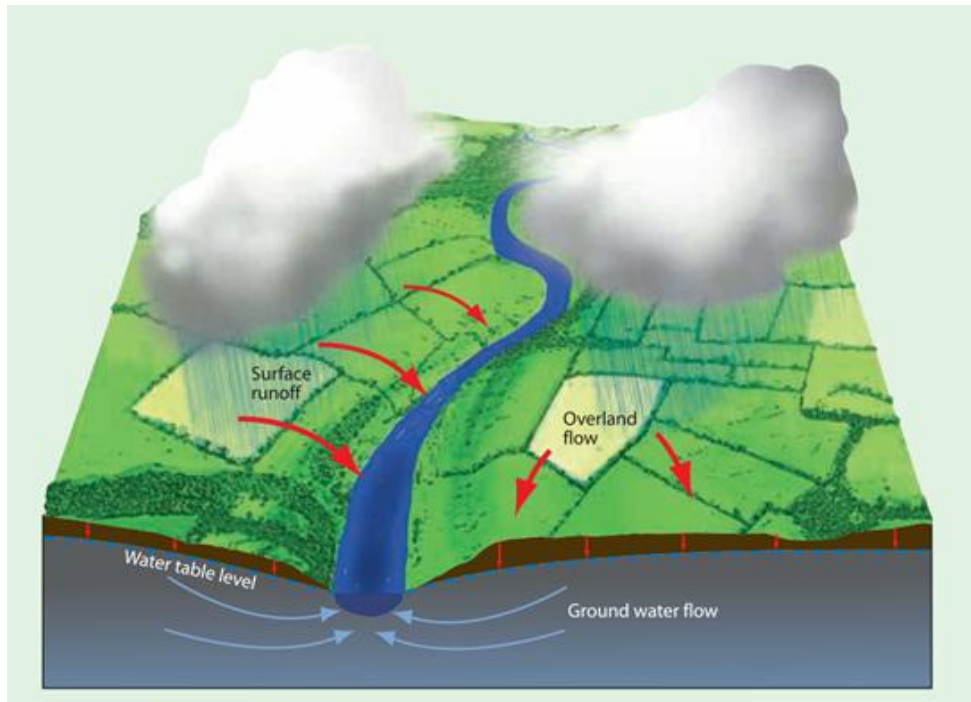


**Fig. 2.3:** Water flow paths to a surface receptor (river), over the soil surface and through subsurface ( $t_u$  and  $t_s$ ) pathways (Ibrahim *et al.*, 2013b).

Potential contaminants, such as nutrients, bacteria or salts, can be transported in water along various hydrological pathways from a source to a receptor (Fig. 2.3), which may be a surface waterbody or a groundwater abstraction point or well (Yang *et al.*, 1996; Jackson *et al.*, 2006; Meals and Davenport, 2010). Within Ireland, the EPA developed a tool for identifying the key hydrological contaminant pathways within a catchment (Archbold, 2010). This ‘Pathways Project’, (established in 2007), (Archbold, 2010) and developed a catchment management tool (CMT) (Mockler *et al.*, 2013; Packham *et al.*, 2013) by which the hydrology of a catchment can be conceptualised. The pathways identified by that project are: overland flow, interflow, shallow and deep groundwater flow, and conduit flow (Archbold, 2010). Certain pathways may facilitate rapid transport, as is the case with P and sediment transport to receptors *via* overland flow (Shore *et al.*, 2014; Mellander *et al.*, 2015), or underground *via* extensive karst conduits (ACP, 2013). Alternatively,  $t_T$  can be prolonged by vertical transport downwards through the unsaturated zone (also called the vadose or variably saturated zone) to the watertable, followed by lateral transport

through groundwater (also referred to as the saturated zone) to the receptor (Fig. 2.3) (Tomer and Burkart, 2003; Fenton *et al.*, 2011; Sousa *et al.*, 2013). In such cases,  $t_T$  can be subdivided to indicate the transport delay through the unsaturated ( $t_u$ ) and saturated/groundwater ( $t_s$ ) zones. The lengths of the  $t_u$  and  $t_s$  zones differ, depending on the depth of the soil overburden, and the proximity of the source to the receptor (Celier *et al.*, 2011; Fenton *et al.*, 2011; Sousa *et al.*, 2013). As discussed by Celier *et al.* (2011), this important influence of landscape position means that it must be incorporated as a component in modelling endeavours intended to quantify N transport. A conceptual landscape diagram is provided in Fig. 2.4. As such, a contaminant source may be located at any position within the landscape (although buffer zones near surface water receptors preclude fertiliser application at close proximity to a receptor).

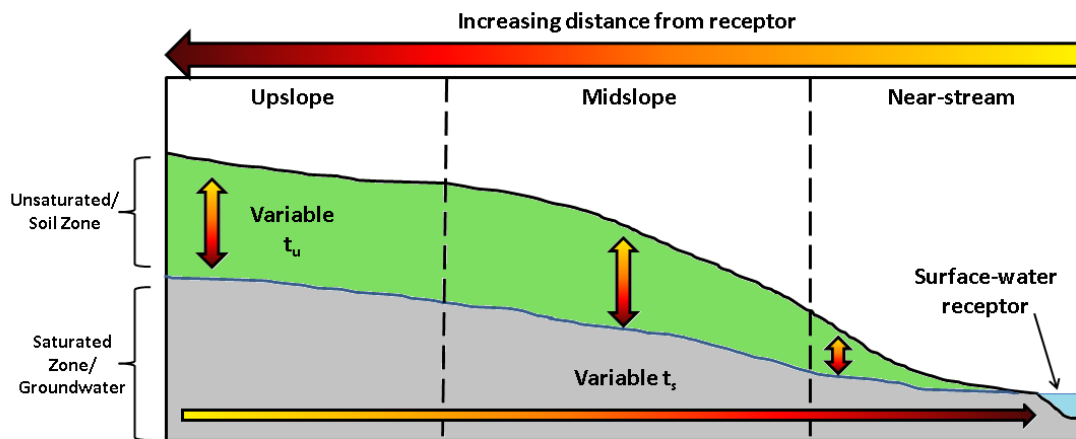


**Fig. 2.4:** Conceptual landscape diagram, indicating the varying distance of a potential contaminant source from a surface water receptor, and consequently, varying  $t_u$  and  $t_s$ .

Typically,  $t_u$  has been simplified and underestimated due to the complexities of its variably saturated and heterogeneous nature (Russo, 1991). As leaching from the root zone occurs over many decades (Schulte *et al.*, 2006; Fenton *et al.*, 2011), a reservoir of nutrients (such as Nitrate) accumulates in the soil profile (Sadej and Prekwas, 2008), beyond the depths from which they are available for plant absorption (Robbins and Carter, 1980). This reservoir, which includes nutrients at various stages of  $t_u$  according to depth (with those nutrients deeper in the profile having passed through the early stages of  $t_u$ ), is gradually released into groundwater

(Richards *et al.*, 2005; Fenton *et al.*, 2011). The full exit of these stored nutrients from the profile must be achieved before the transport of currently applied nutrients and the effects of POM may be discerned (van Grinsven *et al.*, 2012). Unsaturated time lags are influenced by soil/subsoil/bedrock type (Bejat *et al.*, 2000; Helliwell, 2011), unsaturated thickness (Hillel, 2004), variable water content (Nielsen *et al.*, 1986), interactions between the solute and the soil matrix (Leij and van Genuchten, 2011) and climatic factors (Diamond and Shanley, 2003; Stark and Richards, 2008). Bingham and Cotrufo (2015) described how physical protection of labile nitrogen in soil organic matter (common to livestock manures) can further delay the movement of nitrogen through the soil profile. In addition, the spatial (Peck *et al.*, 1977; Gumiere *et al.*, 2013) and temporal variability (Mapa *et al.*, 1986; Fousseureau *et al.*, 2001; Baily *et al.*, 2011; Gladnyeva and Saifadeen, 2013; Sousa *et al.*, 2013) of weather and soil data and the proximity of a particular landscape position relative to groundwater and surface water receptors (Jordan *et al.*, 2005; Schulte *et al.*, 2006; Fenton *et al.*, 2008; Fenton *et al.*, 2011; Sousa *et al.*, 2013) are significant when determining the importance of  $t_u$ . The complexity of water and solute transport in this zone requires a realistic quantification of  $t_u$  for use within hydrological models (Torres *et al.*, 1998, Vereecken *et al.*, 2008; Hooper, 2009). Craig and Daly (2010) indicated the need for ‘further data...to resolve some of the uncertainties surrounding the trend assessment,’ in water quality in response to POM:  $t_u$  represents one such uncertainty.

An additional complicating factor is the concurrent movement of solutes through both matrix and preferential flow pathways (Flury *et al.*, 2003; Richards *et al.*, 2005), meaning that a range of both quick and prolonged  $t_u$  may be observed in a given area. While preferential flow in Irish settings has been addressed in other works (Richards *et al.*, 2005; Kramers *et al.*, 2009; Huebsch *et al.*, 2014), to date no national assessment of matrix  $t_u$  has been established.

## **2.4 Landscape Position**

As discussed in Section 2.3,  $t_u$  is not an isolated process, but rather it reflects the greater hydrologic system. It contributes to  $t_T$ , with the remainder being made up of travel time through the groundwater or saturated zone –  $t_s$ . Depending on the position of the contaminant source within the landscape, depth of the soil profile (to either

bedrock or the watertable) and distance to a receptor (abstraction point or surface water), the relative contributions of  $t_u$  and  $t_s$  will vary, and either one or the other will exert the dominant control over  $t_T$ . Sousa *et al.* (2013) described a methodology to assess the importance of  $t_u$ , by representing the proportion of time lag spent in the unsaturated zone ( $t_r$ ) within the context of  $t_T$  (Eqn. 2.1).

$$t_r = \frac{t_u}{t_T} \quad [\text{Eq. 2.1}]$$

Greater  $t_r$  indicates a larger proportion of total travel time spent in the unsaturated zone. In such instances, thorough characterisation of the unsaturated zone, and hence  $t_u$ , becomes essential. Interpretation of the likely  $t_r$ , based on generic soil series information obtained from maps or soil surveys, and on landscape position and distance from a receptor, can therefore indicate to the practitioner the level of profile characterisation required to adequately define  $t_u$ .

## 2.5 Unsaturated Flow Equations

The rate at which flow occurs through the porous medium is related to its degree of saturation. The simplest approach is to assume fully saturated conditions, as described by Darcy's Law:

$$q = KA(h_1 - h_2)/l \quad [\text{Eq. 2.2}]$$

where  $q$  is the specific discharge,  $K$  is the saturated hydraulic conductivity,  $A$  is the cross-sectional area of flow,  $h_1$  and  $h_2$  are the heights above a reference level of the water, and  $l$  is the thickness of the medium. Fenton *et al.* (2011) used this approach in order to suggest the most rapid possible  $t_u$  ranges. The model presented in that study calculated  $t_u$  is as follows:

$$t_u = \frac{d}{ER/(n_e/100)} \quad [\text{Eq.2.3}]$$

where  $d$  is the depth in metres of the unsaturated zone and  $n_e$  (%) is the effective porosity.  $ER$  represents effective rainfall, as calculated using the hybrid model described by Schulte *et al.* (2005). Even under such rapid-transport assumptions when coupled with estimates of  $t_s$ , Fenton *et al.* (2011) demonstrated that  $t_T$  is likely

to inhibit the capacity of many Irish catchments to achieve EU-WFD targets within the designated reporting periods, and that in many cases  $t_u$  alone (estimated to a depth of 10 m below ground level (BGL)) would exceed current deadlines. Consequently, deadlines have been extended (Daly, 2011).

However, this fully saturated assumption does not hold true in the field, where soil saturation varies depending on weather conditions. Therefore, the hydraulic behaviour of the soil is also variable, as is the rate of solute transport. To account for this, the Richards equation [Eq. 2.4] allows the rate of flow in an unsaturated soil to be determined (Richards, 1931).

$$\frac{\partial \theta}{\partial t} = \frac{\partial}{\partial z} \left[ K(\theta) \left( \frac{\partial \psi}{\partial z} + 1 \right) \right] \quad [\text{Eq.2.4}]$$

where  $K$  is the hydraulic conductivity,  $t$  is time,  $z$  is the elevation above a vertical datum,  $\psi$  is the pressure head and  $\theta$  is the water content. While this equation describes unsaturated flow, it fails to address the effects of fluctuating soil water content present in field soils, because it assumes uniform and constant flow. Knowledge of the saturated conductivity ( $K_{sat}$ ) and soil hydraulic properties can be used to better characterise these transient soil-water conditions (Brooks and Corey, 1966; Mualem, 1976). The van Genuchten-Mualem (VGM) (van Genuchten, 1980) equation is most commonly used approach (Hardie *et al.*, 2013) to assess these properties [Eq. 2.5], although other mathematical models also exist (e.g. Brooks-Corey, 1964; Durner, 1994; Kosugi, 1996).

$$\theta = \theta_r + \frac{\theta_s - \theta_r}{\left[ 1 + (\alpha \psi)^n \right]^m}$$

$$K(\theta) = K_{sat} \Theta^l \left[ 1 - \left( 1 - \theta^{1/m} \right)^m \right]^2$$

$$\Theta = \frac{\theta - \theta_r}{\theta_s - \theta_r} \quad [\text{Eq. 2.5}]$$

where  $\theta_s$  is the saturated soil water content (where all soil pores are filled with water (Shukla, 2014)),  $\theta_r$  is the residual soil water content (beyond which no further

dewatering occurs in response to increasing pressure),  $\alpha$  is an empirical fitting parameter related to the air entry value,  $n$  and  $m$  are empirical constants,  $l$  refers to pore tortuosity, and  $\Theta$  is the degree of saturation. These parameters are derived from the SWCC (Fig. 2.5), also commonly referred to as the soil water retention curve, moisture release curve, or the pF curve (termed SWCC forthwith) (Malaya and Sreedeeep, 2012). The SWCC describes the relationship between volumetric soil water content ( $\theta$ ) and matric potential ( $\Psi$ ). In addition to the modelling of transient soil water content, the SWCC has been used to determine shear strength (Vanapalli *et al.*, 1996), physical quality (Dexter, 2004a/b/c), and pore size distribution (Aschonitis *et al.*, 2012), amongst other applications. Vogel (2014) describes the SWCC as ‘the most important curve in soil physics.’

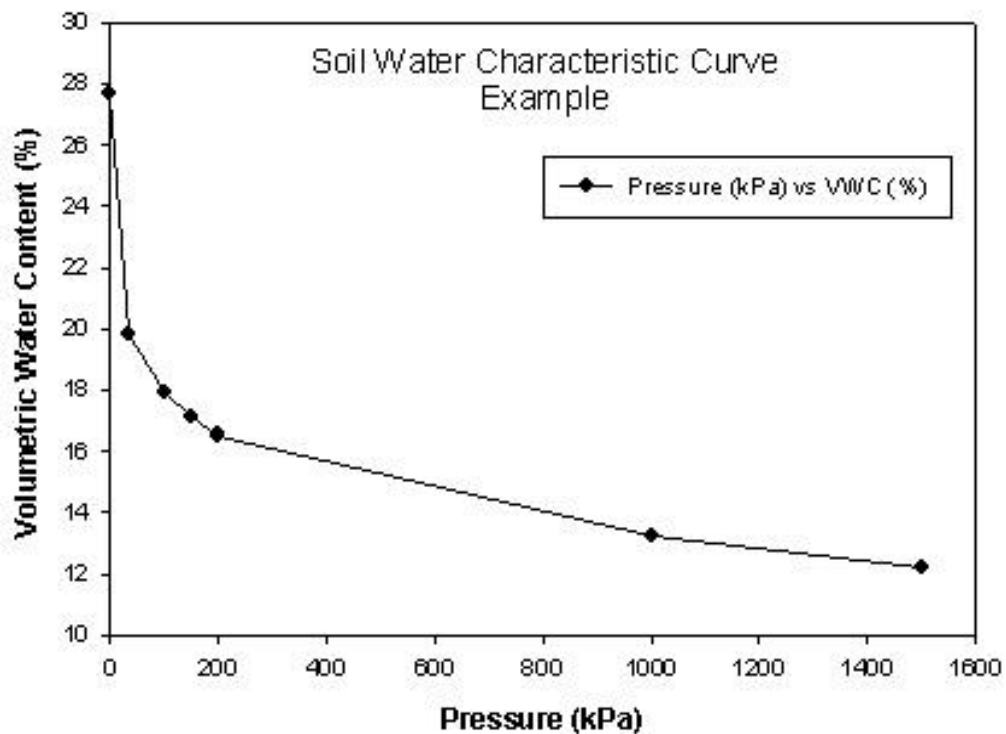


**Fig. 2.5:** Example Soil Water Characteristic Curve (SWCC).

## 2.6 Numerical Modelling

While *in situ* field tracer tests (where a conservative solute or dye is introduced to the soil, and its movement through the unsaturated zone is monitored) represent an exact quantification of  $t_u$  at a specific location, under specific meteorological conditions, there are several key limitations to such an approach.

Tracer testing may be costly and time consuming, with the result that studies of  $t_u$  are implicitly subject to the same delays that they attempt to gauge and so exhibit limited predictive capacity compared to numerical simulations (Konikow, 2011). Furthermore, they are highly specific to the soil and meteorological conditions at that location and time, and so are limited in their ability to reflect larger areas (e.g. a catchment), or to examine various meteorological or management scenarios as an aid to policy design (Bouraoui and Grizzetti, 2014). An alternative approach is to use numerical models capable of simulating the unsaturated zone (see reviews by Arheimer and Olsson, 2003; Jackson *et al.*, 2006) coupled with input parameters reflecting the local soil, solute and meteorological conditions (Keim *et al.*, 2012; Sousa *et al.*, 2013). The ‘demanding timeframe’ of the EU-WFD (Collins and McGonigle, 2008) and somewhat limited opportunity for long-term *in situ* tracer tests have contributed to the popularity of model approaches. Similarly, the capacity for scenario testing led to a preference for models in policy development and river basin management (Bouraoui and Grizzetti, 2013). A wide range of proprietary and free-licence software modelling packages are available (e.g. the Hydrus series (1, 2 or 3 dimensional) (Šimůnek *et al.*, 2013), Hydrogeosphere (Brunner and Simmons, 2012), UnSat Suite (Waterloo Hydrologic Inc., 2004), amongst others). These models incorporate the Richards equation (Richards, 1931), and frequently other relevant functions, enabling simulations of advection-dispersion, root-water/solute uptake, runoff, evaporation, chemical transformations (e.g. the UNSATCHEM module incorporated in the Hydrus series (Šimůnek *et al.*, 1996)), and may impose boundary conditions (Vereecken *et al.*, 2008) and porosity characteristics (single or dual-porosity) appropriate to the particular soil and scenarios in question. Many of these programmes present graphical interfaces, which allow model users to define soil boundaries and horizons. Wagener *et al.* (2001) and Konikow (2011) discussed the importance of selecting a model which best reflects the processes and problems in question, while also taking into consideration the availability of the required data. For example, to estimate  $t_u$  according to Fenton *et al.* (2011), one needs only to know the depth and effective porosity of the soil and the *ER* at the site. However, using a numerical approach, there is an additional requirement for soil hydraulic parameters. Model selection therefore depends on all of the above factors. Konikow (2011) discussed how a model is always ‘a simplification of a very complex reality,’ and indicated the compromise that must occur between model complexity and ease

of use and understanding, particularly in the case of scenarios subject to the innate variability of the natural environment. Models provide a tool for better understanding of a system (Konikow, 2011), rather than providing an inerrant replication of reality.

Bouraoui and Grizzetti (2014) discussed how numerical models at appropriate scales can form a tiered system, with a catchment characterisation model used to identify key areas and pathways for nutrient transport within a river basin. As a subsidiary of this, models capable of simulating the processes in these areas may be employed. The CMT devised by the Pathways Project (Mockler *et al.*, 2013; Packham *et al.*, 2013),, incorporates a model in which nutrient loss from a catchment is assigned to various hydrological pathways (Archbold, 2010). This approach is successful in identifying which pathways are active within specific catchment areas, and can be used to indicate areas in which  $t_u$  requires quantification. However, that model relies on a simplified approach to soil characteristics, in which soil-water parameters are defined according to broad drainage class. Greater accuracy in the quantification of soil moisture dynamics (and hence,  $t_u$ ) may be obtained by increasing input data complexity *via* a dedicated soil hydraulic model, using horizon-specific data. As such, the CMT represents the first tier of catchment characterisation, upon which more detailed assessment of specific pathways using appropriate measurement and modelling approaches may be employed, as a second tier.

In determining which of the many commercial and free-licence numerical models currently available to employ, a practitioner must first identify whether to use one-, two- or three dimensional models. One-dimensional (1D) models assume vertical transport/water flow through the media, without addressing lateral flow. It is frequently used for simulations corresponding to lysimeters (in which lateral flow is prevented by the lysimeter casing) or scenarios in which lateral flow is minimal e.g. in freely drained soils. An advantage of this approach is that horizon-specific soil physical/hydraulic data can be obtained from a single soil profile. A basic principle of numerical modelling is to start with a simple model structure and subsequently to increase complexity (van Genuchten *et al.*, 2013) (so for example, a practitioner might initially model water flow through a profile, and then add a solute component, followed by a chemical attenuation equation). Similarly, 1D modelling can provide a starting point for more comprehensive investigations (Chrysikopoulos *et al.*, 1990). Two-dimensional (2D) models are an example of such an approach. In these models,

both vertical and lateral water and solute movement are simulated. While this may reflect field scenarios well (particularly in less-freely drained soils) and facilitates simulations of entire transects, it also necessitates greater soil data, in order to describe both the vertical and lateral heterogeneity of properties. This requires the excavation of multiple soil profiles or cores over a relatively small area, or detailed geophysical surveys. Similarly, three-dimensional (3D) models require detailed parameterisation and can be considered to be ‘data-hungry’ (Wegener, 2000). This approach may be appropriate to scenarios exhibiting complex geometry such as artificial drainage networks or subsurface tunnels (van Genuchten *et al.*, 2013). Practitioners must select models based on (1) the scenario they are attempting to quantify, and (2) the input data available (Wagener *et al.*, 2001). In a commentary of hydrological modelling principles Bergström (1991), noted that over-simplification and insufficient input data are common impediments to successful and appropriate implementation. As the focus of this thesis is on the vertical pathway, a 1D approach is considered optimum.

There is a multiplicity of both free-licence and proprietary 1D models available. While it is beyond the scope of this chapter to review them all in detail, a brief assessment of some of the most popular software packages is presented here. The Hydrus 1D model (henceforth referred to as ‘Hydrus’) is widely used in the modelling of one-dimensional transport. More than 130 publications from 2014 and 2015 alone (*c.* 800 since 2000) refer to its use. The model employs a finite element method (partitioning the entire subject domain into discrete components) to numerically solve the Richards equation for water flow, and incorporates advective-dispersive equations by which heat (Saito *et al.*, 2006) and solute behaviours can also be approximated (Skaggs *et al.*, 2007). The model accepts hydraulic properties derived according to a variety of fitting equations, and incorporates the ROSETTA soil catalogue (Schaap *et al.*, 2001) for parameter estimation. Hydrus can simulate transport across the full range of soil moisture, from totally unsaturated to saturated, in single or dual porosity systems. In single porosity applications, the soil medium is assumed to be uniform, with all transport occurring through the matrix. Conversely, dual porosity/permeability models (such as MACRO (Jarvis, 1994) or SWAP (Kroes and Van Dam, 2003)) divide the domain into separate regions, exhibiting distinct hydraulic characteristics (Kramers, 2009). Dual porosity models assume matrix water remains stagnant, while dual permeability models allow water movement in

both matrix and macropore regions. These approaches enable both matrix and preferential flow to be simultaneously assessed. The major limitation to this latter approach is the increased model complexity, the requirement for greater expertise on the part of the practitioner, and additional data requirements (Jarvis *et al.*, 1998). As  $t_u$  is likely to be most prolonged through matrix transport, a single porosity model is appropriate for its assessment.

VLEACH (Ravi and Johnson, 1997) has many similarities to Hydrus: one-dimensional transport, finite element model, similar input variables. However, it has two major limitations with respect to the objectives of this thesis. First, moisture content in each horizon is assumed to be steady-state, and does not fluctuate in response to infiltration and drainage. This is highly improbable in field conditions. Secondly, there is no facility to increase the complexity of the chemical processes, as is the case with the Hydrus PHREEQC supplement. This limits the opportunity for tailoring simulations to specific chemicals, subsequent to establishing a basic framework for model use.

STANMOD (Šimůnek *et al.*, 1999a; van Genuchten *et al.*, 2012) has many of the features of the Hydrus series; sharing several of the same development team and a similar graphical user interface. However, unlike VLEACH, the focus of that model is heavily oriented towards the behaviour of specific chemicals, and less on soil-water relations. While it is a powerful program, it is less suitable to the present thesis than a more soil-focused approach. As such, much of the attributes of STANMOD are present within the PHREEQC package, and so may be incorporated to Hydrus simulations where necessary.

Due to the range of add-on packages (Unsatchem, Modflow, PHREEQC) and capacity for upgrade to two or three dimensional simulations (data permitting), Hydrus presents as an ideal basic numerical package for  $t_u$  assessment, which can then be tailored as necessary to specific scenarios. Additionally, the extensive and contemporary literature facilitates its implementation. The duration of this research project precluded examination of more than one model; consequently, the Hydrus single-porosity package was selected, in light of the aforementioned attributes.

## 2.7 Model Inputs

The soil hydraulic properties ( $\theta_s$  and  $\theta_r$ , along with fitting parameters  $\alpha$ ,  $n$  and  $m$ ) can be derived from the SWCC using fitting equations discussed in Section 2.4.

These parameters are used as input values to numerical models, to quantify the soil moisture status, and hence, its capacity for solute transport, and may be obtained directly or indirectly (Durner and Lipsius, 2005). In the direct approach an SWCC is measured and a fitting equation is applied, while in the indirect approach an SWCC and corresponding parameters are inferred using pedotransfer functions from more easily measurable attributes such as texture and bulk density ( $\rho_b$ ). Konikow (2011) suggested that increasing the complexity of a numerical model can improve the accuracy of its outputs (e.g. solute transport and hence  $t_u$ ), but at a cost of lowered ease of understanding and greater data demand. Similarly, increasing the complexity of data inputs to a model, by moving from pedotransfer functions to measured data for example, can likewise improve the performance of that model. Wösten *et al.* (1995) suggested that more complex soil data be employed only when the differences in estimates of soil behaviour were significant as a consequence. Therefore, the results of numerical modelling exercises conducted using direct versus indirect methods cannot be assumed to be synonymous. Sousa *et al.* (2013) indicated that direct/measured rather than indirect or generic data lead to more accurate estimates of  $t_T$ . Chapter 3 examines the effects of data-complexity and landscape position on  $t_u$  estimates.

### *2.7.1 Direct Approach – Soil Water Characteristic Curve*

Laboratory assessment of the SWCC may be conducted on either a wetting (sorption) curve, by which water is gradually imbibed by the soil, or more commonly on a drying (desorption) curve (Hillel, 2004), in which water is expelled, subject to various pressures. The wetting and drying curves of a given soil may exhibit differing  $\theta$  at specific  $\Psi$ , indicating hysteresis (Fig. 2.6) which potentially arises in response to entrapped air, structural changes to the soil (swelling or shrinking), or the effects of pore tortuosity.

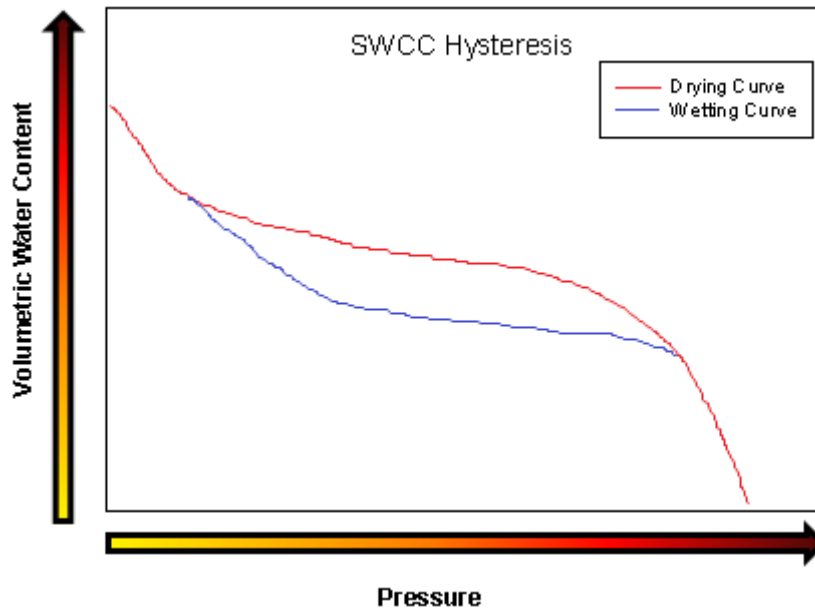


**Fig. 2.6:** Hysteresis in the SWCC, indicating water retention measured via wetting or drying processes.

Rather than measure both curves, the wetting curve may be inversely calculated from the more easily obtained drying curve (Šimůnek *et al.*, 1999b). Traditional methods for assessing the drying curve have included pressure plates (Richards, 1948; 1965), hanging columns (ASTM D6836-02, 2008a) and Tempe Cells (Reginato and Bavel, 1962; ASTM D6836-02, 2008a). These methods have several limitations; chiefly, that they are slow and arduous (Gee *et al.*, 2002; Bittelli and Flury, 2009; Dexter *et al.*, 2012; Gubiani *et al.*, 2012), prone to the shrinkage and cracking of samples (Cresswell *et al.*, 2008) and susceptible to errors, particularly at low water potentials (Peck and Rabbidge, 1969; Campbell, 1988; Cresswell *et al.*, 2008; Bittelli and Flury, 2009). Despite the ubiquity of the method, Cresswell *et al.* (2008) further noted that the shrinkage and dispersion of colloids can impair the ability of clay soils to equilibrate at specified  $\Psi$  using pressure plates. Furthermore, these methods typically pertain to small and disturbed soil samples, which may not reflect the critical influence of soil structure on water content and hydraulic properties (Young *et al.*, 2001; Lin, 2011). As a result of these obstacles, there are limited measurements of SWCCs on Irish soils. To date, the only campaign which took these measurements was the National Soil Survey (NSS) for County Waterford (Diamond and Sills, 2011) in the South of Ireland. That study measured SWCCs for

each horizon of 39 soil profiles, but the endeavour was not implemented over the remainder of the country. Further details of this dataset are provided in Section 3.3.1.

Modern commercial devices are available (e.g. HYPROP (Schindler *et al.*, 2010) or the vapour sorption analyser (Decagon, 2015a)), are not yet in widespread use in many research laboratories. An alternative to the above methods is centrifugation (ASTM D26836-02, 2008a; Nimmo, 1990; Šimůnek and Nimmo, 2005; Reis *et al.*, 2011). This approach was initially proposed by Briggs and McLane (1907), and thereafter by Lebedev (1936) and Russell and Richards (1938). Gardner (1937) [Eqn. 2.6] determined that the radial distance of the midpoint and base of the soil sample, and the speed of rotation (revolutions per minute – RPM) can be manipulated to exert the various target  $\Psi$ .

$$\psi = \frac{\rho\omega^2}{2}(r_2^2 - r_1^2) \quad [\text{Eq. 2.6}]$$

where  $\rho$  is the density of the pore fluid ( $\text{g cm}^{-3}$ ),  $\omega$  is angular velocity ( $\text{rad s}^{-1}$ ),  $r_1$  is radial distance to the midpoint of the soil sample (cm), and  $r_2$  is the radial distance to the free water surface (cm). Khanzode *et al.* (2002) constructed an entire SWCC within a single duration of centrifugation using disturbed, statically compacted samples, by stacking several soil cores 15 mm in height, thus inducing a different degree of pressure in each, corresponding to their radial distance of rotation. While such an approach is difficult to implement on intact field soils, that study ably demonstrated the Gardner equation in practice.

Despite the advantages of this method, high-speed centrifuges were not widely available prior to their commercialisation in the 1940s and 1950s (Thackery and Myers, 2000), allowing the slower methods to become established as standard (Reatto *et al.*, 2008). While modern high-speed, high-capacity, refrigerated centrifuges have allowed the earlier technical limitations to be overcome, there is no commercially available centrifugation kit (to date), by which standard laboratory centrifuges may be adapted to this purpose. Consequently, soil physicists must design and engineer equipment suitable for the application. A schematic of the apparatus used in this thesis (and representative of those in the literature (e.g. Smagin *et al.*, 1998; Khanzode *et al.*, 2002; Caputo and Nimmo, 2005) is shown in Fig. 2.7.

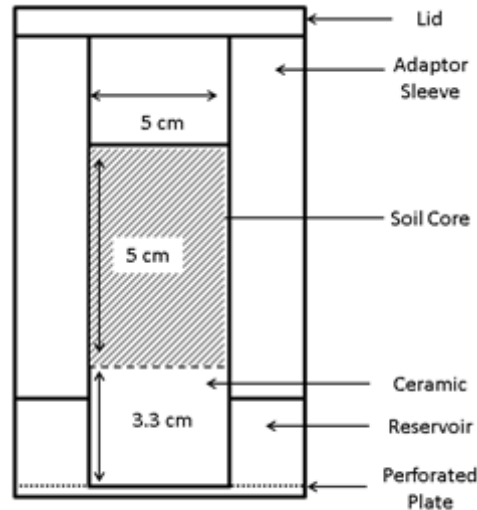


**Fig. 2.7:** A schematic representative of centrifuge bucket adaptors used for retaining a soil sample during centrifugation.

With decreased experimental duration, and the capacity for high-resolution measurements of dewatering over a wide range of  $\Psi$  (Smagin *et al.*, 1998), afforded by the centrifuge method, it is now widely used for the construction of detailed SWCCs and the measurement of hydraulic properties (Nimmo *et al.*, 1987; Nimmo *et al.*, 1989; Smagin *et al.*, 1998; ASTM D6527, 2008b; ASTM D6836-02, 2008a; Khanzode *et al.*, 2002; Caputo and Nimmo, 2005; Reatto *et al.*, 2008; McCartney and Zornberg, 2010; Cropper *et al.*, 2011; Smagin, 2012). This method is not without its limitations: soil structure may be altered by centrifugation, particularly at high-speeds (Nimmo and Akstin, 1988; Khanzode *et al.*, 2002), and by the exertion of a range of  $\Psi$  along the soil sample (Khanzode *et al.*, 2002; Smagin, 2012). Smagin *et al.* (1998) observed that despite some compaction occurring during centrifugation, the change in water retention was within the experimental error, and so, of minor consequence, although Nimmo and Akstin (1988) also noted compaction. Given the range of plasticity observed across soils of various textures (Ball *et al.*, 2000), it seems probable that certain classes or soil types will be more vulnerable, and perhaps less suited to centrifugation than others. However, that is not the objective of this study, although it presents as a fine topic for further investigation.

The centrifuge method avoids the shrinking and cracking commonly observed in traditional approaches, and due to the greater speed of dewatering, enables assessment of the SWCCs of intact soil samples, rather than the disturbed specimens

frequently observed in the literature. This opportunity afforded by the centrifuge method was recognised even in the early study by Russell and Richards (1938). The literature generally reports satisfactory agreement between the results of centrifugation and more traditional methods of SWCC assessment (Khanzode *et al.*, 2002; Caputo and Nimmo, 2005). Smagin *et al.* (1998) noted that while some discrepancies may occur between results obtained by centrifugation and by more traditional means, so too are there deviations within those latter methods, and so the superiority of either approach is by no means definitive. The authors stated that neither this, nor any other method, can serve as a standard against which others may be assessed. Hence, in selecting a method of SWCC assessment for a study or monitoring campaign practitioners must consider whether the results are likely to be satisfactory within the specific context of their application. As the purpose of this current study is to assess  $t_u$  (with a focus on trend analysis) in response to POM applied under the EU-WFD, the method of SWCC analysis employed should not only provide valid SWCCs, but do so in a timely fashion. In scenarios where high-complexity SWCC data are required for appraising  $t_u$ , reliance on those slower, traditional methods will limit the number of sites which may be assessed and so a rapid alternative is pragmatic. Chapter 3 will identify those instances in which these data are optimal, and Chapter 5 will present a methodological framework for determining the optimum measurement duration to be applied to specific soils when using the centrifuge method.

### 2.7.2 Indirect Approach - Pedotransfer Functions

In the absence of laboratory SWCC analysis, fitting equations trained on extensive soil databases (Vereecken *et al.*, 2010; Yang and You, 2013) may be used to infer the hydraulic characteristics from other, more easily ascertained attributes, e.g. texture or  $\rho_b$ . These equations are termed pedotransfer functions (PTF), examples of which include the integrated soil catalogue (Carsel and Parrish, 1988) or Rosetta (Schaap *et al.*, 2001). Mohamed and Ali (2006) found that using more detailed input data in PTFs increased their reliability. Several studies have noted failures of PTFs to wholly characterise the hydraulic behaviour of field soils (Schaap and Leij, 1998; Khodaverdiloo *et al.*, 2011). According to such studies, moving from PTFs to actual measurements of the SWCC is therefore likely to improve estimates

of soil hydraulic parameters, and hence produce more satisfactory simulations of *in situ* water and solute movement using numerical models.

As with the SWCC, there are a range of methods by which the textural characteristics of a soil may be assessed. These range from simple and rapid hand-texturing techniques, commonly used during soil surveys conducted in the field, to slower, more accurate laboratory analyses e.g. the pipette method, laser diffraction, hydrometer. These various approaches are likely to result in small differences in texture (Beuselinck *et al.*, 1998; Taubner *et al.*, 2009), which may or may not have consequences for both soil hydraulic property characteristics, and  $t_u$  estimates obtained *via* PTFs. To date, this has not been addressed in the literature.

As PTFs require input data, e.g. soil texture/particle size distribution, bulk density), a user has two options. They must either measure those properties for their sites, or, where data is required on a larger national or regional scale, may obtain those soil physical data from existing maps. The Irish Soil Information System (SIS) provides a national digital map, detailing soil associations at a 1:250,000 scale, incorporating over 450 soil series and modal profiles detailing horizon specific soil physical and chemical data. A web-based soil information system<sup>1</sup> was launched in September 2014, and the second phase of that project aims to explore derivative soil attributes. This resource presents the most up-to-date and detailed source of national soils data, facilitating greater detail in unsaturated zone analysis than is possible through more generic datasets (for example, the drainage class approach implemented in the Pathways Project (Archbold, 2010)). The SIS map is, therefore, likely to provide a key data-source for any national  $t_u$  investigative toolkit.

### 2.7.3 Meteorological Input Data

In addition to soil hydraulic characteristics and appropriate boundary conditions, the modelling of unsaturated zone processes requires meteorological data inputs (precipitation, temperature, humidity, wind and radiation) (Šimůnek *et al.*, 2012). These factors determine the driving factors behind solute movement i.e. pressure head ( $h$ ) (kPa) and  $\theta$  (%) (Shipitalo *et al.*, 2000). Studies have suggested that smaller time steps/greater resolution will result in more realistic simulations of water contents and pressure heads, and consequently may better account for solute

---

<sup>1</sup> <http://gis.teagasc.ie/soils/index.php>

movement (Wang *et al.*, 2009; Konikow, 2011; Keim *et al.*, 2012; Gladnyeva and Saifadeen, 2013). Co-location of meteorological recording stations in areas where  $t_u$  is of interest is of major importance for accurate simulations, especially where there is a large spatial or temporal influence on weather patterns (Sweeney, 1985; Mapa *et al.*, 1986; Goodale *et al.*, 1998). In Ireland, there is an East-West rainfall gradient (Fig. 2.8), coupled with differences in annual sunshine, and yearly fluctuations, meaning that a generic meteorological dataset is likely to be inadequate to describe the diversity of prevailing conditions, with further implications for  $t_u$  assessment. The locations of the daily rainfall and synoptic meteorological recording stations operated by Met Éireann are shown in Fig. 2.9.

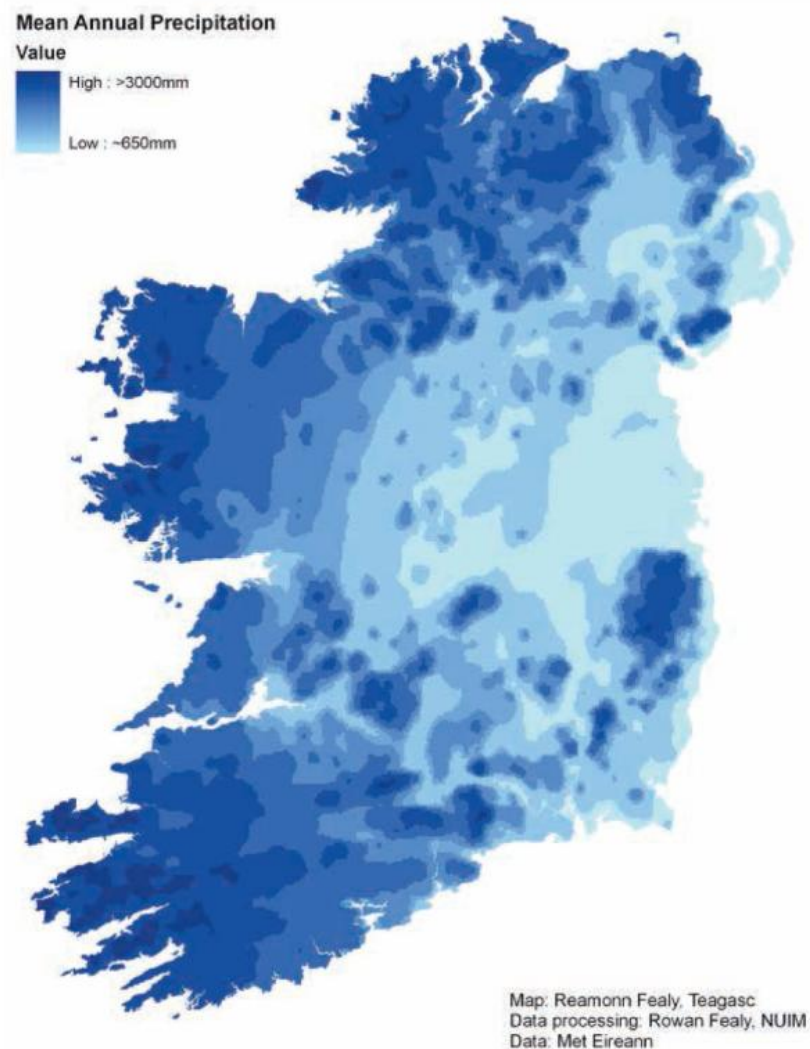


**Fig. 2.8:** Mean annual precipitation across Ireland (Fealy *et al.*, 2010). A gradient is observed which indicates increasing precipitation from East to West.

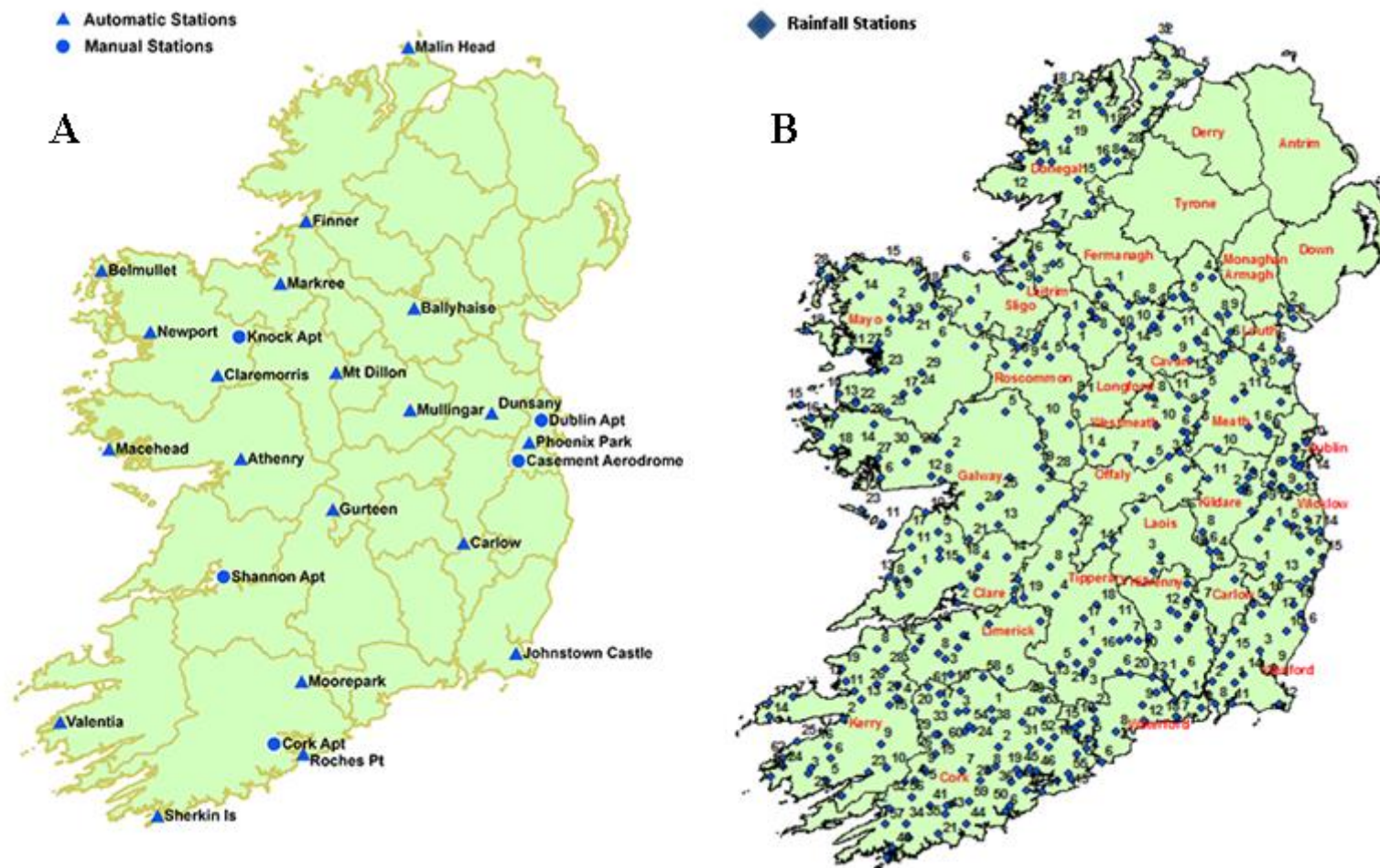


Fig. 2.9: (A) Synoptic stations (automatic and manual), and (B) rainfall recording stations operated by Met Éireann (Met., 2015a/b).

## 2.8 Conclusions and Knowledge Gaps

The objective of this literature review was to introduce the EU-WFD and associated legislation and requirements, the concept of time lag (with a particular focus on the unsaturated zone) and an overview of the principles and requirements of numerical models used for appraising water and solute transport. This review has outlined the role of the unsaturated soil in determining the time lag of waterbodies to POM. Assessing this time lag allows the efficacy of current measures to be assessed and will assist in the development of optimum strategies in the future. Numerical modelling, coupled with appropriate soil and meteorological data, using Hydrus is a suitable means to address this issue. A key target output of this thesis is to develop a toolkit, encompassing data collection and model structure, for  $t_u$  assessment at a catchment scale.

The following knowledge gaps have been identified, and will be addressed in this thesis:

- The importance of  $t_u$  relative to  $t_s$  depending on landscape position has not been assessed in an Irish context.
- There is to date, no detailed assessment of  $t_u$  duration which takes fully into account the variably saturated and heterogeneous nature of the Irish soil landscape. This is essential for both policymakers and monitoring agencies.
- The optimum level of soil and meteorological input data for assessing  $t_u$  are unknown. Identification of these requirements will enable the appropriate use of existing resources such as the Irish Soil Information System (SIS) and indicate when further data collection is required.

## Chapter 3

### Consequences of varied soil hydraulic and meteorological data complexity on unsaturated zone time lag estimates

#### Overview

While the utility of numerical models for assessing  $t_u$  has been indicated in Chapter 2, there is limited information available in the literature as to the optimum resolution of input data. This knowledge gap must be addressed before a model user can embark on a data collection campaign, or a modelling exercise. In this chapter the effects of meteorological and soil data resolution on  $t_u$  estimates using Hydrus are examined, and the optimum input data for  $t_u$  assessment are identified, based on the stage of  $t_u$  in question and the landscape position of the contaminant source. The contents of this chapter have been published in *Journal of Contaminant Hydrology* (Vero *et al.*, 2014) (Appendix B)<sup>2</sup>.

#### 3.1. Introduction

While assessing solute transport *via* numerical models is not new (Pang *et al.*, 2000; Molénat and Gascuel-Oudou, 2002; Amin *et al.*, 2014, and many others), limited consideration has been given to the effects of soil hydraulic data complexity and meteorological input resolution on model outputs, with several studies relying on easily obtained PTF data alone (Heatwole and McCray, 2007; Liu *et al.*, 2012). While this may be sufficient in some instances, such an assumption should be examined, before embarking on investigations of  $t_u$  or  $t_T$ . This is particularly important where results may have legislative or policy implications. Bouraoui and

---

<sup>2</sup> As a result of the work detailed in this chapter, Sara Vero was awarded the AECOM-CIWEM Young Environmentalist 2014. The early results and methodology of this work were presented at the ASA-CSSA-SSSA Annual International Meeting 2013 in Tampa, Florida, thanks to a travel bursary granted by the Irish Grassland Association. In addition, the Irish Geological Association and International Association of Hydrologists (Irish Branch) provided travel bursaries to allow the completed work to be presented at the ASA-CSSA-SSSA Annual International Meeting 2014 in Long, Beach, California. During that event Sara Vero was awarded 2<sup>nd</sup> place in the Soil Physics and Hydrology Lighting Oral and Poster session, for presentations based on this chapter.

Grizzetti (2014) highlighted that the availability of soil data at different scales, and the use of data at appropriate complexity levels are vital components to effective utilisation of hydrological models, with respect to water quality and catchment management issues. As discussed in Sections 2.3 and 2.6, the proximity of a potential contaminant source (such as an area in which fertiliser has been applied) to a receptor (such as a surface waterbody or a groundwater abstraction point) varies across a landscape (Fig. 2.4). Consequently,  $t_r$  is likely to vary, which may affect the utility of the low- and high-complexity input-data options.

It is acknowledged that the unsaturated zone also will inevitably contain a lateral component (Forrer *et al.*, 1999), but for the purposes of this study,  $t_u$  is assumed to represent vertical transport through the unsaturated zone alone. The soil profiles used herein represent profiles in which this pathway prevails. In other settings, for example, where overland flow prevails (as in a P loss scenario), or where there is a large degree of preferential flow, a 1D vertical transport model would not be optimum. Hence, the results of this study should be considered to be reflective only of the scenario in question, although the methodology, by which the results of low- (indirect) versus high-complexity (direct) data are compared, may be applied elsewhere.

### 3.2 Hypotheses and objectives

This chapter examines the range of estimated  $t_u$  when a certain meteorological dataset at a certain temporal resolution is combined with various levels of soil characteristic input data (ranging from generic to soil profile and horizon-specific) derived through fitting of the VGM equation. A numerical model simulating the movement of a surface-applied tracer (analogous to that described in Chapter 7) through the soil profile can then be used to estimate a breakthrough curve (Fig. 3.1) (divided here into initial breakthrough (IBT/Trend), peak concentration (Peak), centre of mass (COM), and total exit of the solute (Exit)) at the base of a soil profile. The combination of these markers presents a comprehensive description of time lag. IBT/Trend can indicate when trend analysis (which is mandatory for 2021 reporting under the EU-WFD (EC, 2000)), should be initiated, as it represents the initial contamination of the receptor after implementation of the POM. The COM equates most closely to saturated (Fenton *et al.*, 2011) condition equivalents and

indicates the period in which the greatest impact of POM on the receptor will be observed. Exit is also important, as it represents the maximum residence time of the solute in the profile, subsequent to which a POM can be considered to have taken full effect.

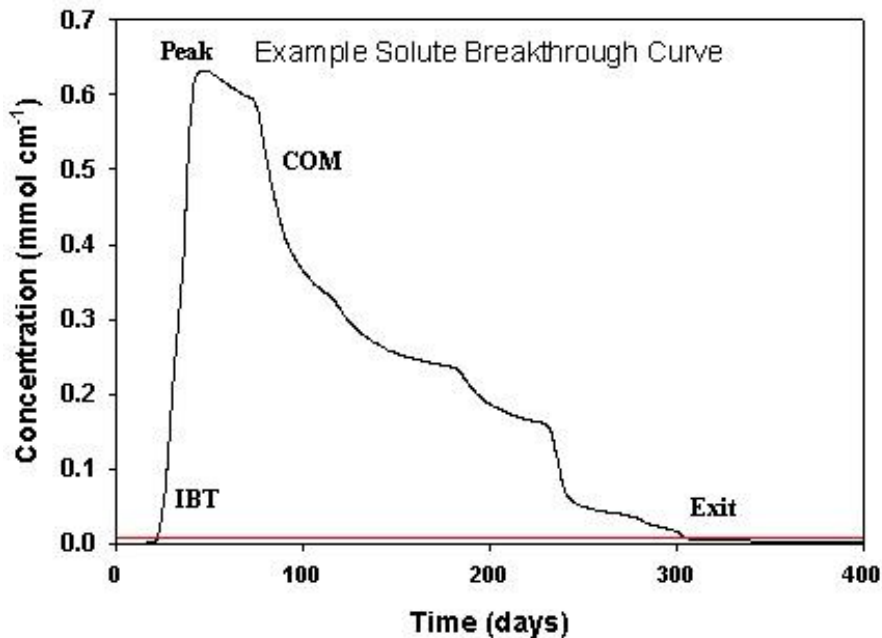


**Fig. 3.1:** Example of a solute breakthrough curve at the base of a soil profile generated using Hydrus. IBT/Trend, Peak, COM and Exit of the solute are indicated.

The first hypothesis of this chapter is that modelled  $t_u$  in freely drained soils is less sensitive to reductions in the temporal resolution of weather data than in more poorly drained soils. The sensitivity of various soil textures to changes in the temporal resolution of meteorological data will be examined, and recommendations will be made regarding the most appropriate time-step to be employed in Hydrus for the purpose of estimating  $t_u$ . The second hypothesis is: increasing the level of complexity (generic/indirect to site-specific/direct) employed to determine the soil hydraulic parameters using the VGM equation will add a higher degree of specificity to the soil hydraulic parameters and consequently improve  $t_u$  estimates. The final hypothesis is:  $t_r$  will differ depending on landscape position, and this has consequences for the complexity of input data required. Therefore, the objectives of this chapter are to (1) assess the sensitivity of various textural classes to changes in temporal resolution of meteorological data and make recommendations regarding the most appropriate time-step to be employed in Hydrus for the purpose of estimating  $t_u$ , (2) assess the sensitivity of Hydrus to the complexity of soil input data and draw

comparisons between the various complexity levels, and (3) use the Sousa *et al.* (2013) equation (Eqn. 2.6) to assess the importance of data complexity in the unsaturated zone relative to various groundwater travel time scenarios; with  $t_r$  indicating the relative importance of  $t_u$  within the context of  $t_T$ .

### 3.3 Materials and Methods

#### 3.3.1 Model simulations

The following model settings were identical for all simulations (both for homogeneous/textural profiles, and real NSS profiles). Hydrus 1D V4.16 (Šimůnek *et al.*, 2013) was used for all model simulations to estimate vertical travel times of a conservative solute through homogenous and heterogeneous real-life soil profiles. Longitudinal dispersivity was set as the Hydrus default of  $1/10^{\text{th}}$  of the profile depth (Fetter, 2008; Šimůnek *et al.*, 2013), which is also within the range (0.8 – 12.8 cm) observed in column studies by Perfect *et al.* (2002). Atmospheric boundary conditions with surface runoff and free drainage were imposed as the upper and lower boundary conditions, respectively (Jacques *et al.*, 2008). A third-type/Cauchy solute upper boundary condition was imposed (Konikow, 2011; Šimůnek *et al.*, 2013). A single-porosity, non-hysteretic VGM model was applied (van Genuchten *et al.*, 1991). As regards the spatial discretisation of the soil profile; a single finite element was assigned for each cm of profile depth. In other words, a profile 1 m deep was assigned 100 finite elements. It is acknowledged that finer discretisation may be required in order for the model to reach a numerical solution for some fine textured soils and also near the soil surface where there may be rapid or large changes in moisture and solute contents (Šimůnek *et al.*, 2012). However, as the present chapter considers primarily the consequences of model input data, a default approach to spatial discretisation is employed. Šimůnek (2009) recommended spatial discretisation at the cm scale for simulations operating on a sub-weekly timestep (as is the case herein) As regards the temporal discretisation; Hydrus incorporates an automated time-step adjustment in response the number of iterations needed to solve the Richards equation. This feature uses the performance index proposed by Perrochet and Berod (1993) [Eq. 3.1] to trigger a decrease in time-step when the threshold value ( $\gamma_s$ ) is exceeded. The index is simply the product of the Peclet number [Eq. 3.2] ( $P_e$  – representing the ratio of advective to dispersive transport, and largely reflecting spatial discretisation) and the Courant number [Eq. 3.3] ( $C_r$  –

which characterises numerical oscillations as influenced by time discretisation). Šimůnek *et al.* (2008) identified  $\gamma_s=2$  for the Hydrus 1D model. A detailed analysis of spatio-temporal discretisation is provided by Jacques *et al.* (2006), whose paper identified the  $\omega_s$  approach as the most appropriate means to assess model performance.

$$P_e * C_r \leq \gamma_s \quad \text{where } \gamma_s=2 \quad [\text{Eq. 3.1}]$$

$$P_e = \frac{\textit{Advective}}{\textit{Diffusive}} \quad [\text{Eq. 3.2}]$$

$$C_r = \frac{u\Delta t}{\Delta x} \leq C_{\max} \quad [\text{Eq. 3.2}]$$

Where  $u$  is magnitude of velocity,  $t$  is timestep,  $x$  is length interval, and  $C_{\max}$  is a predetermined permissible maximum.

The threshold concentration at which IBT/Trend and Exit were considered to have been achieved was  $0.01 \text{ mmol cm}^{-1}$ . COM was calculated according to Payne *et al.* (2008). Meteorological data (hourly) from a synoptic station (Moorepark, Co. Cork;  $52^{\circ}09'50 \text{ N}$ ,  $08^{\circ}15'50 \text{ W}$ ) was obtained and the Penman-Monteith equation (Monteith, 1981; Monteith and Unsworth, 1990; Smith *et al.*, 1991) was used to calculate evapotranspiration (Eta) based on measured precipitation, solar radiation, humidity and windspeed, and assuming an albedo of 0.23 (default value within the model for grassland simulations). This station was selected on account of its long-term, complete dataset, and its proximity and comparable weather patterns (Keane and Sheridan, 2004) to the sites in question. Summary descriptions of the sites are given in Table 3.1, and full details of all soil profiles are provided in Appendix C. To initiate solute movement through the profile, 10 mm of precipitation was applied on Day 1, with a solute concentration of  $10 \text{ mmol cm}^{-1}$ . Fig. 3.2 provides a conceptual model for the Hydrus simulations. In Fig. 3.2 the variable soil input parameters are indicated on the right-hand side and the model settings applied across all simulations are indicated on the left-hand side. Model inputs (meteorological and solute) and outputs at the base of the soil profile (IBT/Trend, Peak, COM and Exit) are also depicted.

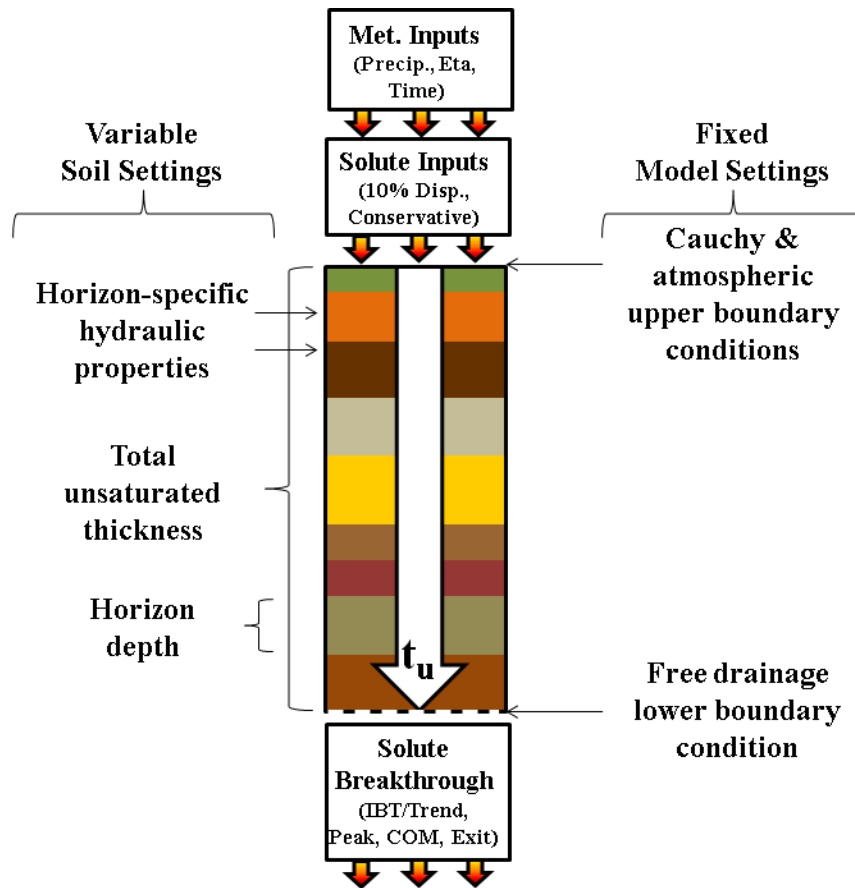


**Fig. 3.2:** Conceptual unsaturated numerical model diagram indicating input parameters, boundary conditions, horizon characteristics and model outputs.

For hypothesis 1, hourly versus daily meteorological data time-steps (converted using SAS V9.1 (SAS, 2003)) from 2004 (a wet year, 1038 mm rainfall) and 2010 (a dry year, 763 mm rainfall) (mean annual Irish rainfall ranges from 750 mm to >1200 mm (Keane and Sheridan, 2004)) were used in conjunction with homogeneous soil profiles, each of 0.5 m depth and each representing 12 textural classes (textural menu) and  $k_s$  ( $\text{cm hr}^{-1}$ ). Such values were used as drainage class proxies, with lower permeability soils assumed to be more poorly drained than higher permeability soils (Gebhardt *et al.*, 2009). Bulk density ( $\rho_b$ ) values for these textural classes were selected from the USDA soil quality test kit guide (USDA, 1999). Sensitivity analysis of the dispersivity value was also performed for these homogeneous soil profiles, in which (for both wet and dry years) dispersivities of 1%, 10% and 20% were applied for the entire soil profile.

**Table 3.1:** Summary of NSS (Waterford) soils (Diamond and Sills, 2011).

Profile No.	Profile Name	Soil Great Group (SIS)	World Reference Base Classification	No. of Layers	Depth	$k_s$ range	Altitude	Saturated $t_u^{**}$
					m	cm hr <sup>-1</sup>	m asl*	Years
Non-converging	Lickey	Humic Surface Water Gley	Haplic Gleysol	6	1.00	0.15-7.90	145	0.35
Non-converging	Dungarvan	Typical Luvisol	Haplic Luvisol	9	1.60	0.11-1.02	30	0.39
Non-converging	Clashmore	Typical Brown Earth	Haplic Phaeozem	8	0.90	0.13-0.92	80	0.29
9	Tramore	Typical Surface Water Gley	Stagnic Cambisol	5	1.20	0.22-0.45	55	0.88
8	Suir	Typical Drained Alluvial Soil	Fluvic Cambisol	7	0.95	1.08-3.81	20	0.55
7	Slievecoiltia	Humic Brown Podzolics	Leptic Cambisol	2	0.20	1.75-3.67	160	0.17
6	Portlaw	Humic Podzol	Albic Folic Podzol	4	1.50	0.23-3.46	65	1.12
5	Newport	Typical Surface Water Gley	Gleyic Phaeozem	6	1.00	0.28-6.62	100	0.60
4	Kill 2	Typical Brown Earth	Haplic Lixisol	7	1.00	0.20-2.27	65	0.75
3	Kill	Typical Brown Earth	Haplic Lixisol	3	0.40	0.86-3.40	90	0.34
2	Callaghane	Typical Brown Podzolics	Haplic Phaezoem	2	0.20	4.01-5.46	20	0.16
1	Ballymacart	Humic Groundwater Gleys	Haplic Gleysol	9	1.25	0.40-8.13	90	0.77

\*metres above sea level: \*\*Fenton *et al.* (2011)

As indicated in Section 2.5.1, the NSS performed soil surveys at a 1:126,720 scale for 44% of Ireland, during the 1960s to the 1980s. As part of this endeavour, soil survey bulletins were produced detailing mapping and soil profile data for individual counties. The County Waterford Bulletin (Diamond and Sills, 2011) was unique amongst that and the later SIS soil characterisation projects, in that it featured SWCC analysis (pressure plate and sand box methods), in addition to more typical soil physical analyses (texture,  $\rho_b$ , particle density) for County Waterford, in the south-east of Ireland (Fig. 3.3). This comprehensive dataset enables the performance of low- and high-complexity soil data as input data to numerical models to be examined. Data from the NSS has since been incorporated into the SIS database. For hypothesis 2, transport through the unsaturated zone was simulated for 12 soil profiles surveyed in Co. Waterford as part of the NSS in the 1980s. The full dataset has been published by Diamond and Sills (2011). Co. Waterford is located on the south coast of Ireland (W6 °58' and 8°11', N51°56' and 52°21'), and has a total area of 185,753 ha (Fig. 3.3), with predominantly undulating topography (Diamond and Sills, 2011). Most of the county experiences *c.* 1,000 mm mean annual rainfall (Diamond and Sills, 2011). Table 3.1 presents abbreviated descriptions of these profiles; complete profile descriptions are provided in Appendix C. No field tracer experiments were conducted at these sites. However, the results of the present Hydrus simulations were compared with published values from a variety of lysimeter studies under similar meteorological conditions (e.g. Ryan *et al.*, 2001; Hooker, 2005, Richards *et al.*, 2005; Kramers *et al.*, 2009/2012; Selbie, 2013). Particular comparison is provided with the results presented by Kramers *et al.* (2009/2012), due to the close similarity between the soil profiles examined in that study, and the NSS profiles herein.



**Fig. 3.3:** Outline map of Ireland; County Waterford (in which the soil series examined in this chapter are located) is highlighted.

The temporal resolution (2004-2008) of meteorological data used in the hypothesis 2 simulations was determined from the results of hypothesis 1. Simulations were conducted for each of the 12 NSS soil profiles using varying levels of soil physical characteristic data complexity to obtain the hydraulic parameters (Fig. 3.4). These were obtained *via* a range of simple-to-complex methods: textural class > ROSETTA > low pressure SWCC > full SWCC. The textural class parameters were selected from the Hydrus textural menu (Carsel and Parrish, 1988). ROSETTA was used to infer parameters based on sand, silt and clay percentages, and  $\rho_b$  (Diamond and Sills, 2011). The SWCC was fitted in RETC using the VGM equation, based on either the full curve (Diamond and Sills, 2011), or excluding the -15 bar pressure step (low pressure).

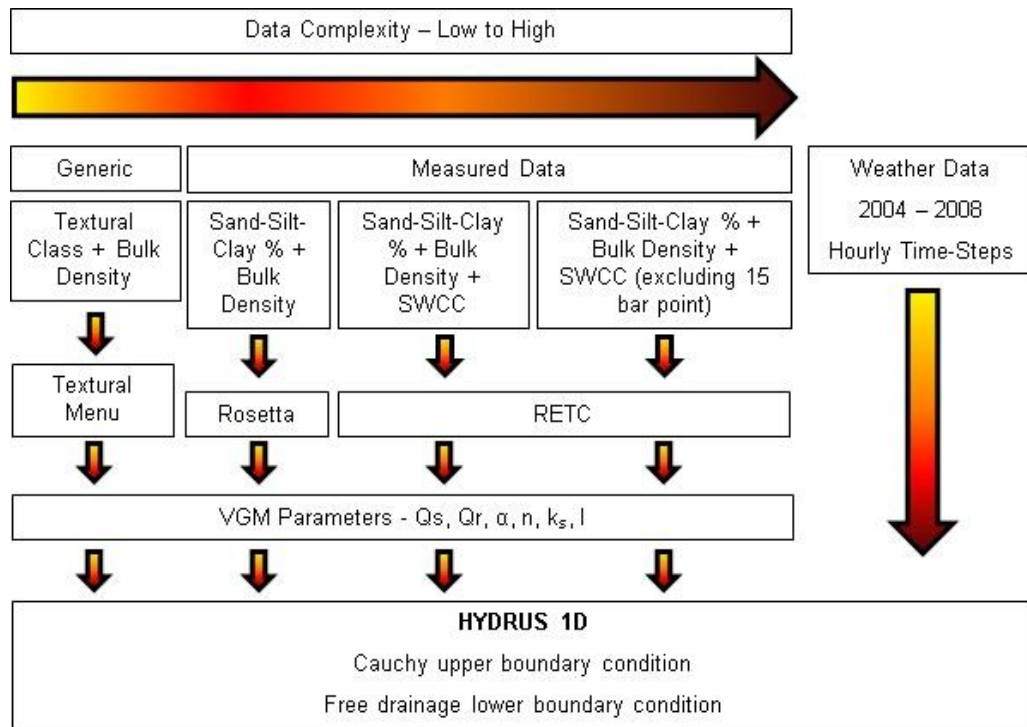


**Fig. 3.4:** Low to high complexity soil characteristic data employed in Hydrus.

### 3.3.2 Landscape Position

For hypothesis 3,  $t_r$  was calculated according to Eqn. 2.1 (Sousa *et al.* 2013). Exit was used to represent  $t_u$  for the purposes of estimating  $t_r$ ; next, each of the soil profiles were placed along a conceptualised catena (Ibrahim *et al.*, 2013b) using their indicative soil groups from the NSS (Diamond and Sills, 2011). The transect ranges in soil group from podzol (typically higher up in the catena) to surface water and groundwater gleys (near a surface water receptor) (Ibrahim *et al.*, 2013b). Saturated  $t_s$  values of 10, 5 and 0.5 years were used.

## 3.4 Results

### 3.4.1 Meteorological Data Resolution

Table 3.2 presents tracer breakthrough times (IBT/Trend, Peak, COM and Exit) for hourly versus daily meteorological inputs (wet and dry year equivalents), combined with hydraulic property characteristics, for the 12 homogenous soil textural classes in the Hydrus textural menu. Hydrus simulations were successful from sand to loam (29.70 to 1.04 cm hr<sup>-1</sup>), with variable success for heavier textured soils (silt loam (0.45 cm hr<sup>-1</sup>) to clay (0.20 cm hr<sup>-1</sup>)). Sandy clay (0.12 cm hr<sup>-1</sup>) to silty clay (0.02 cm hr<sup>-1</sup>) consistently failed to converge (that is, reach a numerical

solution). As  $k_s$  decreased, the model was less likely to converge, leading to failure  $<0.20 \text{ cm hr}^{-1}$  using a daily time-step and at  $<0.45 \text{ cm hr}^{-1}$  using an hourly time-step.

Considering Exit, from sand to loam (better drained) the temporal resolution of simulations (hourly and daily) produced similar results for both wet and dry year equivalents, with IBT/Trend  $<0.04$  years. Irrespective of the soil textural range or wet/dry year simulation, the difference in IBT/Trend between hourly and daily simulations never exceeded 0.01 years. As expected, wet year IBT/Trend was quicker than the dry equivalent. Regarding Peak: within the range of converging soil textures, differences between hourly and daily simulations ranged from 0 to 0.07 years. Average difference in Peak between hourly and daily simulations was 0.02 and 0.01 years for the wet and dry simulations, respectively. With the exception of the sand textural class (most freely drained), the differences between temporal simulations were greater for the wet year than for the dry year. For the soil textures which converged, greater differences between temporal resolutions were observed for COM 0.02 to 0.28 years. The difference in COM between the temporal resolutions for both wet and dry years were as follows: sand (0.02 years for both wet and dry), loamy sand (0.03 wet and 0.06 dry), sandy loam (0.06 wet and 0.13 dry), sandy clay loam (0.15 wet and 0.20 dry), loam (0.16 wet and 0.23 dry). The difference in COM increases as  $k_s$  decreases and is typically greater for dry years. Considering Exit: the differences between temporal simulations ranged from 0.10 to 0.42 years for the wet simulation, and from 0.16 to 0.47 years for the dry simulation. The difference in Exit between the temporal resolutions for both wet and dry years were as follows: sand (0.10 years wet and 0.16 dry), loamy sand (0.06 wet and 0.28 dry), sandy loam (0.39 wet and 0.39 dry), sandy clay loam (0.50 wet and  $>0.47$  dry (full Exit not achieved)), loam (0.42 wet and  $>0.45$  dry (full Exit not achieved)).

As regards the dispersivity value; the sensitivity analysis indicated that, for the range of converging soil types (sand through loam), differences in IBT/Trend did not exceed 0.03 years between the 10% and 20% settings, but greater discrepancies were observed compared to the 1% setting ( $<0.06$  years). For the middle stages of solute transport (Peak and COM); the 1% setting led to greater differences ( $<0.11$  years). For solute exit, differences between the 10% and 20% settings ranged

between 0 and 0.15 years, compared to the 1% setting which underestimated exit time lags by up to 0.57 years. For all soil types, the differences arising as a result of changes to the dispersivity setting were greater for the dry year than for the wet year. The Peclet-Courant stability criteria of  $\gamma_s \leq 2$  (Šimůnek *et al.*, 2008) was achieved for all simulations, indicating that the model remains sufficiently stable irrespective of the imposed dispersivity settings.

**Table 3.2:** Daily versus hourly estimates of IBT/Trend, Peak, COM and Exit (in years) for the 12 textural classes during a wet and a dry year respectively.

Textural Class	k <sub>s</sub>  cm hr <sup>-1</sup>	IBT/Trend				Peak				COM				Exit			
		Wet Year (2004)		Dry Year (2010)		Wet Year (2004)		Dry Year (2010)		Wet Year (2004)		Dry Year (2010)		Wet Year (2004)		Dry Year (2010)	
		Daily	Hourly														
Sand	29.70	0.02	0.02	0.03	0.03	0.03	0.03	0.04	0.03	0.05	0.03	0.07	0.05	0.19	0.09	0.39	0.23
Loamy Sand	14.59	0.02	0.02	0.03	0.03	0.04	0.03	0.04	0.04	0.07	0.04	0.12	0.06	0.24	0.18	0.53	0.25
Sandy Loam	4.42	0.03	0.02	0.03	0.03	0.07	0.05	0.05	0.05	0.12	0.06	0.24	0.11	0.62	0.23	0.83	0.44
Sandy Clay Loam	1.31	0.03	0.02	0.03	0.03	0.10	0.03	0.09	0.07	0.24	0.09	0.37	0.17	0.81	0.31	No Exit (>1)	0.53
Loam	1.04	0.03	0.03	0.04	0.03	0.10	0.07	0.10	0.08	0.26	0.10	0.41	0.18	0.81	0.39	No Exit (>1)	0.55
Silt Loam	0.45	0.04	*	0.04	0.03	0.13	*	0.09	0.08	0.38	*	0.50	0.22	1.00	*	No Exit (>1)	0.66
Clay Loam	0.26	0.03	*	0.03	*	0.12	*	0.35	*	0.37	*	0.49	*	0.98	*	No Exit (>1)	*
Silt	0.25	0.04	*	0.04	*	0.15	*	0.41	*	0.39	*	0.52	*	1.00	*	No Exit (>1)	*
Clay	0.20	*	*	0.03	*	*	*	0.25	*	*	*	0.49	*	*	*	No Exit (>1)	*
Sandy Clay	0.12	*	*	*	*	*	*	*	*	*	*	*	*	*	*	*	*
Silty Clay Loam	0.07	*	*	*	*	*	*	*	*	*	*	*	*	*	*	*	*
Silty Clay	0.02	*	*	*	*	*	*	*	*	*	*	*	*	*	*	*	*

\*Failed to converge

### 3.4.2 Soil Hydraulic Properties

In response to hypothesis 2: estimated soil hydraulic properties were found to vary depending on whether a low- or high- complexity approach was implemented. Tables regarding the soil physical and hydraulic properties of all 12 NSS profiles are available in Appendix C. To give an example of these data, Tables 3.3 and 3.4 show the soil physical and hydraulic properties, respectively, for Profile No. 1 (Ballymacart). As the textural menu and ROSETTA options do not indicate the actual SWCC of the soil, but rather infer hydraulic properties using pedotransfer functions, no  $r^2$  values are available to indicate how well the resulting VGM parameters describe the hydraulic properties of the specific soil in question. For both the full and low pressure SWCCs,  $r^2$  values were typically  $>0.9$ , suggesting a very good fit of the curve for both datasets. For each individual horizon, the  $r^2$  for the full SWCC was not consistently greater than that of the low pressure SWCC. Differences were observed in all hydraulic parameters derived using the textural menu and those obtained by fitting the SWCC. The textural menu assigned values according to textural class. Residual water content ( $\theta_r$ ) and  $k_s$ , determined using the textural menu, typically diverged from values elucidated from the SWCC. In the case of Profile No. 1,  $k_s$  was overestimated by 0.14 to 7.09  $\text{cm hr}^{-1}$ , except for the EG horizons, in which it was underestimated by 2.75 to 3.54  $\text{cm hr}^{-1}$ , while  $\theta_r$  was consistently overestimated. ROSETTA and both SWCC options showed good  $\theta_r$  agreement, but ROSETTA and the low pressure SWCC diverged with respect to  $\theta_s$  relative to the full SWCC. The  $\alpha$  fitting parameter was considerably greater for the low pressure than for the full SWCC. Changes to the fitting parameters allowed RETC to facilitate the fewer data points in the low-pressure SWCC relative to the full SWCC.

**Table 3.3:** Physical properties of Profile No. 1 (Ballymacart) (Diamond and Sills, 2011).

Horizon	Textural Class	Depth cm	Sand %	Silt %	Clay %	$\rho_b$ g cm <sup>-3</sup>	$\rho_s$ g cm <sup>-3</sup>	$n_e$ %	Retained water % volume					
									0 bar	-0.002 bar	-0.059 bar	-0.137 bar	-1 bar	-15 bar
A1	Loam	0-10	47	47	6	1.00	2.26	34	59.5	52.8	47.7	45.4	40.1	21.3
A2	Loam	10-20	46	46	8	1.08	2.17	31	60.0	56.5	52.4	50.1	45.5	18.9
A3.1	Loam	20-30	47	47	6	1.22	2.25	26	50.7	48.7	46.1	45.1	40.6	19.4
A3.2	Loam	30-40	47	47	6	1.23	2.25	27	49.9	47.8	45.8	44.8	40.5	18.8
Eg1	Sandy Loam	40-50	67	23	10	1.69	2.56	23	34.2	32.4	30.5	29.5	25.0	11.1
Eg2	Sandy Loam	50-60	67	23	10	1.53	2.56	26	39.8	36.5	33.7	32.4	28.3	14.4
Bg1	Loam (silty)	60-80	59	32	9	1.51	2.65	33	43.3	37.5	34.1	32.6	25.3	10.3
Bg2	Loam (silty)	80-100	59	32	9	1.63	2.65	29	38.9	35.4	33.0	31.4	27.1	9.5
Cg1	Clay Loam	100-125	45	32	23	1.50	2.64	17	49.1	43.6	41.7	40.8	37.6	25.8

**Table 3.4:** Hydraulic properties of Profile No. 1 (Ballymacart) determined from the textural menu, ROSETTA and by fitting of the full and low pressure SWCC.

Horizon	$\theta_r$	$\theta_s$	$\alpha$	n	$k_s$ (cm hr <sup>-1</sup> )	R <sup>2</sup>	$\theta_r$	$\theta_s$	$\alpha$	n	$k_s$ (cm hr <sup>-1</sup> )	R <sup>2</sup>
<b>Textural Menu</b>							<b>ROSETTA</b>					
<b>A1</b>	0.078	0.430	0.036	1.56	1.04	n/a	0.043	0.452	0.007	1.58	8.13	n/a
<b>A2</b>	0.078	0.430	0.036	1.56	1.04	n/a	0.045	0.436	0.007	1.58	5.21	n/a
<b>A3.1</b>	0.078	0.430	0.036	1.56	1.04	n/a	0.038	0.396	0.009	1.54	3.35	n/a
<b>A3.2</b>	0.078	0.430	0.036	1.56	1.04	n/a	0.038	0.394	0.009	1.54	3.22	n/a
<b>Eg1</b>	0.065	0.410	0.075	1.89	4.42	n/a	0.038	0.333	0.043	1.36	0.88	n/a
<b>Eg2</b>	0.065	0.410	0.075	1.89	4.42	n/a	0.042	0.374	0.033	1.45	1.67	n/a
<b>Bg1</b>	0.067	0.450	0.020	1.41	0.45	n/a	0.038	0.364	0.026	1.42	1.40	n/a
<b>Bg2</b>	0.067	0.450	0.020	1.41	0.45	n/a	0.035	0.337	0.033	1.36	0.91	n/a
<b>Cg1</b>	0.095	0.410	0.019	1.31	0.26	n/a	0.064	0.393	0.014	1.43	0.40	n/a
<b>Full SWCC</b>							<b>Low pressure data - no -15 Bar point</b>					
<b>A1</b>	0.043	0.560	0.023	1.14	8.13	0.93	0.043	0.595	5.621	1.04	8.13	0.98
<b>A2</b>	0.045	0.554	0.001	1.36	5.21	0.96	0.045	0.598	1.070	1.04	5.21	0.98
<b>A3.1</b>	0.038	0.481	0.001	1.32	3.35	0.98	0.038	0.499	0.066	1.05	3.35	0.97
<b>A3.2</b>	0.038	0.474	0.001	1.34	3.22	0.98	0.038	0.490	0.046	1.05	3.22	0.96
<b>Eg1</b>	0.038	0.322	0.002	1.31	0.88	0.98	0.038	0.334	0.032	1.08	0.88	0.97
<b>Eg2</b>	0.042	0.372	0.006	1.45	1.67	0.95	0.042	0.397	2.024	1.04	1.67	0.96
<b>Bg1</b>	0.038	0.399	0.012	1.22	1.40	0.95	0.038	0.431	2.842	1.10	1.40	0.91
<b>Bg2</b>	0.035	0.352	0.002	1.39	0.91	0.95	0.035	0.387	1.982	1.04	0.91	0.95
<b>Cg1</b>	0.064	0.460	0.016	1.43	0.40	0.91	0.064	0.491	66.423	1.02	0.40	0.97

### 3.4.3 Solute Breakthrough

Regarding the effect of low- versus high-complexity data sources on  $t_u$  estimates (hypothesis 2 - continued), Fig. 3.5 shows the standard deviation (SD) in IBT/Trend, Peak, COM and Exit for each of the nine converging NSS profiles, according to the level of data complexity. The overall trend was that SD increased from IBT/Trend to Exit. Exceptions to this were in Peak for Profiles No. 4, 5 and (marginally) 8. Standard deviations in IBT/Trend for each profile depending on input data complexity were typically small, ranging between 0.005 and 0.1 years. Profile No. 1 (Fig. 3.5) showed the greatest difference in IBT/Trend depending on data complexity, with low complexity data overestimating the rate of IBT/Trend relative to the SWCC estimates (SD 0.1 years). Profiles No. 1 and No. 6 showed the greatest SD as regards solute Exit.

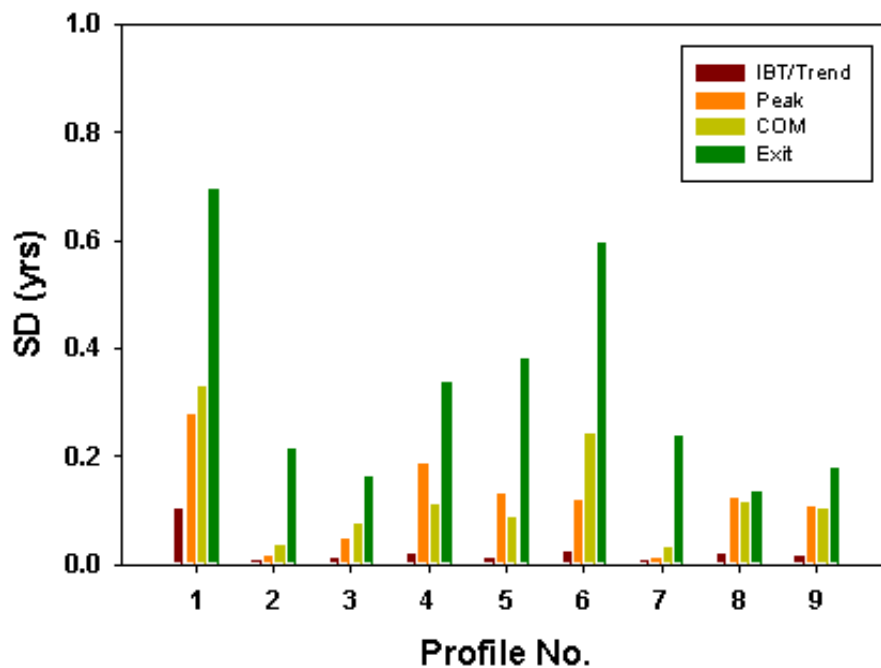


**Fig. 3.5:** Standard deviation (SD) in IBT/Trend, Peak, COM and Exit for each of the 9 NSS profiles, depending on data complexity.

Fig. 3.6 A-D shows IBT/Trend (A), Peak (B), COM (C) and Exit (D) for the nine converging NSS profiles. The bars indicate  $t_u$  in years determined according to the various data complexity levels. Three of the 12 NSS profiles simulated failed to

converge for some or all of the input complexity levels and so have been excluded from the results. Specifically regarding IBT/Trend, the differences between each complexity level were typically minor (0.01-0.05 years) with the exception of Profile No. 1 (0.22 years). Peak concentration and COM were influenced by data complexity for most profiles (Fig. 3.6B and C). Differences in COM between the low pressure and full SWCC simulations were typically minor (SD 0.12 years), except for Profiles No. 1 (0.32 years) and No. 6 (0.24 years) (Fig. 3.5). There is a trend for shorter estimates of COM, as data complexity is decreased relative to the SWCC simulations (Fig. 3.6C). Greater differences in COM are observed for the deeper and more layered profiles (e.g. Profile No. 1) than for the shallow, more homogeneous profiles (e.g. Profile No. 2 – SD of 0.03 years) (Fig. 3.5). The greatest SD amongst the four data complexity levels were found regarding solute Exit (i.e. 0.32 years, Fig. 3.5/Fig. 3.6D). As with COM, there was a trend for shorter estimates of solute Exit when low complexity data were employed, compared to using SWCC data. Differences between full and low pressure SWCCs were greatest for Profile No. 1 (0.66 years), but relatively minor for all other profiles (<0.19 years, Fig. 3.6D). Estimates of Exit based on low complexity data were lesser than those based on the full SWCC by between 0.28 and 0.97 years (Fig. 3.6D). Saturated equivalent  $t_u$  (Table 3.1) underestimated those based on the full SWCC (Fig 3.6D) by 0.34 to 1.71 years; this was typically greater for deeper profiles (e.g. Profiles No. 1, 4 and 6).

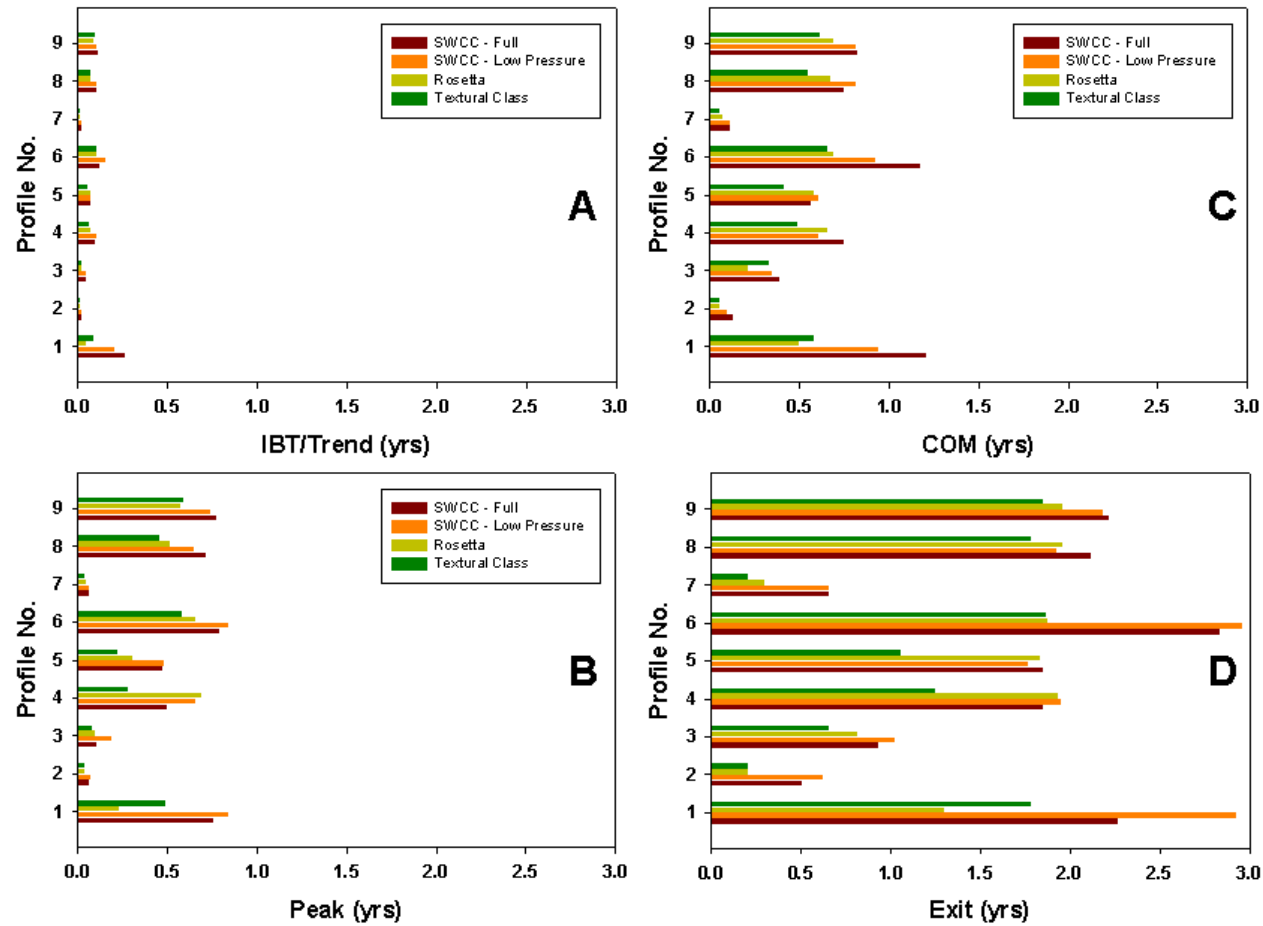


**Fig. 3.6:** Top to bottom: (A) IBT/Trend, (B) Peak, (C) COM and (D) Exit for the NSS profiles using simple to complex input data.

#### 3.4.4 Landscape Position

Based on the Sousa *et al.* (2013) equation, the  $t_r$  depending on data complexity using  $t_s$  of 0.5, 5 or 10 years is shown in Table 3.5. Shorter  $t_s$  led to greater  $t_r$  for all profiles. Increasing the input data complexity led to increases in calculated  $t_r$ . Using low complexity data, as opposed to the full SWCC, led to shorter estimates of  $t_r$  by up to 28%, 10% and 7% for  $t_s$  values of 0.5, 5 and 10 years, respectively. Only the shallow profiles (Profiles No. 2, 3 and 7) typically displayed  $t_r$  values <10%. Differences in  $t_r$ , depending on whether the full or low pressure SWCC was used, were typically minor (<6%). Fig. 3.7A shows the nine NSS profiles placed relative to a surface receptor on a conceptualised catena. The landscape position of Irish soil types is shown in Fig. 3.7B, with those NSS profiles simulated herein, highlighted. The  $t_r$  values shown represent the potential range of  $t_r$  calculated according to soil characteristic data complexity. As distance from the surface water receptor and  $t_s$  increased, there was a general trend towards decreasing  $t_r$ , despite increasing  $t_u$  (e.g. Profiles No. 1 and 6 versus 2). However, even at the maximum simulated distance from the receptor ( $t_s$ , 10 years),  $t_r$  consistently exceeded 10%.

### 3.5 Discussion

#### 3.5.1 Meteorological Data Resolution

The failure of the model to converge when simulating low  $k_s$  soils indicates that hypothesis 1 can only be assessed in soils with less clay and silt contents i.e., more freely drained soils with a more dominant vertical component, and furthermore, suggests that the model may not be ideally suited for the assessment of  $t_u$  in high clay content soils i.e. with imperfectly or poorly drained profiles. Such a limitation has been well documented in the literature (Chiu and Shackelford, 1998; Vereeken *et al.*, 2010), although finer spatial discretisation of the profile (by increasing the number of nodes per cm of profile depth) may allow a numerical solution to be attained, particularly when using high resolution meteorological datasets (Šimůnek, 2009). However, it is reasonable to assume that in such ‘heavy’ soils (which represent 32% of Irish agricultural soils; Humphreys *et al.*, 2008), or those soils possessing a low permeability layer at shallow depth (e.g. due to natural or anthropogenic reasons), mixed contaminant nutrient losses to a surface waterbody are more likely to occur through overland flow rather than sub-surface pathways

(Kurz *et al.*, 2005 a/b; Doody *et al.*, 2006; Fleige and Horn, 2000; Ibrahim *et al.*, 2013a). Although no runoff was generated in the present simulations, the model removes all surplus water from the domain once precipitation exceeds the infiltration capacity of the soil. Hydrus does not report solute lost from the model domain via overland flow, should it occur. However, in those scenarios solute is removed from the simulation according to Eq. 3.2.

$$-Sol = cTop * RO_{cum} \quad [Eq.3.2]$$

where  $-Sol$  is solute removed from the simulation,  $cTop$  is the concentration of the applied solution, and  $RO_{cum}$  is the cumulative runoff. A supplementary package to the 2D version of Hydrus is freely available, which more thoroughly addresses such scenarios. Alternatively, there are a variety of models which focus primarily on these scenarios (Ajmal *et al.*, 2015; Bartlett *et al.*, 2015)

While the dispersivity analysis here is simple, it suggests that the default value of 10% total profile depth, recommended by Fetter (2008) and Šimůnek *et al.* (2013), is sufficient for determining the key IBT/Trend marker, but that the utility of such an approach decreases where assessment of solute exit is of primary interest. Hence, it is recommended that a high-complexity approach, in which actual dispersivity measurements are obtained *via* column tracer tests (Fallico *et al.*, 2012), should be employed where this latter marker is of primary concern.

**Table 3.5:** Importance of  $t_u$  relative to total time lag ( $t_T$ ) in % ( $t_r$ ) across data complexity range, when the saturated time lag ( $t_s$ ) varies (0.5, 5 and 10 years).

Profile No.	$t_s$ (years)											
	0.5 (near receptor)				5 (mid-slope)				10 (upslope)			
	Textural Menu	Rosetta	Full	Low Pressure	Textural Menu	Rosetta	Full	Low Pressure	Textural Menu	Rosetta	Full	Low Pressure
9	79	80	82	81	27	28	31	30	16	16	18	18
8	78	80	81	79	26	28	30	28	15	16	17	16
7	29	37	57	57	4	5	12	12	2	3	6	6
6	79	79	85	86	27	27	36	37	16	16	22	23
5	68	79	79	78	17	27	27	26	10	15	16	15
4	71	79	79	80	20	28	27	28	11	16	16	16
3	57	62	65	67	12	14	16	17	6	7	9	9
2	29	29	50	55	4	4	9	11	2	2	5	6
1	78	72	82	85	26	21	31	37	15	11	18	23

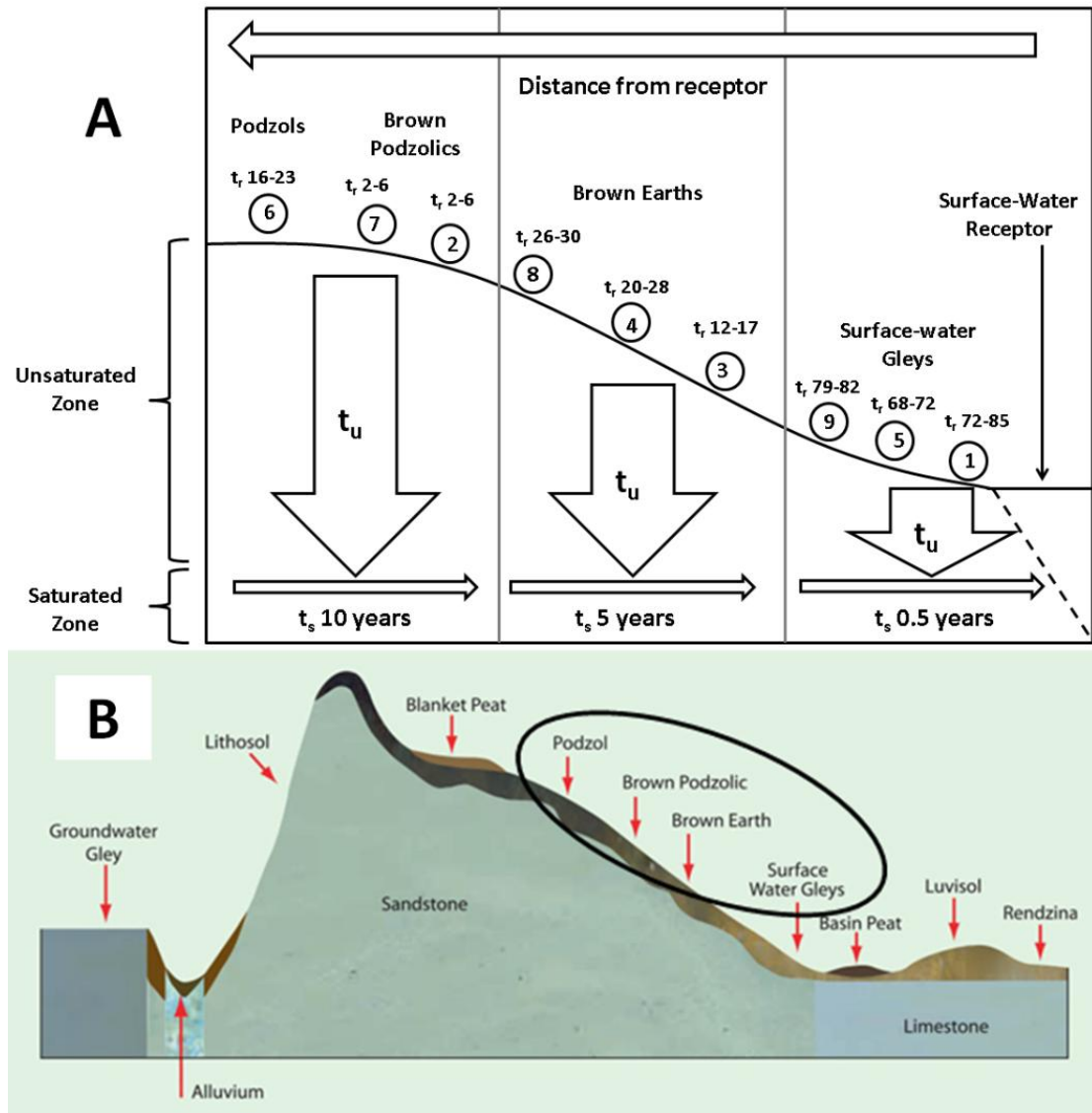


**Fig. 3.7:** (A) Position of NSS profiles No. 1-9 relative to a surface receptor and  $t_r$  ranges, (B) Position of various soil types relative to a surface receptor. Soils simulated in this paper (Podzol to Surface Water Gleys) highlighted. Adapted with permission from Ibrahim *et al.* (2013b).

Within the range of converging textures (i.e.  $>0.20 \text{ cm hr}^{-1}$ ), there is a greater need for higher temporal resolution of meteorological data, as the  $k_s$  of the soil profile (or of specific layers) decreases. This confirms hypothesis 1; that freely drained soils are less sensitive to the temporal resolution of meteorological data than poorly drained soils.

Critical for trend analysis is that temporal resolution is not vital when estimating IBT/Trend (differences <0.04 years) (Table 3.2), which means that a daily time step can be utilised. However, as COM is of primary interest with respect to testing the efficacy of POMs, the hourly time-step is most appropriate (Fenton *et al.* 2011). Mertens *et al.* (2002) found that increasing temporal resolution of weather data improved estimates of runoff obtained using Hydrus. Similarly, Gladnyeva and Saifadeen (2013) found that lower temporal resolution led to errors in estimates of the COM of transported solutes both for hysteretic and non-hysteretic simulations. This is in agreement with the general hydrologic modelling recommendations of Konikow (2011). Furthermore, meteorology and rainfall intensity were shown to play a critical role in determining the rate and nature of solute movement and eventual recharge to groundwater and hence, should be accounted for in numerical models (e.g. Torres *et al.*, 1998; Misstear, 2000; Pot *et al.*, 2005; Schulte *et al.*, 2006; Baily *et al.*, 2011; Keim *et al.*, 2012; Kramers *et al.*, 2012; Fenton *et al.*, 2013; Gladnyeva and Saifadeen 2013; Huebsch *et al.*, 2013; Jahangir *et al.*, 2013b). By increasing time-step, the user essentially averages precipitation over a greater duration, which poorly reflects the intensity of the event and consequently results in errors in model outputs. From a policy perspective, IBT/Trend is the likely the most important marker for indicating initial groundwater quality response to POM, (OECD, 2008; van Grinseven *et al.*, 2012) hence, a daily resolution is sufficient within the context of the present work.

Hydrus has the capacity to accept meteorological inputs in the form of ‘time variable boundary conditions’ (TVBCs), in various time units. However, the graphical user interface (GUI) in Hydrus is limited to 10,000 TVBCs. Consequently, when hourly inputs are supplied, the simulation is limited to 10,000 hours (1.14 years). For many soil profiles, this is an insufficient length of time to wholly account for solute exit from the profile. Alternatives to overcome this limitation are: (1) to manually input additional TVBCs outside of the GUI, (2) to use a lower time resolution such as a daily time-step, or (3) to use the end conditions from the initial simulation as initial conditions for a subsequent simulation. In addition to the daily and hourly temporal resolutions and results presented here, simulations were conducted using 2, 4, 6 and 12-hr temporal discretisation (interim time-steps). However, the results of those simulations were not included as they became

increasingly dissimilar to those obtained using daily or hourly time-steps as temporal resolution decreased, i.e. with the 2-hr discretisation being most similar and the 12-hr being most divergent. Whilst it may be tempting to simply reduce the temporal resolution of weather data, the authors found that this practice led to substantial discrepancies in parameter estimation. It is likely that these errors result from discrepancies between the time-steps over which the boundary conditions are imposed (Šimůnek, 2014). For scenarios where solute breakthrough is likely to exceed 10,000 TVBCs (*c.* one year), instead of attempting to overcome the limitations of the GUI by decreasing the temporal resolution, input data are best supplied outside of the GUI. The failure of these interim time-steps to produce satisfactory results is, in reality, unlikely to be a significant problem to model users, as meteorological data are typically available in daily or hourly resolutions.

The difference in solute Exit and COM between daily and hourly simulations (Table 3.1) suggests that hourly data may better simulate solute movement. While the difference in COM between simulations increased with decreasing  $k_s$ , this was not the case with Exit. As COM represents the bulk of solute movement, this result confirmed the hypothesis that sensitivity to temporal resolution is greater in more poorly drained soils. The failure of Exit to conform to this pattern may be as a result of the physical retardation of solute movement through areas of restricted flow (Kramers *et al.*, 2012; Kartha and Srivastava, 2008), as a result of low mobile water-content (Padilla *et al.*, 1999; Konikow, 2011) or decreased porosity. However, the solute concentrations observed during the tailing period are extremely low and unlikely to contribute significantly to groundwater contamination. Of course, this must be tested further by incorporating data in future time lag analyses on nitrate transformational processes or P adsorption/desorption dynamics. The initiation of this tailing effect corresponded with the driest period of the year, in which differences in  $h$  between the hourly and daily simulations were greatest (up to 124 cm). The failure of Profiles No. 4, 5 and 8 to conform to the overall trend of increasing SD of COM relative to Peak (Fig. 3.3) is indicative of the limited extent of tailing present; with those profiles exhibiting greater tailing (e.g. Profile No. 2.1) also exhibiting a greater SD as regards COM relative to Peak.

Co-location of meteorological stations and collection of soil physical data is important, as the spatial variability of weather within/across catchments and indeed

larger areas can be considerable (Mapa *et al.*, 1986, Sweeney, 1985). In addition, potential errors in site-specific values resulting from unequal distribution of synoptic recording stations can be problematic. In Ireland, synoptic recording stations are both limited in number and unequally distributed across the country, thus limiting the spatial accuracy of weather recording. This difficulty may be offset by supplying precipitation data from the *c.* 750 rainfall recording stations, which are well distributed. The evapotranspiration parameters, which exhibit lower spatial variability, can be interpolated from the 25 synoptic stations operated by Met Éireann (the Irish meteorological service). A digital elevation model, such as that described by Goodale *et al.* (1998), may aid in this. However, in vulnerable catchments, site-specific meteorological data, coupled with actual soil data, will help to elucidate more reliable ranges of  $t_u$ .

### 3.5.2 Soil Hydraulic Properties

Considerable differences were observed in the soil hydraulic properties determined *via* the textural menu, ROSETTA and the full and low-pressure SWCCs, respectively. Assuming that the full SWCC furnishes the most appropriate soil hydraulic properties to describe a specific soil, it is clear that using generic values, such as those obtained *via* the textural menu, can lead to significant errors, and may poorly reflect the properties and consequently processes of a specific soil. These values should at best be considered to give a rough indication of likely solute transport conditions, and may be adequate to estimate IBT/Trend (Table 2.4A). From policy makers' point of view, IBT/Trend is vital as it indicates the initial response of a receptor to a POM and hence informs scientists when their monitoring network can begin to pick up the POM signal. As SD of this marker did not exceed 0.10 years for any of the profiles, it seems imminently practical to accept low complexity, textural data as the preferred input variable. However, such low complexity data appear to be wholly insufficient when bulk effect of POM can be observed by the monitoring network. This is important, as POM efficacy can only be assessed by analysing data collected during the COM period. Therefore, the correct identification of COM requires selecting more complex options as described herein (Fig. 3.2).

The textural menu method also leads to a homogenising effect on the hydraulic properties of the various horizons within a single profile, and hence may

not wholly reflect changes in water and solute movement patterns as influenced by particle size distribution or  $\rho_d$  within a single textural class, e.g. horizons A1 and A2 of Profile No. 1 (Table 3.4). The ROSETTA method was more satisfactory, bearing closer resemblance to the SWCC results. For example, horizon A1 of Profile No. 1 displays  $\theta_s$  values of 0.430, 0.452 and 0.559 according to the textural class, ROSETTA and SWCC methods, respectively. Likewise,  $k_s$  values for that horizon were estimated as 1.04, 8.13 and 8.13  $\text{cm hr}^{-1}$  respectively, depending on input data complexity. Hence, the ROSETTA method can be assumed to more closely reflect hydraulic properties than textural class-based estimates. However, this method still represents a simplified description of the soil and, as resulting  $\theta_s$  values diverged from those obtained using the SWCC, could lead to errors in water and solute transport calculation. Regarding the full and low pressure SWCCs, reasonable similarity was observed between the two, and both presented high  $r^2$  values ( $>0.90$ ), suggesting a good fit of the SWCC using the VGM equation. By removing the -15 bar pressure point, the VGM equation maintained a good fit, but compensated by increasing the  $\alpha$  parameter, e.g. from 0.001 to 1.070 in horizon A2 of Profile No. 1 (Table 3.4). In reality, measurement of the -15 bar pressure step is arduous, slow and expensive. This step may be excluded when IBT/Trend, Peak and COM are of primary concern. This pressure step is only essential for estimation of total solute Exit (Fig. 3.6D).

### 3.5.3 Solute Breakthrough

#### 3.5.3.1 Validity of Hydrus Simulations

The failure of three profiles to converge was related to the clay content and low  $k_s$  of their lower horizons. This corresponds to failures documented in Section 3.3.1. For these NSS soils, nutrient loss is unlikely to occur through the vertical pathway, with runoff, lateral transport and increased dispersion through the subsurface prevailing (Kurz *et al.*, 2005 a/b; Jarvis *et al.*, 2007; Blanco-Canqui and Lal, 2008; Kramers *et al.*, 2012). Consequently, Hydrus 1D is not the optimum model for the simulation of solute transport in these soils, although the 2D package may perform more optimally.

It must be acknowledged that the values of  $t_u$  presented here, regardless of input data complexity employed, do not represent the exact duration of solute

movement through the profile. A model is only ‘a simplification of a very complex reality’ (Konikow, 2011). Due to the complex and dynamic nature of contributing factors, time lag estimates can, at best, provide ranges in which response can be anticipated (Meals *et al.*, 2010). Furthermore, as the Richards equation, upon which the Hydrus single-porosity model is based (Šimůnek *et al.*, 2013), neglects the occurrence of preferential flow, resulting estimates must not be assumed to preclude discrepancies in solute breakthrough, particularly as regards IBT/Trend, in structured soils. In such soils, more rapid solute movement may be observed as a consequence of preferential flow (Gerke, 2006, Kramers, 2009, Kramers *et al.*, 2012), in which case the application of a dual-porosity or permeability model within Hydrus may be more appropriate.

While measured breakthrough curves are not available for the NSS profiles described here, numerous studies under similar soil and meteorological conditions have demonstrated that the results obtained from the Hydrus simulations are likely to be realistic and within the ranges observed during unsaturated tracer and lysimeter experiments (Ryan *et al.* (2001), Hooker *et al.* (2005), Richards *et al.* (2005), Kramers *et al.* (2012), Selbie (2013)). In particular, the lysimeter study by Kramers *et al.* (2012) was conducted using soils which are closely comparable to those detailed herein.

**Table 3.6:** Summary results of Kramers *et al.* (2012) lysimeter study.

Profile Name	Description	World Reference Base Classification	Drainage class	IBT/Trend	Peak	COM	Exit	Tracer Recovery
				yrs				%
Oak Park	Sandy loam (0.45 m) over gravel	Haplic Cambisol	Freely drained	0.08	0.37	0.38	0.99	86
Clonroche	Moderately structured loam	Haplic Cambisol	Relatively well drained	0.05	0.56	0.61	>1.14	70
Elton	Structured loam/silt loam	Cutanic Luvisol	Moderately well drained	0.04	0.84	0.67	1.07	54
Rathangan	Loam to clay loam	Luvic Stagnosol	Poorly drained, some gleying	0.01	0.02	0.18	1.10	33

Table 3.6 presents IBT/Trend, Peak, COM, Exit, and recovery of a Br<sup>-</sup> tracer in 1 m-deep lysimeter profiles (n=4) from Kramers *et al.* (2012). Lysimeters were exposed to an average yearly rainfall of 879 mm during that study. While direct comparison of the NSS profiles and those described by Kramers *et al.* (2012) cannot be drawn as they are essentially discrete sites, there are considerable physical resemblances between them, and both datasets originate from similar climatic and pedogenic environments. The Oak Park soil is roughly analogous to Profiles No. 2 and 3. The Clonroche and Elton soils resemble Profiles No. 5, 6 and 9. The poorly drained Rathangan soil is most similar to Profiles No. 1 and 8. Kramers *et al.* (2012) found IBT/Trend of <0.08 years for all profiles, which compares favourably with the Hydrus NSS simulations (est. IBT/Trend typically <0.09 years, except in the case of Profiles No. 1 and 7). Peak concentration in the NSS soils occurred on average between 0.30 and 0.50 years, which closely resembles peaks observed in the Oak Park and Clonroche soil in the lysimeter study. Peak occurrence for the Elton soil exceeded this for the spring application (0.85 years), but so too did the equivalent Profiles No. 6 and 9 with peak occurrence ranging between 0.58-0.84 and 0.57-0.77 years, respectively (depending on data complexity). Comparing Exit and COM for the Oak Park and Clonroche soils with the results of the data complexity trial suggests that the low complexity data likely underestimates these parameters, and that the high complexity data may result in more realistic estimates. Total solute exit from the Clonroche soil was not achieved during the experimental timeframe of 1.14 years (Kramers, 2012); Exit from the equivalent NSS profiles likewise exceeded this duration regardless of data complexity. Due to the poor recovery of the Br<sup>-</sup> tracer from the Elton and Rathangan soils, the COM and Exit values should not be considered to wholly reflect the total exit of solute from these profiles, which exceeded the experiment duration. Kramers (2012) observed a decrease in Br<sup>-</sup> recovery as the drainage class of the soils decreased (Oak Park>Clonroche>Elton>Rathangan). There is a similarity between the failure to recover the tracer from this profile and the failure to converge of the three heavy NSS soils. This also reflects the slower Exit observed in the Hydrus simulations as clay content increased and k<sub>s</sub> decreased. This gives further evidence to suggest that heavy clay soils are less at risk through the vertical as opposed to lateral pathways, and so their contribution to water contamination is likely to be insufficiently accounted for by a one dimensional, vertical model. The results of the SWCC

simulations more closely resembled the lysimeter results than those obtained using low complexity data, suggesting that measurements of the SWCC may result in more realistic simulations of actual soil profiles than are obtained *via* generic, pedotransfer functions. The low complexity data typically resulted in quicker Exit than was observed in comparable lysimeter studies.

### 3.5.3.2 Comparison of Simple to Complex Input Data

Regarding the Hydrus simulations of the NSS profiles, a general trend was observed in which underestimation of Exit and COM increased as data complexity decreased relative to the full SWCC simulations (Fig. 3.5, and Fig. 3.6C and D). Decreases in complexity resulted in underestimation of Exit by 0.28 to 0.97 years, and in COM by 0.02 to 0.36 years. These errors reflect the limited ability of low complexity data to describe the hydraulic behaviour of specific soils compared to measured values. Likewise, the general trend for increasing SD as regards COM and Exit relative to IBT/Trend and Peak suggests that detailed soil data are more critical where estimation of these markers is intended (Fig. 3.5). Consequently, high quality, measured soil data are required to make site-specific estimates of time lag. Unsaturated estimates exceeded saturated estimates (Fenton *et al.*, 2011) from between 0.34 and 1.71 years. As these estimates performed more poorly in the deeper profiles (e.g. Profiles No. 1, 4 and 6), it should be considered that where the soil layer is thicker, unsaturated conditions are likely to play a greater role in determining solute transport (Sousa *et al.* 2013). The unsaturated simulations, while still representing a simplified conceptualisation of water and solute movement, suggest that generic soil characteristics and saturated assumptions vastly underestimate time lag, are likely to lead to unrealistic expectations regarding groundwater remediation timeframes.

The differences in Exit for the NSS profiles between data complexity levels were greatest for deeper soils displaying many horizons; e.g. Profile No. 1. Therefore, for very simple, shallow profiles, high data complexity may be less critical. Likewise, where IBT/Trend of the solute is of primary interest, low complexity data may suffice. Sousa *et al.* (2013) noted that the importance of potential underestimation of  $t_u$  depends on the context of other uncertainties, and of the potential cost of more detailed analyses, such as measuring the SWCC.

Differences in Exit between full and low pressure SWCC data inputs were typically small - on average 0.08 years. Only one profile (Profile No. 1) exhibited a large difference in Exit depending on the presence or omission of the -15 bar value from the SWCC (Fig. 3.6D). From a monitoring perspective, the signal is likely to be so low it will be difficult to connect such concentrations with specific nutrient losses from the surface. This makes Exit interesting from a theoretical point of view, but in reality will not inform expectations of policy makers with respect to time lag and simply plays into the “generic excuse” category.

#### 3.5.4 Landscape position

It is clear from Table 3.7 and Fig. 3.7A, that even when  $t_s$  is large, the unsaturated zone is always important, and so must typically be accounted for when assessing  $t_T$ . The effect of data complexity on  $t_T$  demonstrates that where  $t_s$  is shorter, such as when the unsaturated zone is underlain by karst geology (Drew, 2008), the use of high complexity data is more critical. Conversely, where  $t_s$  is slow, there may be grounds for a decrease in data complexity. Only the profiles with the most rapid  $t_u$  in conjunction with large  $t_s$  exhibited small  $t_T$  values. This suggests that  $t_u$  is of critical importance for most profiles, and so high quality data are recommended.

Based on Fig. 3.7A, it is clear that  $t_T$  is influenced not only by the properties of the unsaturated zone, but also landscape position. Hence, this factor should also be taken into account when surveying a site for the purpose of determining  $t_u$ , and this may inform the level of data complexity employed. For example, where a shallow profile is distant from the receptor, a decrease in data complexity, which would allow a judicious use of time and resources, may be beneficial. This is in agreement with Sousa *et al.* (2013), who suggested that there is no obvious threshold at which  $t_u$  becomes critical or negligible, but rather that the timescales involved, cost of additional data acquisition, and importance of the receptor (from an abstraction or environmental point of view) should be considered. Consequently, decisions regarding the optimum level of soil data complexity can only be made on a case-by-case basis. The greater context of the profiles simulated herein is demonstrated in Fig. 3.7B, which identifies the likely position of these profiles relative not only to a surface water receptor, but also to other common soil types. The NSS profiles

(highlighted) are representative of those Irish soil types most likely to contribute to water contamination through the vertical dimension.

The small differences in  $t_r$  between the full and low pressure SWCC (<6 years) (Table 3.7) suggests that in many instances, it may not be necessary to measure the entire curve. The -15 bar pressure point is extremely time consuming and difficult to obtain using traditional methods such as pressure plates (Madsen *et al.*, 1986; Gee *et al.*, 2002; Cresswell *et al.*, 2008). The difficulty in measuring this point has contributed in part to the popularity of pedotransfer functions (Saxton *et al.*, 1986; Fredlund and Xing, 1994; Vereecken *et al.*, 2010), but as is shown here, this comes with a loss of site-specific accuracy. Measuring the SWCC excluding this point may present the optimum method of determining  $t_u$ . This will be further investigated in this thesis.

### 3.6 Conclusions

For determining the potential impact of activities in a sensitive catchment, policy makers need to consider the type of data required to model the movement of water through the soils. Where initial (trend analysis) or peak breakthrough of a contaminant is the primary concern, use of a daily, rather than an hourly temporal resolution, is sufficient to describe contaminant transport. However, when determining the latter portion of the solute breakthrough curve (centre of mass (bulk effect of measures) or the total exit of a contaminant from the profile), an hourly time-step is recommended. While higher quality soil physical data with respect to a specific soil profile, allow better estimation of soil hydraulic parameters, a reduction in data resolution, as demonstrated in this chapter, may be sufficient in some circumstances for the attainment of reasonably accurate simulations of water and solute movement using numerical models. For example, when the importance of the unsaturated zone within the context of total time lag (unsaturated and saturated) to a receptor is minor, a reduction in the complexity of the soil physical data analysis may be justified. Data complexity is more critical where the source is closer to the receptor. The estimates of vertical time lag (< 3 years) through the unsaturated zones of nine soil profiles in Ireland using Hydrus were similar to the results of previous studies using tracers in similar soil types and meteorological conditions. This indicates the suitability of this modelling approach to such scenarios. Differences in

vertical time lag estimated using the full soil water characteristic curve and those excluding the -15 bar values, which is difficult to measure in the laboratory, were typically small. Exclusion of this value may therefore be justified for this purpose in certain circumstances.

The methods described herein can facilitate future experimental design and elucidation of when (1) initial trends and (2) bulk effects of POM on water quality in vulnerable catchments occur.

### **Summary**

This chapter explored the implications of various data complexity levels on  $t_u$  assessment, and provides the theoretical framework (including the roles of low versus high complexity data and of landscape position) upon which the remainder of this thesis depends, and which forms the basis for the  $t_u$  toolkit described in Chapter 6. The low-complexity approach is further developed in Chapter 4, in which variation in  $t_u$  subject to the soil textural analysis methods used is examined. A practical approach to the problem of hydraulic equilibrium in the centrifuge method of SWCC assessment is presented in Chapter 5, thus exploring one uncertainty in the high-complexity approach. The low-complexity approach, which is optimum for ascertaining initial trends in water quality is applied to two agricultural study catchments in Chapter 6, the validity of which are examined in Chapter 7.

## Chapter 4

### **Low-complexity approach – Consequences of soil texture evaluation methodologies on hydraulic properties, unsaturated time lag and soil physical quality estimates**

#### **Overview**

In this chapter the influence of various methods of soil textural analysis on characterisation of the soil as regards to textural class, hydraulic parameters derived from these data, and  $t_u$  estimates using these parameters are examined. This should advise practitioners about the consequences of using low-complexity data in  $t_u$  estimation. In addition, the effects of textural analysis method selection on assessments of soil structural quality are also evaluated. The contents of this chapter have been published in the *Journal of Contaminant Hydrology* (Fenton *et al.*, 2015)<sup>3</sup>.

#### **4.1. Introduction**

As demonstrated in Chapter 3, the level of data complexity required by users of numerical models depends on site-specific characteristics, the stage of  $t_u$  in question (IBT/Trend, Peak, COM or Exit), and resource availability (i.e. human and monetary). Trend analysis of groundwater response to POM (as indicated by solute IBT/Trend and COM) can be adequately described using low-complexity data such as soil textural class derived from a knowledge of the site or using actual site-specific textural data and appropriate PTFs. Furthermore, as one migrates further away from the receptor towards upslope areas of a catchment in low  $t_r$  areas, a low-complexity approach may enable the most judicious use of resources (Sousa *et al.*, 2013). In the field, textural class can be rapidly determined using hand texturing techniques (minutes). In the laboratory, the sand-silt-clay percentages of a soil sample can be determined using different methods, requiring different durations e.g. pipette (weeks) (BS 1796; British Standard Institution, 1989), hydrometer (weeks) (BS 1377, Part 2 1990), or laser diffraction (days) (BS ISO 13320, 2009).

---

<sup>3</sup> The text of the published paper was written jointly by Sara Vero and Owen Fenton. Sara Vero conducted the parameter estimation, numerical modelling, and synthesis of results. This work was awarded the Soil Physics Lighting Oral and Poster Award at the SSSA Annual Meeting 2014.

A further application of soil hydraulic parameters is for ascertaining soil physical quality (S value) (Dexter *et al.*, 2004a-c) – that is; well developed structure, good workability, aeration etc. Horizons with low soil physical quality may prolong  $t_u$  and may have low organic matter and carbon contents. Hence, the S value of a soil may inform the practitioner regarding aspects of possible attenuation. Having determined hydraulic parameters using RETC, soil physical quality may be ascertained using the SAWCal model of Asgarzadeh *et al.* (2014). The S term is determined mathematically from the SWCC using the slope of the inflection point (at which the curve changes from convex to concave) (Dexter *et al.*, 2004 a, b, c.; Dexter *et al.*, 2007). A conceptual index of soil physical quality (SPQ) was introduced (Dexter *et al.*, 2004 a) (Table 4.1), and is used in equations for predicting various soil physical properties (Dexter and Czyż, 2007) e.g. hydraulic conductivity, friability, tillage, compaction, penetrometer resistance, plant-available water, root growth, and readily dispersible clay.

**Table 4.1:** Soil physical quality index (Dexter, 2004a, b, c).

<b>S value</b>	<b>SPQ Index</b>
< 0.020	Very Poor
0.020 – 0.035	Poor
0.035 – 0.050	Good
> 0.050	Very Good

The soil/subsoil layer is multi-functional (Schulte *et al.*, 2014; O’Sullivan *et al.*, 2015) providing food, controlling pollutant migration (Richards *et al.*, 2005; Meals *et al.*, 2010), purifying water (e.g. denitrification (Fenton *et al.*, 2009; Jahangir *et al.*, 2013b), sequestering carbon and as a habitat for biodiversity. Its complexity and importance cannot therefore be overstated, and the influence of methodological decisions on various applications (including, but not limited to,  $t_u$  and S assessment) should be of interest to the contaminant hydrology community (Young *et al.*, 2001; Lin, 2011). The primary objective of this soil profile study is therefore to assess how the textural class or sand-silt-clay determination method of a soil sample could dictate hydraulic parameter estimation using PTFs, and  $t_u$  estimates. A secondary objective is to illustrate the implications of selecting one soil texture methodology over another with respect to soil physical quality index designation.

## 4.2. Materials and Methods

### 4.2.1 Site description

The permanent grassland study site was located on a beef farm at the Teagasc, Johnstown Castle Environmental Research Centre, Co. Wexford, south-east Ireland (latitude 52° 12N, longitude 6° 30W). This site has a 30-year average annual rainfall of 1000 mm and a mean daily temperature of 9.6°C (Baily *et al.*, 2011). Typically, approximately 50% of this becomes effective rainfall (ER) (leached).

The soil profile examined was excavated along an open drain that was approximately 2.5 m deep. The soil profile was described by a soil scientist (Table 4.2) following Irish Soil Information System guidelines (Simo *et al.*, 2008; Jones *et al.*, 2011; Teagasc, 2015). Following this, a 1.4 × 1.4 m grid was created on the face of the soil test pit (Fig. 4.1) and divided into 49 equal sampling areas, each of 0.04 m<sup>2</sup> area. Soil samples were taken from each of these sampling areas.



**Fig. 4.1** Soil profile and sample grid location along a deep open drain at a permanent grassland site. C1=Profile A, F1=Profile B.

#### 4.2.2 Soil Textural Analysis

During profile description by the soil scientist, the textural class of a soil sample was determined in the field by hand assessing the constituents of the soil using the method described by Thien (1979). Soil horizons were first identified and described (Table 4.2). A hand sample of mineral soil (excluding stones, roots etc.), judged to be representative of that horizon, was then taken and put through a series of tests to determine soil texture, based on the plasticity, grittiness stickiness etc. of the soil. These were (in order of assessment): ability of moist plastic soil (water was added until soil is plastic) to remain in a ball when squeezed (if no = sand); ability to form a ribbon between thumb and forefinger (if no = loamy sand); and a combination of length of ribbon and feeling of smoothness or grittiness of excessively wet soil in palm when rubbed with forefinger to distinguish the other texture classes. Hand texturing can be somewhat subjective, but such decision keys are designed to limit that subjectivity and make assessment more rigorous. Where texture was heterogeneous within a horizon (e.g. sand lenses), both the dominant and subordinate texture were described.

For laboratory textural analysis, three random replicate samples of approximately 100 g were taken from each sampling area within the grid (Fig. 4.1). Samples were air dried and sieved to < 2 mm. All samples were then analysed for the sand-silt-clay percentages using the laser diffraction methodology with the average of the three replicates recorded. With regard to the hydrometer and pipette methodologies, the three replicates were bulked and a representative sample was taken for textural analysis. The samples for hydrometer analysis were analysed by an external laboratory (Brookside Laboratories, Inc. New Bremen, OH, USA) following BS1377, Part 2 1990 procedures. The pipette method was conducted in accordance with BS 1796 (British Standard Institution, 1989). For laser diffraction laboratory analysis (LDM, BS ISO 13320:2009), a Malvern Mastersizer Hydro 2000G with auto-sampler (Malvern, U.K) was used. The clay/silt particle size boundary (usually 2 µm) was altered to 8 µm, consistent with Konert and Vandenburghe (1997). This modification compensated for the tendency for laser diffraction methods to overestimate the size of clay particles due to their platy shape (and consequently underestimate the proportion of actual clay-sized material within a specific sample).

**Table 4.2:** Field soil profile description. The soil is classified as a Typic Cambisol using the World Reference Base system.

Horizon	Depth	Texture	Clay %	Consistence	Structure	Stones	Roots	Boundary
Ah	0-30	Loam	15	Friable (dry), sticky (wet)	Moderate granular fine to coarse, moderate strength	5%, 1-5 cm, angular/sub-angular greywacke, slate, vein quartz	Fine to very fine, abundant to plentiful	Distinct, level
Bw1	30-80	Clay Loam	30	Firm (dry), Sticky (wet)	Moderate prismatic fine, moderate strength	5%, 1-5 cm, angular/sub-angular greywacke, slate, vein quartz	Very fine, plentiful	Weak, Level
Bw2	80-120	Clay	40	Firm (dry), Sticky (wet)	Weak prismatic fine, moderate strength Compacted	10%, 1-5 cm, angular/sub-angular greywacke, slate, vein quartz	Very fine, plentiful	Weak, Level
Bw3	120-160	Clay	40	Firm (dry), Sticky (wet)	Weak massive Compacted	<1%, <1 cm, angular greywacke, slate, vein quartz	Very fine, very few	Not visible
*clay content based on hand texturing in the field								

### 4.2.3 Applications of soil hydraulic parameters

#### 4.2.3.1 Unsaturated Time Lag

Elucidation of  $t_u$  for the profile as a whole (hand textured method) or for two arbitrary vertical sections (Profile A and Profile B; Fig. 4.1) from the soil profile, were conducted using the Hydrus model, in accordance with Chapter 3, including boundary conditions and meteorological input data for both wet and dry years. The following characteristics were common to all model simulations:

- The  $\rho_b$  of each sampling cell was obtained in the laboratory after extracting metal rings of known volume ( $88.8 \text{ cm}^3$ ) in the field.  $\rho_b$  ranged from 1.2 to  $1.8 \text{ g cm}^3$ . In order to specifically examine the effects of texture,  $\rho_b$  was assumed to be the default value for mineral soils of  $1.20 \text{ g cm}^3$ . Frequently, practitioners using the Hydrus approach to estimate  $t_u$  may not have access to measured  $\rho_b$ , and so will rely on the default of  $1.20 \text{ g cm}^3$  commonly seen in the literature.
- Total depth of the profile was fixed at 140 cm, with solute dispersivity set at 10% of profile depth (Fetter, 2008; Simunek *et al.*, 2013).

Specifically, for the hand-texturing assessment simulation, a four-layered model was set up as in Fig. 4.2 with observational nodes at the end of each layer (0.35, 0.70, 1.05 and 1.4 m). For both the hand textured (Table 4.2) and laboratory textural analyses (Tables 4.3 and 4.4), the required soil hydraulic parameters (Table 4.3, 4.4 and 4.5) were determined for each layer using PTFs in RETC. Initial breakthrough (IBT/Trend) of a tracer to groundwater is very important for contaminant hydrology studies, as it indicates when monitoring networks start to pick up contaminant losses for the first time. As the early stages of  $t_u$  (IBT/Trend and COM) can be estimated using the low-complexity approach (Chapter 3), it is these markers which are presented herein.

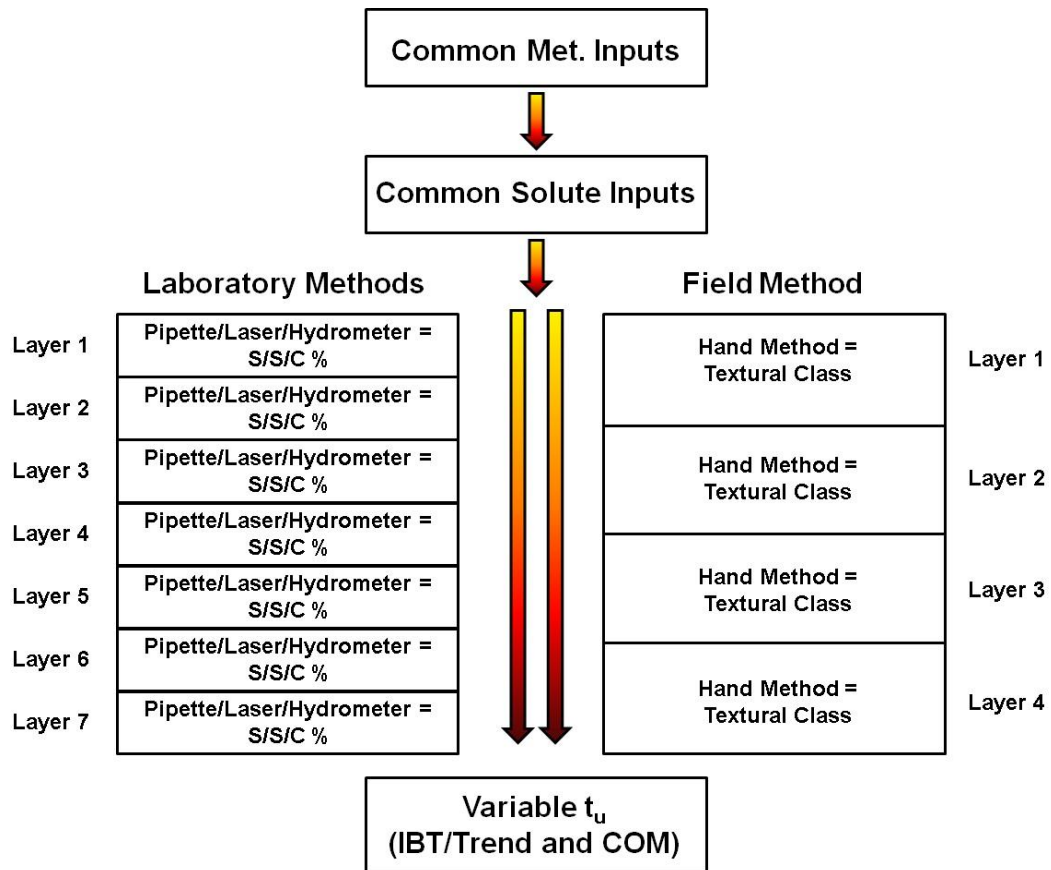


**Fig. 4.2:** Hydrus model setup for Pipette/Hydrometer/Laser (7 layered model) and Hand method (4 layered model). S/S/C% = Sand-Silt-Clay percentage. The four layered model represents the horizons identified by the soil scientist i.e. Ah, Bw1, Bw2, Bw3.

#### 4.2.3.2 Soil physical quality

The S value and associated SPQ rating (Dexter, 2004a, b, c) was determined for each layer in the hand textured profile and at each depth for profiles A and B. The soil hydraulic parameters, coupled with a default mineral soil  $\rho_b$  value of 1.2 mg  $\text{kg}^{-1}$ , were input into the SAWCal model of Asgarzadeh *et al.* (2014). This produced an S value for each soil layer (or depth), and soil physical quality outcomes were compared.

#### 4.2.3.3 Data Analysis

Correlations (Pearson Correlation Coefficients) between the soil textural results derived from hydrometer, pipette and laser diffraction methods were calculated using PROC CORR in SAS 9.3 (SAS Institute Inc., Cary, North Carolina, USA).

### 4.3. Results and Discussion

#### 4.3.1 Soil texture

Table 4.2 presents the soil profile pedological description and includes the hand textured analysis of different soil horizons used to obtain soil hydraulic parameters in RETC. Tables 4.3 and 4.4 present actual sand-silt-clay percentage data determined by pipette, hydrometer and laser diffraction methods. Tables 4.3, 4.4 and 4.5 also present the corresponding soil hydraulic parameters for these textural classes. At lower horizons/depths, there were variations in texture between the hand textural classes and those determined by laboratory measurement. All laboratory methodologies found a similar fining-down (reduction in particle size) trend between samples from 0-20 cm and 20-40 cm depths. At depths greater than 40 cm, the proportions of clay and silt gradually decrease and sand increases.

In general, the agreement between pipette and hydrometer methods with regard to soil texture was good (Tables 4.3 and 4.4). Laser diffraction reported the same trends in soil texture through each profile; however, the proportions showed a consistent, but marginal, difference in value in some cases. With regard to Profile A (Table 4.3), laser diffraction consistently determined a greater proportion of clay than the pipette and hydrometer methods, and in turn, smaller proportions of both sand and silt fractions. Similarly, laser diffraction in Profile B (Table 4.4) assigned a higher proportion of clay. However, this was compensated by the sand fraction; the silt fraction determined by the laser diffraction was comparable to the other laboratory techniques. Difficulties in relating laser and sieve and sediment particle size methods (i.e. hydrometer and pipette) are reported to originate from the clay-sized fraction (Konert and Vandenburghe, 1997). However, any overestimation of clay particles using the laser diffraction method due to the platy structure of fine particles would result in inflation of the silt content. The absence of this trend in the current study is reassuring for the application, and continued use, of the modified clay/silt boundary as applied here (Konert and Vandenburg, 1997). The higher proportion of clay/lower proportion of sand in the laser diffraction results of Profile B, compared to the other laboratory methods, may result from the combined physical and chemical dispersion, which is potentially more efficient at dispersing particles, particularly fine grains aggregated with coarser grains.

Textural class in the field is determined from soil profile description and hand texture assessment methods, from a number of hand samples which represent the dominant matrix of each horizon. In the lowest horizon in the study site, there were distinct sand lenses of quite coarse sand (1-3 cm deep, 5-15 cm long). These were described but were not included in the assessment of texture for that horizon, as they did not dominate. The soil samples for laboratory analysis were taken as representative samples from a regular grid, therefore the contribution of these sand lenses would have been incorporated into an overall “bulked” texture for that horizon. This may, at least partially, explain why the hand texture method tended to identify higher clay content for the lowest horizon. The coarser texture at the level is reflected in all three methods. This is important, as the hydrologic properties of this lowest horizon would likely be dependent on the architecture of these sand lenses. Such lenses could be highly permeable (Scenario 1) and if well connected laterally and vertically, they could be the main flow pathway for transmitting water and contaminants to lower horizons. However, if they are not well connected (Scenario 2), but were isolated lenses in what is a fine-textured matrix, then the overall permeability of this horizon might be quite low. If Scenario 1 were the case, grid sampling, coupled with laboratory analysis, may give a better assessment of transport times, as it incorporates the influence of the sand lenses (to some degree) and would therefore indicate a quicker transport time. If Scenario 2 were the case, the traditional profile and field-assessment approach may give a better assessment of transport times, as the permeability of the dominant fine-textured matrix would be controlling transport times and would therefore lead to slower breakthroughs.

#### *4.3.2 Soil Hydraulic Parameters*

For Profile A (Table 4.3) there was a significant correlation with regard to the  $\theta_s$  between the laser diffraction and the hydrometer ( $r= 0.763$ ,  $P<0.05$ ) and pipette ( $r= 0.947$ ,  $p<0.01$ ) methods, respectively. Although there was no significant correlation in the  $\theta_s$  between the pipette and hydrometer methods ( $r=0.605$ ,  $p=0.1501$ ), the differences in  $\theta_s$  rarely exceeded 4%. With regard to Profile B, there was a significant correlation in the  $\theta_s$  between the pipette and hydrometer methods ( $r=0.954$ ,  $p<0.001$ ). There was also significant correlations between the laser diffraction and the hydrometer ( $r=0.941$ ,  $P<0.01$ ) and pipette ( $r=0.898$ ,  $p<0.01$ ) methods, respectively.

**Table 4.3:** Profile A hydraulic parameters ( $\theta_r$ ,  $\theta_s$ ,  $\alpha$ ,  $n$  and  $k_s$ ) and S value determined from sand-silt-clay percentage and default  $\rho_b$  ( $1.2 \text{ g cm}^{-3}$ ) parameters using pipette, hydrometer or laser.

Pipette									
Depth (cm)	$\theta_r$	$\theta_s$	$\alpha$	$n$	S	$k_s$ cm day <sup>-1</sup>	Sand (%)	Silt (%)	Clay (%)
0-20	0.070	0.458	0.0091	1.54	0.08	32.73	41	37	22
20-40	0.091	0.498	0.0100	1.48	0.07	29.63	22	44	34
40-60	0.091	0.498	0.0100	1.48	0.07	29.63	22	44	34
60-80	0.086	0.487	0.0096	1.50	0.07	29.59	28	41	31
80-100	0.080	0.474	0.0086	1.54	0.07	30.41	32	41	27
100-120	0.092	0.500	0.0130	1.43	0.07	30.41	31	33	36
120-140	0.062	0.448	0.0100	1.53	0.07	43.18	47	35	18
Hydrometer									
Depth (cm)	$\theta_r$	$\theta_s$	$\alpha$	$n$	S	$k_s$ cm day <sup>-1</sup>	Sand (%)	Silt (%)	Clay (%)
0-20	0.066	0.453	0.0094	1.53	0.07	35.84	44	36	20
20-40	0.091	0.498	0.0100	1.48	0.07	29.63	22	44	34
40-60	0.091	0.497	0.0104	1.48	0.07	29.57	24	42	34
60-80	0.089	0.493	0.0109	1.47	0.07	29.39	29	38	33
80-100	0.085	0.487	0.0111	1.47	0.07	29.16	34	35	31
100-120	0.075	0.463	0.0074	1.58	0.07	32.88	32	44	24
120-140	0.068	0.465	0.0133	1.47	0.07	46.58	51	28	21
Laser Diffraction									
Depth (cm)	$\theta_r$	$\theta_s$	$\alpha$	$n$	S	$k_s$ cm day <sup>-1</sup>	Sand (%)	Silt (%)	Clay (%)
0-20	0.080	0.479	0.0115	1.48	0.08	29.12	40	32	28
20-40	0.097	0.514	0.0123	1.43	0.07	29.69	18	43	40
40-60	0.095	0.507	0.0123	1.43	0.07	30.20	23	39	38
60-80	0.092	0.500	0.0117	1.46	0.08	29.99	27	38	36
80-100	0.089	0.495	0.0119	1.45	0.07	29.59	31	35	34
100-120	0.092	0.500	0.012	1.44	0.07	29.68	28	36	35
120-140	0.074	0.468	0.0111	1.50	0.08	32.63	44	32	24

For the deepest soil horizon in Profile A, differences in  $\theta_s$  values between maximum (laser diffraction) and minimum (pipette) was only 2%. This small difference is likely due to slight textural differences (and in clay content in particular) i.e., 47% sand, 35% silt and 18% clay for pipette compared to 44% sand, 32% silt and 24% clay for laser diffraction (Table 4.2). Similarly, for Profile B, differences in  $\theta_s$  values between maximum (laser diffraction) and minimum (hydrometer) was 3%. This difference is once again likely due to textural differences as discussed in the previous section i.e. 46% sand, 36% silt and 19% clay for hydrometer compared to 35% sand, 38% silt and 27% clay for laser diffraction (see Table 4.4).

**Table 4.4:** Profile B hydraulic parameters ( $\theta_r$ ,  $\theta_s$ ,  $\alpha$ ,  $n$  and  $k_s$ ) and S value determined from sand-silt-clay percentage and default  $\rho_b$  ( $1.2 \text{ g cm}^{-3}$ ) parameters using pipette, hydrometer or laser.

Pipette									
Depth (cm)	$\theta_r$	$\theta_s$	$\alpha$	$n$	S	$k_s$ cm day <sup>-1</sup>	Sand (%)	Silt (%)	Clay (%)
0-20	0.078	0.471	0.0095	1.52	0.07	30.22	37	37	26
20-40	0.091	0.498	0.0100	1.48	0.07	29.63	22	44	34
40-60	0.095	0.508	0.0121	1.43	0.07	30.05	22	40	38
60-80	0.085	0.484	0.0096	1.51	0.07	29.56	30	40	30
80-100	0.084	0.485	0.0119	1.47	0.07	28.8	38	32	30
100-120	0.085	0.483	0.0098	1.50	0.07	29.44	31	39	30
120-140	0.070	0.462	0.0106	1.51	0.07	34.88	45	33	22
Hydrometer									
Depth (cm)	$\theta_r$	$\theta_s$	$\alpha$	$n$	S	$k_s$ cm day <sup>-1</sup>	Sand (%)	Silt (%)	Clay (%)
0-20	0.076	0.468	0.0094	1.53	0.08	30.69	38	37	25
20-40	0.090	0.495	0.0097	1.49	0.07	29.72	23	44	33
40-60	0.089	0.495	0.0099	1.49	0.07	29.65	24	43	33
60-80	0.082	0.480	0.0094	1.51	0.07	29.61	32	39	28
80-100	0.082	0.482	0.0113	1.48	0.07	28.84	38	33	29
100-120	0.080	0.474	0.0089	1.53	0.08	30.24	33	40	27
120-140	0.064	0.448	0.0095	1.55	0.08	39.96	46	36	19
Laser Diffraction									
Depth (cm)	$\theta_r$	$\theta_s$	$\alpha$	$n$	S	$k_s$ cm day <sup>-1</sup>	Sand (%)	Silt (%)	Clay (%)
0-20	0.091	0.499	0.0115	1.45	0.08	29.67	27	38	35
20-40	0.099	0.521	0.0131	1.40	0.07	29.03	15	43	42
40-60	0.099	0.519	0.0134	1.40	0.07	29.79	17	41	42
60-80	0.095	0.507	0.0123	1.43	0.07	30.20	23	39	38
80-100	0.089	0.495	0.0119	1.45	0.07	29.59	31	35	34
100-120	0.091	0.499	0.0115	1.45	0.08	29.67	27	38	35
120-140	0.080	0.474	0.0094	1.52	0.08	30.03	35	38	27

In relation to the variation between replicates for textural class analysis using laser diffraction, the relative standard deviation (% RSD) in profiles A and B was small, with the % RSD for clay being 5.47%, silt being 4.19% and sand being 12.58%.

**Table 4.5:** Soil hydraulic parameters and S value of the soil profile derived from texture as determined in the field using hand textured method.

Depth cm	Textural Class	$\theta_r$	$\theta_s$	$\alpha$	$n$	$k_s$ cm day <sup>-1</sup>	S/SPQ
0-35	Loam	0.078	0.430	0.036	1.56	24.96	0.07 (v.good)
35-70	Clay Loam	0.095	0.410	0.019	1.31	6.24	0.04 (good)
70-105	Clay	0.068	0.38	0.008	1.09	4.80	0.01 (very poor)
105-140	Clay	0.068	0.38	0.008	1.09	4.80	0.01 (very poor)

### 4.3.3 Time Lag Estimates

Fig. 4.3A shows the IBT/Trend of the solute at the base of the soil profiles, calculated according to the method of textural analysis. Differences in IBT/Trend determined using the three laboratory methods did not exceed 0.03 years for either sample year simulations. These results suggest that the choice of laboratory soil textural determination technique on the associated hydraulic parameters (Tables 4.3 and 4.4 and outlined in Section 4.3.2) has little impact on IBT/Trend. The difference in IBT/Trend arising from the soil textural methodology employed is significantly smaller than the difference that arises when comparing low and high complexity data sources, as discussed in Chapter 3, and so textural methodology may not be of significant importance within the context of other data selection criteria (Wösten *et al.*, 1995).

Differences in IBT/Trend between profiles A and B was 0.04 years for the 2004 simulation, and 0.02 years for the 2010 simulation (Fig. 4.3A). This indicates that differences in the estimate of soil time lag may arise as a result of soil textural heterogeneity even over a very small scale e.g. a 1.4 m wide pit face. This highlights the importance of collecting replicates, or multiple samples, to ensure a representative texture assessment when implementing a field study on the site-specific analysis of soil time lag. The significance of differences in  $t_u$  (arising either as a result of methodological approaches, or in this case, between soil profiles within an area) is most appropriately considered in light of their consequences (Wösten *et al.*, 1988; Wösten *et al.*, 1995) from a monitoring or policy perspective. The differences between profiles A and B are small in light of the six-year reporting periods defined by the EU-WFD; however, they demonstrate the heterogeneity of soil physical and hydraulic properties over a small scale. Such differences are homogenised and cannot be distinguished based on a hand-texturing approach.

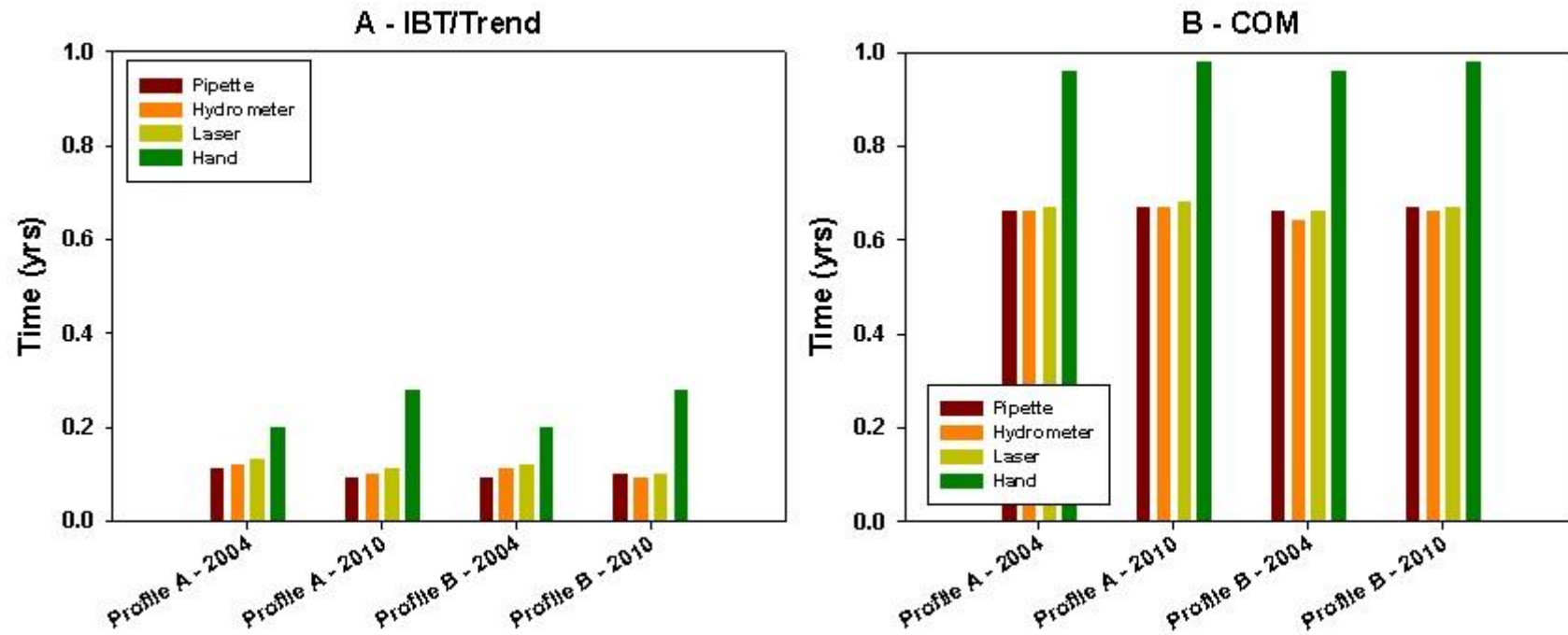


**Fig. 4.3:** (A) Initial Breakthrough at the base of the soil profiles, and (B) Centre of Mass at base of soil profiles, for 2004 and 2010, according to method of textural analysis.

Fig. 4.3A also shows IBT/Trend based on hydraulic parameters inferred from textural analysis using the hand technique. The difference in IBT/Trend between the laboratory and the hand technique was between 0.07 and 0.11 years (for the 2004 simulation). For the 2010 simulation, the hand technique resulted in an overestimation of IBT/Trend times of between 0.16 and 0.19 years. Due to the depth and texture of the soil profiles, time lag was too great to enable the solute to fully exit either profile within the duration of simulations, and so do not wholly reflect time lag in the longer term. However, as discussed in Chapter 3, such low complexity data are of limited value in determining these latter stages of the solute breakthrough curve, and thus differences in exit markers arising as a result of method selection are likely to be of theoretical interest alone, and of limited consequence in practice, as textural analysis is not recommended as a method of parameter estimation in such instances.

As indicated by Fig. 4.3, the difference between the three laboratory methods on both the IBT/Trend and COM stages of  $t_u$  were negligible, and in this instance were unlikely to affect either groundwater monitoring decisions, or to be of consequence from a policy perspective. The method of particle size analysis used is therefore discretionary, where the purpose of such data is to estimate  $t_u$ . Differences in  $t_u$  estimates between laboratory methods and the hand texturing method were far greater, and may lead to underestimation of the speed of solute breakthrough at groundwater. This may impair the efficacy of groundwater monitoring campaigns and tracer studies, which operate at a high temporal resolution. Although within the context of overall trend analysis and policy formulation (which in the EU-WFD operates over six-year periods), the difference in COM appears unlikely to be of major importance. It is critical to recognise that the profiles presented herein are shallow and represent sites with a perched watertable occurring within the soil profile. In other scenarios, the watertable may be much deeper, below the soil layer, within the bedrock. When  $t_u$  estimates are made over the full depth of the unsaturated zone or deep soil profiles, which may extend to several metres, errors resulting from the use of hydraulic parameters generated from hand texture data will be greater, and may lead to flawed predictions regarding the achievability of water policy targets. For this reason, laboratory analysis, regardless of method, should be preferred to simple field assessments. Although there is an element of subjectivity associated

with the hand texturing method, these errors in  $t_u$  estimation arise primarily as a result of the generic nature of PTFs with regards hydraulic parameter estimation. While the laboratory particle size analysis still relies on PTFs to generate hydraulic properties, Mohammed and Ali (2006) found that increasing the accuracy of input data to PTFs, such as by moving from textural class to particle size distribution data, improves the performance of such functions. In accordance with the importance of thorough characterisation of hydraulic parameters in high  $t_r$  areas, the differences arising as a result of hand texturing versus laboratory particle size analysis are likely to be of lesser consequence where the profile is distant from a receptor.

#### *4.3.4 Soil Physical Quality*

Inevitably, as the texture varied between the hand texturing and laboratory methods in the lower horizons of the soil profiles, so too did the soil physical quality i.e. 0.01 (very poor) in hand textured as opposed to 0.07 (very good) in laboratory methods. This is likely to have consequences where other parameters (e.g. chemical and biological values, permeability, recharge coefficients or natural attenuation capacity) are inferred from S values. There was no notable difference between results from the pipette, hydrometer and laser methods (with the same  $\rho_b$ ) in terms of soil physical quality, with the entire profile (A and B) placing as “very good or good” in the SPQ index. Therefore, for sites that are located at a distance from a receptor, the use of simple data (e.g. hand texturing) to assess  $t_u$  may result in inaccurate outcomes with respect to soil physical quality.

#### **4.4. Conclusions**

As examined in Chapter 3, in scenarios where the unsaturated zone does not exert the controlling influence on total time lag (i.e.  $t_u$  is short and the groundwater component of total time lag dominates), or where only IBT/Trend or COM estimates are required, PTFs derived from textural data can be used to ascertain hydraulic parameters for numerical modelling. A toolkit for assessment of  $t_u$ , with a particular focus on detecting trends in water quality beyond the unsaturated zone, is likely to rely on this low-complexity end of the soil input-data spectrum. However, there are several methods for determining the sand, silt and clay percentage of a soil sample. Textural class can be gained in the field through hand texturing or by using pipette, hydrometer and laser diffraction techniques in the laboratory. The difference

between the three laboratory methods on both the IBT/Trend and COM stages of  $t_u$  were negligible, and in this instance were unlikely to affect either groundwater monitoring decisions, or to be of consequence from a policy perspective. When  $t_u$  estimates are made over the full depth of the vadose zone, which may extend to several metres, larger errors will result from the use of hydraulic parameters generated from hand texture data, and may lead to flawed predictions regarding water policy targets. For this reason laboratory analysis, regardless of method, should be preferred to simple field assessments.

Due to the limited availability of high-complexity soil physical data within existing soil maps and the adequacy of low-complexity data for describing the critical IBT/Trend stage of  $t_u$  (Chapter 3), it is likely that data acquired from textural analyses will be relied upon for  $t_u$  assessment as part of a catchment-scale toolkit. Based on the results of this chapter, model users should be reassured that the method of textural analysis (which may vary from laboratory to laboratory, depending on preferred methodologies and facilities/equipment) does not affect IBT/Trend estimates, and so can be used with confidence.

### **Summary**

This chapter has established that three popular methods (pipette, hydrometer and laser diffraction) used for soil particle size analysis all perform equally as regards providing input data for PTFs used to estimate  $t_u$ . The hand texturing approach often employed in field assessment of soil pits, led to discrepancies in  $t_u$  estimates compared to the higher resolution laboratory methods. This chapter should give confidence to model users using the low-complexity approach to  $t_u$  estimation, provided that textural analysis is conducted using a laboratory-based assessment. This allows existing soil maps and datasets which include textural analysis to be relied upon – as is the case in the  $t_u$  toolkit described in Chapter 6. The following chapter (Chapter 5) will explore the subsequent level of data-complexity, which would be employed in areas which are of particular interest (e.g. high  $t_r$  areas – as discussed in Chapter 2).

## Chapter 5

### High-complexity approach - Consequences of truncated dewatering on soil water characteristic curves measured via centrifugation

#### Overview

This chapter presents a methodological framework (consisting of laboratory testing of various experimental durations coupled with statistical analysis) by which the optimum experimental duration to be applied in the centrifuge method may be identified. To date this has not been established in the literature.

#### 5.1. Introduction

Where  $t_r$  is high, or where estimates of the latter stages of  $t_u$  are required, a high-complexity, or direct approach to ascertaining the soil hydraulic parameters is required. In such instances, the SWCC should be assessed by the practitioner, rather than relying on a low-complexity PTF approach. Recent research on the SWCC has addressed knowledge gaps pertaining (but not limited) to hysteresis (Caron *et al.*, 2014), thermal effects (Campbell and Wacker, 2014), the number of applied pressure-steps (Cobos, 2014), modelling approaches (Diamantopoulos and Durner, 2014; Durner, 2014), and the influence of inherent soil properties such as  $\rho_d$ , organic matter content and texture on curve shape (Jensen *et al.*, 2014). Despite these developments, an acute knowledge gap remains pertaining to the identification of hydraulic equilibrium. This is the point at which no pressure gradient exists within the soil sample, and water held in the pores is at an equal potential to the applied pressure or suction. In each of the aforementioned ‘traditional’ methods,  $\Psi$  is applied until dewatering ceases, indicating that hydraulic equilibrium has been attained, at which point the  $\Psi$  is increased incrementally (Briggs and McLane, 1907). However, determining equilibrium presents a major practical challenge, as dewatering of a sample in response to applied  $\Psi$  is non-linear and may continue at low levels over a prolonged period (Cropper *et al.*, 2011; Dexter *et al.*, 2012). Nuth and Laloui (2008) and Malaya and Sreedeeep (2012) note that ‘characteristic’ implies that a unique and distinctive SWCC exists for a specific soil. This suggests that measurement effects may lead to the construction of curves that are neither reflective nor characteristic of the soil in question, with implications for practical applications based on such data

(Fredlund and Xing, 1994), for example, estimating  $t_u$  in high  $t_r$  areas, or when particular soils exhibit non-typical water retention behaviour (as a result of compaction, for example) and so cannot be characterised *via* PTF (Vanapalli *et al.*, 1999).

Traditionally, rules are imposed regarding the duration of the pressure step, which assumes that hydraulic equilibrium is attained after a predetermined duration. A wide range of experimental durations are proposed in the literature, many of which are appealingly brief (Table 5.1), but which typically correspond only to very small or disturbed soil samples, and hence, may not wholly reflect the hydraulic properties of *in situ* soils (Schjønning *et al.*, 1999; Costa *et al.*, 2008; Lin., 2011). Furthermore, a conflicting array of sample dimensions, formats and methods of preparation are documented (Table 5.1), making the identification of the appropriate duration extremely difficult. Even when these rules are well suited to the conditions described therein, the cores used in such experiments tend to be non-standardised and challenging to replicate, and a range of sample sizes, conditions and experimental durations are observed throughout the literature (Table 5.1). Šimůnek and Nimmo (2005) acknowledged that total hydraulic equilibrium was not certain, even subsequent to their designated experimental timeframe. Consequently, determination of the equilibrium state in many instances has relied upon arbitrary decisions (Vomocil, 1965), reflecting methodological limitations. While the importance of achieving equilibrium prior to adjustment of applied pressure is universally acknowledged in the literature (Russell and Richards, 1938; Nimmo, 1990; Khanzode *et al.*, 2002; Hunt and Skinner, 2005; Šimůnek and Nimmo, 2005), there remains no practical method of assessing its status in standard laboratory centrifuges without complex in-flight monitoring equipment (Reis *et al.*, 2011), which may be unavailable in many laboratories. Smagin *et al.* (1998) noted that while 80-90% of moisture held at a specific pressure step may be determined rapidly (within several hours), total equilibrium may require a number of days. Cropper *et al.* (2011) observed similar results.

The objective of the present study was to establish a methodological framework to identify the appropriate experimental duration (at each pressure step) for two soils within the bounds of an imposed experimental design. This framework facilitates reliable raw data collection for the construction of SWCCs.

**Table 5.1:** Summary of methodologies used in the literature to determine the SWCC.

Reference	Method	Sample Description			Pressure-step duration h
		Height Cm	Diameter	Format	
Russell and Richards, 1938	Centrifuge	0.5	3.5	Disturbed	< 4
Nimmo, 1990	Centrifuge	3.8	2.5	Intact	3 - 72
Smagin, 1998	Centrifuge	1 – 3	Unspecified	Disturbed	0.25 - 48
Vanipalli <i>et al.</i> , 1996	Pressure Plates	0.63	10	Disturbed	Unspecified
Khanzode <i>et al.</i> , 2002	Centrifuge	1.2	7.5	Disturbed	2 - 48
	Tempe Cell	Unspecified	Unspecified	Disturbed	336 - 2,688
Bittelli and Flury, 2009	Pressure Plates	3	5.35	Intact	48
		1	5.35	Disturbed	48
McCartney and Zornberg, 2010	Centrifuge	12.6	Unspecified	Compacted	Av. 10
Cropper <i>et al.</i> , 2011	Centrifuge	4.78	3.89	Disturbed	2 - 18
Reis <i>et al.</i> , 2011	Centrifuge	5	2	Intact	Unspecified
Smagin, 2012	Centrifuge	10	1	Intact	4 - 8
				Disturbed	

## 5.2. Materials and methods

### 5.2.1 Centrifuge Method Setup

The SWCC was measured in accordance with the centrifuge method as described by Nimmo *et al.* (1987), Reis *et al.* (2011) and Šimůnek and Nimmo (2005). The apparatus used was a Sigma 6-16KS refrigerated centrifuge (Fig. 5.1), with an 11150 model four bucket rotor and bespoke adaptors designed to fit within the centrifuge buckets (Fig. 5.2) (Ferns Engineering, 2013).



**Fig. 5.1:** Sigma 6-16KS centrifuge used in this study.

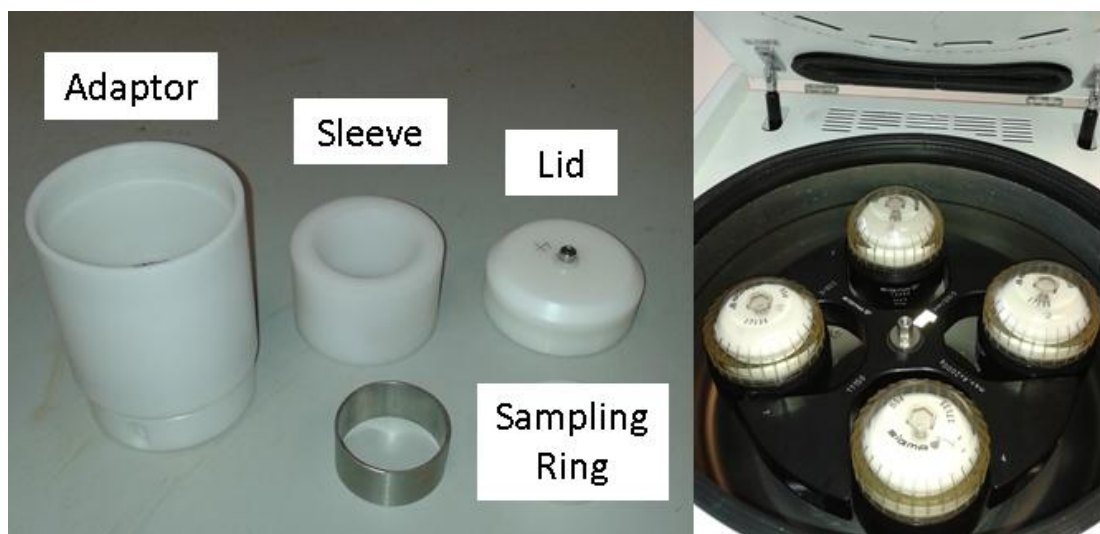


**Fig. 5.2:** Adaptor components and centrifuge loaded with prepared adaptor units.

The bespoke adaptors (Fig. 5.2) were designed to facilitate the use of  $5 \times 5$  cm (Peerlkamp and Boekel, 1960; Reatto *et al.*, 2008; Moncada *et al.*, 2015)  $\rho_b$  rings commonly used in the field (Creamer, 2014). An Acculab Atilon ATL2202 balance, with a precision of 0.01 g was used to weigh the soil cores at specified intervals. During the structured experiment, the following pressure steps were applied: -50, -100, -150, -200, -1,000 and -1,500 kPa (grassland site) and -33, -100, -150, -200, -1,000 and -1,500 kPa (arable site). The RPM applied to achieve the desired pressures were as follows: 670 (544 at -33 kPa), 948, 1161, 1341, 2998 and 3,672 RPM, respectively. Centrifuge speeds were determined according to the Gardner equation (Gardner, 1937) [Eq. 5.1]:

$$\psi = \frac{\rho\omega^2}{2}(r_2^2 - r_1^2) \quad [\text{Eq. 5.1}]$$

where  $\rho$  is the density of the pore fluid ( $\text{g cm}^{-3}$ ),  $\omega$  is angular velocity ( $\text{rad s}^{-1}$ ),  $r_1$  is radial distance to the midpoint of the soil sample (cm), and  $r_2$  is the radial distance to the free water surface (cm). After each specified time step, pressure was incrementally raised by adjusting the RPM of the centrifuge, as discussed in Chapter 2. Further details of the apparatus and methods employed are available in Hassler and Brunner (1945), Croney *et al.* (1952), ASTM D6836 (2008), and Dane and Topp (2002). At the end of each complete cycle, the cores were dried at  $105^\circ\text{C}$  for 48-hr. SWCCs were then constructed for each of the three treatments by plotting  $\theta$  against  $\Psi$  in kPa.

Soil physical characterisation (Table 5.2) was conducted at Teagasc, Environment Research Centre, Johnstown Castle, Co. Wexford, Ireland. Particle size analysis was performed using laser diffraction (Konert and Vandenberghe, 1997) and particle density was determined in accordance with ASTM D854-14 (2014).

**Table 5.2:** Summary of site and soil information.

	Site	Land Use	Texture	Sand %	Silt %	Clay %	$\rho_b$ g cm <sup>-3</sup>	$\rho_s$ g cm <sup>-3</sup>
Initial Testing	Local Soil	Permanent Grassland	Loam	40	36	24	1.41	2.31
Experimental Design	Grassland	Permanent Grassland	Clay Loam	33	31	36	0.86	2.41
	Arable	Malt Barley	Clay Loam	43	24	33	0.93	2.49

### 5.2.2 Initial testing

Intact soil cores (n=4) from a permanent grassland site were excavated from the top 10 cm of soil, within a 1 m<sup>2</sup> area, on a local research farm. Textural analysis is given in Table 5.2. Centrifugation was initially conducted at -20 kPa (424 RPM). During the centrifuge run, samples were weighed every 60 min up to 76-hr. Due to the excessively arduous nature of these data collection, it was impossible to maintain this measurement frequency for the complete SWCC. Centrifugation was also conducted at -100, -300 and -1000 kPa, during which the soil was weighed at less frequent intervals. As an example, the mean high-resolution dewatering curve at -20 kPa is presented in Fig. 5.3. Intervals similar to those observed in the literature (Nimmo, 1990; Smagin *et al.*, 1998; Vanipalli *et al.*, 1996; Bittelli and Flury, 2009): 24-, 48- and 72-hr, are indicated along the SWCC. The 48- and 72-hr measurements exhibited lower  $\theta$  (37.35% and 36.13%, respectively), compared to the 24-hr measurement (38.99%) equivalent. It was therefore decided that three commonly used treatments should be applied in which equilibrium at each  $\Psi$  would be assumed after centrifugation (i.e. 24-, 48- or 72-hr) and the resulting SWCCs should be statistically analysed to develop a framework for other practitioners.

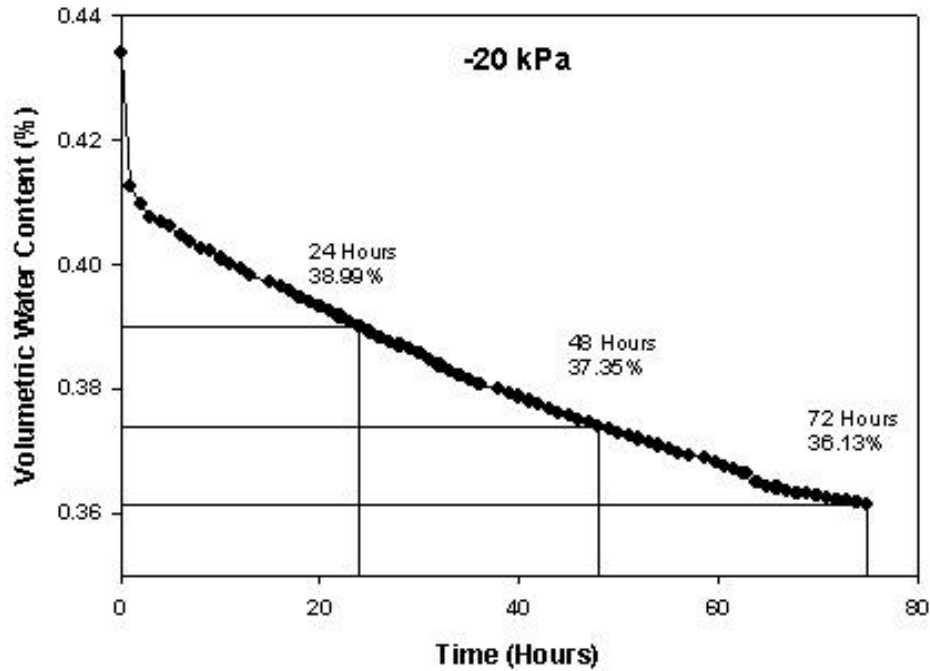


**Fig. 5.3:** Dewatering at -20 kPa, assessed on an hourly basis.

### 5.2.3 Experimental Design and Data Analysis

The experimental treatment was duration of centrifugation which was applied for 24-, 48- or 72-hr at seven pressure steps to the intact soil cores. A completely randomized experimental design with four replicates was used to investigate the treatment effect for two separate sets of soil cores. The first set of soil cores were taken from a well-drained, permanent grassland site and the second set from a well-drained arable site, in the south of Ireland. In both sites, the samples were taken from a 1 m<sup>2</sup> area. In terms of water quality, both catchments are classified as vulnerable to nutrient transport through the vadose zone. A summary of the soils used in the study are presented in Table 5.2. Unlike homogenised soil samples, the nature of intact soil cores is such that there will be variability in the  $\rho_b$  and the initial  $\theta_s$ . This is similar to Šimůnek and Nimmo (2005), who reported significant scatter of  $\theta$ , particularly close to saturation. In order to compare the effects of treatment without the confounding effect of differing initial saturation,  $\theta_s$  (0 kPa) was taken as 100%, and the subsequent water contents were expressed on a relative basis (Fig. 5.4) (Fredlund, 2002). The relative saturation approach enables direct comparison across the treatments, irrespective of initial water content. Henceforth, these adjusted water contents will be referred to as ‘effective saturation’.

The PROC MIXED procedure of SAS 9.3 (© 2002-2010, SAS Institute Inc., Cary, NC, USA) was used to conduct a repeated measures ANOVA to test the effect of treatment on effective saturation over incremental pressure steps for the two sites individually. The parameters included in the model for each site were time (24-, 48- and 72-hr) and pressure (seven steps) and their interaction terms. Pressure was the repeated measure. Using the Aikake Information Criterion to test the fit model the compound symmetry covariance matrix structure was chosen. Least square means (LSMeans) are presented and mean comparisons are by F-protected LSD test.

### 5.3. Results and Discussion

The soils from the grassland and arable sites were similar in textural class, but differed structurally owing to their different management and cropping history. While the  $\rho_b$  values of the grassland samples were low, a 0.80-1.00 cm<sup>-3</sup> range is frequently reported for the surface horizon of Irish grassland sites (Lalor, 2004; Kiely *et al.*, 2009, Herbin *et al.*, 2011; Vero *et al.*, 2013). The values herein reflect minimal trafficking at the site and its high vulnerability to nutrient transport through the vertical pathway (Fenton *et al.*, 2011).

**Table 5.3:** Estimated mean effective saturation (over all  $\Psi$ ), according to treatment, for the grassland and arable sites.

Grassland		Arable	
Treatment effect	Significance Level	Treatment effect	Significance Level
Pressure	***	Pressure	***
Treatment	***	Treatment	***
Pressure x Treatment	n.s	Pressure x Treatment	n.s
Treatment	Estimate	Treatment	Estimate
24-hr	64a <sup>†</sup>	24-hr	67a
48-hr	61b	48-hr	62b
72-hr	59c	72-hr	61b

<sup>†</sup> Letters in common for each site indicate no significant difference between treatments (P<0.05)

\*\*\* significant at P<0.0001

n.s non-significant

Table 5.3 lists the mean effective saturation across all pressure steps, according to treatment and site. There was a significant effect of pressure for both sites ( $P < 0.0001$ ), which is to be expected, as dewatering increases as pressure is raised incrementally. Critically, there was a significant effect of treatment ( $P < 0.0001$ ) for both the grassland and arable sites (Table 5.3). Neither site exhibited a pressure  $\times$  treatment interaction ( $P = 0.5539$  and  $P = 0.0872$ , for the grassland and arable sites, respectively). The 24-hr treatments exhibited significantly greater effective saturation compared with the 48- and 72-hr treatments, for both sites ( $P < 0.001$ ). This suggests that a 24-hr duration is likely to be insufficient to allow dewatering of intact samples. For the grassland site, the 48-hr and 72-hr treatments were also significantly different from one another ( $P = 0.0312$ ), indicating that effective equilibrium was not reached after 48-hr, and that a greater duration would be required to attain equilibrium for this soil. For the arable site there was no significant difference between the 48- and 72-hr treatments, indicating that 48-hr is adequate to characterise the effective saturation of samples from this site. As such, 48-hr can be recommended as the minimum centrifuge run time for soils from this specific arable site, below which dewatering was insufficient to approximate effective equilibrium. For the grassland site, the minimum threshold cannot be established from the treatments described herein. As the P-value is approaching the significance threshold, the methodological framework suggests that the optimum duration for this soil may be close to the 72-hr treatment already applied. These results demonstrate the difference between two sites, having similar textures but different structural properties. Bearing in mind the outcomes in the present study, during field work, additional replicates of soil samples should be taken to facilitate longer durations of centrifugation, if needed. The methodological framework identifies the optimum experimental duration for a particular soil sample and therefore allows for construction of a reliable SWCC. The construction of SWCCs within this methodological framework, gives a practitioner greater confidence with respect to the application of the associated soil hydraulic data.

Although not the case for the present soils, the duration required to attain effective equilibrium at specific  $\Psi$  may differ for other soils, which likely reflects the extent and tortuosity of corresponding pores, and further, will likely be influenced by the composition (texture and structural characteristics) and size of soil samples. This

was alluded to by Šimůnek and Nimmo (2005), who observed that  $\theta$  is less sensitive to pressure head at certain water contents than at others. Herein, the statistical analyses indicated that there was no significant interaction of  $\Psi$  and treatment for either site. Hence, a single duration may be applied across all  $\Psi$  (e.g. 48-hr, for the arable site), where it is not significantly different from a greater duration. The interaction on the arable soil was almost significant ( $P=0.0872$ ), indicating that this should be considered on a soil by soil basis. The important point here is that the present framework (Fig. 5.5), in which the effects of various experimental durations are statistically assessed prior to implementation of an analytical campaign, will identify where this is the case e.g. it is possible that for some soils, a more prolonged treatment would be required at high  $\Psi$ , in accordance with Šimůnek and Nimmo (2005).

It is acknowledged that the soils examined herein are very similar texturally. The occurrence of differences in required duration between two such similar soils demonstrates the need for such a methodological framework, which, although simple in design, has not been implemented in studies of soil physics to date. Should such a methodology be systematically applied, a database may be built up comprising soils of diverse textures,  $\rho_d$ , management and stress history, sample size and format (disturbed or undisturbed) from which a PTF may be determined, as has been done for hydraulic properties in the ROSETTA database. That resource could allow researchers to identify the required experimental duration for their soils without the need for preliminary testing. Unfortunately, such a large endeavour is beyond the scope of this PhD research, and so the framework described in this chapter is recommended.

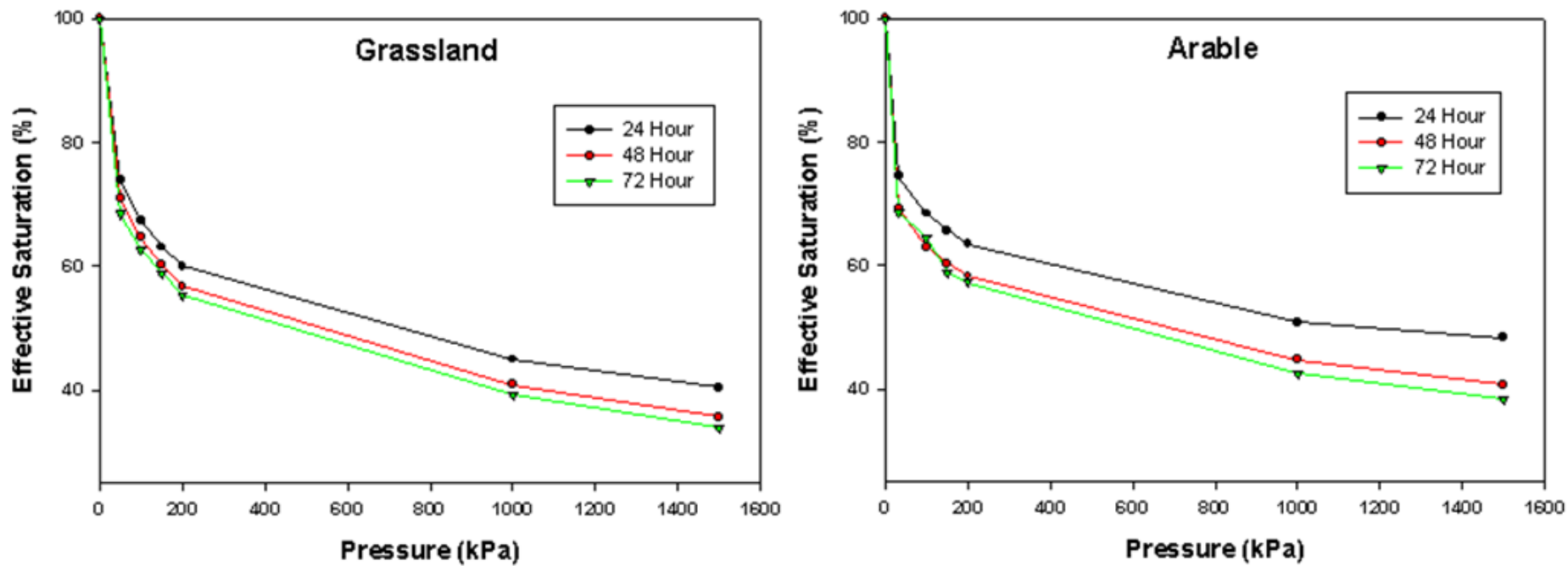
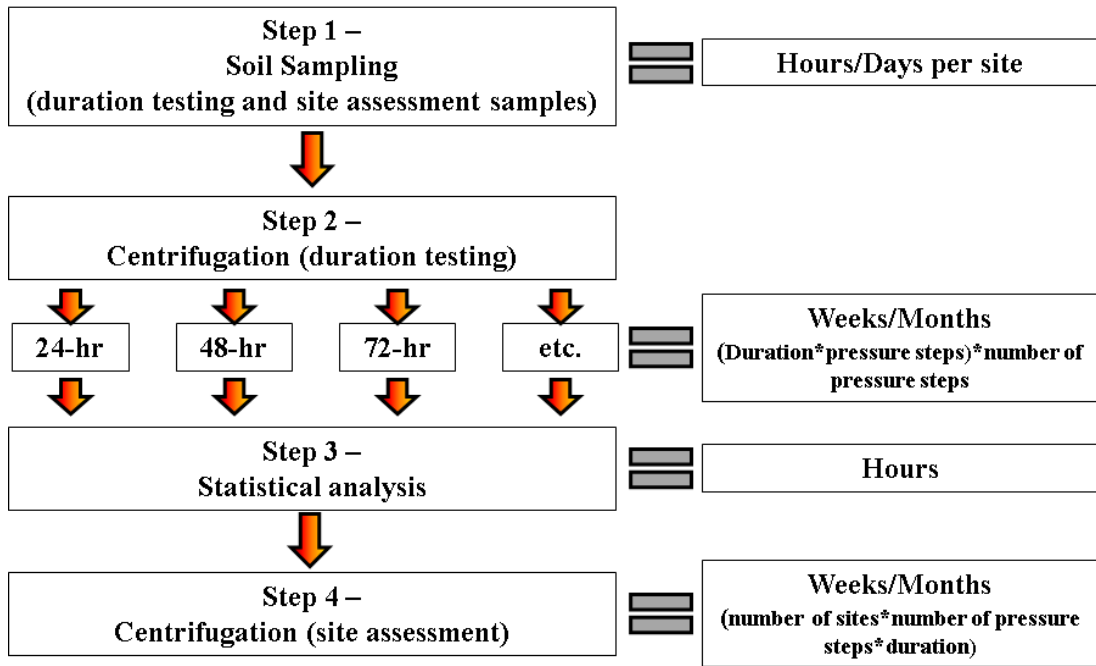


Fig. 5.4: Effective saturation relative to initial water contents for the grassland and arable sites, according to treatment.



**Fig. 5.5:** Methodological framework for experimental duration assessment, and associated timeframes.

These results suggest that where the SWCC is measured, a level of dewatering exists, approaching hydraulic equilibrium ( $E_t$ ) beyond which further centrifugation will not yield significant further information. In the case of the arable soil, this corresponds to 48-hr, while for the grassland soil, the only conclusion which can be drawn from the present results is that the required duration at each pressure-step is not less than 72-hr. Vogel (2014) alluded to the impracticalities of reaching true equilibrium, asking whether “we really need more accurate measurements for a curve that in principle is not really measurable?”, with the implication that such sufficient threshold levels of dewatering likely exist for specific applications. It is proposed that this threshold be termed, ‘effective equilibrium’ ( $E_e$ ), to distinguish from complete  $E_t$ .

## 5.4. Conclusions

High resolution dewatering measurements demonstrated the misleading effect of arbitrary temporal rules in the centrifuge method. However, for practical purposes it remains necessary to identify suitable experimental durations, which will be influenced by soil-specific characteristics. The methodological framework

presented was able to highlight differences in terms of equilibrium duration thresholds between the two soils tested. For the arable soil, a 48-hr time step was deemed most appropriate, whereas for the grassland soil there was no time step within the experimental design (24-, 48-, or 72-hr) that was deemed appropriate, indicating that  $E_e$  in this soil lies somewhere beyond 72-hr. Hence, further prolonged treatment duration (over 72-hr) for this soil may be required. Researchers should consider this need for multiple treatments and hence, endeavour to take many replicates during field work. This methodological framework (including laboratory testing of multiple experimental durations, and statistical review of resulting SWCCs) can be applied by other practitioners to determine optimum durations for the construction of SWCCs using their specific setup (sample sizes, soil types, degree of compaction etc.). In the future this methodological framework can be applied to a greater range of sample sizes, soil textures and structural classifications.

### **Summary**

The comparison of low versus high-complexity data sources (Chapter 3) identified the superior capacity of direct measurements of the SWCC (high-complexity approach) to describe  $t_u$ . However, as discussed in Chapter 2, many of the methods traditionally used for assessing the SWCC are prohibitively time consuming. The centrifuge method presents a more rapid alternative by which the SWCC may be assessed. Statistical assessment of the effects of SWCCs produced *via* this method, subject to various experimental durations as described in this chapter, is a viable approach by which researchers may identify the optimum experimental duration which should be employed in their monitoring campaigns. Monitoring agencies may use this high-complexity approach to closely examine specific critical areas of a catchment. Chapter 6 examines  $t_u$  ranges at a broader scale, using lower-complexity, soil map data. The consequence of the inability to attain  $E_e$  for the grassland soil using the treatments herein is considered in Appendix D.

## Chapter 6

### Indicating Trends in Response to Programmes of Measures in Two Agricultural Catchments – a toolkit approach

#### Overview

In this chapter a toolkit for assessing  $t_u$  ranges within agricultural catchments, with a particular focus on indicating water quality trends beyond the base of the soil layer, is developed. This toolkit incorporates readily available soil and meteorological datasets to provide model input values, in accordance with the low-complexity approach described in Chapters 3 and 4. Two agricultural catchments (grassland and arable), and their respective  $t_u$  ranges are presented as case studies. This toolkit should indicate to policymakers and monitoring agencies when trends in water quality response to POM may first be observed. Practical considerations (e.g. data sources, future developments, suitable catchments), regarding application of this toolkit to other catchments in the future are detailed.

#### 6.1 Introduction

As discussed in Chapter 2, the contamination of groundwaters by  $\text{NO}_3$  from diffuse agricultural sources presents a threat to their quality and status within the EU-WFD (EC, 2000). Numerous studies have identified the application of agricultural manures and fertilisers as a diffuse source of nitrate (Schröder *et al.*, 2004; Collins and McGonnigle, 2008; Fenton *et al.*, 2011), which may then leach through the unsaturated zone pathway (Richards *et al.*, 2005; Gibbons *et al.*, 2006; Mantovi *et al.*, 2006; Sousa *et al.*, 2013), and arrive as a contaminant to groundwater, from which it may be transmitted to surface water receptors or abstraction points such as wells (Molénat and Gascuel-Oudou, 2002; Puckett *et al.*, 2008; Stark and Richards, 2008). There is therefore a demand for implementable methodologies by which the  $t_u$  and  $t_s$  components can be quantified, in order to (1) guide the expectations of policymakers and stakeholders as to trends in water quality, and (2) aid monitoring agencies (such as the EPA) in the design of effective and economical monitoring campaigns (Dworak *et al.*, 2005; Wahlin and Grimvall, 2008).

To date, EU member states have implemented a profusion of different methodologies for ascertaining the effects of POM at different spatial scales; from continental to regional to catchment. As discussed in detail by Bouraoui and Grizzetti (2014), these approaches range from simple, parsimonious empirical models – often used at large scales (e.g. GREEN (Grizzetti *et al.*, 2008; Grizzetti *et al.*, 2012; Thieu *et al.*, 2012), or MITERRA (Velthof *et al.*, 2009)), to more complex, processed-based models (e.g. SWAT (Arnold *et al.*, 1998; Vagstad *et al.*, 2009; Laurent and Ruelland, 2011)). While each of these models (and others) have been successful at their respective scales, a comparative study conducted using seven models and 17 European catchments (Kronvang *et al.*, 2009) found that no individual model performed best in all instances. Nor is there consensus regarding the appropriate scale at which POM effects should be assessed, especially considering that implementation is at a field and farm-scale, but water quality assessments are often conducted at a river basin-scale. Models such as SWAT and the CMT (Mockler *et al.*, 2013; Packham *et al.*, 2013) are highly effective at identifying critical areas associated with specific areas within a catchment. Hence, Bouraoui and Grizzetti (2008) have proposed a tiered approach, in which those physically-based models are used to characterise and delineate areas within a catchment. Subsequently, models appropriate to those sub-catchment regions may be applied, to more thoroughly examine water and solute behaviour via specific hydrological pathways in those areas. In the Irish context, the Pathways CMT (Mockler *et al.*, 2013; Packham *et al.*, 2013) can identify areas within catchments in which the vertical and groundwater pathways are a nutrient vector. Hence, those areas can be targeted for detailed  $t_u$  assessment using the present toolkit.

Ascertaining the unsaturated component ( $t_u$ ) is critical as it (1) can provide the earliest indicator to policymakers as to the progress of POM, (2) dictates when groundwater monitoring should be initiated, and (3) can inform the interpretation of groundwater chemical quality data by disentangling the effects of current and past management practices. Timmerman *et al.* (2010) commented on the ‘data-rich but information-poor syndrome’ affecting water management; quantifying  $t_u$  can help extract the best information from the available data. As trend assessment of water quality must be based on ‘data gathered at individual surveillance and operational monitoring points’ (EC, 2009; Craig and Daly, 2010), generic estimates of  $t_u$  are

limited in their capacity to inform monitoring agencies (although they may still provide a guide at a less site-specific, policy scale). Hence, a methodology to approximate  $t_u$  for trend assessment must take into account the hydrological traits specific to those monitoring points. In order to develop these  $t_u$  estimates, the properties and processes within the unsaturated zone must be examined, at an appropriate scale and incorporate soil characteristics, depths and meteorological controls. Article 5 of the EU-WFD (EC, 2000) requires, amongst other things, characterisation of the physical characteristics of waterbodies, including those ‘overlying strata’ (i.e. the soil and unsaturated bedrock) that influence groundwater, and in turn, surface waters. The 2015 characterisation report (EPA, 2015) identified the physical characteristics of overburden (including soil and unsaturated rock) as exerting a control on water quality pressures, and hence, knowledge of these physical characteristics facilitates the monitoring of waterbodies, trend analysis and determining the efficacy of POM. That document further recognises a lack of ‘clarity on how to carry out the assessments of the risk of not meeting EU-WFD objectives.’ In other words, while the effects of soil properties on  $t_u$  are recognised as a potential impediment to applied POM, no toolkit is yet instrumented by which these limitations and associated timeframes may be assessed. Diffuse contaminant sources (such as those originating from the application of agricultural fertiliser and manures, and subject to  $t_u$ ) were noted as being particularly complex and furthermore, the pathway of the contaminant from its source to receptor is of particular importance. This knowledge gap pertaining to the unsaturated zone presents a major impediment to trend assessment, POM review and the design of future policies (Schröder *et al.*, 2004; Collins and McGonigle, 2008; Wahlin and Grimvall, 2008), and arose in part due a dearth of suitable unsaturated zone data at the time of initial policy design (EPA, 2015). Since that time, the launch of the SIS (September 2014) has provided a more detailed assessment of Irish soil physical (and hence, hydraulic) properties. Incorporating this new resource allows improvement to the more generic drainage class approach currently used to characterise Irish catchments.

Having resolved the requisite data-complexity issues pertaining to  $t_u$  estimation in earlier chapters, the objective of this chapter is to present a toolkit by which this knowledge gap may be addressed, using the low-complexity modelling approach described in Chapters 3 and 4, coupled with meteorological, soil and

bedrock data at appropriate scales. This approach is validated in Chapter 7 by the high-complexity approach and *in situ* hydrological tracer tests. For the first time,  $t_u$  ranges will be presented for two agricultural catchments (grassland and arable) in Ireland in response to the 2012 implementation of POM (Article 11 - EC, 2000) using this method. Furthermore, a 10-yr meteorological dataset was used to assess the likely long-term  $t_u$  ranges, and thus to comment on the achievability of later deadlines (e.g. 2021).

## 6.2 Materials and Methods

### 6.2.1 Toolkit Description and Data Sources

The toolkit for  $t_u$  assessment follows the structure described in Chapter 3, in which conservative solute movement is simulated in Hydrus using meteorological and soil data, and suitable boundary conditions. The sources of these data, and decisions made by the practitioner regarding which of a number of data choices are optimal, are of critical importance to the applicability and implementation of the toolkit. A schematic of the toolkit, including data-source options, is given in Fig. 6.1.

Regarding the meteorological input data (Fig. 6.1, Step 1), Met Éireann operates 25 synoptic recording stations across Ireland (see Fig. 2.5, Chapter 2), in addition to over 400 rainfall recording stations. Long-term records from these stations can provide meteorological data pertaining to specific periods of interest, e.g. 2012 to present, or may be used to identify years exhibiting specific meteorological patterns, e.g. drought or wet years, thus facilitating scenario testing. Alternatively, *in-situ* recording stations supply data (as is the case for the six catchments currently partaking in the ACP). As discussed in Chapter 3, the choice of daily or hourly data should be made based on the stage of  $t_u$  (IBT/Trend, Peak, COM, or Exit) in question, although for trend assessment (as indicated by IBT/Trend), daily data are sufficient. Atmospheric boundary conditions (typically allowing surface runoff) are applied within the Hydrus model, to correspond with these meteorological inputs.

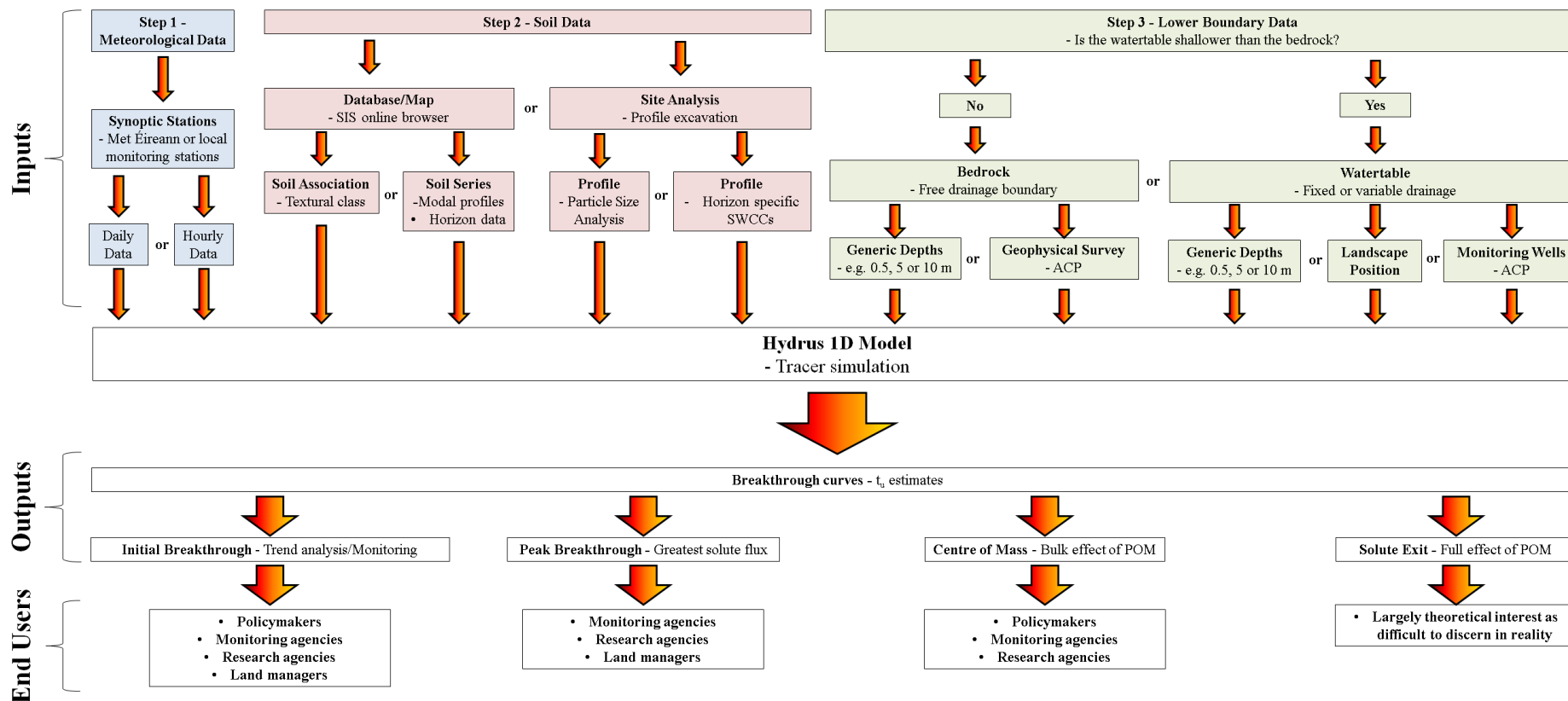


**Fig. 6.1:** Unsaturated zone time lag toolkit, including data-sources and outputs. Input data complexity within each step is increased by moving from left to right.

Regarding the soil input data (Fig. 6.1, Step 2), the practitioner has two primary options. The SIS provides a national soil map at a scale of 1:250,000 (Creamer, 2014), which is available in the form of an online database (<http://gis.teagasc.ie/soils/>). The practitioner may select a map area (the SIS divides Ireland into polygons covering areas of >250 ha) in this database, and will be presented with a number of soil associations which occur in this region (Fig. 6.2). Soil association indicates the broadly dominant soil texture of the area, based on the lead series textural composition (e.g. loam), but does not differentiate based on horizon, depth or location. Hence, a practitioner may produce an extremely low-complexity  $t_u$  estimate based on these data alone, corresponding to the lowest level of complexity, as discussed in Chapter 3, and providing only a very generic estimate of  $t_u$ . As the SIS database is hierarchical in nature, a number of soil subgroups and hence, series are also specified within association, which provides greater detail regarding soil properties (Fig. 6.2). Each soil series is associated with a modal soil profile, considered to be representative of the characteristics of that series. The number of soil series within a catchment varies depending on both its size and the pedogenic processes in that area. It is judicious therefore, that only those series representing a significant proportion of the catchment be simulated. At present (with the exception of those within the ACP), sufficient mapping resolution is not yet available to subdivide most Irish catchments in this manner. Where a catchment exhibits poor or declining water quality, it is therefore recommended that high-resolution soil mapping be conducted in order to provide these data. In addition, many catchments will exhibit at least some soil series, in which the vertical pathway is an unlikely vector for nutrient loss, e.g. soil types where runoff or lateral flow prevails. Estimating  $t_u$  for these profiles is likely to be misleading, and so they should be excluded.

The modal profiles provide horizon-specific characteristic data, including particle size distribution and bulk density information, from which soil hydraulic parameters can be derived *via* PTF (ROSETTA), and also other information pertaining to its structural and chemical properties. While these data should not be extrapolated to exactly describe the horizon-specific traits or depths of soil at locations other than those at which they were studied, they are indicative of the defining characteristics and hydrology of these series. Moving from the generic soil

Chapter 6 – Indicating Unsaturated Soil Time Lag in Agricultural Catchments – A Toolkit Approach

association approach (which indicates a single textural class for the whole depth of the profile) to the modal profile approach (indicating horizon-specific soil characteristics) allows the influence of both vertical and horizontal heterogeneity of soil properties to be considered (Mohanty and Zhu, 2007) (Fig. 6.3). This approach determines  $t_u$  for the soil series present within a catchment, and thus, can indicate to policymakers and monitoring agencies the ranges of  $t_u$  which may be observed in a given area, using an existing resource – the SIS database.

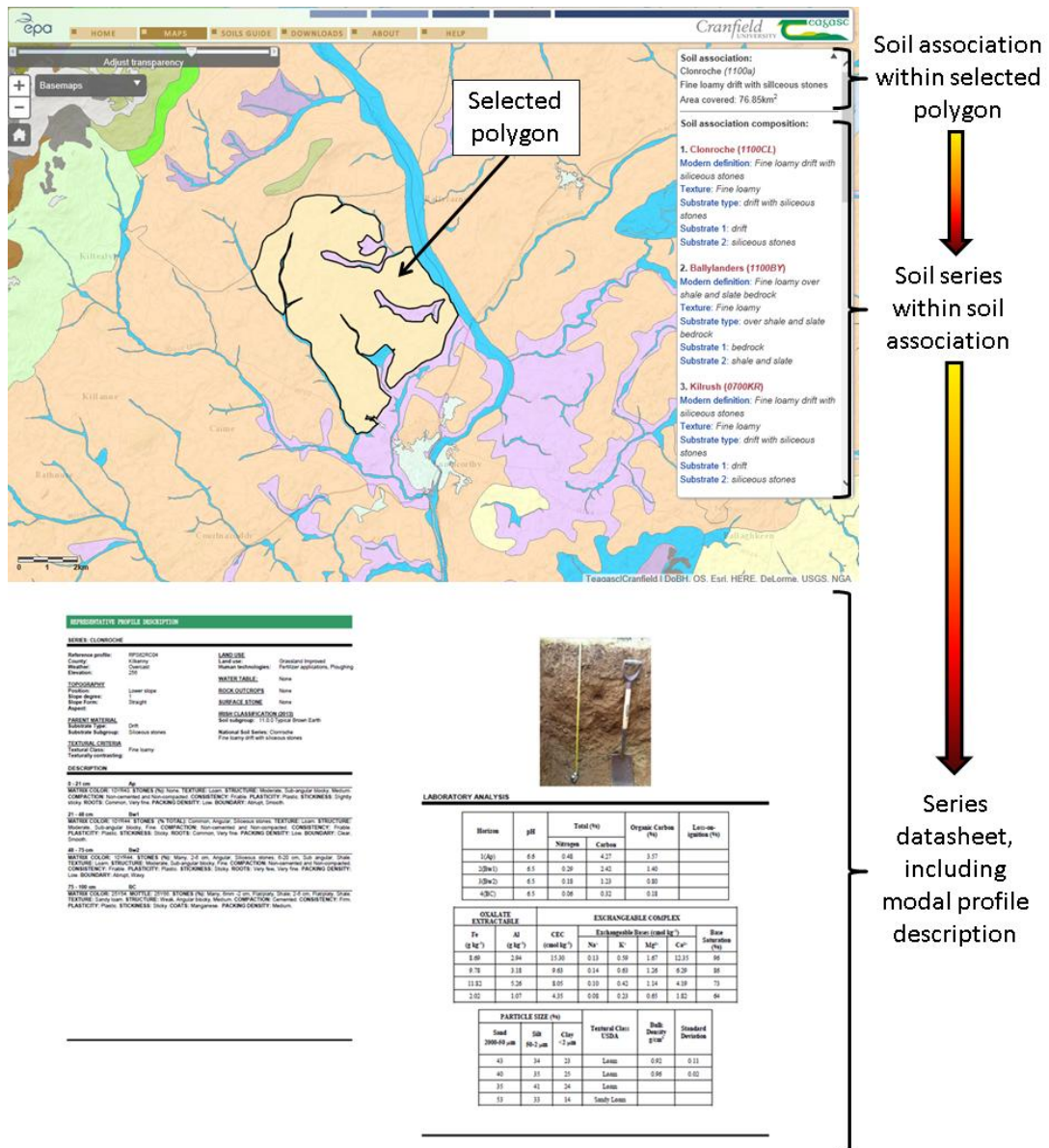


**Fig. 6.2:** SIS map interface, indicating a polygon and affiliated soil association, and soil series within that association. The lower image indicates a sample data-sheet for a modal profile associated with the Clonroche series – see Appendix E for a high resolution version of this data-sheet (SIS, 2015).

However, where specific areas within a catchment are of particular interest, exhibiting unique characteristics that preclude characterisation at the 1:250,000 scale, site-specific assessment may be desirable. In these instances, a soil profile should be excavated and described in accordance with SIS guidelines (Simo *et al.*, 2008). The profile description may be used to ascertain soil hydraulic parameters *via* PTF, or alternatively, soil cores may be taken from which the SWCC may be assessed and hydraulic properties directly calculated. The results of this approach are highly site-specific, and require additional time for laboratory analysis. This represents the maximum complexity level, as discussed in Chapter 3.

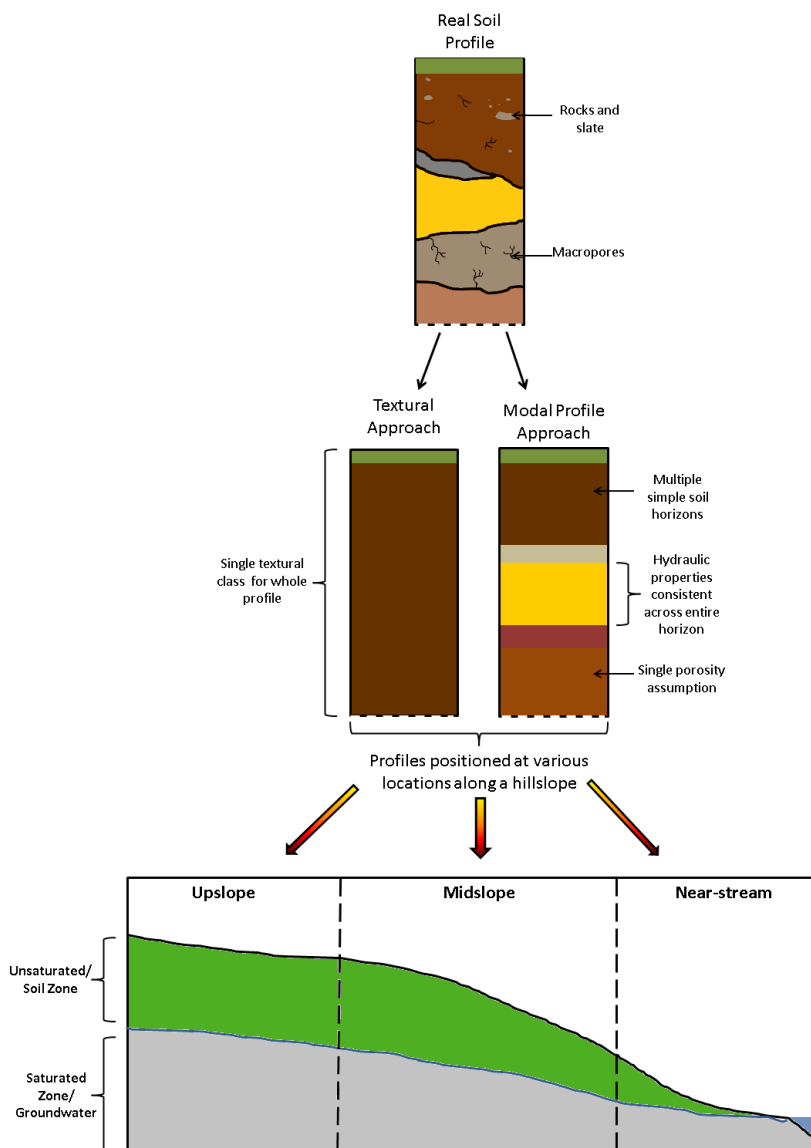


**Fig. 6.3:** Conceptual diagram of textural and modal profiles, as interpretations of a real soil profile. In the current study, simulations of  $t_u$  are ascertained for textural and modal profiles, subject to various hillslope positions.

Lower boundary data (Fig. 6.1, Step 3) is determined based on the depth of the watertable. The hydraulic properties of unsaturated bedrock cannot be quantified using the PTF and SWCC approaches used in regard to the soil parameters, and so only the soil component of the unsaturated zone may be accounted for using the toolkit approach. It is acknowledged that the full depth to groundwater may exceed these depths, particularly in upslope areas (Fig. 6.4), however, transport through the unsaturated bedrock to the watertable is often extremely rapid. Therefore its contribution to  $t_T$  may be relatively unimportant compared to that of the soil and saturated components. Where the watertable is deeper than the soil/bedrock interface (i.e. no part of the soil profile is saturated), a free drainage lower boundary condition should be imposed. This condition assumes that water and solute outflow at the base of the profile is unimpeded. As soil pits are not typically excavated to the bedrock depth due to safety concerns and practical challenges, the bottom-most surveyed soil horizon must be assumed to account for the remainder of this region. While this is an assumption, it is based on the increased vertical homogeneity observed in deep soil horizons (e.g. C horizons), which are less subject to the weathering, biological and management practices influencing shallower horizons, and more closely resemble the parent material (van Breemen and Buurman, 2002). So for example, a soil pit is excavated to a depth of 1.2 m, and the bedrock interface is assumed at a depth of 2.5 m. The profile built within Hydrus should equate to 2.5 m in depth, with the properties of the bottom-most horizon extrapolated across this unaccounted for region. Bedrock depths may be identified from geophysical survey (as in the ACP catchments), or generic depths may be used, e.g. 0.5, 5 or 10 m. From a policy perspective, it seems apt to use depths corresponding to the subsoil thickness vulnerability rating depths (3, 5 or 10 m) delineated by the Geological Survey of Ireland (GSI) (DELG/EPA/GSI, 1999).

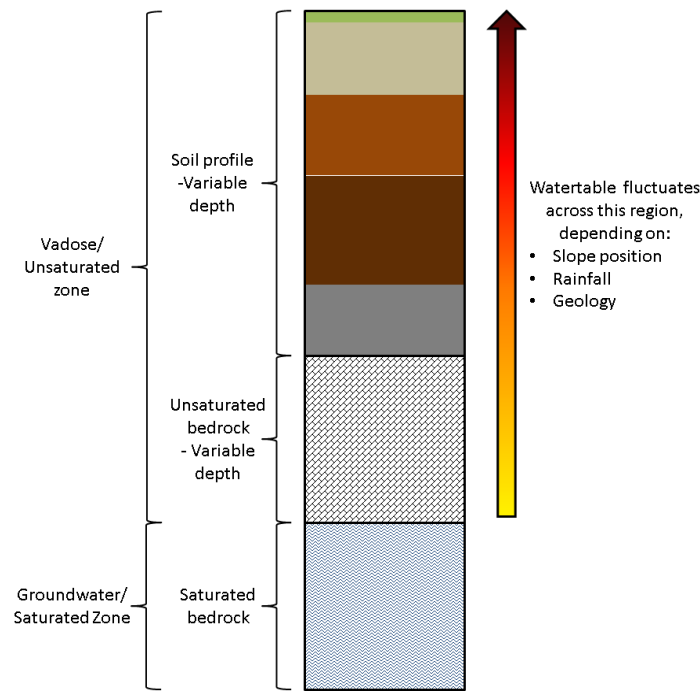


**Fig. 6.4:** Diagram of the unsaturated and saturated zones. The depths of both the soil and unsaturated bedrock vary spatially, and the position of the watertable may fluctuate, both spatially and temporally.

Where the watertable is shallower than the bedrock, a fixed pressure head may be imposed at the base of the simulated soil profile (a variable pressure head may alternately be applied, but this requires additional data pertaining to the fluctuations of watertable depth at a similar resolution to the meteorological input data, which are unknown to many practitioners). There are three approaches by which watertable depths may be derived. The simplest approach is to assume generic depths e.g. 0.5, 5 or 10 m (Fenton *et al.*, 2011). Alternatively, depths may be estimated based on landscape position, for example, in near-stream areas the watertable is likely encountered at less than 1 m below ground level. In such instances where the watertable is shallower than the modal profile, the profile should be truncated to correspond to that depth. Greatest detail pertaining to watertable depths is obtained *via* monitoring wells. In the ACP catchments, these are installed along transects, spanning from the top of the hill-slope to the near-stream area. These allow watertable depths at a range of slope positions and times to be ascertained; however, such data may not be readily available for catchments outside of this program, and so a landscape position approach may be more easily implemented.

### 6.2.2 Description of study sites

Two actively farmed catchments (designated Grassland A and Arable A by the ACP – referred to hereafter in this thesis as ‘grassland’ and ‘arable’) were selected as part of the ACP (Fig. 6.5), descriptions of which are given in Fealy (2010), Mellander *et al.* (2012), ACP (2013), and Mellander *et al.* (2014). Summaries of the sites are given in Table 6.1, and maps of the respective catchments are shown in Fig. 6.6 and 6.7. Although these sites are texturally similar, the land management, rainfall, and geology differ, allowing the toolkit to be reviewed in different scenarios, and also contributes to the thorough and on-going characterisation of these ACP study catchments.

These sites were selected due to their capacity for rapid unsaturated zone transport, allowing assessment of  $t_u$  within observable timescales (Mellander *et al.*, 2014). Nitrate was identified as the primary contaminant at these sites, with leaching through the soil to groundwater representing the main  $\text{NO}_3$  loss pathway in both watersheds (ACP, 2013). As both catchments are freely-draining, they exhibit risk to declining groundwater (and hence, surface water) quality as a result of  $\text{NO}_3$  transport through the vertical pathway. The already intensive stocking rate at the grassland site (1.9 livestock units/ha) is likely to increase in light of milk quota removal. However, improved nutrient use efficiency may offset further risk induced by this factor. The arable site exhibits limited capacity within the soil for denitrification, however, further investigation by the ACP is underway in order to ascertain future risk, as influenced by soil, landscape, management and climatic factors. Despite this, water quality at both sites was generally good. Groundwater 3-yr mean  $\text{NO}_3$  concentrations at the grassland site were below the drinking water MAC, but at times exceeded these thresholds for prolonged periods, probably as a result of mineralisation during reseeded (Mellander *et al.*, 2014). Mean (3 yr) groundwater  $\text{NO}_3$  concentrations at the arable site were below the drinking water MAC, although did exhibit spatio-temporal variability, resulting in occasional and temporary surpassing of this threshold (Mellander *et al.*, 2014). These instances coincided with fertilizer application, high rainfall and a high watertable in areas of thin soil, which were not observed in catchment areas having thicker soil layers. In both sites, despite these

temporary peaks, N concentrations are considered to be below EU-WFD thresholds (Mellander *et al.*, 2014).

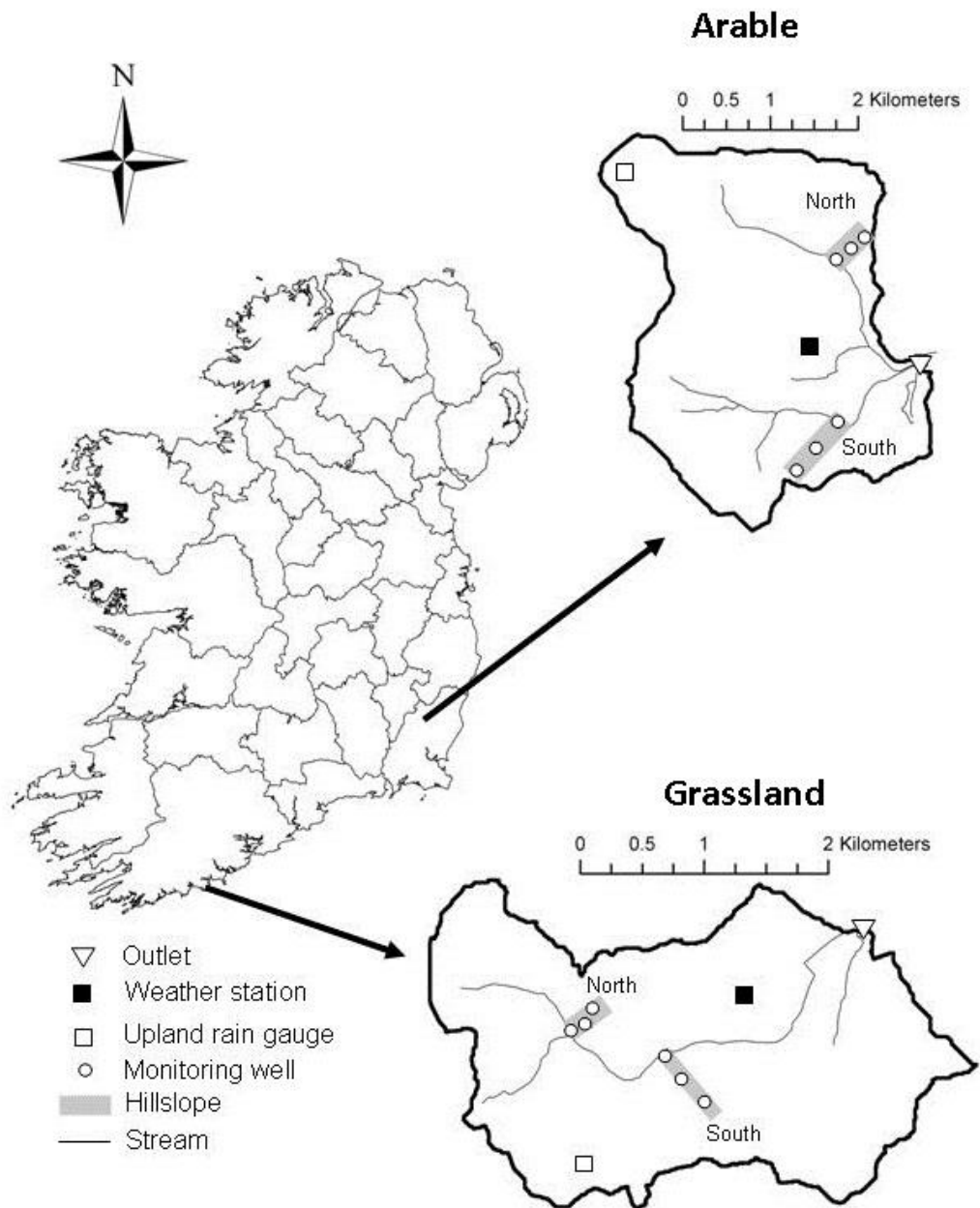


**Fig. 6.5:** Locations of the grassland and arable catchments (Mellander *et al.*, 2014).

**Table 6.1:** Summary of the grassland and arable catchments.

	<b>Grassland</b>	<b>Arable</b>
<b>Location</b>	Co. Cork, Southern Ireland	Co. Wexford, South East Ireland
<b>Area</b>	758 ha	1,117 ha
<b>Land Use</b>	Intensive Dairy Grazing, Perennial Ryegrass	Malt Barley
<b>30-Year Average Rainfall (1981-2010)</b>	1228 mm	1060 mm
<b>Permeability Characteristics</b>	Dominantly moderate permeability topsoil overlying highly permeable subsoil	Freely drained soil and fractured slate overlying poorly permeable bedrock
<b>Geology</b>	Devonian old red sandstone and mudstone, some gravel lenses	Ordovician slate and shale, decreased weathering with depth
<b>Unsat. Soil Depths</b>	0.5 – 10 m	1 – 5 m
<b>Aquifer Type</b>	Productive	Poorly Productive

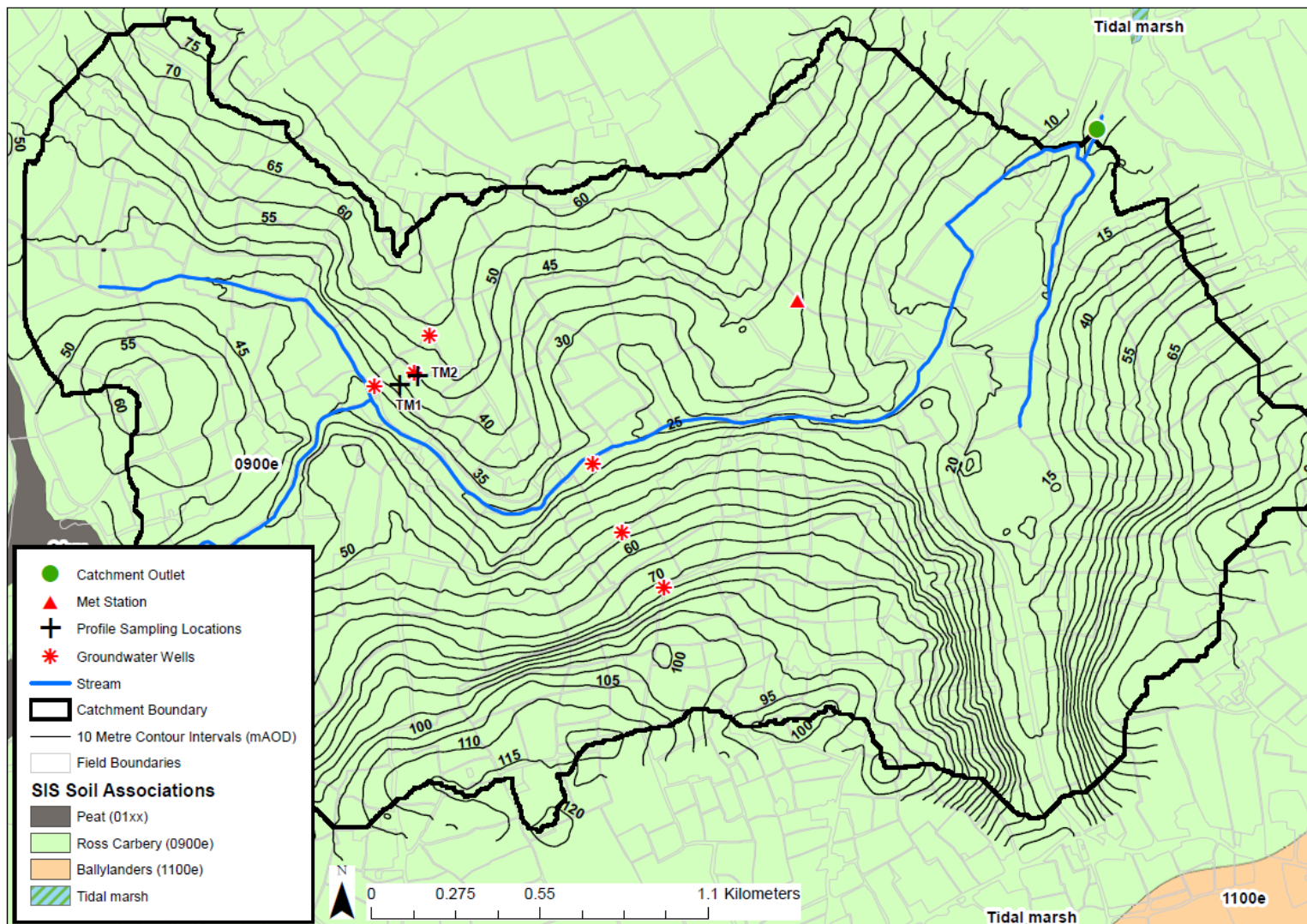


**Fig. 6.6:** Map of the grassland catchment, indicating soil association, synoptic station, monitoring wells, catchment outlet, profile sampling locations and elevation.

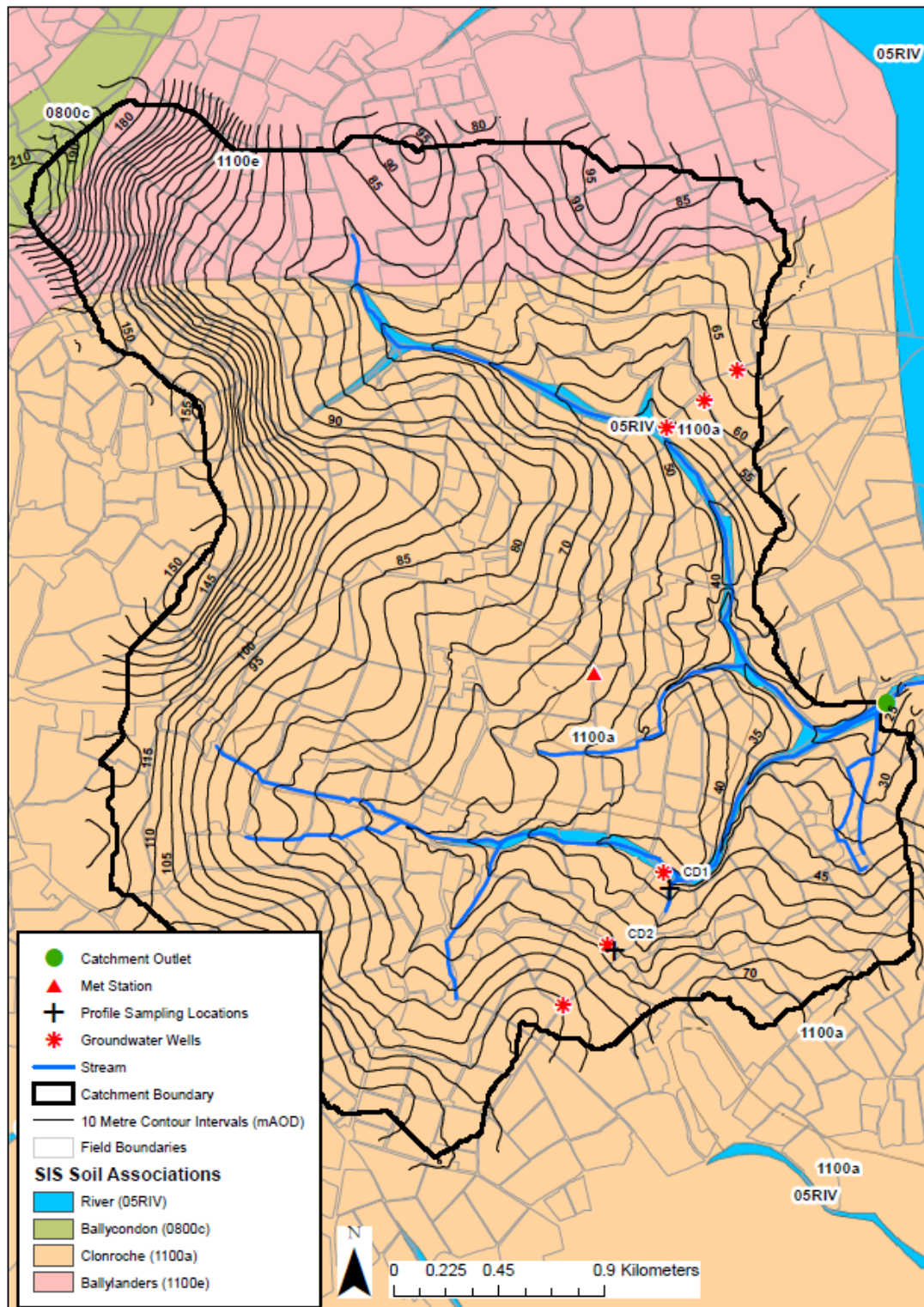


**Fig. 6.7:** Map of the arable catchment indicating soil association, synoptic station, monitoring wells, catchment outlet, profile sampling locations and elevation.

### 6.2.3 Data sources for the study sites

#### 6.2.3.1 Meteorological data

Two modelling exercises are conducted, using separate meteorological datasets. In order to estimate  $t_u$  at the study sites in response to POM applied in 2012, and so to comment on the 2015 reporting period, a 3-yr daily meteorological dataset (rainfall and evapotranspiration) (Fig. 6.8) was obtained from onsite synoptic recording stations run by the ACP. As this study was conducted in 2015, data for that year was incomplete and was therefore omitted. Therefore, the dataset spanned from 1<sup>st</sup> January 2012 to 10<sup>th</sup> December 2014.

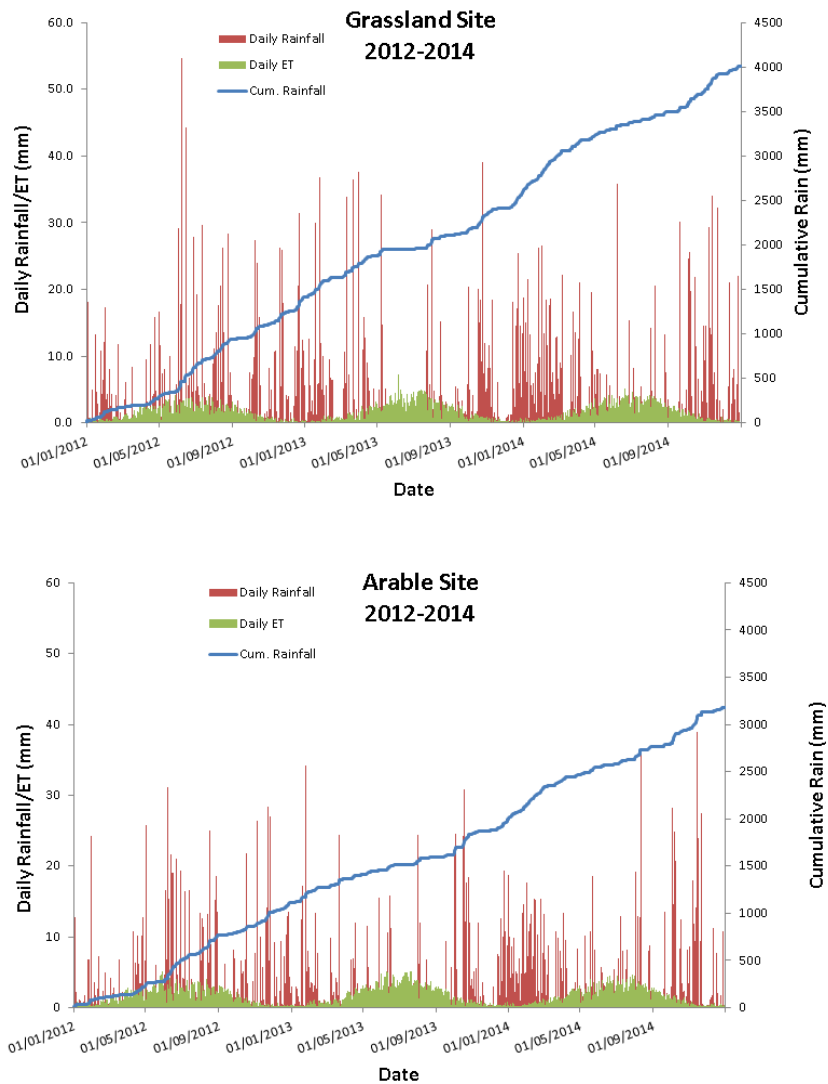


**Fig. 6.8:** Daily rainfall and potential evapotranspiration (PET) and cumulative rainfall for the grassland and arable sites, respectively, from 2012 to 2014 (ACP, Personal Communication).

Due to the relatively recent installation of those monitoring stations (2009), insufficient data were available to reliably determine 30-yr average meteorological conditions for either site. The Rosslare synoptic station was used to furnish a complete 30-yr meteorological dataset (1961-2008), from which minimum (263 mm), maximum (777 mm) and median (422 mm) yearly effective rainfall (ER) values were determined. Hence, a typical year (1991), having median rainfall (865 mm), evapotranspiration (443 mm), and hence, ER (422 mm), values, and exhibiting stereotypical rainfall distribution, was selected. Daily rainfall and potential evapotranspiration (PET), and cumulative rainfall are displayed in Fig. 6.9. This dataset was duplicated, to provide a decade of moderate conditions, and used as input data to assess long-term  $t_u$  patterns. It is acknowledged that such consistent meteorology is not observed in reality; the purpose of this exercise was to exclude the influence of single periods of high rainfall or drought. For example, a year of exceptionally high rainfall may have a large effect on  $t_u$  should it occur shortly after the application of a potential contaminant to the soil surface, or conversely, may be of relatively low importance should it occur a number of years later, coinciding with the latter part of solute movement.

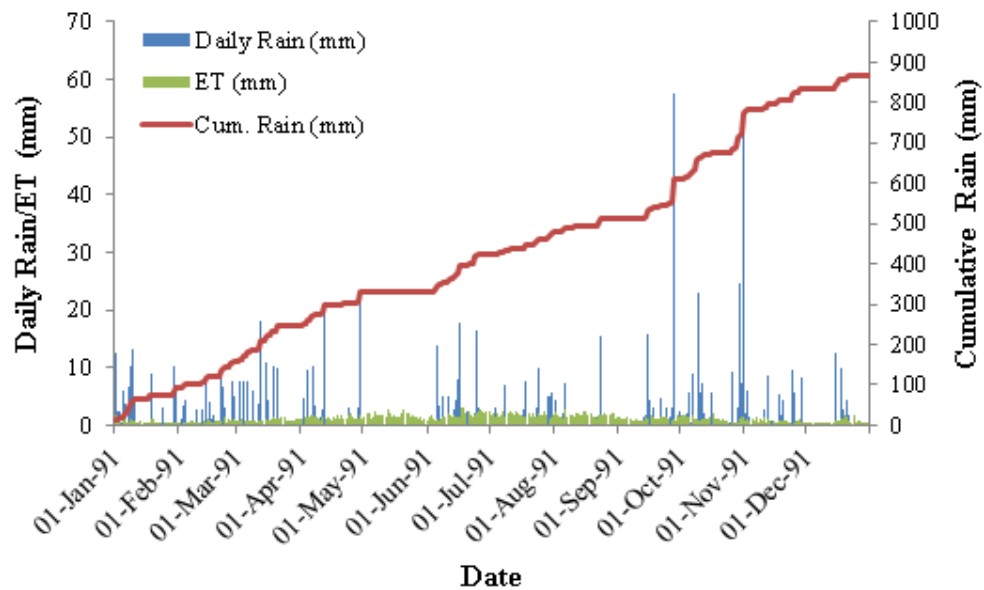


**Fig. 6.9:** Daily and cumulative rainfall, and daily evapotranspiration at the Rosslare synoptic station (ACP, Personal Communication).

### 6.2.3.2 Soil data

The SIS online database (<http://gis.teagasc.ie/soils/>) was used to obtain soil association, subgroup and series data for the catchments in question. As the shape of these catchments does not correspond exactly with the polygons defined in the SIS, the outline maps of the two study catchments were overlain on the SIS map using GIS and the affiliated associations and series were hence determined (Fig. 6.6 and 6.7). In total, 6 and 11 associations were indicated for the grassland and arable catchments, respectively. The soil series appearing within the soil associations for the respective catchments are shown in Fig. 6.10. While not yet available on the SIS webpage (Autumn 2015), topographic and geophysical maps of the catchments, developed as part of the larger ACP studies in these catchments, allowed the respective areas represented by each series to be estimated. Ground-truthing (in which areas of the catchment are sampled and assessed) of these assumptions is ongoing within the ACP, and particular areas of interest, identified from the maps, were examined *via* soil auguring in accordance with (Simo *et al.*, 2008) in June 2015 (Fig. 6.11). This was conducted in order to delineate the location and extent of soil associations in the landscape. Although such validation is not possible at a national scale, it was within the remit of the ACP for intensive characterisation and monitoring of these study catchments, and essential for validation of the assumptions in this chapter. Only the dominant associations and their affiliated soil series for each catchment were selected for the modelling exercise, as marginal soil types poorly represent overall catchment behaviour. Horizon-specific data (particle size distribution and  $\rho_d$ ) for each of the modal profiles were processed using RETC to derive soil hydraulic properties (datasheets included in Appendix E). For horizons in which  $\rho_d$  was not available, a default value of  $1.20 \text{ g cm}^3$  for Irish mineral soils observed in the literature (Kiely *et al.*, 2009), was applied.

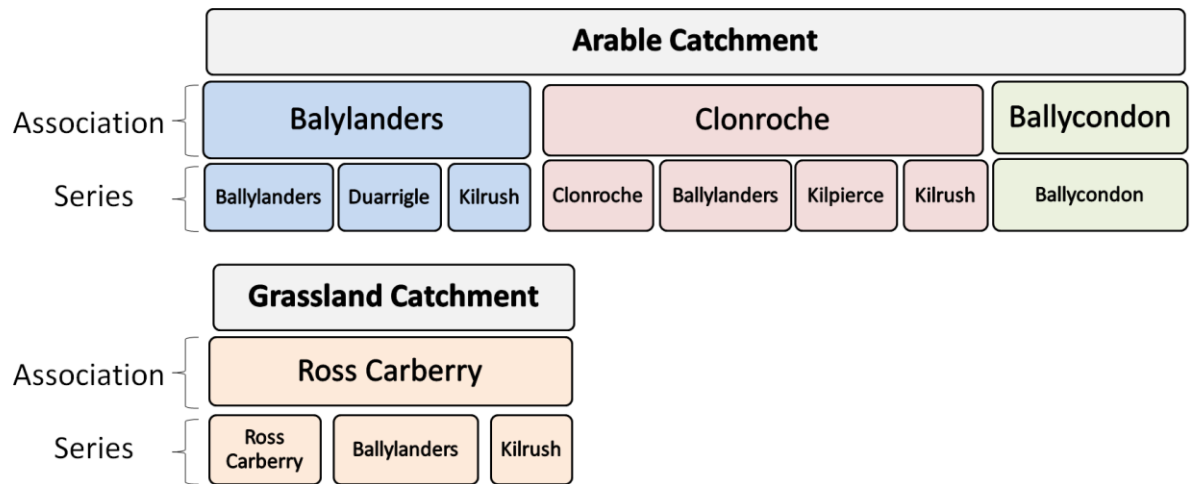


**Fig. 6.10:** Hierarchy, indicating soil association and affiliated soil series for the arable (top) and grassland (bottom) catchments.

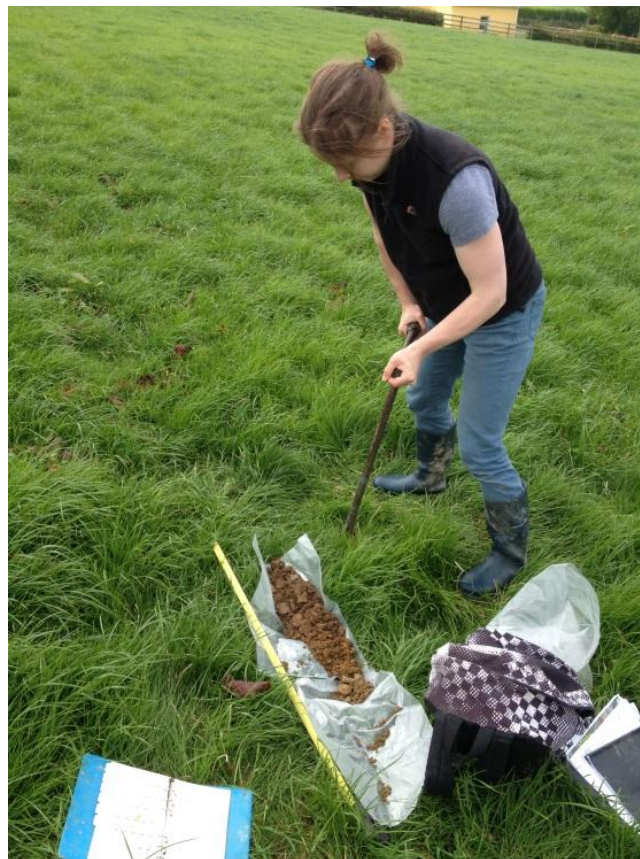


**Fig. 6.11:** Validation (ground-truthing) of soil series in the grassland catchment via soil sampling.

### 6.2.3.3 Boundary data

Geophysical surveys conducted in both catchments used ground penetrating radar (GPR) to determine the depths of soil to bedrock, and hence the maximum and minimum profile depths used in the model were determined (Mellander *et al.*, 2014). For the grassland site, four soil depths were simulated – 0.5, 3, 5 and 10 m, while three depths were simulated at the arable site – 1, 3 and 5 m. These depths were selected to correspond with subsoil thickness vulnerability rating depths (DELG/EPA/GSI, 1999). At the grassland site, the shallowest depths correspond to near-stream or low-slope positions, in which the watertable is present within the soil profile, while the deeper scenarios reflect the greater soil overburden commonly seen at mid- or upslope positions. At the arable site, the GPR survey revealed undulating bedrock along the hillslope. Consequently, slope position and distance from the receptor cannot be determined for this site, based on depth of the soil profile, and the intermediate and deep scenarios should be considered to occur at multiple slope positions.

Multilevel groundwater monitoring wells, each with three piezometers, were installed along Northern and Southern hillslope transects in each catchment as part of the ACP, in near-stream, midslope and upslope positions. Piezometer screen depths ranged between 2 to 30 and 1 to 52 m below ground-level, in the grassland and arable catchments, respectively. Monitoring of these wells at a monthly resolution (McAleer *et al.*, Personal Communication) between 2013 and 2014, indicated watertable depths, which in some instances (near-stream areas) was less than the bedrock depth. Constant pressure head, indicating a fixed watertable depth, was assumed at the base of the shallowest soil profiles, while free drainage was assumed for other slope positions, indicating the presence of unsaturated bedrock below the soil layers.

## 6.3 Results

### 6.3.1 Catchment mapping

The relative area within each catchment represented by each soil series is shown in Fig. 6.12. Both sites are dominated by the Ballylanders (and in the arable; Clonroche) series. The arable site exhibits a greater diversity of soil series, which is

in agreement with the observations of Mellander *et al.* (2014). For both catchments, the broad textural class of the soils therein is loam (thereby justifying the soil type examined in Chapter 5). The National Soil Map of Ireland (Creamer, 2014) indicates a greater variety of soil associations in western areas, and so it is reasonable to expect catchments in those regions to exhibit a correspondingly wide range of hydraulic properties and  $t_u$  than either of the catchments herein. The Driminidy series within the grassland catchment is one of a limited number of soil series for which no modal profile is available. Consequently, the Newport modal profile has been substituted, due to their similarity.

### 6.3.2 Soil Hydraulic Parameters - Modal Profile Approach

Hydraulic parameters derived *via* the modal profile approach are shown in Tables 6.2 and 6.3. Consistent with the range of soil series present in the arable catchment, a wider variety of hydraulic characteristics are observed than in the grassland catchment, with ramifications for  $t_u$  ranges. The dominant series in each catchment were Brown Earths (typically well drained/permeable with good structure (Simo *et al.*, 2008; Ibrahim *et al.*, 2013b)); whilst in the arable catchment the minor series exhibited a greater diversity of hydraulic properties. The implication of this is that certain areas within a catchment may exhibit unique hydrological behaviour and hence vulnerability, consistent with the phosphorus critical source area (CSA) concept, in which source areas subject to high nutrient loads are hydrologically connected to water receptors (Gburek and Sharpley, 1998; Pionke *et al.*, 2000; Thomas *et al.*, 2015). Phosphorus CSAs identify areas in which the overland-flow pathway predominates. This implicitly indicates other areas within a catchment, in which the vertical pathway is important, and hence, may be subject to  $t_u$ . A possible future development to this concept would be nitrate CSAs, which could be used to target high-complexity investigations within a catchment exhibiting poor status as a result of N concentration within surface- or groundwater. As discussed in Section 6.1, this tiered approach has been recommended for examining POM under EU-WFD by Bouraoui and Grizzetti (2008).

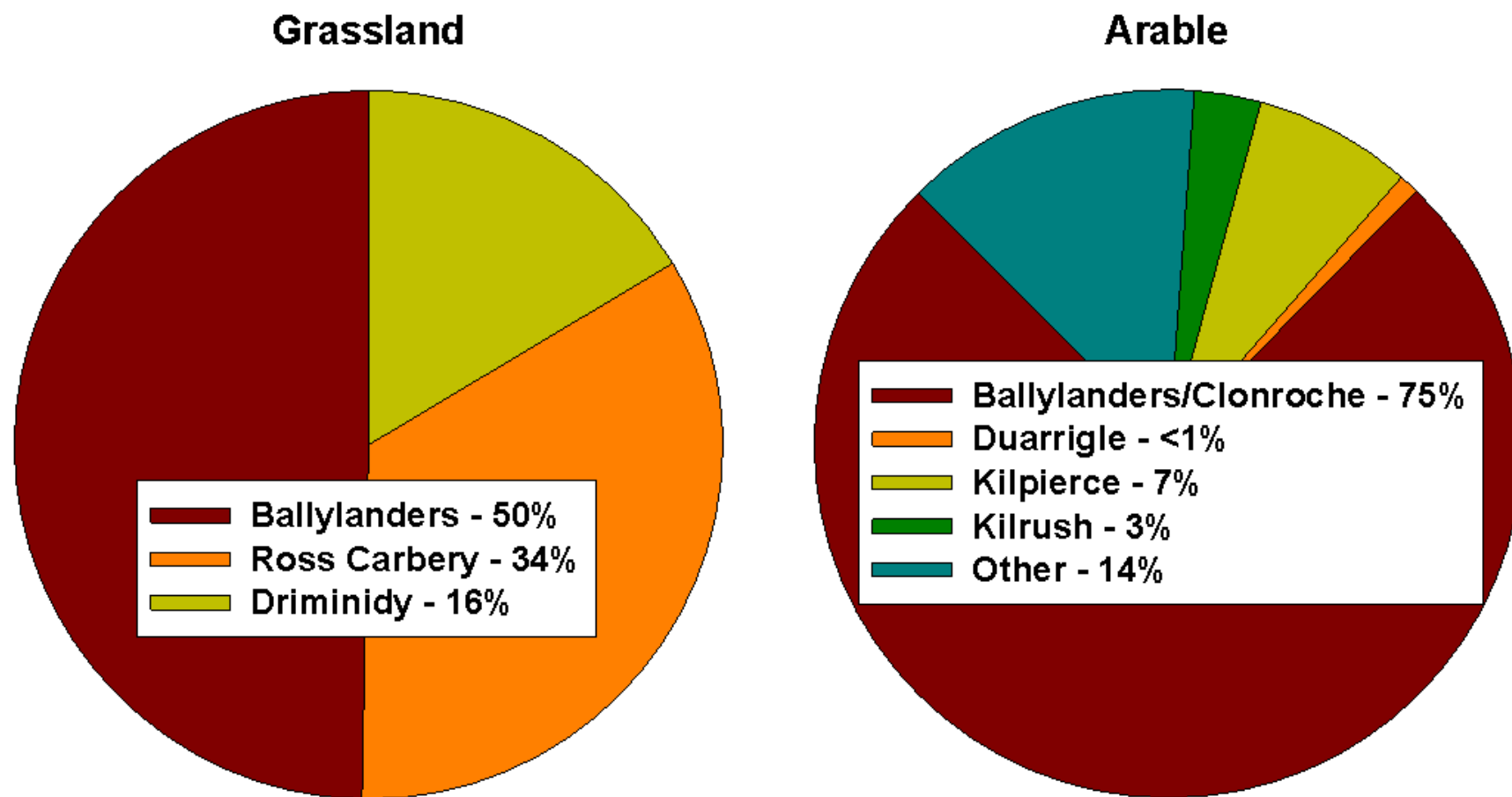


**Fig. 6.12:** Relative area represented by each soil series within the grassland and arable catchments.

**Table 6.2:** Horizon-specific hydraulic parameters for soil series at the grassland site derived via the low-complexity modal profile approach, using PTFs. \* indicates default mineral  $\rho_d$  value of  $1.20 \text{ g cm}^{-3}$ .

Site	Association & Number	Series	Horizon	Horizon Depth (cm)	$\rho_d$ ( $\text{g cm}^{-3}$ )	$\theta_r$	$\theta_s$	$\alpha$	n	$k_s$ ( $\text{cm hr}^{-1}$ )
Grassland	Ross Carbery (0900e)	Ballylanders (Fine Loamy)	Ap	0-25	0.89	0.086	0.566	0.0108	1.478	5.77
			Bw1	25-45	0.80	0.080	0.580	0.0092	1.504	9.10
			Bw2	45-75	1.20*	0.056	0.395	0.0149	1.439	0.62
			Cr	75-85	1.20*	0.039	0.389	0.0232	1.413	1.60
		Ross Carbery (Fine Loamy)	Ap	0-35	1.19	0.063	0.4775	0.0214	1.435	3.78
			AB	35-70	0.97	0.060	0.5265	0.0181	1.416	7.58
			Bs buried	70-100	1.20*	0.044	0.3896	0.0175	1.433	1.17
			2C buried	100-150	1.20*	0.034	0.3961	0.0208	1.429	1.98
		Driminidy/Newport (Coarse Loamy)	Ap	0-10	0.87	0.059	0.5693	0.0263	1.372	10.78
			Apg	10-30	1.35	0.050	0.4310	0.0315	1.538	4.23
			Bg	30-65	1.70	0.043	0.3369	0.0373	1.321	0.64
			BCg	65-120	1.77	0.041	0.3180	0.0431	1.314	0.59
			2Ctg	120-140	1.20*	0.076	0.4276	0.0108	1.453	0.35

**Table 6.3:** Horizon-specific hydraulic parameters for soil series at the arable site derived via the low-complexity modal profile approach, using PTFs. \* indicates default mineral  $\rho_d$  value of  $1.20 \text{ g cm}^{-3}$ .

Site	Association & Number	Series	Horizon	Horizon Depth (cm)	$\rho_d$ ( $\text{g cm}^{-3}$ )	$\theta_r$	$\theta_s$	$\alpha$	n	$k_s$ ( $\text{cm hr}^{-1}$ )
Arable	Ballylanders (1100e) & Clonroche (1100a)	Ballylanders (Fine Loamy)	Ap	0-25	0.89	0.086	0.566	0.0108	1.478	5.77
			Bw1	25-45	0.80	0.080	0.580	0.0092	1.504	9.10
			Bw2	45-75	1.20*	0.056	0.395	0.0149	1.439	0.62
			Cr	75-85	1.20*	0.039	0.389	0.0232	1.413	1.60
		Clonroche (Fine Loamy)	Ap	0-21	0.92	0.079	0.546	0.0100	1.497	5.14
			Bw1	21-48	0.96	0.082	0.539	0.0099	1.499	4.29
			Bw2	48-75	1.20*	0.070	0.419	0.0091	1.496	0.46
			BC	75-100	1.20*	0.050	0.390	0.0174	1.427	0.90
		Duarrigle (Fine Loamy)	Ap	0-28	1.11	0.092	0.521	0.0117	1.456	2.04
			Bw1	28-45	1.20*	0.077	0.432	0.0095	1.477	0.47
			Bw2	28-65	1.20*	0.066	0.396	0.0221	1.354	0.50
			Cg	65-70	1.20*	0.080	0.443	0.0082	1.504	0.52
		Kilpierce (Fine Loamy)	Ap1	0-15	1.20*	0.079	0.433	0.0114	1.434	0.34
			Ap2	15-25	1.20*	0.076	0.424	0.0122	1.429	0.28
			Bg	25-41	1.20*	0.070	0.417	0.0104	1.473	0.35
			BCG	41-60	1.20*	0.075	0.426	0.0104	1.464	0.38
		Kilrush (Fine Loamy)	Apg	0-25	1.04	0.089	0.533	0.0114	1.467	2.89
			Bg	25-55	1.50	0.070	0.400	0.0123	1.430	0.28
			BCg	55-80	1.48	0.075	0.417	0.0165	1.362	0.40
			Cg1	80-110	1.58	0.072	0.386	0.0122	1.392	0.17
Cg2	110-140		1.20*	0.077	0.429	0.0114	1.439	0.33		
Other	Series representing minor land area									

*6.3.3 Time Lag Estimates – 2012 implementation*

6.3.3.1 Modal Profile Approach

Results of the modal profile simulations subsequent to 2012 implementation of POM are shown in Table 6.4. IBT/Trend at the base of the soil profile were observed between 0.03 and 1.45 yrs, and 0.12 and 1.07 yrs, for the grassland and arable sites, respectively, depending on profile depth. Exit of the solute was only achieved at shallow depths in either catchment (1.05 to 2.93 and 1.23 to 1.98 yrs, grassland and arable, respectively) within the three-year simulation period. However, for deeper profiles, higher along the slope, total exit of the solute from the soil was not achieved. Differences in  $t_u$  between series within either catchment was greater for the latter markers (COM and Exit), but for IBT/Trend ranged between 0.02 to 0.11 yrs, depending on soil depth. This suggests that the superiority of the modal profile approach vs. the textural class approach is of greater importance where the soil is deeper, i.e. in upslope positions. Conversely, it must be considered that in both of the catchments presented herein, the prevalent soil series represents a relatively small range of soil types (largely brown earths). Hence, in catchments exhibiting a more diverse soilscape, the differences between series are likely to be greater, and an increased preference for the modal approach should be observed.

**Table 6.4:** Results of modal profile simulations, subsequent to 2012 implementation, according to various profile depths indicative of slope position. X indicates failure to achieve that  $t_u$  stage within the simulation period.

Site	Association	Series	Area %	Depth M	Breakthrough Stage (yrs) (subsequent to 2012 implementation)							
					IBT/Trend	Peak	COM	Exit				
Grassland	Ballylanders	Ballylanders (Fine Loamy)	50	0.5	0.05	0.27	0.39	1.05				
				3	0.43	1.10	1.52	X				
				5	0.74	2.04	1.97	X				
				10	1.54	X	2.40	X				
	Rosscarbery	Rosscarbery (Fine Loamy)	34	0.5	0.03	0.15	0.29	0.98				
				3	0.32	1.08	1.40	2.93				
				5	0.68	1.64	1.90	X				
				10	1.45	X	2.37	X				
	Driminidy/Newport	Driminidy/Newport (Coarse Loamy)	16	0.5	0.01	0.11	0.25	0.92				
				3	0.54	1.14	1.58	X				
				5	1.09	2.19	2.1	X				
				10	2.34	X	2.54	X				
Arable	Ballylanders/Clonroche	Ballylanders (Fine Loamy)	75	1	0.14	0.56	0.76	1.98				
				3	0.65	1.17	1.71	X				
				5	1.04	2.21	2.16	X				
				1	0.13	0.54	0.73	1.84				
	Clonroche (Fine Loamy)	3	5	0.94	2.15	2.06	X					
								1	0.13	0.56	0.74	1.77
								3	0.62	1.18	1.64	X
								5	1.04	2.18	2.14	X
	Duarrigle (Fine Loamy)	1	3	1.02	2.16	2.12	X					
								1	0.12	0.51	0.69	1.23
								3	0.59	1.14	1.59	X
								5	1.02	2.16	2.12	X
Kilpierce (Fine Loamy)	7	3	1.02	2.16	2.12	X						
							1	0.13	0.54	0.72	1.32	
							3	0.67	1.20	1.71	X	
							5	1.07	2.21	2.19	X	
Kilrush (Fine Loamy)	3	3	1.07	2.21	2.19	X						
							5	1.07	2.21	2.19	X	
Other			14	Series representing minor land area								

### 6.3.3.2 Time Lag Estimates – Long-term Simulations

The results of long-term simulations, using an average yearly meteorological data set, for each of the modal profiles are shown in Table 6.5. For the grassland site, IBT/Trend was typically observed in <1.25 yrs, but where in deep soil profiles (10 m) lags in this initial marker exceeded 2 yrs. Under those scenarios, Exit of the solute, indicating the complete effect of POM, was not achieved until 9.25 to 9.62 yrs. Even under more moderate profile depths (3 to 5 m), which are likely to be observed at mid-slope positions across a catchment, Exit ranged from just under 4 to *c.* 5.5 yrs. In the arable catchment, IBT/Trend in all simulations was observed in <1.28 yrs. This is due to the depth of the profiles (<5 m), caused by the shallow, undulating bedrock observed throughout the catchment. Exit was likewise, lesser than that observed in the grassland catchment, and ranged between 1.99 and 6.94 yrs.

## 6.4 Discussion

### 6.4.1 Catchment Mapping

As indicated in Section 6.2.3.2, although the soil associations present within any catchment can be rapidly determined by the SIS, the proportion of area represented by each constituent series has not been determined for all Irish catchments, only those within the ACP. These catchments have been subject to more thorough mapping and characterisation than is typical. This means that  $t_u$  ranges can be determined for any catchment outside of the ACP sites, but it is not yet possible to discern which soil series (and hence,  $t_u$  estimates) predominate at a given location. This increase in detail would be a valuable addition to the toolkit, in areas which have been identified by the Pathways Project as being particularly vulnerable to nutrient transport and associated time lags through the vertical and groundwater pathway. In such areas, higher resolution soil mapping will be required in order to improve toolkit performance.

**Table 6.5:** Results of long-term modal profile simulations, using an average yearly meteorological dataset. Profile depths are indicative of various slope positions.

Site	Association	Series	Area	Depth	Breakthrough Stage (yrs) (long-term mean weather dataset)			
					%	M	IBT/Trend	Peak
Grassland	Rosscarbery	Ballylanders (Fine Loamy)	50	0.5	0.10	0.23	0.53	1.23
				3	0.56	1.49	2.08	4.13
				5	1.11	2.40	3.26	6.16
				10	2.41	4.74	5.95	9.96
	Rosscarbery	Rosscarbery (Fine Loamy)	34	0.5	0.09	0.18	0.44	1.09
				3	0.45	1.33	1.93	3.94
				5	1.05	2.29	3.07	5.66
				10	2.29	4.55	5.72	9.55
	Rosscarbery	Driminidy/Newport (Coarse Loamy)	16	0.5	0.07	0.17	0.42	1.00
				3	0.67	1.80	2.22	4.28
				5	1.26	2.97	3.75	6.66
				10	2.96	5.79	6.84	11.57
Arable	Ballylanders/ Clonroche	Ballylanders (Fine Loamy)	75	1	0.16	0.76	0.85	2.03
				3	0.56	1.49	2.08	4.13
				5	1.11	2.40	3.26	6.16
		Clonroche (Fine Loamy)		1	0.16	0.76	0.86	2.06
				3	0.68	1.72	2.17	4.22
				5	1.16	2.53	3.43	6.24
	Ballylanders/ Clonroche	Duarrigle (Fine Loamy)	1	1	0.17	0.80	0.88	2.04
				3	0.83	1.89	2.34	4.47
				5	1.28	3.02	3.81	6.85
	Ballylanders/ Clonroche	Kilpierce (Fine Loamy)	7	1	0.16	0.75	0.80	1.99
				3	0.82	1.82	2.25	4.28
				5	1.25	2.88	3.68	6.45
	Ballylanders/ Clonroche	Kilrush (Fine Loamy)	3	1	0.17	0.79	0.85	2.01
				3	0.87	1.93	2.45	4.86
Ballylanders/ Clonroche	Kilrush (Fine Loamy)	3	5	1.33	3.13	4.00	7.13	
			Other	14	Series representing minor land area			

#### 6.4.2 Modal Profiles – 2012 Implementation

The results of the modal profile simulations demonstrate that a single figure, such as those suggested based on broad textural classes, cannot quantify the range of  $t_u$  durations exhibited across a catchment, having various soil series and watertable depths. Hence, the effects of POM on water quality may not be directly observable where specific areas within a catchment are transmitting solutes over a prolonged period, despite flushing in shallower or more rapidly drained regions. This is consistent with Mellander *et al.* (2015), who reported both temporal and spatial variation in groundwater response in these study catchments. Regarding water quality monitoring; the results suggests that monitoring of groundwater at low-slope locations with shallow overburden should have been initiated in early 2013, but that trends at upslope locations could not have been detected prior to July 2014. Regarding the 2015 EU-WFD deadline, these results indicate that assuming implementation of POM at a latest date of 2012, achieving full effects (indicated by Exit) within this timeframe is unrealistic, even when the unsaturated bedrock and saturated zone time lags are not considered.

#### 6.4.3 Long-term time lag estimates

The results of long-term simulations (Table 6.5) indicated that even under average meteorological conditions, for many soil depths, it may take in excess of a 6-yr reporting period for the full effects of POM to be observed at the base of the soil profile. While these results present a simplistic approach to the complexity of meteorological scenario testing, they are indicative of the timeframes in which  $t_u$  operates, and in which policy and POM should be designed. The results suggest that, assuming the full and timely implementation of POM by the end of 2012, water quality trends should be observed in the two study catchments within the first reporting period in both catchments, for all soil series and profile depths within these catchments. However, considering COM as an indicator of the bulk effect of POM, it is likely to be towards the latter stages of the reporting period that substantial responses are marked. As indicated in Chapter 3, the saturated approach of Fenton *et al.* (2011) approximates the COM stage of  $t_u$ . The results of that paper (under ER conditions of *c.* 800 mm-yr and  $n_e$  of 40%) are in good agreement with those results presented here. Furthermore, Exit of the solute from the soil profile (although

potentially hard to discern during monitoring campaigns due to low concentrations), was for many soil series and profile depths, approaching or exceeding 6 yrs. This indicates that while the length of the reporting periods will allow trend assessment, they are too short to allow the full effects of POM to be observed. While it is not within the objectives or scope of this thesis to indicate  $t_T$ , the similarity between the results herein and those of Fenton *et al.* (2011) suggest that their assertion of remediation timeframes between 2019 and 2033, depending on unsaturated zone depth and proximity to receptor, are realistic.

#### 6.4.4 Comparison of textural vs. modal profile approaches

As a textural approach can only provide a generic description of the soil characteristics within a catchment, it fails to reflect the unique hydrologic and pedogenic processes occurring at various landscape positions. Hence, the textural approach assigns a single value for each stage of  $t_u$  for each landscape position, across a catchment. Contrary to this, mapping endeavours (e.g. Creamer, 2014) demonstrate that a variety of distinct soil series may be observed within a single catchment, and so, taking the grassland site as an example, a mid-slope position may exhibit one of two different  $t_u$  durations, dependant on which soil series is present. Regarding the arable catchment in the current study, the range of soil series and the undulating depth to bedrock (3 m to 5 m) across the entire slope indicated up to ten different  $t_u$  durations. This is in agreement with Mellander *et al.* (2014), who likewise observed a spatial variability in N transfer in this catchment, as a result of heterogeneous soil characteristics and bedrock depths. Therefore, a range of potential  $t_u$  (for each marker: IBT/Peak/COM/Exit) provides a more realistic tool by which policymakers and land managers can assess the timescales within a catchment. In accordance with Chapter 3, the latter stages of breakthrough curves (COM and Exit) generated from textural simulations decreased in their similarity to modal profile based results, and so further emphasis must be placed on the modal profile approach where these latter markers are of interest. IBT/Trend estimates derived *via* the textural approach typically differed from those derived *via* the modal profile approach, in accordance with Chapter 3, but the differences did not exceed 0.26 yrs, and were less than 0.14 yrs for most soil depths/slope positions. For the purpose of trend analysis, and for indicating when data generated by groundwater monitoring

campaigns can first be correlated with POM, these differences may or may not be important, and should be considered on a contextual basis. For example, for indicating to policymakers when trends in mitigation effects should be observed in groundwater in a region having a low-slope position and shallow soil, a textural approach may suffice, as a difference of *c.* 0.04 yrs is minor within the context of six year reporting periods. However, for disentangling groundwater response to POM from background signals at a greater elevation, having deeper soils, a difference of 0.13 to 0.26 yrs between textural and modal approaches, may lead to poorly timed water sampling or incorrect interpretation of the data, and hence, a failure to capture a realistic assessment of POM effects. In such scenarios, a modal profile approach is recommended.

The soil series data provided in the SIS online browser includes subgroup classification for all series. For certain soil types (Groundwater Gleys and Alluvial soils) this can indicate where along a hill transect they are likely to be positioned, and consequently, which of the soil depths (suggesting low-slope/near-stream, midslope or upslope positions) should be considered. Other soil types such as Typical Brown Earths, may be observed anywhere within a catchment, and so the full range of slope positions should be considered. For example, in the arable catchment, the Ballylanders and Clonroche series approximate 75% of the catchment. As these soils are Typical Brown Earths, they may develop at any slope position, and so the full range of potential profile depths are possible. Conversely, the Kilpierce series is identified as a typical groundwater gley, implying a lower slope position. Hence, for the portion of the catchment assigned to this series (7.22%), the shallowest groundwater estimates become vital. It should be noted that assignation of percentages to soil series is not yet possible within most catchments, and so the full range of  $t_u$  estimates should be acknowledged. However, a recommendation forthcoming from this chapter is that in catchments where groundwater exhibits (1) poor chemical ( $\text{NO}_3$ ) quality (1.5% of Irish groundwater (EPA, 2015)), or (2) trends of increasing  $\text{NO}_3$  concentration (15% of Irish groundwater (EPA, 2015)), further soil surveys should be conducted, to aid characterisation and allow subdivision of the catchment as detailed herein.

#### 6.4.5 Implications for policy and monitoring

Analysis of the trends in water quality response to POM is inherently limited by spatio-temporal factors; namely, the position of the monitoring points within the landscape and the stage of  $t_u$  which may be assessed at those locations. For example, the quality of surface waters is influenced by the sum of multiple hydrological pathways in the catchment, including lateral subsurface flow, baseflow etc. Consequently, for subsurface pathways (both vertical and lateral) it is challenging to disentangle the trend effects of recent POM from the legacy effects of past practices, or those effects arising from measures implemented in different parts of the catchment. Likewise, monitoring of groundwater will indicate chemical concentrations reflective of both past and present measures, and at low-slope positions, will be subject to the import of water/contaminants from higher along the transect. As such, monitoring at ground- or surface water represents  $t_T$ , or  $t_u$  plus some portion of  $t_s$ , and cannot discriminate between the components of time lag (saturated versus unsaturated), or its various stages (early versus late stages of the breakthrough curve). Unsaturated zone modelling according to the methodology described in this chapter, or based on site-specific analyses of soil properties in vulnerable regions of the catchment (Chapter 5), enabled trends at the base of the soil profile to be indicated independent from confounding influences. This provides an earlier indication of trend responses than is possible *via* monitoring of ground- or surface waters.

As the focus of this thesis is on ascertaining the specific stages or markers of  $t_u$  rather than assess specific N loadings, it is not possible to deliver reliable mass fluxes at the base of the profiles. This would require further data, such as crop uptake, attenuation (including both dilution and denitrification), microbial action, physical immobility etc. However, the results herein are in agreement with those of Fenton *et al.* (2009), who observed uneven contaminant mass fluxes across an area as a result of soil physical heterogeneity. That study identified regions of high attenuation/low mass flux, which reduced overall delivery to the receptor (in that case; groundwater) sufficient to maintain sub-MAC values. Such a scenario could easily occur at the grassland site, where slow IBT/Trend as a result of deep soil profiles may sufficiently offset more rapid delivery elsewhere in the catchment.

Fenton *et al.* (2009) also identified ‘hot-spots’ exhibiting high mass flux. Should such soils be located adjacent to a receptor, the brief  $t_u$  could lead to intermittently high concentration peaks and hence, high observed fluxes, should monitoring coincide with the early stages of  $t_u$ . Fenton *et al.* (2009) suggested that such areas be targeted for environmental remediation such as denitrifying bioreactors. Reported mass fluxes at receptors should be considered in light of both the  $t_u$  and  $t_s$  influencing observations.

There are 6278 river catchments in Ireland (and a further 2470 coastal sub-basins) (Fealy, 2015) which range in size from less than 12 km<sup>2</sup> to 473 km<sup>2</sup> (Fig. 6.13). In those catchments exhibiting poor or declining water quality and dominated by the vertical pathway, the methodology described in this chapter could be applied. This would enable trends to be anticipated, and facilitate a better understanding of water quality results in relation to past and current management practices. Wahlen and Grimvall (2008) highlighted the need for discernment of anthropogenic effects on water quality during environmental modelling from confounding influences arising from methodological choices and meteorological factors, to which this thesis adds, time lag, and particularly,  $t_u$ .

It should further be noted that the toolkit described herein has not accounted for any element of N attenuation or transformation, which are likely to occur in reality. The  $t_u$  estimates generated therefore represent only perfectly conservative behaviour. As this toolkit provides a basic framework, a future research objective should be the incorporation of these aspects using the PHREEQC geochemical code developed for this purpose as an adjunct to the standard Hydrus program (Parkhurst and Appelo, 1999; Šimůnek *et al.*, 2006).

## 6.5 Conclusions

The results of this modelling exercise indicate a range of potential  $t_u$  within each catchment, depending on the stage of transport in question, soil series, and depth of the soil profile (or slope position). These projections represent the best estimate of  $t_u$  using the available data, but should not be considered to preclude either shorter or longer durations in specific locations within the catchment. In the catchments examined in this chapter, the Hydrus model simulations suggested that

trends may first be observed at the base of the soil profile up to 2.24 yrs subsequent to the implementation of POM, the full effects of which (as indicated by the Exit marker of the breakthrough curve) may exceed 10 yrs to be exhibited at some locations within the grassland catchment, and *c.* 7 yrs in the arable catchment. These lags are long, particularly in light of the 6-yr reporting period cycles defined by the EU-WFD.

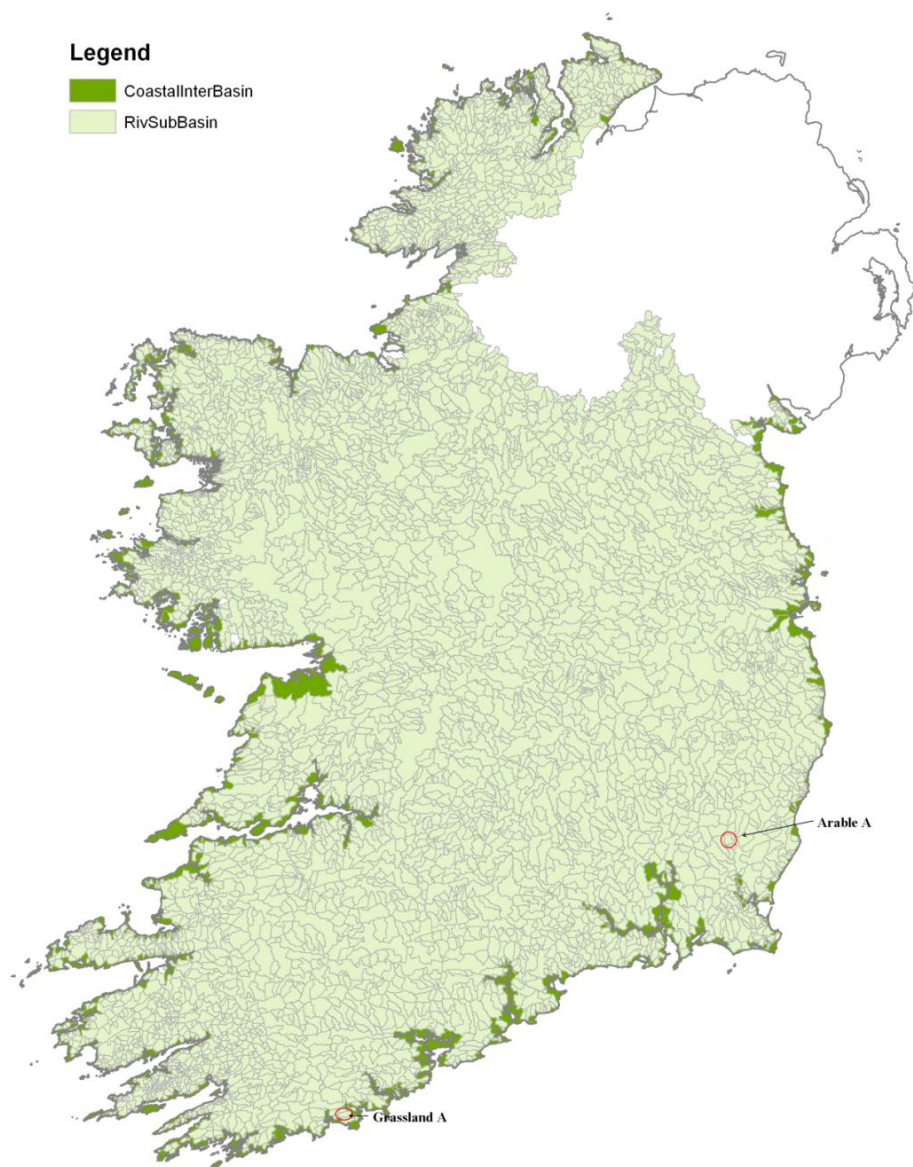


**Fig. 6.13:** Irish hydrological catchments (including both river and marine catchments). The grassland and arable sites used in this study are indicated (Fealy, 2010).

Furthermore, research into  $t_s$  in these catchments (McAleer *et al.*, Personal Communication) suggests that groundwater travel times may approach 2 yrs in the grassland catchment, and 1 yr in the arable catchment. The 2015 deadline therefore allows insufficient time for POM, implemented in 2012, to have full effect on water quality. However, based on the long-term simulations, a groundwater response (changes in quality) should be expected at these sites within the next reporting period (2021). It is important to recognise however, that these catchments are considered to be dominantly well drained, and so more prolonged durations are highly likely at other locations. Employing the methodology described herein allows water quality trends and  $t_u$  ranges to be estimated, and allows the likely trends in water quality beyond the soil zone to be discerned, based on readily available, existing soil data. Such an approach can be rapidly implemented at other sites, requiring only appropriate soil and meteorological input data, and access to the Hydrus model. In catchments exhibiting poor or declining water quality, additional soil mapping at higher resolution may be conducted in order to indicate the proportions of the constituent soil series, and thus, add greater context to the estimated trend and long-term  $t_u$  ranges.

The following additions/developments could in future be made to the basic structure of the toolkit as detailed herein:

- Incorporation of the Pathways catchment management tool (Tier 1) in order to identify areas within a catchment in which the prevailing nutrient loss pathway is vertical transport through the soil, and hence, to target these areas for  $t_u$  assessment using the toolkit (Tier 2).
- Identify catchments exhibiting poor or declining water quality as a result of N contamination, and conduct high spatial resolution soil mapping, in accordance with Section 6.3.1. Hence, trend and long-term  $t_u$  estimates at those sites can be contextualised and fine-tuned, based on the proportions of the catchment represented by each constituent soil series.

- Incorporate the PHREEQC package in order to better quantify nutrient attenuation and speciation, and so, modify  $t_u$  estimates to closely resemble N, or any other potential contaminant of interest.
- Develop a classification system by which a catchment can be subdivided into upslope, midslope and lowslope/near-stream components. This could potentially be based upon slope, elevation, proximity to receptor, or some integration of each of these factors. Hence, in addition to soil series percentages, a toolkit user could determine which landscape position predominate, and therefore, which trend/long-term  $t_u$  ranges are of most significance from a policy or monitoring perspective.

Validation of the present toolkit approach detailed herein is using *in-situ* tracer tests was conducted, and is discussed in Chapter 7.

### **Summary**

This chapter presents two case studies of the low complexity approach as applied to grassland and arable agricultural catchments, in which the transport of  $\text{NO}_3$  is a primary concern as regards achieving water quality standards under the EU-WFD. Ranges of  $t_u$  were identified in each catchment, which may preclude attainment of these goals within imminent reporting periods. The low-complexity approach was implemented using data readily available from the existing SIS and ACP resources. Chapter 7 presents an *in-situ* assessment of  $t_u$  at the study catchments using a potassium bromide tracer, allowing the suitability of the modelling approach to be examined. That chapter also details unsaturated zone monitoring arrays, which may be installed in vulnerable catchments in order to track contaminant transport, and indicate the effects of POM earlier than is possible using groundwater or catchment outlet monitoring apparatus.

## Chapter 7

### Validation of time lag estimates using field tracer tests

#### Overview

This chapter presents field investigations of time lag using a conservative, surface-applied tracer, the results of which are compared to estimates of  $t_u$  generated according to the methodology presented in Chapter 3. This work was conducted in conjunction with a separate PhD project (Eoin McAleer, Trinity College Dublin), which investigated groundwater time lag. These projects contribute to the comprehensive characterisation of the ACP sites, and form the basis of a toolkit by which  $t_T$  (both  $t_u$  and  $t_s$  components) may be assessed in Irish agricultural catchments.

#### 7.1 Introduction

In their commentary on the advantages and limitations of models as tools by which the hydrological environment may be understood, Pachepsky *et al.* (2004) noted that while hydrologic models are becoming increasingly complex and parameterised, some degree of parsimony is required in acquiescence to data availability. Furthermore, the suitability of the model must be considered within the context of what is required by the end-user (Bouraoui and Grizzetti, 2013). As described by Schoups *et al.* (2008), a model should be ‘complex enough to explain the data, but not more complex than necessary.’ It is recommended that model users evaluate the performance and suitability of their methodological framework (in this case; the low- vs high-complexity approach - Chapter 3; and the  $t_u$  toolkit – Chapter 6) against some empirical measure of the process they are simulating (Bouraoui and Grizzetti, 2013).

Frequently, tracer studies provide such a measure, against which specific modelling approaches described in the literature are compared, in order to assess their capacity to describe the conditions and hydrologic response in question (Saxena and Jarvis, 1995; Kramers, 2009; Dann *et al.*, 2010). Köhne *et al.* (2009) provided a comprehensive synthesis of modelling approaches used in comparison to tracer studies at various scales (lysimeter/plot/field) (although that study focussed of preferential rather than matrix flow). As such, tracer studies provide the standard

against which the accuracy and utility of modelling or conceptual approaches can be gauged. The Hydrus model has been extensively tested, calibrated and validated against tracer studies at a variety of scales (Šimůnek *et al.*, 2012). These studies have used a multiplicity of different tracer and solute types, and range in scale from relatively small, laboratory soil column experiments (Adhikari *et al.*, 2011; Ladu and Zhang, 2012; Wen-Zhi *et al.*, 2013.), to lysimeter studies (Jiang *et al.*, 2010; Afrous *et al.*, 2012), to *in situ* plot and field-scale investigations (Merdun, 2012; Saso *et al.*, 2012; Horel *et al.*, 2014).

In order to ascertain the performance of the low- versus high-complexity approaches described in Chapter 3, and to comment on the utility of the catchment-scale toolkit for  $t_u$  assessment described in Chapter 6, an *in situ* investigation of  $t_u$  was required. Due to the complexity of  $t_u$ , and the role of landscape position (see Chapter 2, Section 2.6), it was decided that for this study, a field-scale approach was most appropriate. In this chapter the transport through the soil profile of a surface-applied conservative tracer (as an indicator of  $t_u$ ) was compared to the low- and high-complexity modelling approaches described in Chapter 3 and to the modal profile toolkit described in Chapter 6. The specific objective of this chapter is to examine the validity of  $t_u$  estimates made in accordance with the methodologies described in the previous chapters.

## 7.2 Materials and Methods

### 7.2.1 Tracer Study

The grassland and arable agricultural catchments described in Chapter 6 were used for this exercise, and are detailed therein. In order to provide an empirical measurement of  $t_u$  at these locations, against which the low and high-complexity approaches could be examined, a tracer study was initiated, in which a  $KBr^-$  solution was applied to the soil surface and its movement through the unsaturated zone was observed. This tracer was selected due to its low background levels in the soil and its generally conservative behaviour (Gilley *et al.*, 1990) and low toxicity. It has been frequently used in unsaturated zone studies as a proxy for nitrate e.g. Owens *et al.* (1985); Richards *et al.* (2005), and was considered an ‘index tracer’ by Bowman (1983), against which the performance of other tracers could be evaluated. Rapidly

drained catchments were selected in order to facilitate results within the timescale of the research project (Mellander *et al.*, 2014).

### 7.2.1.1 Profile Instrumentation

Soil pits were excavated at two locations (low- and mid-slope) within each catchment (Fig. 7.1). At each site, the mid-slope pits were situated adjacent to mid-slope monitoring wells, while the low-slope pits were situated roughly 1/3<sup>rd</sup> upslope from the lower well. This was done to ensure that soil monitoring apparatus were not saturated during seasonally high watertables.

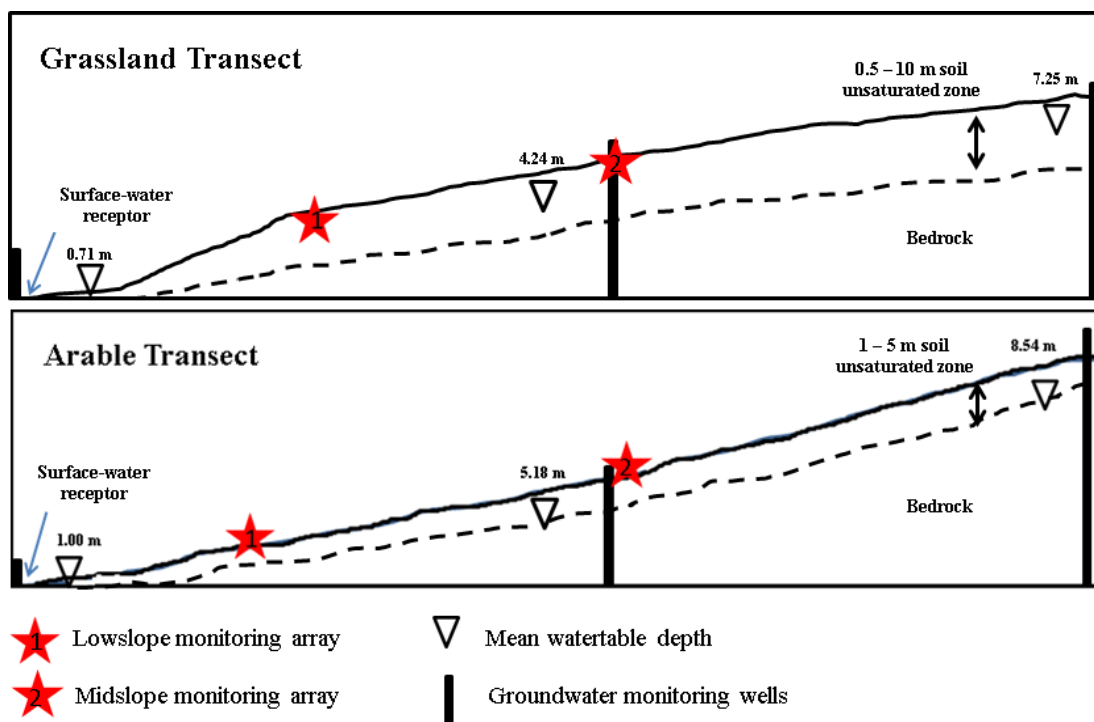


**Fig. 7.1:** Cross-section of the grassland and arable hillslopes, indicating position of the soil monitoring arrays, the surface water receptors, groundwater monitoring wells, bedrock and mean annual watertable depths.

These soil pits were excavated within areas characterised by the dominant soil series of each catchment (Ballylanders in both instances). Soil profile characterisation was conducted in the field according to SIS protocol (Simo *et al.*, 2013). The soil profiles, instrumentation and soil characteristics for each location are indicated in Fig. 7.11a-d. In each soil pit, the following monitoring devices were installed (installation depths are specified in Fig. 7.2):

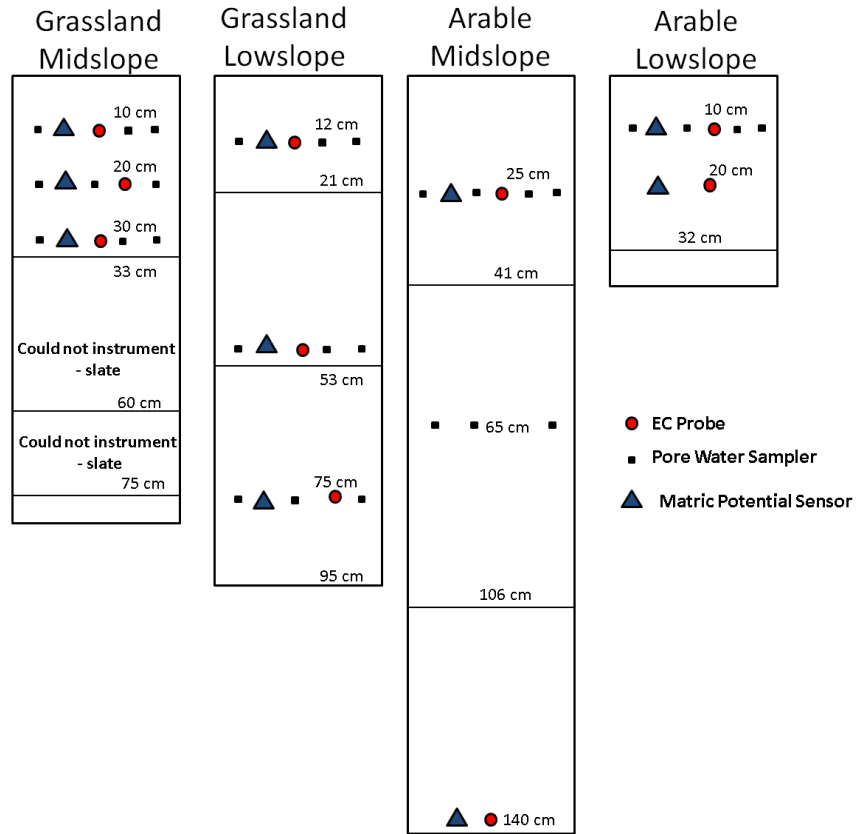


**Fig. 7.2:** Instrumentation depths of the soil profiles (indicating pore water samplers, EC probes and matric potential sensors). Horizontal lines indicate horizon boundaries.

- Pore water samplers - Macrorhizon pore water samplers (Rhizosphere) (3-4 replicates per horizon) (Fig. 7.3).

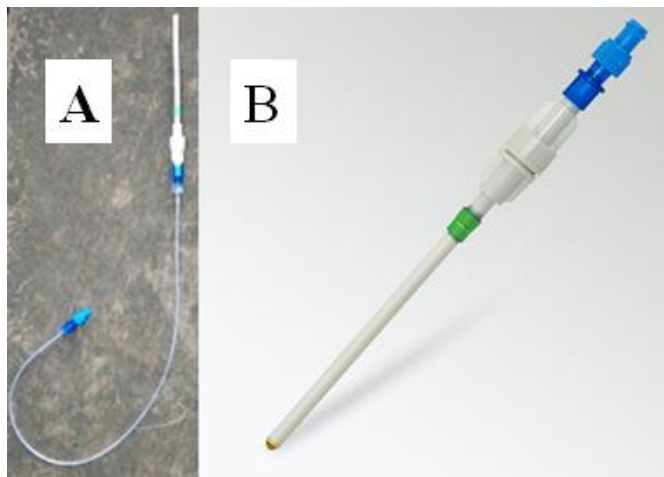


**Fig. 7.3:** (A): Rhizosphere Macrorhizon pore water sampler, including ceramic head, piping, and lauer-lock extraction point. (B): Ceramic sampling head which is inserted into the pit face.

- Soil moisture probes - Decagon 5TE ( $\theta$ , electrical conductivity ( $EC$ ) and temperature ( $^{\circ}C$ )) (Fig. 7.4 - A).
- Matric potential probes - Decagon matric potential probes (MPS2) ( $\Psi$ ) (Fig. 7.4 - B).

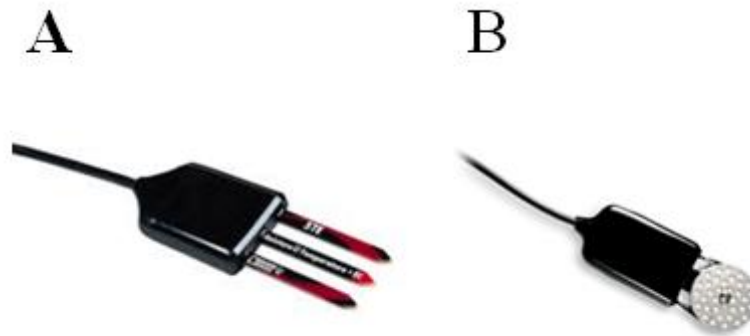


**Fig. 7.4:** (A) 5TE soil moisture and  $EC$  probe and (B) MPS2 matric potential probe (Decagon, 2015).



**Fig. 7.5:** Installation of the instruments into the pit-face (grassland, midslope location), using guide holes and soil paste.

All monitoring equipment was installed laterally into the pit-face towards the field and wiring/piping was routed to the surface *via* plumbing piping (Fig. 7.5). This method of installation prevented preferential flow to the monitoring equipment, which can occur with vertical installation (Decagon, 2015). Sensors and probes were

inserted into the pit-face to their full depth by first driving a small-bore insertion tool into the horizon, in order to provide a guide hole for the equipment (Doležal *et al.*, 2012), preventing damage to the delicate instruments (Figs. 7.5 and 7.6). A soil and water paste was used to coat the instruments prior to insertion (Doležal *et al.*, 2012). This ensured good soil-sensor contact, which is essential for accurate readings (Decagon, 2015). Colour-coded tags were affixed to the luer-lock extraction point of the pore water samplers at the soil surface. These tags indicated the depth of the instrument, so that extracted pore water could be associated with the appropriate horizon. Solar powered Decagon CR1000 data-loggers recorded hourly sensor measurements. Data-loggers and batteries were housed within resilient, waterproof logger-boxes, which were affixed to steel support posts adjacent to the soil pits (Fig 7.7). Data-loggers were programmed and downloaded using the Loggernet™ software (Campbell Scientific, 2015). Subsequent to installation, the soil pits were backfilled by hand to prevent damage to the equipment. Installation occurred six months prior to application of the tracer. This ensured that 1) the equipment became settled within the soil profile, limiting preferential flow and biased measurements (Decagon, 20015), and 2) background readings were established. Synoptic weather stations located within each catchment recorded hourly measurements of precipitation (mm), temperature (°C), windspeed (kph) and humidity (%). These data were used to calculate effective rainfall (ER), which provided the meteorological inputs to the Hydrus model. Prior to application of the KBr<sup>-</sup> tracer, pore water samples were taken roughly every two weeks, to establish background concentrations. The sampling and monitoring arrays were established six months prior to application of the tracer, in order to establish antecedent conditions and to allow the soil profile to settle after the disturbance of the excavation.



**Fig. 7.6:** (A): Instruments routed from pit-face to surface via piping, prior to backfilling of the excavation. Hammer indicates scale. (B): Lauer-lock syringes collecting pore water at the soil surface, subsequent to backfilling of the excavation. Colour coded tag indicates the depth of the pore water samplers. Both photographs obtained at the grassland, lowslope location.

#### 7.2.1.2 Tracer Application and Monitoring

Laboratory testing was conducted in order to examine the ability of the 5TE probes to detect changes in *EC* in response to application of  $\text{KBr}^-$  solution at various concentrations. Dry soil from the arable midslope pit (upper horizon) was packed to a  $\rho_d$  of  $1.20 \text{ g cm}^3$  in 100 ml containers.  $\text{KBr}^-$  solution was prepared from stock solution, to concentrations of 0.5%, 1%, 1.5%, 2% and 5%, in addition to a control containing only filtered water (0%). Soil samples were adjusted to 10-50%  $\theta$ , using the various  $\text{KBr}^-$  solutions (Fig 7.7). Samples were allowed to equilibrate overnight. The *EC* of each of the soil/ $\text{KBr}^-$  mixtures was tested using a 5TE probe connected to a handheld datalogger (Decagon ProCheck<sup>tm</sup>). The sensor was inserted into the container and allowed to equilibrate for ten minutes, subsequent to which the *EC* measurement was recorded. The 5% concentration (Fig. 7.8) provided a distinct indication of increased *EC*.

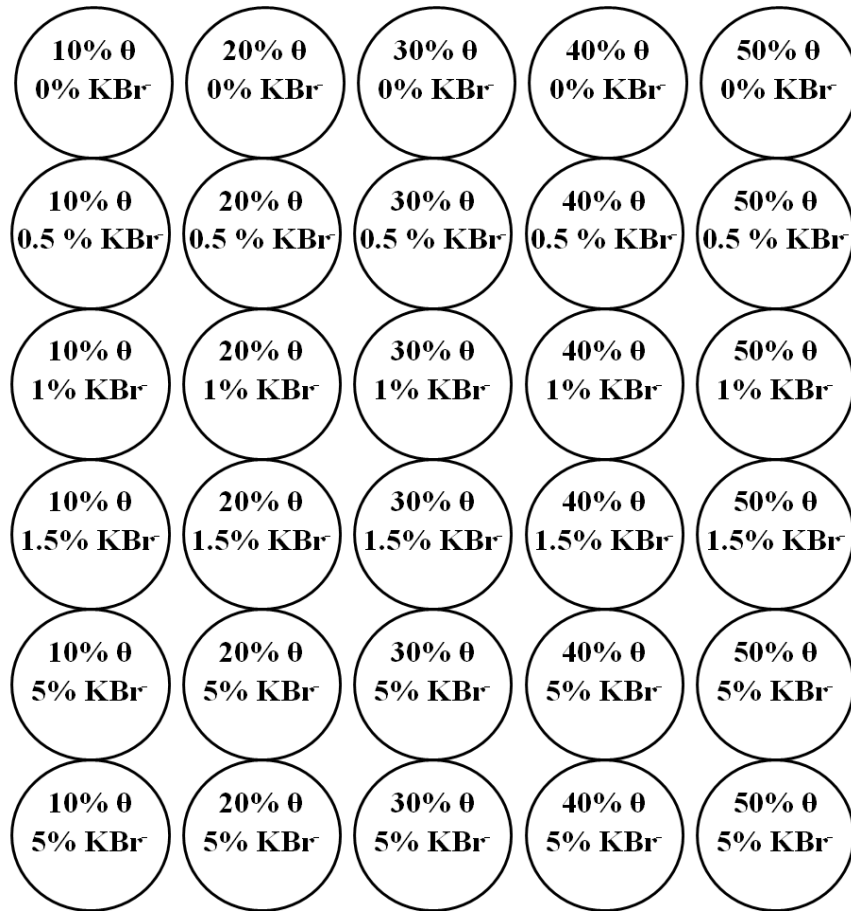


**Fig. 7.7:** Schematic of EC response test in the laboratory; indicating volumetric water content ( $\theta$ ) of the soil and concentration of the KBr- solution.

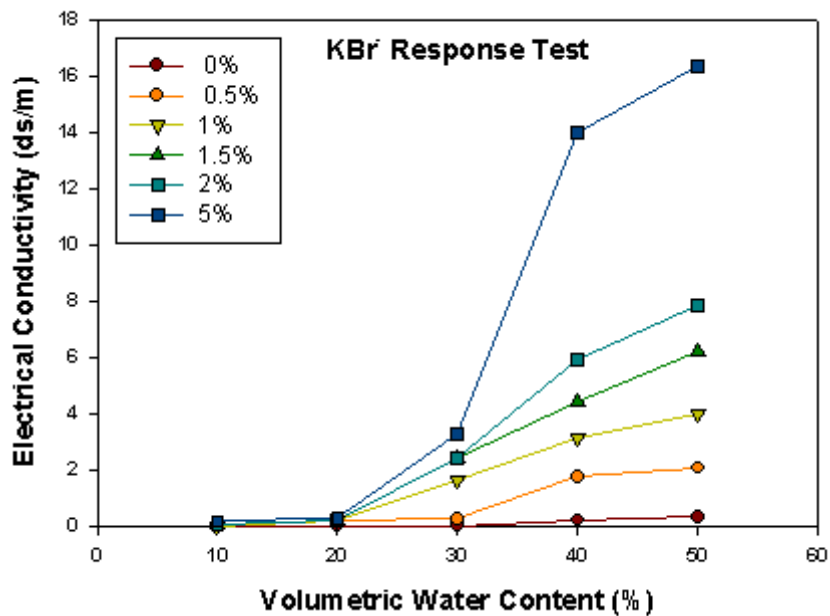


**Fig. 7.8:** Electrical conductivity response (ds/m) to various KBr- solute concentrations (0-5%) and soil volumetric water content (0-50%).

Based on the laboratory concentration testing and values observed in the literature, a 5% solution of  $\text{KBr}^-$  was applied at all four study sites (grassland midslope, grassland lowslope, arable midslope, arable lowslope), at a rate of  $200 \text{ kg ha}^{-1}$ , over a  $5 \times 5 \text{ m}$  application area surrounding the monitoring arrays, as in similar studies such as Brandi-Dohrn *et al.* (1996), Fleming and Butters (1995), and Premrov (2011). Background soil pore water  $\text{KBr}^-$  concentrations prior to tracer application did not exceed  $0.0001 \text{ g L}^{-1}$ , suggesting that additions of this solute would be clearly detectable. The tracer was prepared from stock solutions at Johnstown Castle, Environmental Research Centre, Co. Wexford, and transported to the study sites in 20-L drums. Watering-cans with a 50 cm wide T-bar attachment were used to equally distribute solution across the application zone (Richards *et al.*, 2005). The application area was subdivided into 1-m-wide strips, and trial-runs were performed prior to application, to ensure even and uniform, application of the solution over each strip. Mean surface soil moisture content of the application plots prior to tracer application was assessed by taking 25 evenly distributed measurements using a 5TE probe and a handheld data-logger. Antecedent volumetric soil moisture was 28% and 26% at the grassland and arable sites, respectively. Application was conducted at the arable site on 1<sup>st</sup> December 2014 and at the grassland site on 8<sup>th</sup> December 2014. Timing of tracer application was determined in order to correspond to the main drainage/recharge season, in which water (and consequently, nutrient) transport is most likely. Furthermore, this timing corresponded with the fewest land management practices at both sites, thus eliminating background ‘noise’ which could have rendered the interpretation of results more difficult.

Hourly *EC* readings (corrected for moisture content (Decagon, 2015) were used to indicate presence of the tracer. In addition, soil pore water sampling (for  $\text{KBr}^-$  concentration measurement) was attempted on a *c.* weekly basis. All pore water samplers from the mid- and lowslope at the arable site were irreparably vandalised (Fig. 7.10), and so no chemistry results are available for this location.

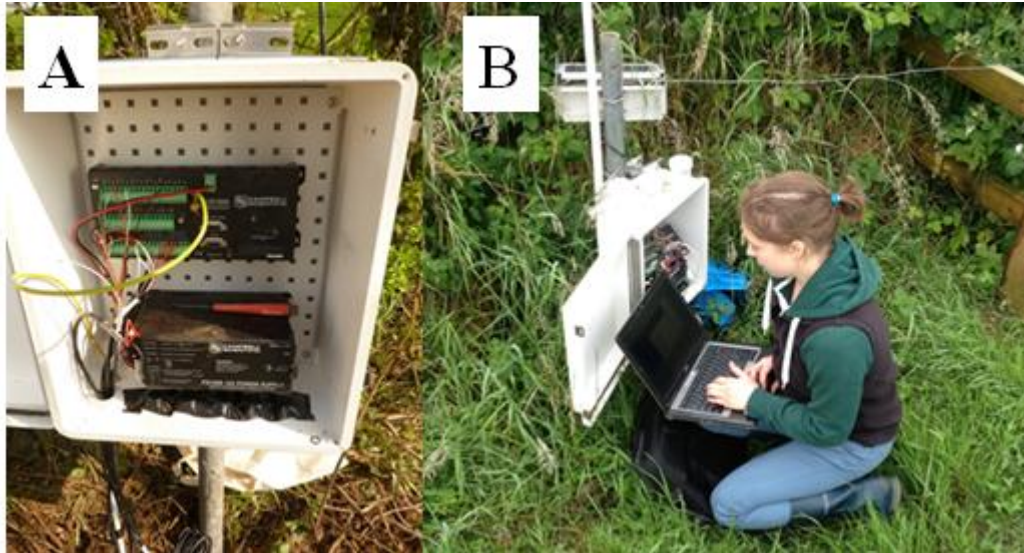


**Fig. 7.9:** (A): Data-logger and solar charged battery, inside waterproof loggerbox, affixed to steel support. (B): Downloading data using Loggernet<sup>tm</sup> software, at the grassland site.



**Fig. 7.10:** Damaged piping for pore water samplers, as a result of vandalism.

There was also an incident of vandalism at the grassland lower pit, in which the A horizon samplers were destroyed. However, the deeper samplers were effectively repaired. Samples were obtained by attaching 30 ml lauer-lock syringes and applying suction for *c.* 48-hr prior to sample collection (Fig. 7.6B). Pore water from samplers in each horizon was bulked to ensure sufficient quantities for

chemical analysis. Data were downloaded from the data-loggers at weekly-fortnightly intervals (Fig. 7.9).  $\text{KBr}^-$  analysis was performed using ion chromatography (Metrohm 790, Switzerland), and a conductivity detector and analytical column (Brennan *et al.*, 2012; Selbie, 2014). Cessation of monitoring occurred in June 2015 (up to 7 months after  $\text{KBr}^-$  application), although the monitoring arrays remained *in situ* to facilitate prolonged unsaturated zone observations (Drummond *et al.*, 2012) as part of the ACP.

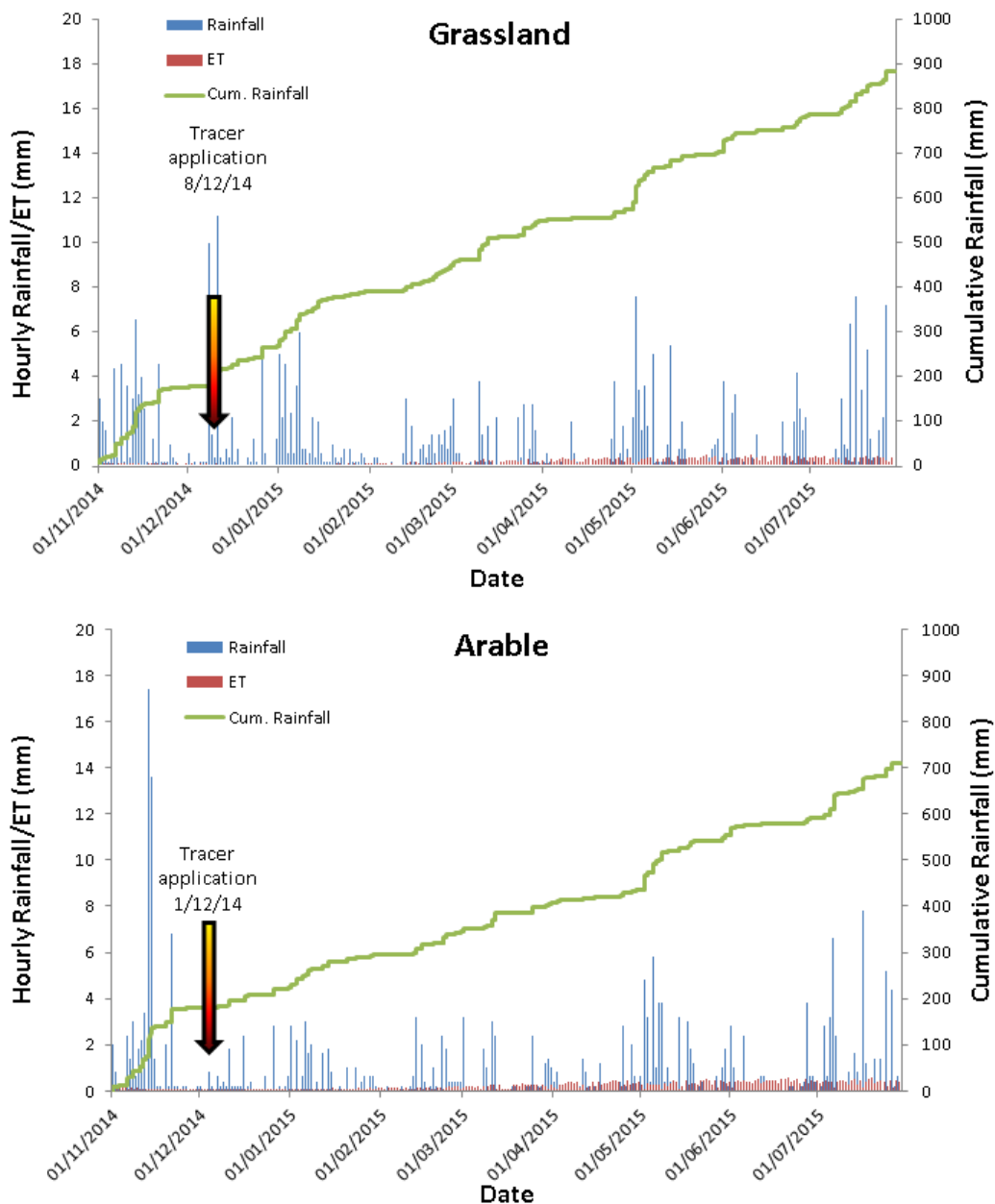


**Fig. 7.11:** Hourly rainfall and evapotranspiration (ET), and cumulative rainfall at the grassland (top) and arable (lower) sites, respectively, during the tracer study period (ACP, Personal Communication).

### 7.2.2 Model Simulations

Movement of the field tracer was compared to various model simulations, in order to assess their performance as predictors of  $t_u$ . The  $t_u$  was determined using Hydrus, with model settings in accordance with Chapter 3. Common to all the simulations was the meteorological input data (Fig. 7.11), which was recorded hourly at the respective catchments, during the monitoring period. This allowed the results to be compared directly to the field observations. Breakthrough curves are likewise divided into the respective  $t_u$  markers: IBT/Trend, Peak, COM and Exit, with  $0.01 \text{ mmol cm}^3$  used as the threshold solute concentration for IBT/Trend and Exit. The modelling approaches were as follows:

#### 1. Modal Profile Approach

Simulations were conducted for each of the modal profiles described in Chapter 6 using meteorological data corresponding to the tracer study period, and with breakthroughs assessed at depths corresponding to the probe depths. This approach allows comparison between the modal approach to reality, for comparable depths, and to infer the efficacy of this low complexity methodology. This is likely the most suitable approach for policymakers, as it represents typical soil characteristics within a catchment (and so minimises the potentially confounding influence of small-scale heterogeneity), and is cost-effective and rapidly implementable due to the presence of existing soil maps.

#### 2. In-Situ Profile Approach – Low complexity

Soil textural and bulk density data, ascertained from the same samples used in the high-complexity analyses, were used to derive hydraulic properties *via* PTF in accordance with Chapters 3 and 4. This represents the low-complexity (indirect) approach. Hydraulic parameters are described in Fig. 7.13 a-b. This approach might be applied in scenarios where high site-specificity is required (e.g. for monitoring of areas of a catchment which are of particular concern), but where the time or facilities required for SWCC assessment are not available. This approach bears a low level of data complexity, but a high level of site-specificity (Fig. 7.12).

### 3. *In-Situ Profile Approach – High complexity*

In order to supply the data for a high-complexity (or direct) approach to soil characteristics and  $t_u$ , four intact soil cores ( $5 \times 5$  cm) were obtained from each horizon of the soil pits, during installation of the monitoring arrays. SWCCs were constructed from these cores using the centrifuge method described by Nimmo *et al.* (1987), Reis *et al.* (2011), Šimůnek and Nimmo (2005) and Chapter 5 of this thesis. Cores were excavated in a vertical orientation (as opposed to the common horizontal extraction method, where cores are used for bulk density assessment alone). In some instances (arable site, mid-slope pit, horizons Ap2, Bc and C), it was not possible to obtain sufficiently intact cores due to the presence of stones and poor soil consistency. A 48-hr duration was applied at each time-step, in accordance with Chapter 4. It is acknowledged that this duration is sub-optimal at the grassland site; the implications of this are discussed in Appendix D. The following pressure steps were applied: 0, -33, -100, -150, -200, -1000 and -1,500 kPa. The resulting SWCCs were fit using the VGM equation in the RETC program, in order to obtain the soil hydraulic parameters for high-complexity simulations. Subsequent to centrifugation, samples were oven-dried at 105°C for 48-hr, and weighed to determine  $\rho_b$  (Shukla, 2014). ASTM D854-14 (2014) was used to determine  $\rho_s$ . Effective porosity ( $n_e$  %) was calculated as  $\rho_s/\rho_b$  (Shukla, 2014). As with the low-complexity modelling approach, an atmospheric boundary condition was imposed at the surface, while a free drainage condition was imposed at the base of the profile, in order to reflect the absence of a watertable within the observed region. The depths of the simulations correspond to the depths for which the SWCCs were assessed. This approach combines both high data complexity and high site-specificity (Fig. 7.12).

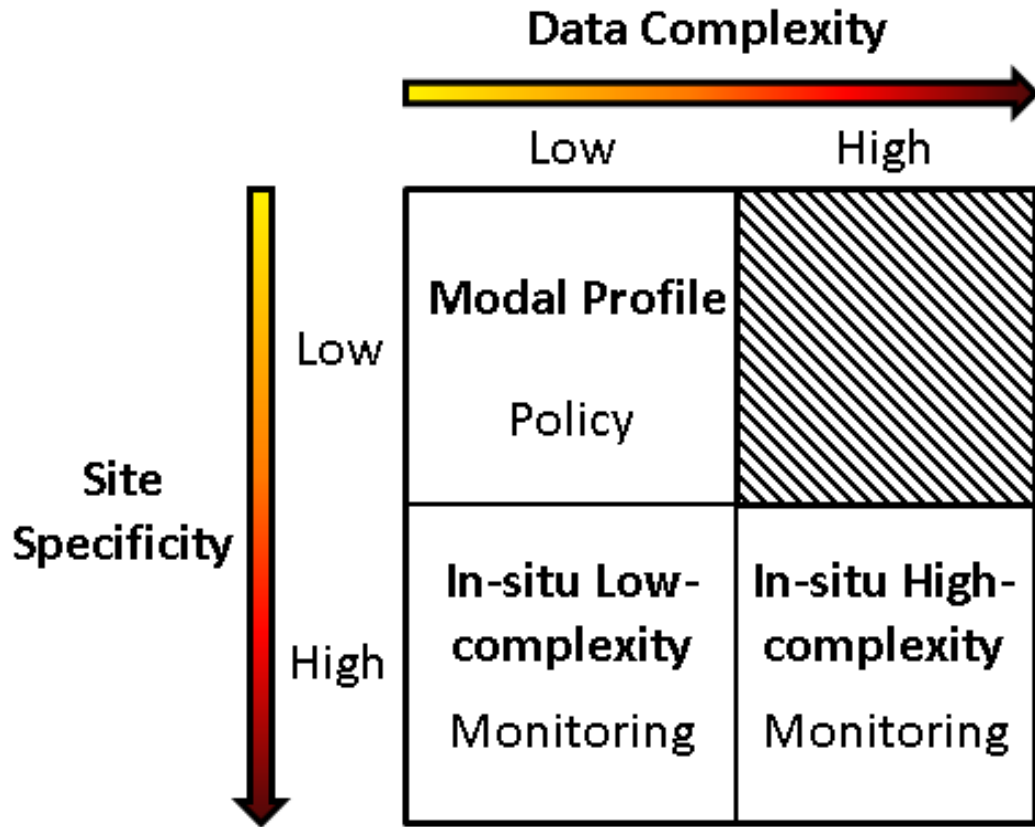


**Fig. 7.12:** Eisenhower box indicating data complexity/site specificity interactions, and appropriate end-users/stakeholders. Data complexity increases from left to right, while site-specificity increases from top to bottom.

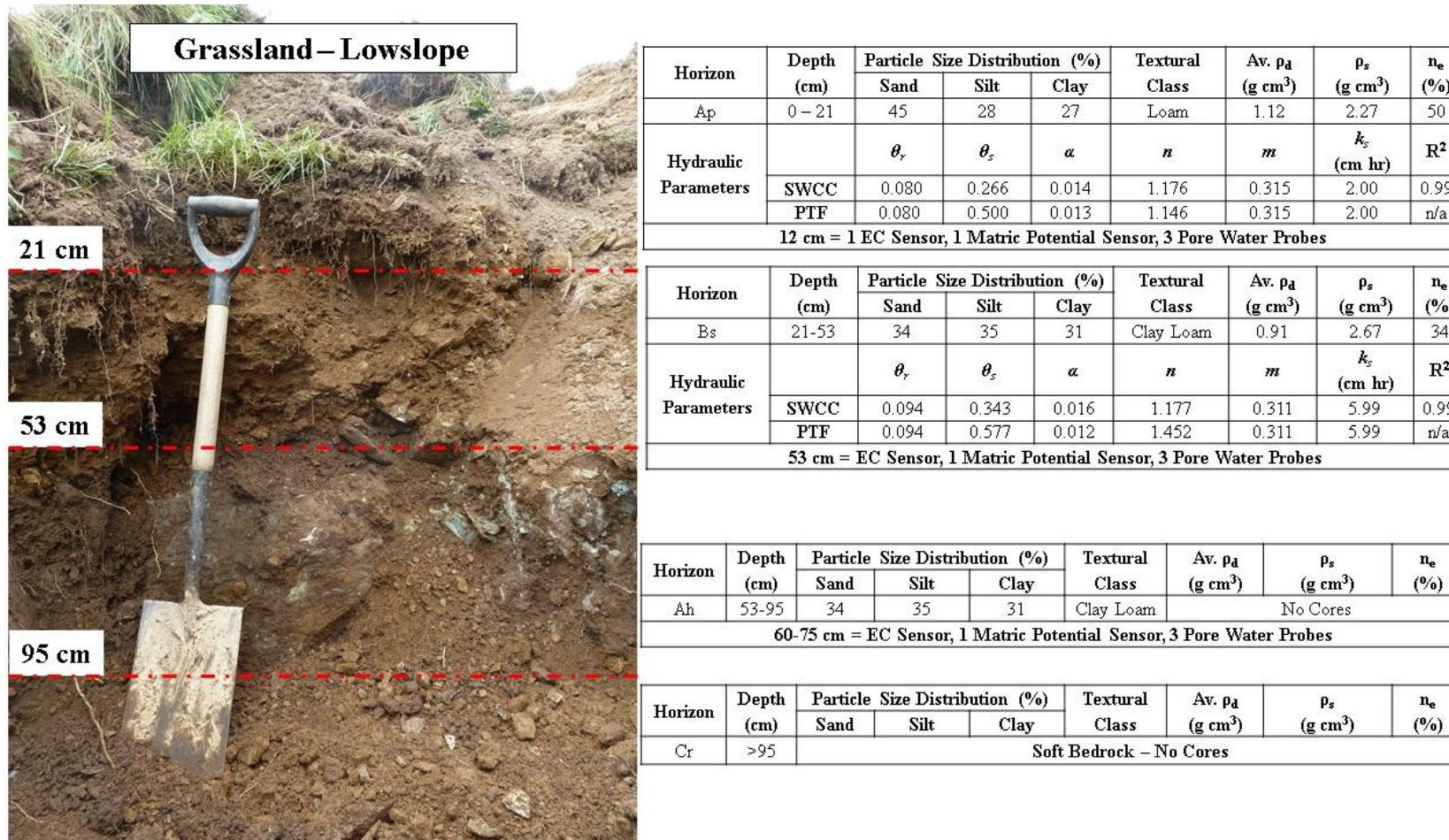


Fig. 7.13a: Profile description of the lowslope installation at the grassland site.

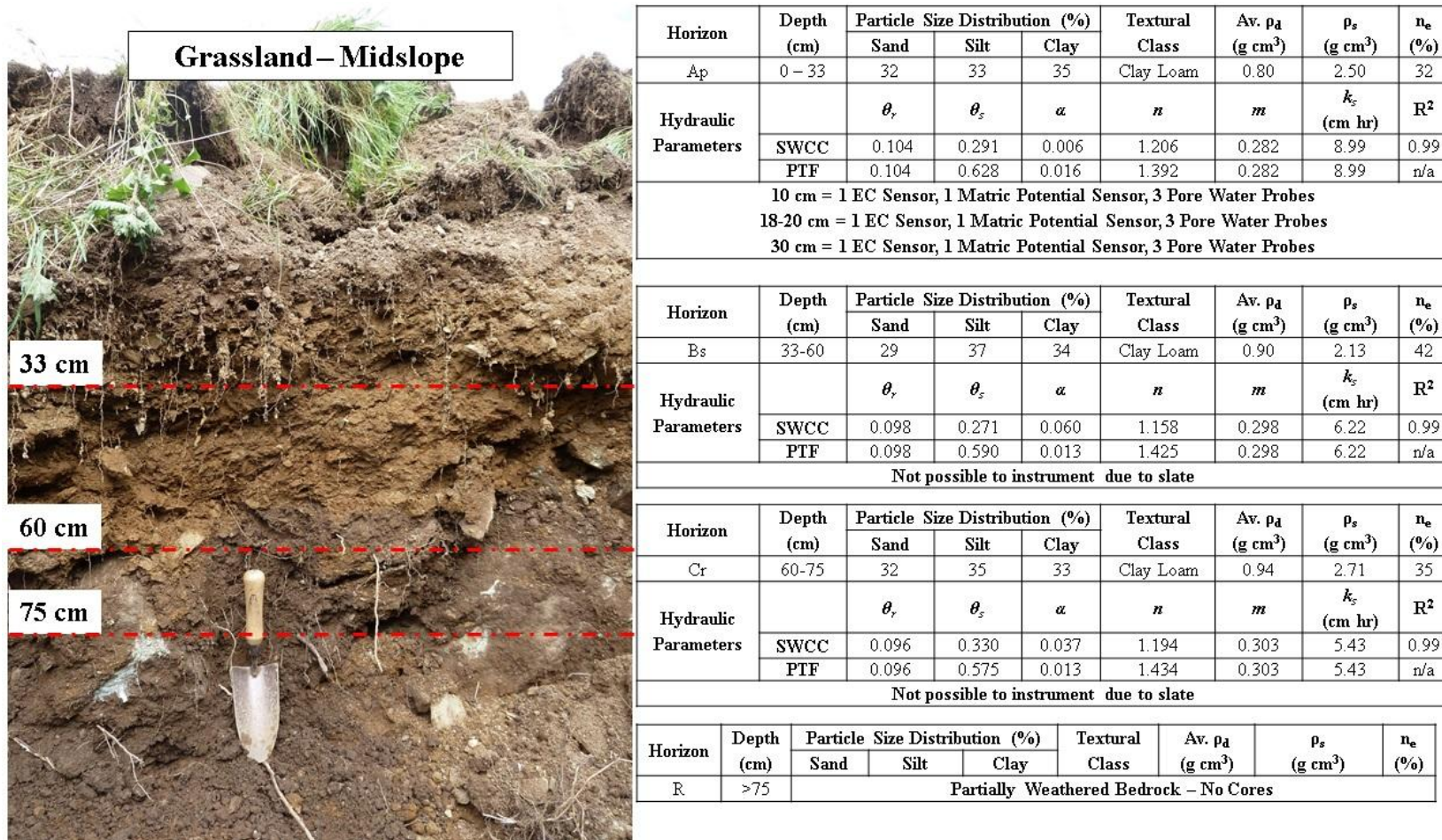


Fig. 7.13b: Profile description of the midslope installation at the grassland site.



Horizon	Depth (cm)	Particle Size Distribution (%)			Textural Class	Av. $\rho_d$ (g cm <sup>3</sup> )	$\rho_s$ (g cm <sup>3</sup> )	$n_e$ (%)
		Sand	Silt	Clay				
Ap	0 – 32	42	24	24	Clay Loam	0.96	2.37	40
Hydraulic Parameters		$\theta_r$	$\theta_s$	$\alpha$	$n$	$m$	$k_s$ (cm hr)	R <sup>2</sup>
	SWCC	0.094	0.299	0.079	1.153	0.285	4.26	0.99
	PTF	0.094	0.569	0.017	1.398	0.285	4.26	n/a
10 cm = 1 EC Sensor, 1 Matric Potential Sensor, 4 Pore Water Probes								
20 cm = 1 EC Sensor, 1 Matric Potential Sensor								

Horizon	Depth (cm)	Particle Size Distribution (%)			Textural Class	Av. $\rho_d$ (g cm <sup>3</sup> )	$\rho_s$ (g cm <sup>3</sup> )	$n_e$ (%)
		Sand	Silt	Clay				
Cr	>32	22	31	47	Clay	0.97	2.42	42
Hydraulic Parameters		$\theta_r$	$\theta_s$	$\alpha$	$n$	$m$	$k_s$ (cm hr)	R <sup>2</sup>
	SWCC	0.108	0.307	0.108	1.139	0.250	4.32	0.99
	PTF	0.108	0.598	0.021	1.331	0.248	4.32	n/a
Not possible to instrument below this depth								

Fig. 7.13c: Profile description of the lowslope installation at the arable site.



**Arable – Midslope**

41 cm

106 cm

Horizon	Depth (cm)	Particle Size Distribution (%)			Textural Class	Av. $\rho_d$ (g cm <sup>3</sup> )	$\rho_s$ (g cm <sup>3</sup> )	$n_e$ (%)
		Sand	Silt	Clay				
Ap	0 – 41	27	30	43	Clay	1.23	2.51	49
Hydraulic Parameters		$\theta_r$	$\theta_s$	$\alpha$	$n$	$m$	$k_s$ (cm hr)	R <sup>2</sup>
	SWCC	0.100	0.613	0.203	1.049	0.270	1.31	0.99
	PTF	0.097	0.508	0.016	1.370	0.270	1.31	n/a
25 cm = 1 EC Sensor, 1 Matric Potential Sensor, 4 Pore Water Probes - Vandalised								

Horizon	Depth (cm)	Particle Size Distribution (%)			Textural Class	Av. $\rho_d$ (g cm <sup>3</sup> )	$\rho_s$ (g cm <sup>3</sup> )	$n_e$ (%)
		Sand	Silt	Clay				
Bc	41-106	34	31	35	Clay Loam	No Cores Obtained		
Hydraulic Parameters		$\theta_r$	$\theta_s$	$\alpha$	$n$	$m$	$k_s$ (cm hr)	R <sup>2</sup>
	No Cores Obtained							
65 cm = 3 Pore Water Probes								

Horizon	Depth (cm)	Particle Size Distribution (%)			Textural Class	Av. $\rho_d$ (g cm <sup>3</sup> )	$\rho_s$ (g cm <sup>3</sup> )	$n_e$ (%)
		Sand	Silt	Clay				
C	>106	29	34	37	Clay Loam	No Cores Obtained		
Hydraulic Parameters		$\theta_r$	$\theta_s$	$\alpha$	$n$	$m$	$k_s$ (cm hr)	R <sup>2</sup>
	No Cores Obtained							
140 cm = 1 EC Sensor, 1 Matric Potential Sensor								

**Fig. 7.13d:** Profile description of the midslope installation at the arable site.

### 7.3 Results

#### 7.3.1 Tracer Results – Pore Water Samples

Vandalism to the pore water samplers at both locations prevented consistent sampling of pore water (Fig. 7.10). For this reason, no bromide concentrations can be presented from the arable site. For the grassland site, sampling was attempted on a fortnightly basis, but the performance of the repaired samplers was impaired. This is a hazard implicit in environmental monitoring outside of a dedicated research facility. Unfortunately, this dearth of pore water samples rendered regression between measured solute concentrations and *EC* impossible. Consequently, chemical concentrations cannot be inferred from *EC* data, but are sufficient to indicate the breakthrough markers.

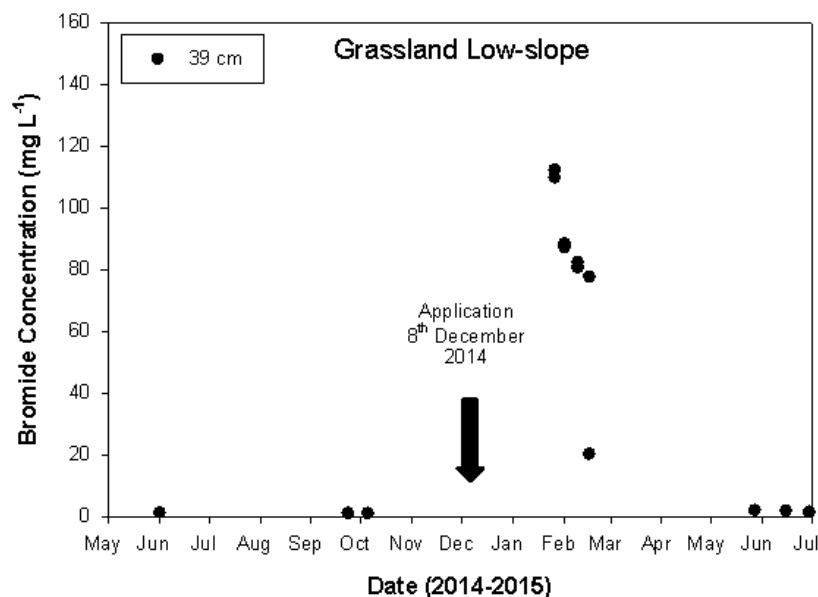


**Fig. 7.14:** Bromide concentration from pore water samples at the grassland low-slope position.

From the results available for the grassland site (Figs. 7.14, 7.15 and 7.16); the following conclusions can be drawn. Both pore water samples and *EC* results indicated peak concentration in February. IBT/Trend could not be reliably ascertained from the pore samples due to insufficient data. Likewise, while there are too few post-peak samples to determine the precise date of solute exit, concentrations declined sharply after peak, and returned to baseline levels prior to June 2015. This is in good agreement with the *EC* results, which indicated exit of the

tracer in early May 2015. An observed peak concentration of  $112.35 \text{ mg L}^{-1}$  was recorded on 26<sup>th</sup> January 2015. Regarding the mid-slope array: pore samples indicated breakthrough of the solute at each of the instrumented depths (10, 20 and 30 cm). Peaks were observed at each of these depths in early February, and declined to baseline levels by June 2015 (June corresponds to 0.40 yrs post application). This is in good agreement with the results of the *EC* probes at the low slope location (Fig. 7.17).

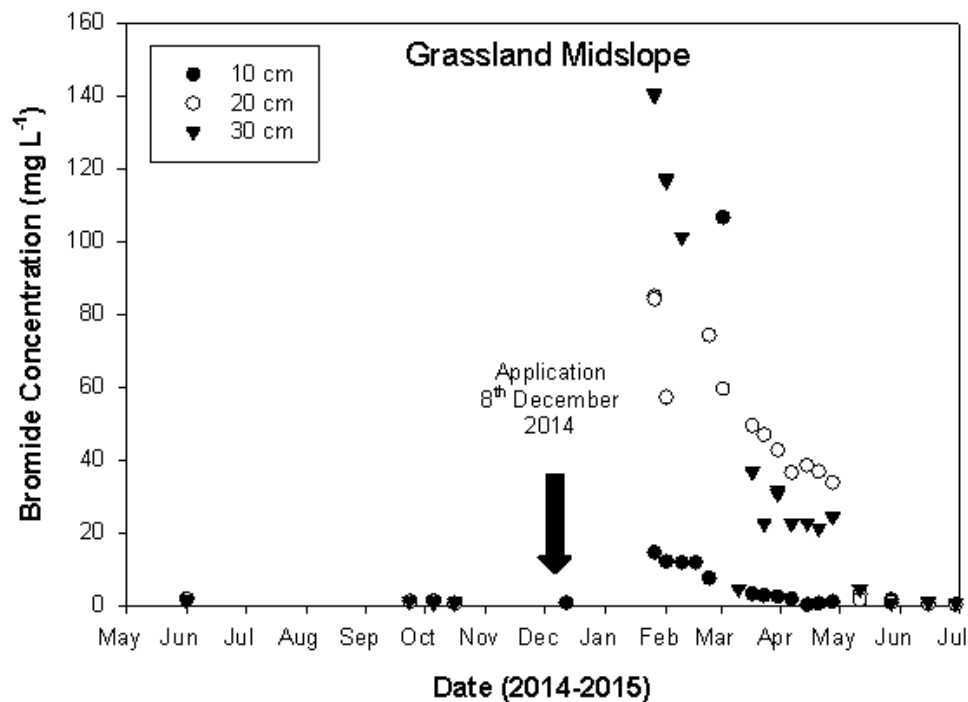


**Fig. 7.15:** Bromide concentration from pore water samples at the grassland midslope position.

Greater peak concentrations were observed at increasing depths, which is counterintuitive, as natural dispersion of the solute with depth would suggest the opposite (Fig. 7.16; scenario A). However, the results did not have sufficient temporal resolution to indicate a staggered breakthrough, i.e. first at 10 cm, then 20 cm, followed by 30 cm below the ground surface. Rather, these suggest that the COM of the solute had already passed the upper sensors, and was now positioned at *c.* 30 cm below the ground surface (Fig 7.16; scenario B). It is important also to remember that these sensors are very shallow and in relatively close proximity to one another, and so dispersion may not be meaningfully exhibited at such a scale. Schulte *et al.* (2006) described similar scenarios as occurring in southern and eastern

areas, in which effective rainfall is often sufficient to facilitate movement of nitrogen to groundwater through the vertical pathway, but insufficient to dilute concentrations below critical loads.

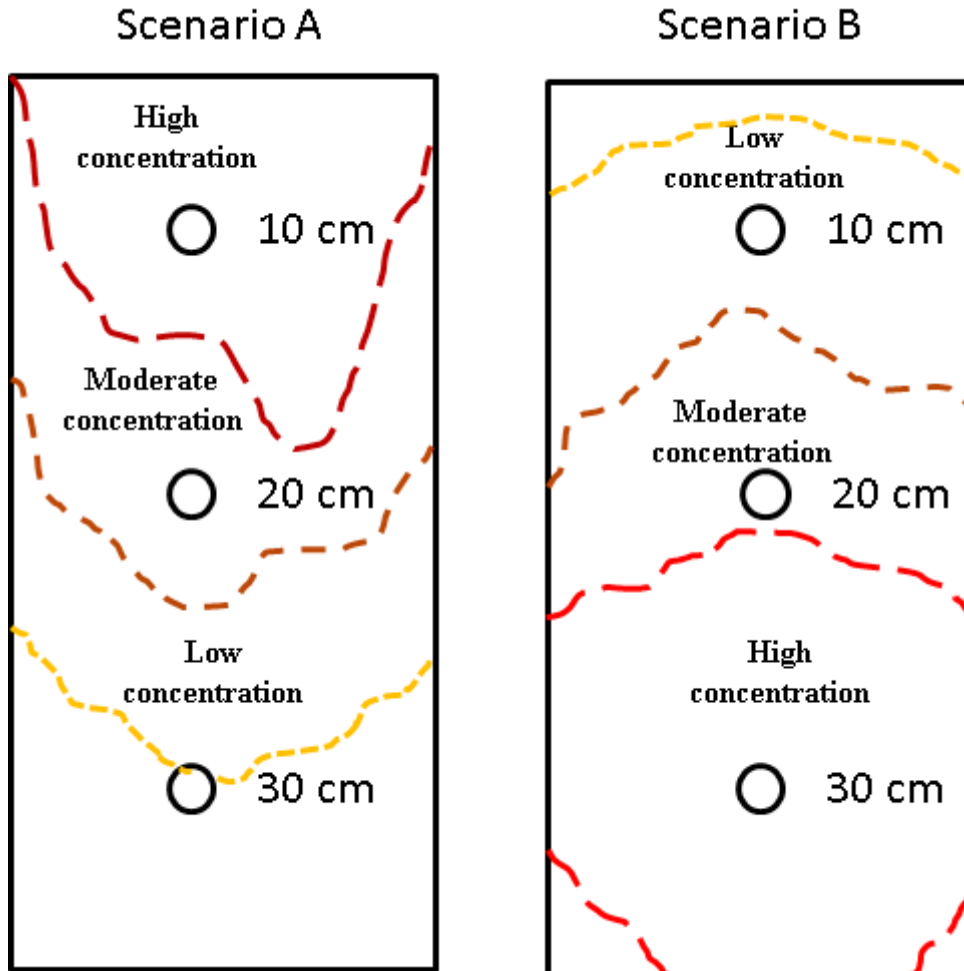


**Fig. 7.16:** Solute transport scenarios, where Scenario A indicates early stages of transport, with the bulk of the solute in the upper horizons, and Scenario B indicates later stage transport, where centre of mass is lower in the soil profile.

### 7.3.2 Tracer Results - Electrical Conductivity

Breakthrough of the KBr- tracer was primarily indicated by changes in *EC* above a baseline level. Baseline *EC* was determined from the maximum values of the week preceding application of the tracer. Baselines were different for the various sensors, reflecting the specific textural, structural, chemical, and saturation conditions at their specific locations. Despite the shallowness of the *EC* sensors, with the exception of the grassland lowslope array, full exit of the tracer (as indicated by

*EC*) was not observed in any study location during the monitoring period. Where markers are not shown (e.g. for the Exit marker) this indicates that this stage of solute time lag was not observed within the experimental timeframe. No measured breakthrough is shown for the grassland midslope site, as there was no discernible increase in *EC* above baseline for that monitoring array. The failure of the grassland midslope *EC* monitoring array to reflect  $\text{KBr}^-$  movement should not be considered to preclude the results from the pore water samples, which indicated a distinct breakthrough of the tracer. This discrepancy may result from an overbearing influence of the properties of the soil matrix itself (including clay content,  $\rho_b$ , temperature, pH, etc.) on *EC* (Rhoades *et al.*, 1999). In this case, the pore water results alone are used to indicate solute transport. *EC* data alone is relied upon for the arable site, due to an absence of pore water samples as a result of vandalism. As the installation of the sensors and samplers were relatively shallow, the duration of time lags should not be considered indicative of  $t_u$  to groundwater, but rather are used solely to assess the model approaches.

### 7.3.3 Model Simulation Results

Figs. 7.17 to 7.19 indicate the estimated breakthrough of the tracer according to the modal profile approach, the textural (low-complexity) and SWCC (high-complexity) approaches assessed from the soil pit, and the measured breakthrough of the  $\text{KBr}^-$  tracers, as detected by changes in *EC*. Full exit of the tracer from these shallow unsaturated zone monitoring arrays was not achieved except for at the grassland midslope location. Good agreement was observed for the IBT/Trend and Peak stages of time lag, between reality and simulations, except for the arable midslope location. While the modal profile estimates differed from the site-specific estimates, the discrepancy was marginal (days) within the context of the 6-yr reporting periods under the EU-WFD.

For the grassland low-slope tracer study (Fig. 7.17), there was a generally good agreement between  $t_u$  estimates derived from measured SWCCs, and actual tracer movement. Peak and COM exhibited particular similarity, although the simulation did not anticipate exit of the solute within the simulated duration, despite observation this marker in the field by 139 days post-application. The simulation did underestimate IBT/Trend relative to the tracer study by *c.* seven days; likely to be

inconsequential in light of trend analysis. The profile-textural approach also performed satisfactorily, approximating IBT/Trend, Peak and COM to within 22 days of tracer results. The model approaches did not anticipate exit within the simulation period, and rather, indicated a more prolonged tailing than was observed in reality. Regarding the grassland mid-slope study, Peak tracer breakthrough at *c.* 47 days, and Exit at *c.* 177 days post-application indicated a greater  $t_u$  than suggested by model approaches.

*EC* measurements at the arable sites similarly indicated later IBT/Trend than estimated by either SWCC or profile-textural simulations. For the arable site study,  $t_u$  at the mid-slope position was underestimated by the modelling approach; with real IBT/Trend (153 days (0.42 yrs)) more closely approximated by COM 112 days (0.31 yrs) than by IBT/Trend 17 days (0.05 yrs) estimates. A similar mismatch of observed and simulated tracer movement was reported by Durner and Weyer (2007).

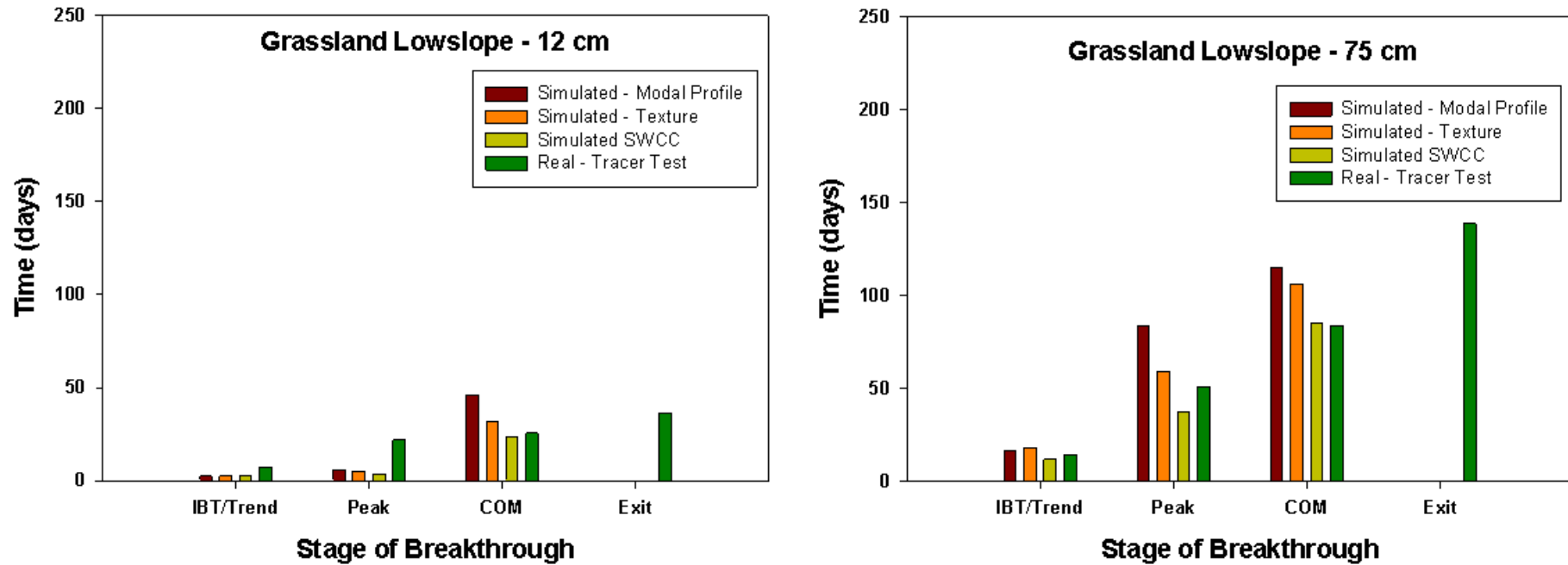


**Fig. 7.17:** Results of the modal and *in situ* (texture and SWCC) simulations, and the field tracer (as detected from *EC*), at the grassland, lowslope location. Model simulations failed to anticipate Exit within the monitoring/simulation period.

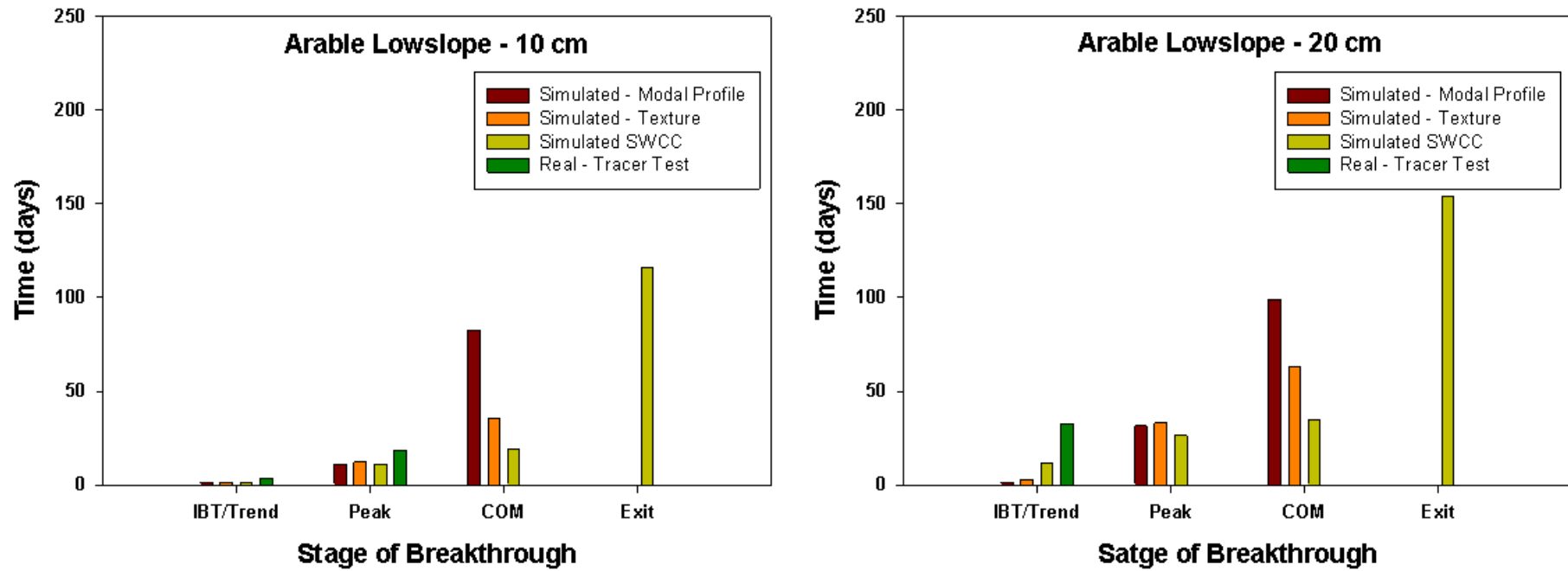


**Fig. 7.18:** Results of the modal and *in situ* (texture and SWCC) simulations, and the field tracer (as detected from *EC*), at the arable, lowslope location. COM and Exit (and Peak at the shallowest sensor) were not observed from tracer test results within the monitoring period.

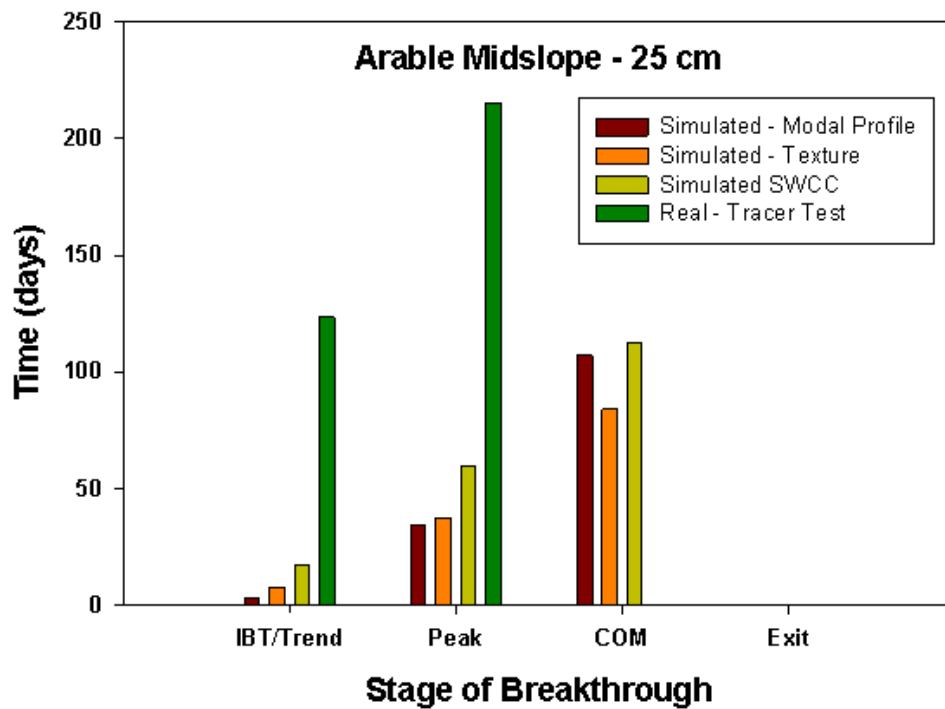


**Fig. 7.19:** Results of the modal and in situ (texture and SWCC) simulations, and the field tracer (as detected from *EC*), at the arable, midslope location. Exit of the solute was not observed in the simulations/tracer results, and COM was not detected from the tracer test.

For the arable midslope location (Fig. 7.19), IBT/Trend at 25 cm was not observed from the tracer study until 123 days post application. This was underestimated by over 100 days by each of the model approaches. This discrepancy was greater for the Peak marker, and neither COM nor Exit of the tracer was observed in the field within the monitoring period.

## 7.4 Discussion

### 7.4.1 General Discussion

Results of the modal approach for both catchments generally resembled the results of the high-complexity simulations. This suggests a minimal advantage to the high-complexity approach, particularly in light of the heterogeneity of soil characteristics on a catchment (Sonneveld and Bouma, 2003), or even on a field scale. For the grassland site, the modal approach estimated  $t_u$  ranges which

encompassed breakthroughs of the  $\text{KBr}^-$  tracer. Contrarily,  $t_u$  at the arable site was underestimated for the mid-slope position, but acceptable for the lower position.

A possible reason for the underestimation of  $t_u$  by the model approaches is an overestimation of the  $k_s$  parameter used in the model, leading to a perceived greater rate of transport. Wösten and van Genuchten (1988) noted the reliance of practitioners on estimates of this parameter derived *via* PTF from more easily measured attributes (texture,  $\rho_d$ ), and suggested that such an approach may ‘*provide the only viable means of characterising the hydraulic properties of a large area of land.*’ As the methodology employed in data assessment herein calculates the retention function only, the  $k_s$  parameter is not adjusted from PTF estimates during the optimization process due to a lack of measured conductivity data. Further investigation following the same input data (real versus estimated) methodology described for the parameters  $\theta_r$ ,  $\theta_s$ ,  $\alpha$  and  $n$ , pertaining rather to  $k_s$  is therefore, strongly recommended. As such, the difference between the three modelling approaches was relatively minor from a policy perspective, which is primarily concerned with  $t_u$  relative to multi-year remediation timescales. There is, therefore, no advantage gained by moving from a modal profile approach to a site-specific assessment for ascertaining trend response. In agreement with the conclusions of Fenton *et al.* (2011), these similarities indicate the dominant influence of rainfall as a control on  $t_u$ . From a groundwater monitoring perspective, in order to implement timely sampling and observation, it is essential that  $t_u$  is predicted as accurately as possible, as an error of just a few days could result in a failure to capture key solute markers. Site-specific data are therefore preferred. Recalling Chapter 3, the differences between high and low-complexity data sources is relatively minor for IBT/Trend assessment, but becomes greater towards the latter stages of transport. Monitoring agencies should consider which stage of transport they wish to observe, and select complexity level accordingly.

The discrepancy between the tracer study and the model estimates at the arable site results from overestimation of soil moisture by the model throughout the simulation period. Assuming that these errors do not originate as a result of problems with the soil water sensors, there are two possible reasons for this discrepancy: 1) runoff, and 2) preferential flow, both of which could lead to scenarios in which the modelled water contents poorly resemble those observed *in situ*.

Regarding the runoff scenario, Mellander *et al.* (2016) indicated a typically greater annual runoff coefficient for the arable site than for the grassland site. This suggests that less of the applied water (in the form of rainfall) infiltrates into the soil profile. This coefficient is controlled not only by soil factors, but by slope, vegetation, rainfall intensity etc. Due to the relatively simple approach to upper boundary conditions herein, it is possible that runoff at this slope position is underestimated, and so, estimated soil water contents poorly reflect reality.

Regarding the preferential flow scenario, the profile exhibited high macroporosity and is highly tilled. Consequently, it may be vulnerable to lateral transport of water and nutrients, and rapid, preferential flow through the vertical pathway. Insufficient sampling precludes quantification of this likely preferential behaviour, but it is evidenced by the highly responsive nature of waterbodies within the catchment to rainfall events (Mellander *et al.*, 2014). As a result, water which may otherwise have saturated the soil matrix (enabling matrix flow), was rapidly removed from the profile. In such scenarios, two time lags are evidenced: one rapid – indicating preferential flow of the bulk of transported nutrients through macropores, and one slow – indicating  $t_u$  through the soil matrix. This has been reported in the literature by solute breakthrough curves exhibiting double peaks (Li and Ghodrati, 1996; Sugita and Nakane, 2007; Durner and Weyer, 2007). This was not reflected by the results of the *EC* probes, which primarily indicate matrix transport. The small diameter and limited spatial reach (Rhoades *et al.*, 1999) means that such probes may not necessarily intercept important, but spatially diverse, macropores (Doležal *et al.*, 2012).

In the present context, it appears more likely that preferential flow at the arable site is responsible. The soil water content never approached field capacity, nor was rainfall intensity sufficient to initiate infiltration-excess overland flow. It must therefore be assumed that the supplied precipitation did infiltrate into the soil. However, that site exhibits high soil porosity and rapid groundwater flow (McAleer *et al.*, manuscript in preparation). Hence, water arriving at the soil surface is rapidly transmitted to the groundwater below, and flushed from the catchment. High  $\text{KBr}^-$  concentrations may therefore have been lost *via* preferential flow, while the remainder of the solute was more slowly transmitted (due to low saturation) *via* matrix flow, and detected by the *EC* probes. Unfortunately, the damage done to the

pore water samplers forestalls confirmation of this hypothesis, but it presents as the most likely explanation based on the contextual evidence.

Where preferential flow is responsible for such differences, a dual-porosity model is more appropriate than the single porosity version used herein. Durner and Weyer (2007) concluded that the discrepancy in their lysimeter/Hydrus 1D study arose from a dual-porosity scenario and Merdun (2012) reported a similar scenario. Practitioners may avail of the dual-porosity facility incorporated in Hydrus, or alternatively, may employ a dedicated dual-porosity model such as MACRO (Jarvis, 1998), used in leaching studies by Larsson (1999), Vasiljev *et al.* (2004), Kramers (2009), and others. The difficulty therefore lies in determining which package, dual- or single-porosity, is appropriate to a given scenario. Kramers (2009) identified that preferential flow is not infrequent in Irish soils, although this by no means rules out matrix associated lags occurring both on other soils, and simultaneously through the matrix of highly structured profiles. At present, hydrological parameters required for the simulation of preferential flow are not readily available at a national scale, nor would such an approach be ubiquitously appropriate. This lack of data has been noted by Kramers (2009), Flühler *et al.* (2000) and Šimůnek *et al.* (2003). Preferential flow is typically studied at a highly localised scale (plot or lysimeter) (Flühler *et al.*, 2000) and hence, extrapolation of this behaviour to a catchment scale is challenging. While site-specific profile assessment may indicate the likelihood of such behaviour, based on root patterns and distribution, or presence of anecic earthworms, etc. (Šimůnek and van Genuchten, 2006), there is no established methodology by which a single- or dual-porosity condition may be ascertained from modal profiles. Köhne *et al.* (2012) noted that PTFs may suffice to roughly approximate the characteristics of dual-porosity systems, but that further development is required to overcome the limitations of that approach. A single-porosity approach as detailed herein, is more implementable, when data availability and scale factors are considered.

A potential limitation of the high-complexity approach pertains to the unquantified heterogeneity of soil hydraulic properties over a given area (Huang *et al.*, 1995; Sonneveld and Bouma, 2003). Textural characteristics, such as those used in the low-complexity approaches, are largely derived from pedogenic factors (weathering, climate, parent material etc.) which typically occur at a relatively broad

scale (Jenny, 1994), e.g. a catchment subject to alluviation will exhibit associated textural properties. Hence, the hydraulic parameters derived from this approach can be assumed to generally characterise that area. Conversely, the SWCC used in the high-complexity approach, reflects extremely site-specific soil structural characteristics (Wang and Zhang, 2011), originating from influences at a much smaller scale, e.g. compaction by vehicles (Vero *et al.*, 2013, Barik *et al.*, 2014 earthworm activity (Whalen, 2004; Johnston *et al.*, 2014), root distribution (Lynch, 1995). The results of this approach are accordingly, appropriate only to the area they are measured in, or which can reliably be understood to reflect those same geneses. Results of the high-complexity approach cannot reliably be extrapolated across a large scale, for instance a catchment, but may be well suited to investigations of  $t_u$  at a localised scale. For example, where a small parcel of land exhibits characteristics unique within the larger landscape (buffer strips, a particularly wet or dry area of a field) or in areas in which  $t_u$  is likely to exert a dominant control over  $t_T$  (in shallow profiles, adjacent to surface receptors), such a high-complexity approach may be justified.

A further limitation is the difficulty in obtaining intact, vertically oriented soil cores in deeper soil profiles, e.g. arable catchment, mid-slope (Fig. 7.13d). An example of a poor soil core is shown in Fig. 7.20. In such cases, a practitioner developing  $t_u$  estimates must revert to PTF-derived hydraulic parameters. The likely soil conditions, both transient, such as moisture and consistency, and characteristic, such as stone or organic matter content, should therefore be considered prior to implementing a high-complexity approach. In such instances, a lower-complexity approach may be judicious, particularly if  $t_r$  is minor. Exempt from this study were measurements of  $k_s$ , with all values inferred *via* PTF. It is not possible therefore, to quantify the effect of measured versus inferred values for this parameter. This presents as a key recommendation for further research.

It should also be acknowledged that even within a catchment, there is spatial and temporal variability in rainfall distribution (Faures *et al.*, 1995), and hence, infiltration and runoff. This lends an element of uncertainty to highly-site specific lag times that is difficult to quantify. However, from a policy perspective,  $t_u$  at a point location is of minimal importance, compared to the prevailing  $t_u$  at the catchment scale – which is indicated in Chapter 5. Regarding  $t_u$  assessment on a

catchment scale, the modal profile approach is optimal, as it allows ranges of  $t_u$  within a catchment to be determined, as opposed to overly-site-specific estimates, as may occur where the highest-resolution approach is employed.



**Fig. 7.20:** An example of a poor soil core, exhibiting both a large stone and an air space. This core is not suitable for SWCC assessment.

#### 7.4.2 Tracer Study

There are limitations to the tracer study presented herein, chiefly the limited observation time, which in some instances, precluded full exit of the solute, and impaired performance of the pore water samplers as a result of vandalism. Such incidents are common outside of dedicated research facilities, and are one of the inherent challenges when operating in ‘real-life’ settings (Macdonald and Jefferies, 2003; Brown and Musil, 2004). This impediment has precluded detailed analyses of tracer concentrations in this study; however, in the absence of absolute concentration values, the changes in *EC* allowed breakthrough markers to be identified. For the purposes of validating the toolkit presented in Chapter 6 primarily as a means to assess IBT/Trend at a catchment scale, the results herein suggest that sufficient similarity exists between IBT/Trend observed in the tracer study and estimated *via* the low-complexity toolkit approach to recommend the toolkit for implementation.

However, it is acknowledged that in some scenarios (e.g. preferential flow), this approach may not be ideal, and investigation of a more suitable approach is required at such locations.

## 7.5 Conclusions

The results of the tracer study indicate that good estimates of  $t_u$  are obtained *via* the modal profile approach. While the high-complexity approach may allow slightly more accurate estimates, these differences are likely to be inconsequential on a catchment scale (given the heterogeneity of the soil medium) and within EU-WFD reporting period timescales. The failure of the toolkit approach to reflect the midslope tracer at the arable location indicates that small-scale variations do exist, and that  $t_u$  ranges obtained *via* the toolkit approach should be considered indicative of catchment behaviour over relatively small timescales (months), rather than prescriptive of rigid dates by which specific  $t_u$  stages will necessarily be observed.

## Summary

This chapter has explored real unsaturated zone time lags, across different soil profiles in two agricultural catchments, as a means to comment on the suitability of the toolkit described in Chapter 6. The modal profile approach produced  $t_u$  estimates which are sufficient to indicate IBT/trends in water quality response, with minimal advantage to increasing input data complexity (by measuring the SWCC). Model approach should be identified primarily on the goals of the end-users/stakeholders, although data availability and the practicalities of sampling play an important role. Chapter 8 will summarise and draw conclusions from the entire thesis, and make recommendations as regards further research.

## Chapter 8

### Conclusions and Recommendations

#### Overview

The primary objective of this thesis was to develop a toolkit to model the “time lag” in the unsaturated zone of a soil between the enactment of programme of measures (POMs) for good agricultural practice and their impact on groundwater quality. This toolkit may be used to guide monitoring agencies and policymakers in the determination of realistic mitigation timeframes, particularly those specified in the EU-WFD. This chapter presents a summary of the findings of this thesis, and suggests how these advances may be applied to catchment monitoring and policy development in the future. Research outcomes are discussed within the context of the Irish environment and its governing policies. This chapter also identifies areas requiring further investigation.

#### 8.1 Synopsis of main research findings

Review of the existing literature (**Chapter 2**) revealed that although hydrological time lag is recognised as a potential limitation to achieving water quality standards within EU-WFD deadlines, no practical assessment method has been established. Particularly challenging is unsaturated zone time lag. Neglecting to account for this region can result in unrealistic expectations regarding POM efficacy. While Fenton *et al.* (2011) presented a simplified methodology (assuming saturated conditions and generic soil properties) by which reasonable estimates of  $t_u$  may be made, a more detailed approach, investigating unsaturated conditions, is required to accurately reflect the complex reality. Numerical models (such as Hydrus) capable of simulating solute transport through a complex soil medium may address this knowledge gap. Input data required by such models include soil properties and meteorological data. In practice, little research has been conducted on the ramifications of decisions made regarding input data selection, sources and methodologies. Clarification of these issues is critical for developing a scientifically reliable and justified framework for  $t_u$  assessment.

The effects of input data resolution on  $t_u$  estimates produced with Hydrus are examined in **Chapter 3**. Results of that chapter identified that low-complexity soil

data (soil texture and bulk density) may indicate trends in POM effects at the base of the soil profile, but where long-term response is of interest, or in particularly vulnerable areas of a catchment, higher-resolution soil data are required (i.e. the measured SWCC). A further conclusion of that study was that increasing the temporal resolution of meteorological input data improved numerical simulations, but for the purposes of trend analysis, a daily time-step provides sufficient resolution.

Regarding the low-complexity data; in **Chapter 4** the consequences of four popular approaches to textural analysis (three of which are laboratory based - laser diffraction, pipette and hydrometer, and one of which is a field assessment – the hand method) and  $t_u$  estimation, are examined. No significant difference in  $t_u$  was observed between the three laboratory techniques, but results of the hand method (which is vulnerable to subjectivity and the expertise of the analyst) differed significantly. This illustrates that for  $t_u$  analysis, whichever laboratory particle size assessment methodology is available to the analyst, should produce acceptable estimates. Prior to this study, no information was available as to the consequences of such methodological decisions (which may be out of the control of the practitioner – subject to the availability of specific equipment in their research facility) on hydrological models.

A practical approach to determining the optimum experimental duration, of centrifugation when constructing SWCCs, has not been established. **Chapter 5** addresses this aspect of the high-complexity approach, by presenting a framework in which SWCCs are constructed, contingent on statistical analysis of various experimental durations. Applying this new, simple methodology to test samples prior to initiation of a soil measurement campaign allows practitioners to ascertain the optimum duration, to allow sufficient dewatering to describe the properties of that soil.

Having established the ability of the low-complexity approach to indicate trends in Chapter 3; a ‘toolkit’ for  $t_u$  assessment was developed in **Chapter 6**, and applied to a grassland and an arable catchment. The toolkit describes data-sources and model assumptions. The practicality of the toolkit approach to provide trend ranges according to the soil series present within agricultural catchments was

demonstrated *via* the two case studies. A critical result of this study was that achieving the full effects of POM within the 6 yr reporting periods designated by the EU-WFD is unrealistic, as  $t_u$  for the deeper soil profiles are estimated at *c.* 5 to 11, and *c.* 6 y yrs, for the grassland and arable catchments, respectively. Ireland has a total of 6,278 river-basin catchments, and over 450 soil series; thus presenting a diversity of hydrological conditions. This catchment-specific approach allows time lag to be understood not as a ‘generic excuse’ to escape stringent policy measures (Scheure and Naus, 2010) but as an intrinsic controlling mechanism, which can be characterised and accounted for.

In **Chapter 7**, *in-situ*  $t_u$  in each of the catchments, introduced in Chapter 6, is examined, *via* surface applied  $KBr^-$  tracers. Reasonable similarity was observed between estimated and measured  $t_u$  for the grassland site, and for one of the tracer locations in the arable site. However, at the second arable location (midslope) a poor similarity was observed. This stemmed from a dissimilarity of simulated and observed soil moisture contents, which may be attributed to runoff or preferential flow at that location. This indicates the importance of appropriate model settings, for a given scenario. However, from a policy perspective, the discrepancy is likely to be of minor importance. The toolkit presented in Chapter 6 still presents as a useful strategy by which policymakers can grasp the likely timeframes in which POMs operate, within the context of catchment heterogeneities.

In summary, the main findings of this thesis are:

- Low-complexity soil input data is sufficient to estimate IBT/Trends in water quality response to POM.
- High-complexity soil input data may be required where the nutrient source is adjacent to a receptor, or to estimate long-term  $t_u$ .
- There is negligible difference in  $t_u$  estimates depending on whether pipette, laser diffraction or hydrometer methods are used for particle size analysis (low-complexity approach), but the hand texturing method leads to discrepancies compared to the laboratory approaches.

- Applying centrifugation for 24-hr (at each pressure step) is insufficient to describe the SWCC. Statistical analysis of the difference in SWCCs constructed according to various temporal treatments can allow the appropriate experimental duration to be determined.
- The toolkit described in this thesis can be used to determine  $t_u$  ranges in agricultural catchments.

## 8.2 Recommendations for Further Research

- This thesis has demonstrated that  $t_u$  alone may preclude agricultural catchments from exhibiting remediation in response to POM. Preliminary incorporation of these results with catchment specific  $t_s$  assessments has begun (McAleer *et al.*, Personal Communication). A more detailed synthesis of these two research projects is required, in order to provide a comprehensive analysis of  $t_T$  at a national level.
- Diverse values of  $t_u$  have been observed in this study, dependent on soil characteristics. Using the SIS database, geological data from the GSI, and regional meteorological data supplied by Met Éireann, a trend map for POM response across Ireland can now be developed in accordance with the methodology applied to the two study catchments in Chapter 6. This would complement existing GIS layers in the above databases, and provide a valuable tool for policy, monitoring and research agencies.
- In this study it was only possible to assess the appropriate centrifuge duration for a single textural class and sample size. Testing of a wide array of soil textural types, management/stress histories, sample sizes, sample formats (disturbed vs. undisturbed), etc. would enable future researchers to determine the appropriate duration for their unique samples. In order to develop an extensive database from which a PTF could be developed, it seems optimum that all researchers applying the centrifuge methodology would utilise the methodological framework presented in Chapter 4. Hence, meta-analysis could be performed, and rules could be formulated based on an extensive database.
- Soil hydraulic conductivity is recognised as an important soil parameter exerting a control on water and solute movement. It was beyond the scope of

this research to apply the low- versus high-complexity methodology used in Chapter 3 to compare inferred versus measured values of conductivity. This would be a valuable addition to the series of papers published in Journal of Contaminant Hydrology assessing the importance of input-data resolution (Vero *et al.*, 2014; Fenton *et al.*, 2015).

- Lidar remote sensing technology has recently been used to develop digital elevation models (DEM) from which critical source areas (CSAs) may be identified. These CSAs indicate zones within a catchment which are vulnerable to phosphorus (Galzski *et al.*, 2011; Thomas *et al.*, 2015) and nitrogen (Tomer *et al.*, 2013) losses to waterbodies. At a sub-catchment scale, this approach could be used to identify areas in which  $t_u$  is important, and thus to target high-complexity soil assessment. This approach should be trialled on existing ACP catchments.
- The toolkit presented herein addresses  $t_u$  through the soil; however, unsaturated zones may also include unsaturated bedrock, exhibiting varying depths, degrees of weathering and hydraulic properties. This region is difficult to characterise, commonly leading to a reliance on literature-derived estimates of water retention characteristics. A methodology by which these characteristics may be assessed should ideally accompany the soil characterisation methodologies described in Chapters 4 and 5.
- This toolkit represents water movement through the soil, and as such, resulting  $t_u$  ranges pertain to a solute exhibiting utterly conservative behaviour. In reality, nutrient attenuation and transformation is likely to further delay waterbody remediation (Burchill *et al.*, 2016). A further refinement to the toolkit would be the incorporation of geochemical software (e.g. the Hydrus-PHREEQC tool, aka HP1 (Jacques and Šimůnek 2005; Jacques *et al.* 2006; Šimůnek *et al.* 2006, 2008)) which would enable these challenges to be addressed.
- This study assumed a single-porosity approach to soil structure, which sufficiently characterises many soils, and for which hydraulic parameters are relatively easy to assess. However, this does not preclude dual-porosity behaviour in other circumstances (Kramers, 2009), in which case, a single-porosity approach will lead to errors in  $t_u$  estimation (as in the arable

midslope location). An addendum is therefore required to Step 2 of the toolkit described in Chapter 6, by which the appropriate approach may be selected, based on a preliminary assessment of soil properties. This may involve identification of soil macropores in the field (earthworm burrows, plant roots, cracks or fractures, etc.). This is more challenging where the modal profile approach is applied, as dual-porosity at a site cannot be reliably inferred to another. A decision-support methodology is therefore, required.

### **8.3 Concluding Remarks**

The results of this study are in agreement with earlier investigations (Fenton *et al.*, 2011) suggesting that  $t_u$  is a critical component of  $t_T$ , and may preclude certain agricultural catchments from exhibiting the full effects of current POM within the designated EU-WFD reporting periods. This thesis has expanded current understanding of  $t_u$ , by presenting ranges for agricultural catchments based on the most up to date Irish soil mapping endeavour (which was conducted at a national 1:1250,000 scale), and presents a toolkit for assessment at a catchment level which may be readily implemented using existing datasets. This provides a structure for high quality characterisation of catchments, as required by the EU-WFD, which has hitherto, not been accomplished. Furthermore, the methodology presented for determining optimum model input data complexity has been accepted by peer-review, and will enable judicious use of resources in future data collection and application.

## Bibliography

Adhikari, K., Pal S, Chakraborty, B., Mukherjee, S.N. and Gangopadhyay, A 2011. Assessment of phenol infiltration resilience in soil media by HYDRUS-1D transport model for a waste discharge site. *Environmental Monitoring Assessment*. 186(10)

Afrous, A., Dejangah, S. and Gholami, A. 2013. Simulation of leaching nitrate with HYDRUS-1D in lysimetry studies under wheat cultivated in arid and semi-arid conditions of Dezful, Iran. *Caspian Journal of Applied Sciences Research*. 2(1): 76-79

Agricultural Catchments Program. 2013. Phase 1 Report: 2008-2011. Teagasc, Johnstown Castle Environment Research Centre. pp110

Ajmal, M., Waseem, M., Wi, S. and Kim, T-W. 2015. Evolution of a parsimonious rainfall-runoff model using soil moisture proxies. *Journal of Hydrology*. 530: 623-633

American Society for Testing and Materials (ASTM), 2008. D6836-02 (Reapproved 2008) Standard test methods for determination of the soil water characteristic curve for desorption using hanging column, pressure extractor, chilled mirror hygrometer, or centrifuge.

American Society for Testing and Materials (ASTM), 2008. D6527. Standard test methods for determining unsaturated and saturated hydraulic conductivity in porous media by steady-state centrifugation.

American Society for Testing and Materials (ASTM), 2014. D854-14. Standard test methods for specific gravity of soil solids by water pycnometer.

Amin, M.G.M., Šimůnek, J. and Lægdsmand, M. 2014. Simulation of the redistribution and fate of contaminants from soil-injected animal slurry. *Agricultural Water Management*. 131: 17-29

Anon. 2014. Timetable and work programme for the development of the second cycle river basin management plans. Consultation document. Water Quality Section, Dept. of the Environment, Community and Local Government, Newtown Road, Wexford.

## Bibliography

<http://www.environ.ie/en/Publications/Environment/Water/FileDownload,38703,en.pdf> Last downloaded 22/10/15

Archbold, M., Bruen, M., Deakin, J., Doody, D., Flynn, R., Kelly-Quinn, M., Misstear, B. and Ofterdinger, U. 2010. Contaminant movement and attenuation along pathways from the land surface to aquatic receptors – A review. STRIVE Report Series No. 56. [https://www.epa.ie/pubs/reports/research/water/STRIVE\\_56\\_Archbold\\_Contaminant\\_sPathwaysReview\\_web.pdf](https://www.epa.ie/pubs/reports/research/water/STRIVE_56_Archbold_Contaminant_sPathwaysReview_web.pdf) Last downloaded 1/11/15

Arheimer, B. and Olsson, J. 2003. Integration and coupling of hydrological models with water quality models: Applications in Europe. Report of the Swedish Meteorological and Hydrological Institute, Norrköping Sweden. pp 49

Arnold, J.G., Srinivasan, R., Muttiah, R.S. and Williams, J.R. 1998. Large area hydrologic modelling and assessment. Part I: Model development. *Journal of American Water Resources Association*. 34: 73-89

Aschonitis, V.G., Kostopoulou, S.K. and Antonopoulos, V.Z. 2012. Methodology to assess the effects of rice cultivation under flooded conditions on van Genuchten's model parameters and pore size distribution. *Transport in Porous Media*. 91(3): 861-876

Asgarzadeh, H., Mosaddeghi, M.R., Nikbakht, A.M., 2014. SAWCal: A user-friendly program for calculating soil available water quantities and physical quality indices, *Computers and Electronics in Agriculture*, 109, 86-93

Azevedo, L.B., van Zelm, R., Leuven, R.S.E.W., Hendriks, A.J. and Huijbregts, M.A.J. 2015. Combined ecological risks of nitrogen and phosphorus in European freshwaters. *Environmental Pollution*. 200: 85-92

Baily, A. Rock, L., Watson, C.J. and Fenton, O. 2011. Spatial and temporal variations in groundwater nitrate at an intensive dairy farm in south-east Ireland: insights from stable isotope data. *Agriculture, Ecosystems & Environment*. 144: 308-318

## Bibliography

- Ball, B.C., Campbell, D.J. and Hunter, E.A. 2000. Soil compactability in relation to physical and organic properties at 156 sites in UK. *Soil and Tillage Research*. 57(1-2): 83-91
- Barik, K., Aksakal, E.L., Islam, K.R., Sari, S. and Angin, I. 2014. Spatial variability in soil compaction properties associated with field traffic operations. *Catena*. 120: 122-133
- Bartlett, M.S., Daly, E., McDonnell, J.J., Parolari, A.J. and Porporato, A. 2015. Stochastic rainfall-runoff model with explicit soil moisture dynamics. *Proceedings of the Royal Society A*. 471(2183)
- Bechmann, M., Deelstra, J., Stålnacke, P., Eggestad, H.O., Øygarden, L., Pengerud, A. 2008. Monitoring catchment scale agricultural pollution in Norway: policy instruments, implementation of mitigation methods and trends in nutrient and sediment losses. *Environmental Science & Policy*. 11: 102-114.
- Behrendt, H., Huber, P., Kornmilch, M., Opitz, D., Schmoll, O., Scholz, G., Uebe, R. 2000. Nutrient Emissions into river basins of Germany. UBA-Texte, 23/00, p 266.
- Bejat, L., Perfect, E., Quisenberry, V.L., Coyne, M.S. and Hazler, G.R. 2000. Solute transport as related to soil structure in unsaturated intact soil blocks. *Soil Science Society of America Journal*. 64(3): 818-826
- Bergström, S. 1991. Principles and confidence in hydrological modelling. *Nordic Hydrology*. 22: 123-136.
- Beuselinck, L., Govers, G., Poesen, J., Degraer, G., Froyen, L. 1998. Grain-size analysis by laser diffractometry: comparison with the sieve/pipette method. *Catena*. 32, 193–208.
- Bingham, A.H. and Cotrufo, M.F. 2015. Organic nitrogen storage in mineral soil: Implications for policy and management. *Soil Discussions*. 2: 587-618.
- Bittelli, M. and Flury, M. 2009. Errors in water retention curves determined with pressure plates. *Soil Science Society of America Journal*. 73(5): 1453-1560
- Blanco-Canqui, H. and Lal, R. 2008. Principles of soil conservation and management. Springer. pp 617

## Bibliography

Bouraoui, F. and Grizzetti, B. 2008. An integrated modelling framework to estimate the fate of nutrients: Application to the Loire (France). *Ecological Modelling*. 212: 450-459

Bouraoui, F. and Grizzetti, B. 2014. Modelling mitigation options to reduce diffuse nitrogen water pollution from agriculture. *Science of the Total Environment*. 468-469: 1267-1277

Bowman, R.S. 1983. Evaluation of some new tracers for soil water studies. *Soil Science Society of America Journal*. 48(5): 987-993

Boyle, G., O'Mara, F. and Schulte, R.P.O. 2013. The science of sustainability – Food Harvest 2020 and beyond. <http://www.ifa.ie/wp-content/uploads/2013/11/The-Science-of-Agrifood.pdf> Last downloaded 1/11/2015

Brandi-Dohrn, F.M., Dick, R.P., Hess., M. and Selker, J.S. 1996. Suction cup sampler bias in leaching characterisation of an undisturbed field soil. *Water Resources Research*. 32(5): 1173-1182

Breathnach, P. 2000. The evolution of the spatial structure of the Irish dairy processing industry. *Irish Geography*. 33(2): 166-184

Brennan, F.P., Kramers, G., Grant, J., O'Flaherty, V., Holden, N.M. and Richards, K.G. 2012. Evaluating E-coli transport risk in soil using dye and bromide tracers. *Soil Science Society of America Journal*. 76(2):663-676

Briggs L.J. and McLane, J.W. 1907. The moisture equivalent of soils. USDA Bureau of Soils Bulletin. 45: 23

British Standard, 1989. Pipette Method, (BS 1796, 1989). Methods of test for soils for civil engineering purposes

British Standard, 1990. Hydrometer Method (BS1377:Part 2:1990). Methods of test for soils for civil engineering purposes: Classification tests

British Standard, 2009. Particle size analysis. ISO 13320: Laser diffraction methods.

Brooks, R.H. and Corey, A.T. 1964. Hydraulic properties of porous media. Hydrology Papers. Colorado State University, fort Collins, Colorado.

## Bibliography

- Brooks, R.H. and Corey, A.T. 1966. Properties of porous media affecting fluid flow. *Journal of Irrigation, Drainage Division*. American Society of Civil Engineering. 72(IR2): 61-88
- Brown, P. and Musil, S.A. 2004. Automated data acquisition and processing. In. *Environmental Monitoring and Characterisation*. Eds. Artiola, J.F., Pepper, I.L. and Brusseau, M. Elsevier Academic Press
- Brunner, P., & Simmons, C. T. 2012. HydroGeoSphere: a fully integrated, physically based hydrological model. *Groundwater*, 50(2), 170-176.
- Buckley, C. and Carney, P. 2013. The potential to reduce the risk of diffuse pollution from agriculture while improving economic performance at farm level. *Environmental Science and Policy*. 25: 118-126
- Buckley, C., Wall, D., Moran, B. and Murphy, P. 2015. Expanding milk production while achieving water quality targets. *T Research*. 10(2): 50-51
- Burchill, W., Lanigan, G.J., Li, D., Williams, M. and Humphreys, J. 2016. A system N balance for a pasture-based system of dairy production under moist maritime climatic conditions. *Agriculture, Ecosystems and Environment*. 220: 202-210
- Campbell, G.S. and Wacker, K. 2014. Moisture sorption at high temperature and low water potential effects water content measurements. Revisiting The Most Important Curve In Soil Physics I. ASA-CSSA-SSSA Annual International Meeting. 3-5 Nov. 2014. Long Beach, California.
- Campbell Scientific. 2015. Loggernet Manual. V.4.3. <https://s.campbellsci.com/documents/us/manuals/loggernet.pdf>. Last accessed 14/10/15
- Caputo, M.C. and Nimmo, J.R. 2005. Quasi-steady centrifuge method for unsaturated hydraulic properties. *Water Resources Research*. 41(11): W11504
- Caron, J., Bonin, S., Pepin, S., Vanderleest, C. and Bland, W. 2014. Hysteresis phenomenon and threshold water potentials for cranberry irrigation. Revisiting The Most Important Curve In Soil Physics I. ASA-CSSA-SSSA Annual International Meeting. 3-5 Nov. 2014. Long Beach, California.

## Bibliography

Carpenter, S.R., Caraco, N.F., Correll, D.L., Howarth, R.W., Sharpley, A.N. and Smith, V.H. 1998. Nonpoint pollution of surface waters with phosphorus and nitrogen. *Ecological Applications*. 8: 559-568

Carsel, R.F. and Parrish, R.S. 1988. Developing joint probability distributions of soil water retention characteristics. *Water Resources Research*. 24: 755-769

Celier, P., Durand, P., Hutchings, N., Dragosits, U., Theobald, M., Drouet, J-L. and Oenema, O., Bleeker, A., Breuer, L., Dalgaard, T., Duret, S., Kros, J., Loubet, B., Olesin, J.E., Merot, P., Viaud, V., de Vries, W. and Sutton, M.A. 2011. Nitrogen flows and fate in rural landscapes. In. *The European Nitrogen Assessment*. Eds. Sutton, M.A., Howard, C.M., Erisman, J.W., Billen, G., Bleeker, A., Grennfelt, P., van Grinsven, H. and Grizzetti, B. pp 229-248

Cherry, K.A., Shepherd, M., Withers, P.J.A. and Mooney, S.J. 2008. Assessing the effectiveness of actions to mitigate nutrient loss from agriculture: A review of methods. *Science of the Total Environment*. 1-23

Chiu, T-F, and Shackleford, C.D. 1998. Unsaturated hydraulic conductivity of compacted sand-kaolin mixtures. *Journal of Geotechnical and Geoenvironmental Engineering*. 124(2): 160-170

Chrysikopoulos, C.V., Roberts, P.V. and Kitanidis, P.K. 1990. One-dimensional solute transport in porous media with partial well-to-well recirculation: Application to field experiments. *Water Resources Research*. 26(6): 1189-1195

Chyzheuskaya, A. 2015. Modelling the economics of water pollution improvement in the agricultural context. Ph.D thesis. National University of Ireland, Galway.

Cobos, D.R. and Rivera, D. 2014. Can the dry-end (-1 to -1000 MPa) soil water characteristic curve be well characterised with a single point? Revisiting The Most Important Curve In Soil Physics I. ASA-CSSA-SSSA Annual International Meeting. 3-5 Nov. 2014. Long Beach, California.

Collins, A.L. and McGonigle, D.F. 2008. Monitoring and modelling diffuse pollution for agriculture policy support: UK and European experience. *Environmental Science and Policy*. 11: 97-101.

## Bibliography

Cook, P.G., Jolly, I.D., Walker, G.R. and Robinson, N.I. 2003. From drainage to recharge to discharge: some timelags in subsurface hydrology. In: Alsharhan, A.S., Wood, W.W. (Eds). *Water Resources Perspectives: Evaluation, Management and Policy*. Elsevier Science, Amsterdam, pp. 319-326

Costa, W.A., Oliveira, C.A. and Eiyti, K. 2008. Adjustment models and methods for determining the soil water retention curve of a red-yellow Latosol. *Revista Brasileira de Ciência do Solo*. 32(2): 515-523

Craig, M. and Daly, D. 2010. Methodology for establishing threshold values and the assessment of chemical and quantitative status of groundwater, including an assessment of pollution trends and trend reversal. Hydrometric and Groundwater Section, Office of Environmental Assessment, EPA, Dublin.

Creamer, R. 2014. Irish SIS Final Technical Report 10: Soil Profile Handbook. Associated datasets and digital information objects connected to this resource are available at: Secure Archive for Environmental Research Data (SAFER) managed by Environmental Protection Agency Ireland <http://erc.epa.ie/safer/resource?id=a1b872a2-3b8c-11e4-b233-005056ae0019> (Last Accessed: 2015-03-19)

Cresswell, H.P., Green, T.W. and McKenzie, N.J. 2008. The adequacy of pressure plate apparatus for determining soil water retention. *Soil Science Society of America Journal*. 72: 41-49

Croney, D., Coleman, J.D. and Bridge, P.M. 1952. The suction of moisture held in soil and other porous materials. Department of Scientific and Industrial Research. Road Research Technical Paper No. 24. H.M. Stationery Office, London.

Cropper, S.C., Perfect, E., van den Berg, E.H. and Mayes, M.A. 2011. Comparison of average and point capillary pressure-saturation functions determined by steady state centrifugation. *Soil Science Society of America Journal*. 75(1): 17-25

Daly, D. 2011. Some implications of implementing the EU Water Framework Directive for developing agriculture – an EPA view. National Agrienvironment Conference 2011.

## Bibliography

Dane, J.H. and Topp, G.C. (Eds) 2002. Methods of soil analysis: Part 1, Physical methods. 3rd ed. Soil Science Society of America. Madison, Wisconsin.

Dann, R., Bidwell, V., Thomas, S. Wöhling, T. and Close, M. 2010. Modelling of nonequilibrium bromide transport through alluvial gravel vadose zones. *Vadose Zone Journal*. 9: 731-746

Decagon. 2015. Vapor Sorption Analyzer: Operator's manual. 2365 NE Hopkins Court, Pullman WA 99163

Decagon. 2015. 5TE Water content, EC and temperature sensor manual. 2365 NE Hopkins Court, Pullman WA 99163. Last downloaded 15/10/15

DELG/EPA/GSI, 1999. Groundwater Protection Schemes. Department of the Environment and Local Government, Environmental Protection Agency and Geological Survey of Ireland, Ireland.

Dept. of Agriculture, Food and the Marine. 2010. Food Harvest 2020. A Vision for Irish Agri-Food and Fisheries. <https://www.agriculture.gov.ie/media/migration/agri-foodindustry/foodharvest2020/2020FoodHarvestEng240810.pdf> Last downloaded 1/11/15

Dept. of Agriculture, Food and the Marine. 2015. Food Wise 2025. A 10-year vision for the Irish agri-food industry. <http://www.agriculture.gov.ie/media/migration/agri-foodindustry/foodwise2025/report/FoodWise2025.pdf>. Last downloaded 15/10/15

Dexter AR., 2004a. Soil physical quality. Part I: Theory, effects of soil texture, density and organic matter, and effects on root growth. *Geoderma* 120, 201–214.

Dexter AR., 2004b. Soil physical quality. Part II: Friability, tillage, tith and hard-setting. *Geoderma* 120, 215–226.

Dexter AR., 2004c. Soil physical quality. Part III: Unsaturated hydraulic Conductivity and general conclusions about S-theory. *Geoderma* 120, 227–239.

Dexter, A.R., Czyż, E.A., 2007. Applications of S-theory in the study of soil physical degradation and its consequences.

Dexter A.R., Czyż E.A., and Richard G., 2012. Equilibrium, non-equilibrium and residual water: consequences for soil water retention. *Geoderma*, 177/178, 63-71.

## Bibliography

Diamantopoulos, E. and Durner, W. 2014. Closed-form model for hysteretic hydraulic properties based on angular pores with variable contact angles. Revisiting The Most Important Curve In Soil Physics I. ASA-CSSA-SSSA Annual International Meeting. 3-5 Nov. 2014. Long Beach, California.

Diamond, J. and Shanley, T. 2003. Infiltration rate assessment of some major soils. *Irish Geography*. 36(1): 32-46

Diamond, J. and Sills, P. 2011. Soils of Co. Waterford. Soil Survey Bulletin No. 44. National Soil Survey of Ireland. Teagasc, Oakpark, Co. Carlow. pp314

Dillon, E.J., Hennessy, T., Buckley, C., Donnellan, T., Hanrahan, K., Moran, B. and Ryan, M. 2014. The sustainable intensification of the Irish dairy sector. 88th Annual Conference of the Agricultural Economics Society, AgroParisTech, Paris, France. 9<sup>th</sup> -11<sup>th</sup> April 2014.

Doležal, F., Matula, S. and Moreira Barradas, J.M. 2012. Percolation in macropores and performance of large time-domain reflectometry sensors. *Plant Soil and Environment*. 58: 503-507

Doody, D., Moles, R., Tunney, H., Kurz, I., Bourke, D., Daly, K. and O'Regan, B. 2006. Impact of flow path length and flow rate on phosphorus loss in simulated overland flow from a humic gleysol grassland soil. *Science of the Total Environment*. 372: 247-255

Drew, D.P. 2008. Hydrogeology of lowland karst in Ireland. *Quarterly Journal of Engineering*,

Drummond, J.D., Covino, T.P., Aubeneau, A.F., Leong, D., Patil, S., Schumer, R. and Packman, A.I. 2012. Effects of solute breakthrough curve tail truncation on residence time estimates: A synthesis of solute tracer injection studies. *Journal of Geophysical Research*. 117

Durner, W. 1994. Hydraulic conductivity estimation for soils with heterogeneous pore structure. *Water Resources Research*. 30(2): 211-223

## Bibliography

Durner, W. and Lipsius, K. 2005. Chapter 75: Determining soil hydraulic properties. In. *Encyclopaedia of Hydrological Sciences*. Ed. Anderson, M.G. John Wiley and Sons Ltd.

Durner, W. and Weyer, J. 2007. Bromide Transport in a Sandy and a Silty Soil - A Comparative Lysimeter Study - Research Report. Technische Universität Braunschweig. <http://www.soil.tu-bs.de/download/downloads/reports/2007.Bromide-report.Weyer.pdf> Accessed 1/10/15

Durner, W. 2014. Soil hydraulic functions revisited: Challenges and solutions. Revisiting The Most Important Curve In Soil Physics I. ASA-CSSA-SSSA Annual International Meeting. 3-5 Nov. 2014. Long Beach, California.

Dworak, T., Gonzalez, C., Laaser, C. and Interwies, E. 2005. The need for new monitoring tools to implement the WFD. *Environmental Science and Policy*. 8: 301-306

Environmental Protection Agency. 2005. Submission in accordance with Article 5 of Directive 2000/60/EC of the European Parliament and of the Council of 23 October 2000 establishing a framework for Community action in the field of water policy, and in accordance with EC-DG Environment D.2 document "Reporting Sheets for 2005 Reporting" dated 19 November 2004. Version 2. EPA, Johnstown Castle, Wexford, Ireland.

Environmental Protection Agency. 2008. Water Quality in Ireland 2004-2006. EPA, Johnstown Castle, Wexford, Ireland

Environmental Protection Agency. 2015. An approach to characterisation as part of implementation of the Water Framework Directive. V2 Revised. [http://www.epa.ie/pubs/reports/water/other/WFD%20Characterisation%20Approach%20\(May%202015\).pdf](http://www.epa.ie/pubs/reports/water/other/WFD%20Characterisation%20Approach%20(May%202015).pdf) Last accessed 8/9/15

Environmental Protection Agency. 2015. Water Quality in Ireland: 2010-2012. Prepared for the EPA by Aquatic Environment, Office of Environmental Assessment. Eds. Byrne, C. and Fanning, A.

## Bibliography

<http://www.epa.ie/pubs/reports/water/waterqua/wqr20102012/WaterQualityReport.pdf> Last accessed 26/10/15

European Commission, 1991. Council Directive (1991/676/EC). EC Directive of the European Parliament and of the Council of 12 December 1991 on the protection of waters against pollution caused by nitrates from agricultural sources. Brussels. pp 1-8

European Commission, 2000. Council Directive (2000/60/EC). EC Directive of the European Parliament and of the Council 200/60/EC establishing a framework for community action in the field of water policy. Brussels. pp72

European Commission, 2006. Statutory Instrument 378. (Good Agricultural Practice for the Protection of Waters) Regulations 2006. Statutory Office, Dublin, Ireland.

European Commission, 2009. Statutory Instrument 101. (Good Agricultural Practice for the Protection of Waters) Regulations 2009. Statutory Office, Dublin, Ireland.

European Commission. 2009. Guidance on groundwater status and trend assessments. CIS Guidance Document co. 18. Luxembourg. Office for Official Publications of the European Communities. 84 pp

European Commission, 2010. Statutory Instrument 610. (Good Agricultural Practice for the Protection of Waters) Regulations 2010. Statutory Office, Dublin, Ireland.

European Commission, 2014. Statutory Instrument 31. (Good Agricultural Practice for the Protection of Waters) Regulations 2014. Statutory Office, Dublin, Ireland.

European Environment Agency. 2013. Chemical status indicators for water across Europe. <http://www.eea.europa.eu/data-and-maps/indicators/wfd-indicator-chemical-status/assessment> Last accessed 26/10/15

Fallico, C., Chidichimo, F. And Straface, S. 2012. Solute dispersion in porous media at different transport velocities and distances. *International Water Technology Journal*. 2(2)

Faures, J-M, Goodrich, D.C., Woolhiser, D.A. and Sorooshian, S. 1995. Impact of small-scale spatial rainfall variability on runoff modelling. *Journal of Hydrology*. 173: 309-326

## Bibliography

- Fealy, R., Buckley, C., Mechan, S., Melland, A., Mellander, P., Shortle, G, Wall, D. and Jordan, D. 2010. The Irish Agricultural Catchments Programme: catchment selection using spatial multi-criteria decision analysis. *Soil Use and Management*. 26: 225-236
- Fenton, O., Healy, M.G. and Rogers, M. 2008. Preliminary steps in the location of a farm-scale groundwater remediation system. Proceedings of ESAI Environ 2007.
- Fenton, O., Richards, K.G., Kirwan, L., Khalil, M.I., Healy, M.G. 2009. Factors affecting nitrate distribution in shallow groundwater under a beef farm in South Eastern Ireland. *Journal of Environmental Management*. 90, 3135–3146.
- Fenton, O., Schulte, R.P.O., Jordan, P., Lalor, S.T.J. and Richards, K.G. 2011. Time lag: A methodology for estimation of vertical and horizontal travel and flushing timescales to nitrate threshold concentrations in Irish aquifers. *Environmental Science and Policy*. 14(4): 419-431
- Fenton, O., Vero, S.E., Ibrahim, T.G., Murphy, P.N.C., Sherriff, S. and Ó'hUallachian, D. 2015. Consequences of using different soil texture determination methodologies for soil physical quality and unsaturated zone time lag estimates. *Journal of Contaminant Hydrology*. 182: 16-24
- Ferns Engineering. 2013. Kileens, Co. Wexford, Ireland
- Fetter, C.W. 2008. Contaminant Hydrogeology 2<sup>nd</sup> Ed. Waveland Press Inc.
- Fleige, H. and Horn, R. 2000. Field experiments on the effect of soil compaction on soil properties, runoff, interflow and erosion. *Advances in Geoecology*. 32: 258-268
- Flury, M. and Wai, N.N. 2003. Dyes as tracers for vadose zone hydrology. *Reviews of Geophysics*, 41, 1 / 1002 2003 doi:10.1029/2001RG000109
- Fleming, J. B., and Butters, G.L. 1995. Bromide transport detection in tilled and nontilled soil-Solution samplers vs. soil cores. *Soil Science Society of America Journal*. 59(5), 1207–1216.
- Flühler, H., Ursino, N., Bundt, M., Zimmerman, U. and Stamm, C. 2000. The preferential flow syndrome – A buzzword or a scientific problem. ASAE. Preferential Flow: Water movement and chemical transport in the environment. Proceedings of the 2<sup>nd</sup> International Symposium.

## Bibliography

Forrer, I., Kasteel, R., Flury, M. and Flühler, H. 1999. Longitudinal and lateral dispersion in an unsaturated field soil. *Water Resources Research*. 35(10): 3049-3060

Foussereau, X., Graham, W.D., Akpoji, G.A., Destouni, G. and Rao, P.S.C. 2001. Solute transport through a heterogeneous coupled vadose-saturated zone system with temporally random rainfall. *Water Resources Research*. 37(6): 1577-1588

Fredlund, D.G. and Xing, A. 1994. Equations for the soil-water characteristic curve. *Canadian Geotechnical Journal*. 31: 521-532

Fredlund, D.G. 2002. Use of soil-water characteristic curve in the implementation of unsaturated soil mechanics. Keynote address. In Proceedings of the 3rd International Conference on Unsaturated Soils, UNSAT 2002, Recife, Brazil, 10–13 March 2002. Edited by J.F.T. Juca, T.M.P. de Campos, and F.A.M. Marinho. Taylor and Francis, London. Vol. 3, pp. 887–902.

Frind, E.O., Molson, J.W. and Rudolph, D.L. 2006. Well vulnerability: A quantitative approach for source water protection. *Groundwater*. 44(5): 732-742

Galzki, J.C., Birr, A.S. and Mulla, D.J. 2011. Identifying critical agricultural areas with three-meter LiDAR elevation data for precision conservation. *Journal of Soil and Water Conservation*. 66(6): 423-130

Gardner, R. 1937. A method of measuring the capillary tension of soil over a wide moisture range. *Soil Science*. 43: 277 – 283

Gburek, W.J. and Sharpley, A.N. 1998. Hydrologic Controls on Phosphorus Loss from Upland Agricultural Watersheds. *Journal of Environmental Quality*. 27: 267-277.

Gebhardt, S., Fliege, H. and Horn, R. 2009. Effect of compaction on pore functions of soils in a Saalean moraine landscape in North Germany. *Journal of Plant Nutrition and Soil Science*. 172(5): 688-695

Gee, G.W., Ward, A.L., Zhang, Z.F., Campbell, G.S. and Mathison, J. 2002. The influence of hydraulic nonequilibrium on pressure plate data. *Vadose Zone Journal*. 1: 172-178

## Bibliography

Gerke, H.H., 2006. Preferential flow descriptions for structured soils. *Journal of Plant Nutrition and Soil Science*. 169(3): 382-400

Gibbons, P., Rogers, M. and Mulqueen, J. 2006. Nitrate leaching – Soil investigation. Final Report. Environmental Protection Agency. Wexford, Ireland. 128 pp.

Gilley, J.E., Finkner, S.C., Doran, J.W. and Kottwitz, E.R. 1990. Adsorption of bromide racers onto sediment. *Applied Engineering in Agriculture*. 6(1): 35-38

Gladnyeva, R. and Saifadeen, A. 2013. Effects of hysteresis and temporal variability in meteorological input data in modelling of solute transport in unsaturated soil using Hydrus-1D. *Journal of Water Management and Research*. 68: 285-293

Goodale, C. L., Aber, J.D. and Ollinger, S.V. 1998. Mapping monthly precipitation, temperature and solar radiation for Ireland with polynomial regression and a digital elevation model. *Climate Research*. 10: 35-49

Goodchild, R.G. 1998. EU policies for the reduction of nitrogen in water: The example of the Nitrates Directive. *Environmental Pollution*. 102 (S1): 737-740

Granlund, K., Räike, A., Ekholm, P., Rankinen, K., Rekolainen, S., 2005. Assessment of water protection targets for agricultural nutrient loading in Finland. *Journal of Hydrology*. 304: 251-260

Grizzetti, B., Bouraoui, F. and De Marsily, G. 2008. Assessing nitrogen pressures on European surface water. *Global Biogeochemical Cycles*. 22

Grizzetti, B., Bouraoui, F. and Aloe, A. 2012. Changes of nitrogen and phosphorus loads to European seas. *Global Change Biology*. 18: 769-782

Gubiani, P.I., Reichert, J.M., Campbell, C., Reinert, D.J. and Gelain, N.S. 2012. Assessing errors and accuracy in dew-point potentiometer and pressure plate extractor measurements. *Soil Science Society of America Journal*. 77: 19-24

Gumiere, S.J., Caron, J., Périard, Y. and Lafond, J. 2013. Effects of spatial variability of soil hydraulic properties on water dynamics. EGU General Assembly 2013. 7th-12th April, Vienna, Austria

## Bibliography

Hamilton, S.K. 2012. Biogeochemical time lags may delay responses of streams to ecological restoration. *Freshwater Biology*. 57(1): 43-57

Hardie, M., Doyle, R., Cotching, W., Holz, G. and Lisson, S. 2013. Hydropedology and preferential flow in the Tasmanian texture-contrast soils. *Vadose Zone Journal*. 12(4): 1539-1663

Hassler, G.L. and Brunner, E. 1945. Measurement of capillary pressures in small core samples. Transactions of the American Institute of Mining, Metallurgical and Petroleum Engineers. 160: 114-123

Heatwole, K.K. and McCray, J.J. 2007. Modelling potential vadose-zone transport of nitrogen from onsite wastewater systems at the development scale. *Journal of Contaminant Hydrology*. 91(1-2): 184-201

Helliwell, J. 2011. An assessment of nitrate leaching risk for different buffer strip establishments. *Bioscience Horizons*. 4(1): 79-89

Hennessy, T. and Kinsella, A. 2013. 40 Years of Irish farming since joining the European Union: A journey with the Teagasc National Farm Survey 1972 to 2012. Teagasc Rural Economy and Development Programme, Athenry.

Herbin, T., Hennessy, D., Richards, K.G., Piwawarczyk, A., Murphy, J.J. and Holden, N.M. 2011. The effects of dairy cow weight on selected soil physical properties indicative of compaction. *Soil Use and Management*. 27: 36-44

Hillel, D. 2004. Introduction to Environmental Soil Physics. Elsevier Academic Press.

Hooker, K.V. 2005. A field study of nitrate leaching from tillage land in south east Ireland. M.Sc. thesis. Trinity College, Dublin, Ireland

Hooper, R.P. 2009. Towards and intellectual structure for hydrologic sciences. *Hydrological Processes*. 23: 353-355

Horel, A., Lichner, L., Alaoui, A., Czachor, H., Nagy, V. and Tóth, E. 2014. Transport of iodide in structured clay-loam soil under maize during irrigation experiments analysed using HYDRUS model. *Biologia*. 69(11): 1531-1538

## Bibliography

Huang, K., Toride, N. and van Genuchten, M. Th. 1995. Experimental investigation of solute transport in large, homogeneous and heterogeneous, saturated soil columns. *Transport in Porous Media*. 18(3): 283-302

Huebsch, M., Horan, B., Richards, K., Blum, P., Grant, J. and Fenton, O. 2013. Impact of agronomic practices of an intensive dairy farm on nitrogen concentrations in a karst aquifer in Ireland. *Agriculture, Ecosystems and Environment*. 179: 187-199

Huebsch, M., Fenton, O., Horan, B., Hennessy, D., Richards, K. G., Jordan, P., Goldscheider, N., Butscher, C., Blum, P., 2014. Mobilisation or dilution? Nitrate response of karst springs to high rainfall events, *Hydrol. Earth Syst. Sci. Discuss.*, 11, 4131–4161.

Humphreys, J., Casey, I.A., Darmody, P., O'Connell, K., Fenton, O. and Watson, C.J. 2008. Soil mineral N and nitrate-N losses to groundwater from four grassland-based systems of dairy production on a clay-loam soil under moist temperate climatic conditions. *Grass and Forage Science*. 63: 481-494

Hunt, A.G. and Skinner, T.E. 2005. Hydraulic conductivity limited equilibration: Effect on water retention characteristics. *Vadose Zone Journal*. 4: 145-150

Ibrahim, T.I., Fenton, O., Richards, K.G., Fealy, R.M. and Healy, M.G. 2013a. Spatial and temporal variations in nutrient loads in overland flow and subsurface drainage from a marginal land site in South-East Ireland. *Biology and Environment: Proceedings of the Royal Irish Academy*. 113B(2): 1-18

Ibrahim, T., Fenton, O. and Creamer, R.E. 2013b. Chapter 2: Soil and drainscapes. In: Teagasc Manual on Drainage and Soil Management. Ed. Moore, M., Fenton, O., Tuohy, P. and Ibrahim, T. Teagasc.

Irish Cooperative Organisation Society, 2015. Food Wise 2025 Environmental Analysis Consultation Feedback Form. <http://www.icos.ie/wp-content/uploads/2013/12/August-2015-ICOS-Submission-re-Food-Wise-2025-EA-Report.pdf> Last downloaded 01/11/2015

Jackson, B.M., Wheeler, H.S., Mathias, S.A., McIntyre, N. and Butler, A.P. 2006. A simple model of variable residence time flow and nutrient transport in the chalk. *Journal of Hydrology*. 330: 221-234

## Bibliography

Jacques, D., and Šimůnek, J. 2005. User Manual of the Multicomponent Variably-Saturated Flow and Transport Model HP1, Description, Verification and Examples, Version 1.0, SCK•CEN-BLG-998, Waste and Disposal, SCK•CEN, Mol, Belgium, 79 pp.,

Jacques, D., Šimůnek, J., Mallants, D. and van Genuchten, M. Th.. 2006. Operator-splitting errors in coupled reactive transport codes for transient variably saturated flow and contaminant transport in layered soil profiles, *Journal of Contaminant Hydrology*. 88, 197-218,

Jacques, D., Šimůnek, J., Mallants, D. and van Genuchten, M. Th. 2008 Modelling coupled water flow, solute transport, and geochemical reactions affecting heavy metal migration in a podzol soil. *Geoderma*. 145(3-4): 449-461

Jahangir, M.M.R., Johnston, P., Addy, K., Khalil, M.I., Groffman, P.M. and Richards, K.G. 2013a. Quantification of in situ denitrification rates in groundwater below an arable and a grassland system. *Water Air and Soil Pollution*. 224:1693

Jahangir, M.M.R., Johnston, P., Barrett, M., Khalil, M.I., Groffman, P.M., Boeckx, P., Fenton, O., Murphy, J. and Richards, K.G. 2013b. Denitrification and indirect N<sub>2</sub>O emissions in groundwater: Hydrologic and biogeochemical influences. *Journal of Contaminant Hydrology*. 152: 70-81

Jarvis, N.J. 1994. A review of non-equilibrium water flow and solute transport in soil macropores: principles, controlling factors and consequences for water quality. *European Journal of Soil Science*. 58: 523-546

Jarvis N.J. and Larsson M.H. 1998. The MACRO model (Version 4.1) – Technical description. <http://130.238.110.134:80/bgf/Macrohtm/macro.htm>, Department of Soil Sciences, Swedish University of Agricultural Sciences, Uppsala. Jarvis, N., Larsbo, M., Roulier, S., Lindahl, A. and Persson, L. 2007. The role of soil properties in regulating non-equilibrium macropore flow and solute transport in agricultural topsoils. *European Journal of Soil Science*. 58(1): 282-292

Jenny, H. 1994. Factors of soil formation. A system of quantitative pedology. Dover Publications. New York.

## Bibliography

- Jensen, D.K., Moldrup, P., Arthur, E., Tuller, M. and de Jonge, L.W. 2014. Impact of texture, bulk density, and organic carbon on the soil water characteristic from oven dryness to saturation. Revisiting The Most Important Curve In Soil Physics I. ASA-CSSA-SSSA Annual International Meeting. 3-5 Nov. 2014. Long Beach, California.
- Jiang, S., Pang, L., Buchan, G.D., Simunek, J., Noonan, M.J. and Close, M.E. 2010. Modelling water flow and bacterial transport in undisturbed lysimeters under irrigations of dairy shed effluent and water using HYDRUS-1D. *Water Resources*. 44(4): 1050-1061
- Johnston, A.S.A., Holmstrup, M., Hodson, M.E., Thorbek, P., Alvarez, T. and Sibly, R.M. 2014. Earthworm distribution and abundance predicted by a process-based model. *Applied Soil Ecology*. 84: 112-123
- Jones, R.J.A., Hannam, J.A., Creamer, R.E., 2011. Ireland Soil Information System: Description and classification of soils in the field Version 6.1, Cranfield University and Teagasc.
- Jordan, P., Menary, W., Daly, K., Kiely, G., Morgan, G., Byrne, P. and Moles, R. 2005. Patterns and processes of phosphorus transfer from Irish grassland soils to rivers – integration of laboratory and catchment studies. *Journal of Hydrology*. 304: 20-34
- Kartha, S.A. and Srivastava, R. 2008. Effect of immobile water content on contaminant transport in unsaturated zone. *Journal of Hydro-Environment Research*. 1: 206-215
- Keane, T. and Sheridan, T. 2004. Climate of Ireland. In: Climate, Weather and Irish Agriculture 2<sup>nd</sup> Edition. Eds: Keane, T. and Collins, J.F. Joint Working Group on Applied Agricultural Meteorology. pp392
- Keim, D.M., West, L.J. and Odling, N.E. 2012. Convergent flow in unsaturated fractured chalk. *Vadose Zone Journal*. 11(4) Khodaverdiloo, H., Homaei, M., van Genuchten, M. Th. and Dashtaki, S.G. 2011. Deriving and validating pedotransfer functions for some calcareous soils. *Journal of Hydrology*. 399: 93-99

## Bibliography

- Khazode, R.M., Vanipalli, S.K. and Fredlund, D.G. 2002. Measurement of soil-water characteristic curves for fine grained soils using a small-scale centrifuge. *Canadian Geotechnical Journal*. 39: 1209-1217
- Khodaverdiloo, H., Homaei, M., van Genuchten, M.Th., Dashtaki, S.G., 2011. Deriving and validating pedotransfer functions for some calcareous soils. *Journal of Hydrology*. 399, 93–99.
- Kiely, G., McGoff, N., Eaton, J.M., Xu, X., Leahy, P. and Carton, O. 2009. Soil C. Measuring and modelling of soil carbon stocks and stock changes in Irish soils. In: STRIVE, pp 42. Environmental Protection Agency, Johnstown Castle Estate, Co. Wexford, Ireland.
- Köhne, J.M., Köhne, S. and Šimůnek, J. 2009. A review of model applications for structured soils: a) Water flow and tracer transport. *Journal of Contaminant Hydrology*. 104: 4-35
- Konert, M., Vandenburghe, J., 1997. Comparison of laser grain size analysis with pipette and sieve analysis: a solution for the underestimation of the clay boundary, *Sedimentology*, 44, 523-535.
- Konikow, L.F., 2011. The secret to successful solute-transport modelling. *Ground Water*. 49 (2), 144–159.
- Kosugi, K., 1996. Lognormal distribution model for unsaturated soil hydraulic properties. *Water Resources Research*. 32 (9), 2697–2703.
- Kramers, G., Holden, N.M., Brennan, F., Green, S., Richards, K.G., 2012. Water content and soil type effects on accelerated leaching after slurry application. *Vadose Zone Journal*. 51(1)
- Kramers, G. 2009. Preferential flow in Irish grassland soils. Ph.D thesis. University College Dublin, Ireland.
- Kroes, J.G. and J.C. van Dam (eds), 2003. Reference Manual SWAP version 3.0.3. Wageningen, Alterra, Green World Research.. Alterra-report 773. Reference Manual SWAP version 3.0.3.doc.

## Bibliography

Kronvang, B., Andersen, H.E., Børgesen, C., Dalgaard, T., Larsen, S.E., Bøgestrand, J. and Blicher-Mathiasen, G., 2008. Effects of policy measures implemented in Denmark on nitrogen pollution of the aquatic environment. *Environmental Science and Policy*. 11, 144-152.

Kronvang, B., Behrendt, H., Andersen, h.E., Arheimer, B., Barr, A., Borgvang, S.A. Bouraoui F., Granlund K., Grizzetti B., Groenendijk, P., Schwaiger, E., Hejzlar, J., Hoffmann, L., Johnsson, H., Panagopoulos, Y., Lo Porto, A., Reisser, H., Schoumans, O., Anthony, S., Silgram, M., Venohr, M., Larsen, S.E. 2009. Ensemble modelling of nutrient loads and nutrient load partitioning in 17 European catchments. *Journal of Environmental Monitoring*. 11: 572-583

Kurz, I., Coxon, C., Tunney, H. and Ryan, D. 2005a. Effects of grassland management practices and environmental conditions on nutrient concentrations in overland flow. *Journal of Hydrology*. 304: 35-50

Kurz, I., Tunney, H. and Coxon, C. 2005b. The impact of agricultural management practices on nutrient losses to water: data on the effects of soil drainage characteristics. *Water science and technology*. 51(3-4): 73-81

Ladu, J.L.C. and Zhang, D-R. 2011. Modelling atrazine transport in soil columns with HYDRUS-1D. *Water Science and Engineering*. 4(3): 258-269

Lalor, S.T.J. 2004. Soils of UCD research farm, Lyon's Estate, Cellbridge, Co. Kildare. Agriculture, Food Science and Veterinary Medicine. University College Dublin, Dublin.

Larsson, M. 1999. Quantifying macropore flow effects on nitrate and pesticide leaching in a structured clay soil field experiments and modelling with the MACRO and SOILN models. PhD thesis. Swedish University of Life Sciences. Uppsala, Sweden.

Laurent, F. and Ruelland, D. 2011. Assessing impacts of alternative land use and agricultural practices on nitrate pollution at the catchment scale. *Journal of Hydrology*. 409: 440-450

Lebedev, A.F. 1936. Soil and Ground Waters. Moscow (In Russian)

## Bibliography

Leij, F.J. and van Genuchten, M. Th. 2011. Chapter 6. Solute Transport. In. Handbook of Soil Science. Ed. Sumner, M. CRC Press. 183-227

Li, Y. and Ghodrati, M. 1996. Preferential transport of solute through soil columns containing constructed macropores. *Soil Science Society of America Journal*. 61(5): 1308-1317

Lin, H., 2011. Hydropedology: Towards new insights into interactive pedologic and hydrologic processes across scales. *Journal of Hydrology*. 406: 141-145

Liu, X., Sun, S., Ji, P, and Šimůnek, J. 2012. Evaluation of historical nitrate sources in groundwater and impact of current irrigation practices on groundwater quality. *Hydrological Sciences Journal*. 58(1): 1-15

Lynch, J. 1995. Root architecture and plant productivity. *Plant Physiology*. 109: 7-13

Macdonald, K. and Jefferies, C. 2003. Performance and design details of SUDS. National Hydrology Seminar 2003. 93-102

Madsen, H.B., Jensen, C.R. and Boysen, T. 1986. A comparison of the thermocouple psychrometer and the pressure plate methods for determination of soil water characteristic curves. *Journal of Soil Science*. 37: 357-362

Malaya, C. and Sreedeeep, S. 2012. Critical review on the parameters influencing soil-water characteristic curve. *Journal of Irrigation and Drainage Engineering*. 138: 55-62

Mantovi, P., Fumagalli, L., Berretta, G.P. and Guermandi, M. 2006. Nitrate leaching through the unsaturated zone following pig slurry applications. *Journal of Hydrology*. 316 (1-4): 195-212

Mapa, R.B., Green, R.E. and Santo, L. 1986. Temporal variability of soil hydraulic properties with wetting and drying subsequent to tillage. *Soil Science Society of America Journal*. 50(5): 1133-1138

McCartney, J.S. and Zornberg, J.G. 2010 Centrifuge permeameter for unsaturated soils II: Measurement of the hydraulic characteristics of an unsaturated clay. *Journal of Geotechnical and Geoenvironmental Engineering*. 136(8): 1064-1076

## Bibliography

Meals, D.W., Dressing, S.A. and Davenport, T.E. 2010 Lag time in water quality response to best management practices: A review. *Journal of Environmental Quality*. 39: 85-96

Mellander P-E., Jordan, P., Wall, D.P., Melland, A.R., Meehan, R., Kelly, C. and Shortly, G. 2012a. Delivery and impact bypass in a karst aquifer with high phosphorus source and pathway potential. *Water Research*. 46(7): 2225-2236

Mellander, P-E., Melland, A.R., Jordan, P., Wall, D.P., Murphy, P.N.C. and Shortle, G. 2012. Quantifying nutrient transfer pathways in agricultural catchments using high temporal resolution data. *Environmental Science and Policy*. 24: 44-57

Mellander, P-E., Melland, A.R., Murphy, P.N.C., Wall, D.P., Shortle, G. and Jordan, P. 2014. Coupling of surface water and groundwater nitrate-N dynamics in two permeable agricultural catchments. *Journal of Agricultural Science*. 152: 107-124

Mellander, P-E., Jordan, P., Shore, M., Melland, A.R. and Shortle, G. 2015. Flow paths and phosphorus transfer pathways in two agricultural streams with contrasting flow controls. *Hydrological Processes*.

Mellander, P-E., Jordan, P., Shore, M., McDonald, N.T., Wall, D.P., Shortle, G. and Daly, K. 2016. Identifying contrasting influences and surface water signals for specific groundwater phosphorus vulnerability. *Science of the Total Environment*.

Merdun, H. 2012. Effects of different factors on water flow and solute transport investigated by time domain reflectometry in sandy clay loam field soil. *Water, Air and Soil Pollution*. 223(8): 4905-4923

Mertens, J., Raes, D. and Feyen, J. 2002. Incorporating rainfall intensity into daily rainfall records for simulating runoff and infiltration in soil profiles. *Hydrological Processes*. 16: 731-739

Met Éireann. 2015a. Current synoptic stations <http://www.met.ie/about/weatherobservingstations/synopmap.asp> Last accessed 22/10/15

## Bibliography

Met Éireann. 2015b. Current rainfall stations  
<http://www.met.ie/about/weatherobservingstations/rainmap.asp> Last accessed  
22/10/15

Missteart, B.D.R. 2000. Groundwater recharge assessment: A key component of river basin management. National Hydrology Seminar 2000. pp 51- 58

Missteart BDR and Brown L. 2008. Water Framework Directive: Recharge and Groundwater Vulnerability. Final Report, Environmental Protection Agency, Wexford.

Mockler, E., Packham, I. and Bruen, M. 2013. Pulling it all together: Information from FSU and EPA datasets in parameterising hydrology in the Pathways Catchment Management Tool. National Hydrology Conference 12<sup>th</sup> November 2013. Tullamore, Co. Offaly, Ireland.

Mohamed, J. and Ali, S. 2006. Development and comparative analysis of pedotransfer functions for predicting soil water characteristic content for Tunisian soils. Proceedings of the 7<sup>th</sup> Edition of TJASSST. 170-178

Mohanty, B.P. and Zhu, J.T. 2007. Effective hydraulic parameters in horizontally and vertically heterogeneous soils for steady-state land-atmosphere interaction. *Journal of Hydrometeorology*. 8(4), 715–729

Molénat, J. and Gascuel-Oudou, C. 2002. Modelling flow and nitrate transport in groundwater for the prediction of water travel times and of consequences of land use evolution on water quality. *Hydrological Processes*. 16: 479-492

Moncada, M.P., Ball, B.C., Gabriels, D., Lobo, D. and Cornelis, W.M. 2015. Evaluation of soil physical quality index S for some tropical and temperate medium-textured soils. *Soil Science Society of America Journal*. 79(1): 9-19

Monteith, J.L. 1981. Evaporation and surface temperature. *Quarterly Journal of the Royal Meteorological Society*. 107(451): 1-27

Monteith, J.L. and Unsworth, M.H. 1990. Principles of Environmental Physics. 2<sup>nd</sup> edition. Ed. Edward Arnold, New York. pp 53-54

## Bibliography

Mualem, Y.I. 1976. A new model for predicting the hydraulic conductivity of unsaturated porous media. *Water Resources Research*. 12: 513-522

Nielsen, D.R., van Genuchten, M. Th. and Biggar, J.W. 1986. Water flow and solute transport processes in the unsaturated zone. *Water Resources Research*. 22(9S): 89-108

Nimmo, J.R., Rubin, J. and Hammermeister, D.P. 1987. Unsaturated flow in a centrifugal field: Measurement of hydraulic conductivity and testing of Darcy's law. *Water Resources Research*. 23(1): 124-137

Nimmo, J.R. and Akstin, K.C. 1988. Hydraulic conductivity of a sandy soil at low water content after compaction by various methods. *Soil Science Society of America Journal*. 52(2): 303-310

Nimmo, J.R. 1990. Experimental testing of transient unsaturated flow theory at low water content in a centrifugal field. *Water Resources Research*. 26(9): 1951-1960

Nuth, M. and Laloui, L. 2008. Advances in modelling hysteresis water retention curve in deformable soils. *Comput. Geotech*. 110: 835-844

O'Donoghue, C. and Hennessy, T. 2014. Chapter 3: The agri-food sector. In. Rural economic development in Ireland. Eds. O'Donoghue, C., Coneely, R., Frost, D., Heanue, K., Leonard, B. and Meredith, D. Teagasc, Oak Park, Carlow, Ireland

O'Donovan, M., Lewis, E. and O'Kiely, P. 2011. Requirements of future grass-based ruminant production systems in Ireland. *Irish Journal of Agriculture and Food Research*. 50: 1-21

O'Sullivan, L., Creamer, R.E., Fealy, R., Lanigan, G., Simo, I., Fenton, O., Carfrae, J., Schulte, R.P.O. 2015. Functional Land Management for managing soil functions: A case-study of the trade-off between primary productivity and carbon storage in response to the intervention of drainage systems in Ireland, *Land Use Policy*. 47, 42-54

Organisation for Economic Co-operation and Development (OECD). 2008. Environmental performance of agriculture in OECD countries since 1990. Paris, France.

## Bibliography

- Owens, L.B., Van Keuren, R.W. and Edwards, W.M. 1985. Groundwater quality changes resulting from a surface bromide application to a pasture. *Journal of Environmental Quality*. 14(4): 543-548
- Pachepsky, Y.A., Smettem, K.R.J., Vanderborght, J., Herbst, M., Vereecken, H. and Wösten, J.H.M. 2004. Reality and fiction of models and data in soil hydrology. In: *Unsaturated Zone Modelling*. Vol. 6: Progress, Challenges and Applications. Feddes, R.A.; Rooij, G.H.de; Dam, J.C. van (Eds.).
- Packham, I., Mockler, E. and Bruen, M. 2013. Development of a Catchment Management Tool to assess environmental risk from nutrient loadings using open source GIS. In. *Environmental Software Systems: Fostering information sharing*. Eds. Hřebíček, J., Schimak, G., Kubásek, M. and Rizzoli, A.E. Springer Berlin Heidelberg
- Padilla, I.Y., Yeh, T-C. J. and Conklin, M.H. 1999. The effect of water content on solute transport in unsaturated porous media. *Water Resources Research*. 35(11): 3303-3313
- Pang, L., Close, M.E., Watt, J.P.C. and Vincent, K.W. 2000. Simulation of picloram, atrazine, and simazine leaching through two New Zealand soils and into groundwater using HYDRUS-2D. *Journal of Contaminant Hydrology*. 44: 19-46
- Parkhurst, D.L. and Appelo, C.A.J. 1999. User's guide to PHREEQC (Version 2) – A computer program for speciation, batch-reaction, one-dimensional transport, and inverse geochemical calculations. U.S.G.S. Water-Resources Investigations Report. 99-4259
- Payne, F.C., Quinnan, J.A. and Potter, S.T. 2008. *Remediation Hydraulics*. CRC Press. Taylor & Francis Group. pp 432
- Peck, A.J. and Rabbidge, R. 1969. Design and performance of an osmotic tensiometer for measuring capillary potential. *Soil Science Society of America Journal*. 33:196-202
- Peck, A.J., Luxmoore, R.J. and Stolzy, J.L. 1977. Effects of spatial variability of soil hydraulic properties in water budget modeling. *Water Resources Research*. 13(2): 348-354

## Bibliography

- Peerlkamp, P.K. and Boekel, P. 1960. Moisture retention curves. Proceedings of the technical meetings of the Committee for Hydrological Research T.N.O. 5: 122-138
- Perfect, E., Sukop, M.C. and Haszler, G.R. 2002. Prediction of dispersivity for undisturbed soil columns from water retention parameters. *Soil Science Society of America Journal*. 66: 696-701
- Pionke, H.B., Gburek, W.J. and Sharpley, A.N., 2000. Critical source area controls on water quality in an agricultural watershed located in the Chesapeake Basin. *Ecological Engineering*. 14: 325-335.
- Pot, V., Šimůnek, J., Benoit, P., Coquet, Y., Yra, A. and Martínez-Cordón, M-J. 2005. Impact of rainfall intensity on the transport of two herbicides in undisturbed grassed filter strip soil cores. *Journal of Contaminant Hydrology*. 81: 63-88
- Premrov, A., Coxon, C.E., Hackett, R., Kirwan, L. and Richards, K.G. 2014. Effects of over-winter green cover on soil solution nitrate concentrations beneath tillage land. *Science of the Total Environment*. 470-471: 967-974
- Puckett, L.J., Zamora, C. Essiad, H., Wilson, J.T. and Johnson, H.M. 2008. Transport and fate of nitrate at the groundwater/surface-water interface. *Journal of Environmental Quality*. 37: 1034-1050
- Ravi, V. and Johnson, J.A. 1997. VLEACH: A one-dimensional finite difference vadose zone leaching model. Version 2.2. Developed for the United States Environmental Protection Agency Office of Research and Development, Robert S. Kerr Environmental Research Laboratory, Centre for Subsurface Modeling Support, P.O. Box 1198, Ada, Oklahoma 74820
- Reatto, A., da Silva, E.M., Bruand, A., Martins, E. and Lima, J.E.F.W. 2008. Validity of the centrifuge method for determining the water retention properties of tropical soils. *Soil Science Society of America Journal*. 72(6): 1547-1553
- Reginato, R.J. and van Bavel, C.H.M. 1962. Pressure cell for soil cores
- Reis, R.M., Sterck, W.N., Ribeiro, A.B., Dell'Avanzi, E., Saboya, F., Tibana, S., Marciano, C.R. and Sobrinho, R.R. 2011. Determination of the soil-water retention

## Bibliography

curve and the hydraulic conductivity function using a small centrifuge. *Geotechnical Testing Journal*. 34(5): 457-466

Rhoades, J.D., Chanduvi, F. and Lesch, S. 1999. Soil salinity assessment: Methods of interpretation of electrical conductivity measurements. FAO Irrigation and drainage paper 57.

Richards, L.A. 1931. Capillary conduction of liquids through porous mediums. *Physics*. 1(5): 318–333

Richards, L.A. 1948. Porous plate apparatus for measuring moisture retention and transmission by soils. *Soil Science*. 66:105-110

Richards, L.A. 1965. Physical condition of water in soil. P128-152. In. C.A. Black (ed.) Methods of soil analysis. Part 1. Agron. Monograph. 9. ASA and SSSA, Madison, WI

Richards, K., Coxon, C.E. and Ryan, M. 2005. Unsaturated zone travel time to groundwater on a vulnerable site. *Irish Geography*. 38(1): 57-71

Robbins, C.W. and Carter, D.L. 1980. Nitrate-nitrogen leached below the root zone during and following alfalfa. *Journal of Environmental Quality*. 9(3): 447-450

Russell, M.B. and Richards, L.A. 1938. The determination of soil moisture energy relations by centrifugation. Journal Paper No. J590 of the Iowa Agricultural Experiment Station, Ames, Uowa. Project No. 487

Russo, D. 1991. Stochastic analysis of simulated vadose zone solute transport in a vertical cross section of heterogeneous soil in nonsteady water flow. *Water Resources Research*. 27(3): 267-283

Ryan, M., Sherwood, M. and Fanning, A. 2001. Leaching of Nitrate (NO<sub>3</sub>-N) from cropped and fallow soil – a lysimeter study with ambient and imposed rainfall regimes. *Irish Geography*. 34(1): 34-49

Sadej, W. And Prekwas, K. 2008. Fluctuations of nitrogen levels in soil profiles under conditions of a long-term fertilization experiment. *Plant Soil Environment*. 54(5): 197-203

## Bibliography

Saito, H., Šimůnek, J. and Mohanty, B.P. 2006. Numerical analysis of coupled water, vapour and heat transport in the vadose zone. *Vadose Zone Journal*. 5(2): 784-800

SAS, 2003. SAS for Windows. Version 9.1. SAS Inst, Cary, NC.

SAS Institute Inc. 2011. SAS® 9.3 System Options: Reference, Second Edition.

Saso, J.K., Parkin, J.W., Drury, C.F., Lauzon, J.D. and Reynolds, W.D. 2012. Chloride leaching in two Ontario soils: Measurement and prediction using HYDRUS-1D. *Canadian Journal of Soil Science*. 92(2): 285-296

Saxena, R.K. and Jarvis, N.J. 1995. Measurements and modelling of tracer transport in a sandy soil. In: Biogeochemical monitoring in small catchments. Eds. Čerňý, J., Novák, M., Pačes, T. and Wieder, R.K. Reprinted from *Water, Soil and Air Pollution*. 79(1-4)

Saxton, K.E., Rawls, W.J., Romberger, J.S. and Papendick, R.I. 1986. Estimating generalised soil-water characteristics from texture. *Soil Science Society of America Journal*. 50(4): 1031-1036

Schaap, M.G. and Leij, F.J. 1998. Database-related accuracy and uncertainty of pedotransfer functions. *Soil Science*. 163(10): 765-779

Schaap, M.G., Leij, F.J. and van Genuchten, M.Th. 2001. ROSETTA: A computer program for estimating soil hydraulic parameters with hierarchical pedotransfer functions. *Journal of Hydrology*. 251: 163-176

Scheure, S. and Naus, J. 2010. 10 Years of the Water Framework Directive: A toothless tiger? A snapshot assessment of EU environmental ambitions. Ed. Hontelez, J. European Environmental Bureau.

Schindler, U., Durner, W., von Unold, G., Mueller, L. and Wieland, R. 2010. The evaporation method: Extending the measurement range of soil hydraulic properties using the air-entry pressure of the ceramic cup. *Journal of Plant Nutrition and Soil Science*. 173: 563-572

Schjønning, P., Thomsen, I.K., Møberg, J.P., de Jong, H., Kristensen, K. and Christensen, B.T. 1999. Turnover of organic matter in differently textured soils: I.

## Bibliography

Physical characteristics of structurally disturbed and intact soils. *Geoderma*. 89(3-4): 177-198

Schoups, G., van de Giesen, N.C. and Savenije, H.H.G. 2008. Model complexity control for hydrologic prediction. *Water Resources Research*. 44(12)

Schröder, J.J., Scholefield, D., Cabral, F. and Hofman, G. 2004. The effects of nutrient losses from agriculture on ground and surface water quality: The position of science in developing indicators for regulation. *Environmental Science and Policy*. 7:15-23

Schulte, R.P.O., Diamond, J., Finkle, K., Holden, N.M. and Brereton, A.J. 2005. Predicting the soil moisture conditions of Irish grasslands. *Irish Journal of Agriculture and Food Research*. 44: 95-110

Schulte, R.P.O., Richards, K., Daly, K., Kurz, I., McDonald, E.J. and Holden, N.M. 2006. Agriculture, meteorology and water quality in Ireland: A regional evaluation of pressures and pathways of nutrient loss to water. *Biology and Environment: Proceedings of the Royal Irish Academy*. 106B(2): 117-133

Schulte, R.P.O., Creamer, R., Donnellan, T., Farrelly, N., Fealy, R., O'Donoghue, C., O'hUallachain, D. 2014. Functional land management: a framework for managing soil-based ecosystem services for the sustainable intensification of agriculture. *Environ. Sci. Policy*, 38, 45–58.

Selbie, D. 2013. The fate of nitrogen in an animal urine patch as affected by urine nitrogen loading rate and the nitrification inhibitor dicyandiamide. Ph.D thesis. Lincoln University, Canterbury, New Zealand.

Shipitalo, M.J., Dick, W.A. and Edwards, W.M. 2000. Conservation tillage and macropore factors that affect water movement and the fate of chemicals. *Soil and Tillage Research*. 53: 167-183

Shore, M., Jordan, P., Mellander, P-E., Kelly-Quinn, M., Wall, D.P., Murphy, P.N.C. and Melland, A.R. 2014. Evaluating the critical source area concept of phosphorus loss from soils to water-bodies in agricultural catchments. *Science of the Total Environment*. 490: 405-415

## Bibliography

Shukla M.K. 2014. Soil Physics: An Introduction. CRC Press, Boca Raton, FL, USA.

Simo, I., Creamer, R.E., Reidy, B., Jahns, G., Massey, P., Hamilton, B., Hannam, J.A., McDonald, E., Sills, P. and Spaargaren, O. 2008. Irish Soil Information System technical report 10: Soil profile handbook. Environmental Protection Agency, Johnstown Castle, Co. Wexford, Ireland.

Šimůnek, J., Suarez, D.L. and Šejna, M. 1996. The UNSATCHEM software package for simulating one-dimensional variably saturated water flow, heat transport, carbon dioxide transport, and multi-component solute transport with major ion equilibrium and kinetic chemistry. Version 2.0. Research Report No. 141. U.S. Salinity Laboratory, USDA, ARS, Riverside, California pp186

Šimůnek, J., van Genuchten, M.Th., Šejna, M., Toride, N. and Leij, F.J. 1999a. The STANMOD Computer Software for Evaluating Solute Transport in Porous Media Using Analytical Solutions of Convection-Dispersion Equation Versions 1.0 and 2.0. U.S. Salinity laboratory, Agricultural Research Service, USDA. Riverside, California.

Šimůnek, J., Kodešová, R., Gribb, M.M. and van Genuchten, M.Th. 1999. Estimating hysteresis in the soil water retention function from cone permeameter experiments. *Water Resources Research*. 35(5): 1329-1345

Šimůnek, J., Jarvis, N.J., van Genuchten, M.Th., and Gärdenäs, A. 2003. Review and comparison of models for describing non-equilibrium and preferential flow and transport in the vadose zone. *Journal of Hydrology*. 272:14–35.

Šimůnek, J. and Nimmo, J.R. 2005. Estimating soil hydraulic parameters from transient flow experiments in a centrifuge using parameter optimization technique. *Water Resources Research*. 41

Šimůnek, J., Jacques, D., van Genuchten, M.Th. and Mallants, D. 2006. Multicomponent geochemical transport modeling using the HYDRUS computer software packages, *Journal of American Water Resources Association*. 42(6), 1537-1547.

## Bibliography

- Šimůnek, J. 2009. Notes on spatial and temporal discretisation (when working with Hydrus). [http://www.pc-progress.com/Documents/Notes\\_on\\_Spatial\\_and\\_Temporal\\_Discretization.pdf](http://www.pc-progress.com/Documents/Notes_on_Spatial_and_Temporal_Discretization.pdf) Last accessed 28<sup>th</sup> January 2016
- Šimůnek, J., van Genuchten, M. Th. and Šejna, M. 2012. Hydrus: Model use, calibration and validation. *Transactions of the ASABE*. 55(4): 1261-1274
- Šimůnek, J., Šejna, M., Saito, H., Sakai, M and van Genuchten, M. Th. 2013. The HYDRUS 1D software package for simulating the movement of water, heat and multiple solutes in variably saturated media. Version 4.16 HYDRUS software series 3, Department of Environmental Science, University of California Riverside, Riverside, California, USA. pp 340
- Šimůnek, J. 2014. 31/1/2014 PC-Progress discussion forum. <http://www.pc-progress.com/forum/viewtopic.php?f=4&t=2391&sid=22af64777a79eab232fbf7470f204bb3>
- Soil Information Survey (SIS). 2015. <http://gis.teagasc.ie/soils/index.php> Last accessed 3/11/15
- Skaggs, T.H., Jarvis, N.J., Pontedeiro, E.M., van Genuchten, M Th. and Cotta, R.M. 2007. Analytical advection-dispersion model for transport and plant uptake of contaminants in the root zone. *Vadose Zone Journal*. 6: 890-898
- Smagin, A.V., Sadovnikova, N.B. and Ben Ali, M.M. 1998. The determination of the primary hydrophysical function of soil by the centrifuge method. *Eurasian Soil Science*. 31(11):1362-1370
- Smagin, A.V. 2012. Column-centrifugation method for determining water retention curves of soils and disperse sediments. *Eurasian Soil Science*. 45(4):416-422
- Smith, M., Allen, R.G., Monteith, J.L., Perrier, A., Pereira, L. and Segesen, A. 1991. Report on the expert consultation on procedures for revision of FAO guidelines for prediction of crop water requirements. FAO, Rome.

## Bibliography

Sonneveld, M.P.W. and Bouma, J. 2003. Methodological considerations for nitrogen policies in the Netherlands including a new role for research. *Environmental Science and Policy*. 6: 501-211

Sousa, M.R., Jones, J.P., Frind, E.O. and Rudolph, D.L. 2013. A simple method to assess unsaturated zone time lag in the travel time from ground surface to receptor. *Journal of Contaminant Hydrology*. 144: 138-151

Stark, C.H. and Richards, K.G. 2008. The continuing challenge of nitrogen loss to the environment: Environmental consequences and mitigation strategies. *Dynamic Soil, Dynamic Plant*. 2(1): 1-12

Sugita, F. and Nakane, K. 2007. Combined effects of rainfall patterns and porous media properties on nitrate leaching. *Vadose Zone Journal*. 6:548–553

Sweeney, J.C. 1985. The changing synoptic origins of Irish precipitation. *Transactions of the Institute of British Geographers*. 10(4): 467-480

Taubner, H., Roth, B. and Tippkötter, R. 2009. Determination of soil texture: Comparison of sedimentation method and the laser-diffraction analysis. *Journal of Plant Nutrition and Soil Science*. 172: 161-171

Teagasc, 2015. <http://gis.teagasc.ie/soils/> accessed 19<sup>th</sup> February 2015.

Tedd, K.M., Coxon, C.E., Misstear, B.D.R., Daly, D., Craig, M., Mannix, A. and Hunter Williams, N.H. 2014. An integrated pressure and pathway approach to the spatial analysis of groundwater nitrate: A case study from the southeast of Ireland. *Science of the Total Environment*. 476-477. p460-476

Tesoriero, A.J., Duff, J.H., Saad, D.A., Spahr, N.E. and Wolock, D.M. 2013. Vulnerability of streams to legacy nitrate sources. *Environmental Science and Technology*. v. 47, 3623-3629

Thackery, A. and Myers, M. 2000. Arnold O. Beckman: One hundred years of excellence. Volume 1. Chemical Heritage Foundation

Thien, S.J., 1979. A flow diagram for teaching texture- by-feel analysis. *Journal of Agronomic Education*. 8:54-55.

## Bibliography

Thieu, V., Bouraoui, F., Aloe, A. and Bidoglio, G. 2012. Scenario analysis of pollutant loads to European regional seas for the year 2020. Part I: Policy options and alternative measures to mitigate land based emission of nutrients. EUR 25159 EN. Luxembourg: EC-JRC p80

Thomas, I., Murphy, P.N.C., Shine, O., Fenton, O., Mellander, P-E., Dunlop, P. and Jordan, P. 2015. Development of a phosphorus critical source area index using high resolution DEMs. Catchment Science into Policy Briefing. March 13<sup>th</sup> 2015. Killeshin Hotel, Portlaoise. [http://www.teagasc.ie/publications/2015/3556/presentations/Pres\\_Nutrient%20Pathways%20and%20Critical%20Source%20Areas%20-%20Mr.%20Ian%20Thomas.pdf](http://www.teagasc.ie/publications/2015/3556/presentations/Pres_Nutrient%20Pathways%20and%20Critical%20Source%20Areas%20-%20Mr.%20Ian%20Thomas.pdf)

Timmerman, J.G., Beinat, E., Termeer, K. and Cofino, W. 2010. Analysing the data-rich-but-information-poor syndrome in Dutch water management in historical perspective. *Environmental Management*. 45: 1231-1242

Tomer, M.D., Burkart, M.R. 2003. Long-term effects of nitrogen fertilizer use on ground water nitrate in two small watersheds. *Journal of Environmental Quality*. 32, 2158–2171.

Tomer, M.D., Crumpton, W.G., Bingner, R.L., Kostel, J.A. and James, D.E. 2013. Estimating nitrate load reductions from placing constructed wetlands in a HUC-12 watershed using LiDAR data. *Ecological Engineering*. 56: 69-78

Torres, R., Dietrich, W.E., Montgomery, D.R., Anderson, S.P. and Loague, K. 1998. Unsaturated zone processes and the hydrologic response of a steep, unchanneled catchment. *Water Resources Research*. 34(8): 1865-1879

Tunney, H., Kurz, I., Bourke, D. and O'Reilly, C. 2007. Eutrophication from Agricultural Sources: The Impact of the Grazing Animal on Phosphorous Loss from Grazed Pasture. Synthesis Report. Teagasc, Johnstown castle, Wexford, Ireland. [https://www.epa.ie/pubs/reports/research/water/LS-212ppcalice\\_Web1.pdf](https://www.epa.ie/pubs/reports/research/water/LS-212ppcalice_Web1.pdf) Last downloaded 1/11/15

USDA. 1999. Soil Quality Test Kit Guide. Ed. United States Department of Agriculture. Washington D.C.

## Bibliography

Vagstad, N., French, H.K., Andersen, H.E., Behrendt, H., Grizzetti, B., Groenendijk, P., Lo Porto, A., Reisser, H., Siderius, C., Stromquist, J., Hejzlar, J., and Deelstra, J. 2009. Comparative study of model prediction of diffuse nutrient losses in response to changes in agricultural practices. *Journal of Environmental Monitoring*. 11: 594-601

van Breemen, N. and Buurman, P. 2002. *Soil Formation*. 2<sup>nd</sup> Ed. Kluwer Academic Publishers.

van Genuchten, M. Th. 1980. A closed-form equation for predicting the hydraulic conductivity of unsaturated soils. *Soil Science Society of America Journal*, 44: 892-898.

van Genuchten, M.Th., Leij, F.J. and Yates, S.R. 1991. The RETC code for quantifying the hydraulic functions of unsaturated soils. Version 1.0 EPA Report 600/2-91/065, U.S. Salinity Laboratory, USDA, ARS, Riverside, California

van Genuchten, Šimůnek, J., Leij, F.J., Toride, N and Šejna, M. 2012. STANMOD: Model use, calibration, and validation. *Transactions of the ASABE*. 55(4): 1353-1366

van Genuchten, Šimůnek, J. and Kodešová, R. 2013. Advanced modelling of water flow and contaminant transport in porous media using the HYDRUS and HP1 software packages. PC-Progress Ltd. Prague, Czech Republic. March 18<sup>th</sup>-20<sup>th</sup>, 2013

van Grinsven H.J.M., ten Berge H.F.M., Dalgaard T., Fraters B., Durand P., Hart A., Hofman G., Jacobsen B.H., Lalor S.T.J., Lesschen J.P., Osterburg B., Richards K.G., Techen A.-K., Vertès F., Webb J., Willems W.J. 2012. Management, regulation and environmental impacts of nitrogen fertilization in northwestern Europe under the Nitrates Directive; a benchmark study, *Biogeosciences*. Special issue: Nitrogen and global change 9, 5143–5160.

van Grinsven, H.J.M., Holland, M., Jacobsen, B.H., Klimont, Z., Sutton, M.A. and Willems, J. 2013. Costs and benefits of nitrogen for Europe and implications for mitigation. *Environmental Science and Technology*. 47(8): 3571-3579

Vanapalli, S.K., Fredlund, D.G. and Pufahl, D.E. 1996. The relationship between the soil-water characteristic curve and the unsaturated shear strength of a compacted glacial till. *Geotechnical Testing Journal*. 19(3): 259-268

## Bibliography

- Vasiljev, A., Grimvall, A. and Larsson, M. 2004. A dual-porosity model for nitrogen leaching from a watershed. *Hydrological Sciences*. 49(2): 313-322
- Velthof, G.L., Oudendag, D., Witzke, H.R., Asman, W.A.H., Klimont, Z. and Oenema, O. 2009. Integrated assessment of nitrogen losses from agriculture in EU-27 using MITERRA-EUROPE. *Journal of Environmental Quality*. 38: 402-417
- Vereecken, H., Huisman, J.A., Bogaen, H., Vanderborght, J., Vrugt, J.A. and Hopmans, J.W. 2008. On the value of soil moisture measurements in vadose zone hydrology: A review. *Water Resources Research*. 44(4):
- Vereecken, H., Weynants, M., Javaux, M., Pachepsky, Y., Schaap, M.G. and van Genuchten, M. Th. 2010. Using pedotransfer functions to estimate the van Genuchten-Mualem soil hydraulic properties: A review. *Vadose Zone Journal*. 9: 795-820
- Vero, S.E., Antille, D.L., Lalor, S.T.J. and Holden, N.M. 2013. Field evaluation of soil moisture deficit thresholds for limits to trafficability with slurry spreading equipment on grassland. *Soil Use and Management*. 30(1): 69-77
- Vero, S.E., Ibrahim, T.G., Creamer, R.E., Grant, J., Healy, M.G., Henry, T., Kramers, G., Richards, K.G., Fenton, O., 2014. Consequences of varied soil hydraulic and meteorological complexity on unsaturated zone time lag estimates. *Journal of Contaminant Hydrology*, 170: 53-67
- Vogel, H.J. 2014. Moving away from the lamppost of the most important curve in soil physics. Revisiting The Most Important Curve In Soil Physics I. ASA-CSSA-SSSA Annual International Meeting. 3-5 Nov. 2014. Long Beach, California.
- Vomocil, J.A. 1965. Ch. 21: Porosity. In. Methods of soil analysis. Part 1. Physical and mineralogical properties, including statistics of measurement and sampling. *Agronomy Monograph* 9.1
- Wagener, T., Boyle, D.P., Lees, M.J., Wheatler, H.S., Gupta, H.V. and Sorooshian, S. 2001. A framework of development and application of hydrological models. *Hydrology and Earth System Sciences*. 5(1): 13-26

## Bibliography

- Wahlin, K. and Grimvall, A. 2008. Uncertainty in water quality data and its implications for trend detection: lessons from Swedish environmental data. *Environmental Science and Policy*. 115-124
- Wall, D., Jordan, P., Melland, A.R., Mellander, P-E., Buckley, C., Reaney, S.M., Shortle, G. 2012. Using the nutrient transfer continuum concept to evaluate the European Union Nitrates Directive National Action Programme. *Environmental Science and Policy*. 14(6): 664-674
- Wang, P., Quinlan, P. and Tartakovsky, D.M. 2009. Effects of spatio-temporal variability of precipitation on contaminant migration in the vadose zone. *Geophysical Research Letters*. 36
- Wang, K. and Zhang, Z. 2011. Heterogeneous soil water flow and macropores described with combined tracers of dye and iodine. *Journal of Hydrology*. 397(1-2): 105-117
- Wang, L., Stuart, M.E., Bloomfield, J.P., Butcher, A.S., Goody, D.C., McKenzie, A.A., Lewis, M.A. and Williams, A.T. 2012. Prediction of the arrival of peak nitrate concentrations at the water table at the regional scale in Great Britain. *Hydrological Processes*. 26(2): 226-239
- Waterloo Hydrologic, Inc. 2004. [http://trials.swstechnology.com/archive/Software/UnSatSuite/UnSat2203/UNSAT\\_User\\_Manual.pdf](http://trials.swstechnology.com/archive/Software/UnSatSuite/UnSat2203/UNSAT_User_Manual.pdf)
- Wegener, M. 2000. Chapter 1: Spatial Models and GIS. In. *Spatial Models and GIS: New and Potential Models*. Eds. Fotheringham, S. and Wegener, M.
- Wen-zhi, Z., Jie-sheng, H., Jing-wei, W and Chi, W. 2013. Modelling soil salt and nitrogen transport under different fertigation practices with HYDRUS-1D. *Advance Journal of Food Science and Technology*. 5(5): 592-599
- Whalen, J.K. 2004. Spatial and temporal distribution of earthworm patches in cornfield, hayfield, and forest systems of south-western Quebec, Canada. *Applied Soil Ecology*. 27: 143–151

## Bibliography

Wösten, J.H.M., Finke, P.A. and Jansen, M.J.W. 1995. Comparison of class and continuous pedotransfer functions to generate soil hydraulic characteristics. *Geoderma*. 66(3-4): 227-237

Wösten, J.H.M., and van Genuchten, M. Th. 1988. Using texture and other soil properties to predict the unsaturated soil hydraulic functions. *Soil Science Society of America Journal*. 52: 1762-1770

Yang, C-C., Prasher, S.O. and Lacroix, R. 1996. Applications of artificial neural networks to simulate water-table depths under subirrigation. *Canadian Water Resources Journal*. 21(1): 27-44

Yang, X. and You, X. 2013. Estimating parameters of van Genuchten model for soil water retention curve by intelligent algorithms. *Applied Mathematics and Information Sciences*. 7(5): 1977-1983

Young, I.M., Crawford, J.W. and Rappoldt, C., 2001. New methods and models for characterising structural heterogeneity of soil. *Soil and Tillage Research*. 61: 33-45

## **Appendices**

## Appendix A

### List of Publications and Presentations

#### Journal Papers (Published)

**Vero, S.E.**, Ibrahim, T.G., Creamer, R.E., Grant, J., Healy, M.G., Henry, T., Kramers, G., Richards, K.G., Fenton, O., 2014. Consequences of varied soil hydraulic and meteorological complexity on unsaturated zone time lag estimates. *Journal of Contaminant Hydrology*, 170: 53-67

Fenton, O., **Vero, S.E.**, Ibrahim, T.G., Murphy, P.N.C., Sherriff, S. and Ó'hUallachian, D. 2015. Consequences of using different soil texture determination methodologies for soil physical quality and unsaturated zone time lag estimates. *Journal of Contaminant Hydrology*. 182: 16-24

#### Manuscripts in Preparation

**Vero, S.E.**, Healy, M.G., Henry, T., Creamer, R.E., Ibrahim, T.G., Forrestal, P.J., Richards, K.G. and Fenton, O. A methodological framework to determine optimum durations for the construction of soil water characteristic curves. Due for submission December 2015

**Vero, S.E.**, Healy, M.G., Henry, T., Creamer, R.E., Ibrahim, T.G., McDonald, N.T., Mellander, P-E., Richards, K.G. and Fenton, O. Unsaturated zone time lag: A toolkit for assessment in agricultural catchments. Due for submission December 2015

#### Non-Peer Reviewed

**Vero, S.E.**, Henry, T. and Healy, M.G. 2014. NUIG/Teagasc Research – NUI Galway/Teagasc research collaboration advancing the Irish agri-food sector. *Research Matters*. 7. Spring 2014.

**Vero, S.E.**, Fenton, O., Creamer, R.C. and Richards, K.G. 2014. *Soil time lag and water quality*. T-Research Soils Special.

### **International Conference Papers**

**Vero, S.E.**, Creamer, R.E. Henry, T., Healy, M.G., Forristal, P. Richards, K.G. and Fenton, O. 2015 ASA, CSSA and SSSA Annual International Meeting. November 2014. Minneapolis, Minnesota.

Fenton, O., Murphy, P.N.C., Sherriff, S.C., **Vero, S.E.**, and Ó hUallacháin, D. 2015 Consequences of textural analysis methods on time lag estimates. ASA, CSSA and SSSA Annual International Meeting. 16<sup>th</sup>-18<sup>th</sup> November 2014. Minneapolis, Minnesota.

**Vero, S.E.**, Mellander, P-E., Creamer, R.E., Henry, T., Healy, M.G., Richards, K.G. and Fenton, O. 2015. A toolkit for assessing soil time lag in agricultural catchments. Catchment Science 2015. 28<sup>th</sup> – 30<sup>th</sup> September 2015. Wexford, Ireland. Poster presentation.

**Vero, S.E.**, Fenton, O., Mellander, P-E., Richards, K.G., Coxon, C., Creamer, R.E., Henry, T., Healy, M.G. and McAleer, E. 2015. Modelling of unsaturated and saturated zone time lag at hillslope scale. Catchment Science 2015. 28<sup>th</sup> – 30<sup>th</sup> September 2015. Wexford, Ireland. Poster presentation.

**Vero, S.E.**, Creamer, R.E., Henry, T., Healy, M.G., Ibrahim, T.G., Richards, K.G., Fenton, O., 2014. Unsaturated time lag: Managing the expectations of policymakers using numerical models. ASA, CSSA and SSSA Annual International Meeting. 2<sup>nd</sup> – 5<sup>th</sup> November 2014. Long Beach, California. Poster and Oral presentation – Awarded 2<sup>nd</sup> place in the Student Hydrology Session.

**Vero, S.E.**, Creamer, R.E., Healy, M.G., Henry, T., Ibrahim, T.G., Richards, K.G., Fenton, O., 2014. Hydraulic equilibrium: Is it ever reached? ASA, CSSA and SSSA Annual International Meeting. 2<sup>nd</sup> – 5<sup>th</sup> November 2014. Long Beach, California. Oral presentation.

**Vero, S.E.**, Reidy, B., Creamer, R.E., Henry, T., Healy, M.G., Ibrahim, T.G., Richards, K.G., Fenton, O., 2014. Using field instrumentation to validate numerical modelling. ASA, CSSA and SSSA Annual International Meeting. 2<sup>nd</sup> – 5<sup>th</sup> November 2014. Long Beach, California. Poster presentation.

**Vero, S.E.**, Ibrahim, T.G., Richards, K.G., Creamer, R.E., Healy, M.G., Fenton, O., 2013. Consequences of simplification versus complexity in estimating unsaturated vertical travel times in a multi-layered soil. ASA, CSSA and SSSA Annual International Meeting. 3<sup>rd</sup> - 6<sup>th</sup> November 2013. Tampa, Florida. Poster and Oral presentation.

### **National Conference Papers**

**Vero, S.E.**, Reidy, B., Creamer, R.E., Henry, T., Healy, M.G., Ibrahim, T.G., Richards, K.G., Fenton, O., 2015. Using field instrumentation to validate numerical modelling. Catchment Science into Policy Briefing. March 2015. Poster presentation.

**Vero, S.E.**, Ibrahim, T.G., Creamer, R.E., Grant, J., Healy, M.G., Henry, T., Kramers, G., Richards, K.G., Fenton, O., 2015. Effects of meteorological and soils data on unsaturated time lag estimates. Agricultural Research Forum. 9<sup>th</sup> and 10<sup>th</sup> March 2015. Tullamore, Ireland. Oral presentation.

**Vero, S.E.**, Creamer, R.E., Henry, T., Healy, M.G., Ibrahim, T.G., Richards, K.G., Fenton, O., 2014. Unsaturated time lag: correlating water quality changes with programs of measures. Walsh Fellowships Seminar. 5<sup>th</sup> December 2014. Wexford, Ireland.

**Vero, S.E.**, Healy, M.G., Creamer, R.E., Ibrahim, T.G., Richards, K.G. and Fenton, O. 2013. Use of the Centrifuge Method for Determining the Soil Water Characteristic Curve. NUIG-UL Research Day 2013. 11th April 2013. National University of Ireland, Galway. Poster presentation

**Vero, S.E.**, Healy, M.G., Creamer, R.E., Ibrahim, T.G., Richards, K.G. and Fenton, O. 2013 Consequences of using different levels of input data on estimates of vertical travel time through the vadose zone. Ryan Institute Research Day. 24th September 2013. National University of Ireland, Galway. Oral and poster presentations.

### **Other**

**Vero, S.E.** 2015. Getting your message to the people that matter. *Elsevier Scitech Connect Blog*. July 2015.

Appendix A – Publications and Presentations

**Vero, S.E.** 2015. Communicating your research – there's more than one route. *CSA News Magazine*. 60(6)

**Vero S.E.** 2015. How soil goes against the grain of groundwater quality legislation in Ireland. Ryan Institute Podcast Series. 1(3). <http://www.ryaninstitute.ie/education-outreach/ryan-institute-radio/>

**Vero, S.E.** 2015. Public communication of science for the early career researcher. *T-Research*. 10(1). Spring 2015.

**Vero, S.E.** 2015. Unsaturated Soil Time Lag: Correlating water quality changes with programmes of measures. IAH Technical Meeting 24<sup>th</sup> March, GSI, Ballsbridge, Dublin. Ireland.

**Vero, S.E.** 2014. From the Earth to the stars: putting soil into orbit. *Astronomy Ireland Lecture Series*. September 2014. Trinity College Dublin, Ireland

**Vero, S.E.,** 2014. Crops in space. *Research Matters*. 9. Autumn 2014.

**Vero, S.E.,** 2014. Presentation to the International Science Advisory Board, Teagasc, Ashtown, Dublin. July 2014.

**Vero, S.E.,** 2014. Famelab Communicating Science National Finals.

**Vero, S.E.,** 2014. Threesis National Finals

**Vero, S.E.,** 2014. NUIG Threesis Finals

**Vero, S.E.,** 2014. Pint of Science – public science presentations.

**Vero, S.E.,** 2013. NUIG Threesis Finals – 2<sup>nd</sup> place

## **Appendix B**

### **Published Journal Papers**

## **Appendix C**

### **Soil profile descriptions and hydraulic parameters for all soil profiles appearing in Chapter 3**

Presented in this appendix are tables showing descriptions and soil water retention data for each of the soil profiles used in Chapter 3. Subsequently, tables are given detailing the hydraulic parameters calculated according low- to high-complexity approaches (textural class, ROSETTA, Full-SWCC and Partial-SWCC).

Appendix B – Full Soil Profile Descriptions and Hydraulic Properties (Chapter 3)

<b>Profile No. 1 - Ballymacart</b>														
<b>Horizon</b>	<b>Textural Class</b>	<b>Depth</b>	<b>Sand</b>	<b>Silt</b>	<b>Clay</b>	<b><math>\rho_b</math></b>	<b><math>\rho_s</math></b>	<b><math>n_e</math></b>	<b>Retained water</b>					
									<b>% volume</b>					
									<b>cm</b>	<b>%</b>	<b>%</b>	<b>%</b>	<b><math>g\ cm^{-3}</math></b>	<b><math>g\ cm^{-3}</math></b>
A1	Loam	0-10	47	47	6	1.00	2.26	34	59.5	52.8	47.7	45.4	40.1	21.3
A2	Loam	10-20	46	46	8	1.08	2.17	31	60.0	56.5	52.4	50.1	45.5	18.9
A3.1	Loam	20-30	47	47	6	1.22	2.25	26	50.7	48.7	46.1	45.1	40.6	19.4
A3.2	Loam	30-40	47	47	6	1.23	2.25	27	49.9	47.8	45.8	44.8	40.5	18.8
Eg1	Sandy Loam	40-50	67	23	10	1.69	2.56	23	34.2	32.4	30.5	29.5	25.0	11.1
Eg2	Sandy Loam	50-60	67	23	10	1.53	2.56	26	39.8	36.5	33.7	32.4	28.3	14.4
Bg1	Loam (silty)	60-80	59	32	9	1.51	2.65	33	43.3	37.5	34.1	32.6	25.3	10.3
Bg2	Loam (silty)	80-100	59	32	9	1.63	2.65	29	38.9	35.4	33.0	31.4	27.1	9.5
Cg1	Clay Loam	100-125	45	32	23	1.50	2.64	17	49.1	43.6	41.7	40.8	37.6	25.8

Appendix B – Full Soil Profile Descriptions and Hydraulic Properties (Chapter 3)

**Profile No. 2 - Callaghane**

Horizon	Textural Class	Depth cm	Sand %	Silt %	Clay %	$\rho_b$ g cm <sup>-3</sup>	$\rho_s$ g cm <sup>-3</sup>	$n_e$ %	Retained water % volume					
									0	-0.002	-0.059	-0.137	-1	-15
									bar	bar	bar	bar	bar	bar
A1	Loam	0-10	66	18	16	1.21	2.47	36	54.9	42.5	41.2	39.8	32.4	15.2
A2	Loam	10-20	68	16	16	1.13	2.51	39	57.2	41.6	39.9	38.5	31.3	15.9
Bs	Loamy Sand	20-40	68	20	12	n/a	n/a	n/a		No SWCC data				
C	Coarse Sand	40+	86	6	8	n/a	n/a	n/a		No SWCC data				

Appendix B – Full Soil Profile Descriptions and Hydraulic Properties (Chapter 3)

<b>Profile No. 3 – Kill</b>														
<b>Horizon</b>	<b>Textural Class</b>	<b>Depth</b>	<b>Sand</b>	<b>Silt</b>	<b>Clay</b>	$\rho_b$	$\rho_s$	$n_e$	<b>Retained water</b>					
									<b>% volume</b>					
									<b>cm</b>	<b>%</b>	<b>%</b>	<b>%</b>	<b>g cm<sup>-3</sup></b>	<b>g cm<sup>-3</sup></b>
A1	Loam	0-10	47	34	19	1.04	2.42	43	61.3	54.6	53.7	49.9	-	13.6
A2	Loam	10-25	48	31	21	1.20	2.48	40	60.7	55.6	53.7	50.5	-	11.7
A3	Loam	25-40	45	34	21	1.33	2.54	36	54.2	48.5	43.8	39.3	-	11.2
C1	Loam	40-60	36	39	25	n/a	n/a	n/a						No SWCC data
C2	Loam	60-80	32	42	26	n/a	n/a	n/a						No SWCC data
C3	Loam	80-120	32	41	27	n/a	n/a	n/a						No SWCC data

Appendix B – Full Soil Profile Descriptions and Hydraulic Properties (Chapter 3)

<b>Profile No. 4 - Kill II</b>														
<b>Horizon</b>	<b>Textural Class</b>	<b>Depth</b>	<b>Sand</b>	<b>Silt</b>	<b>Clay</b>	$\rho_b$	$\rho_s$	$n_e$	<b>Retained water</b>					
									<b>% volume</b>					
									<b>cm</b>	<b>%</b>	<b>%</b>	<b>%</b>	<b>g cm<sup>-3</sup></b>	<b>g cm<sup>-3</sup></b>
A1	Loam	0-10	35	43	22	1.18	2.46	36	59.4	52.9	51.2	49.0	-	15.7
A2	Loam	10-20	33	46	21	1.29	2.45	30	59.4	52.5	50.3	47.6	-	17.5
A3	Loam	20-30	32	47	21	1.23	2.5	38	54.6	47.6	41.5	37.6	-	12.4
A4	Loam	30-40	33	46	21	1.21	2.53	41	56.7	49.9	41.1	37.1	-	10.9
Bs	Loam	40-50	26	55	19	1.16	2.57	46	60.0	49.4	43.5	39.6	-	9.0
C1	Loam	50-75	42	42	16	1.67	2.64	27	41.9	35.7	34.3	32.7	-	9.6
C2	Silt Loam	75-100	37	50	13	1.81	2.65	23	35.6	31.2	30.0	29.2	-	9.1

Appendix B – Full Soil Profile Descriptions and Hydraulic Properties (Chapter 3)

<b>Profile No. 5 – Newport</b>														
<b>Horizon</b>	<b>Textural Class</b>	<b>Depth</b>	<b>Sand</b>	<b>Silt</b>	<b>Clay</b>	$\rho_b$	$\rho_s$	$n_e$	<b>Retained water</b>					
									<b>% volume</b>					
									<b>cm</b>	<b>%</b>	<b>%</b>	<b>%</b>	<b>g cm<sup>-3</sup></b>	<b>g cm<sup>-3</sup></b>
A1	Loam	0-12	51	32	17	0.91	2.43	45	63.0	58.1	54.6	52.7	43.6	17.4
A2	Sandy Loam	12-25	54	31	15	1.32	2.55	35	48.4	43.1	41.4	40.4	35.7	13.7
Eg1.1	Loam	25-45	50	36	14	1.65	2.70	26	39.6	35.7	34.2	33.3	28.7	12.5
Eg1.2	Loam	45-60	50	36	14	1.78	2.70	20	34.6	32.0	31.3	30.6	27.4	14.1
Eg2.1	Sandy Loam	60-80	68	18	14	1.86	2.69	18	32.4	30.6	30.0	29.5	26.4	12.6
Eg2.2	Sandy Loam	80-100	68	18	14	1.9	2.67	22	29.9	28.0	27.4	26.4	17.3	6.5
Bg	Loam	100-140	44	33	23	n/a	n/a	n/a			No SWCC data			
C	Loam	140+	64	20	16	n/a	n/a	n/a			No SWCC data			

Appendix B – Full Soil Profile Descriptions and Hydraulic Properties (Chapter 3)

<b>Profile No. 6 – Portlaw</b>														
<b>Horizon</b>	<b>Textural Class</b>	<b>Depth</b>	<b>Sand</b>	<b>Silt</b>	<b>Clay</b>	$\rho_b$	$\rho_s$	$n_e$	<b>Retained water</b>					
									<b>% volume</b>					
									<b>cm</b>	<b>%</b>	<b>%</b>	<b>%</b>	<b>g cm<sup>-3</sup></b>	<b>g cm<sup>-3</sup></b>
Oa	Peat	0-10	No data			0.20	1.51	29	87.5	82.0	77.4	67.7	-	10.7
E	Loam	10-30	45	43	12	1.83	2.60	21	38.1	33.8	34.8	34.4	-	9.1
Bh	Loam	30-33	29	33	38	No data			No SWCC data					
Bs1	Loam	33-60	40	36	24	1.01	2.55	52	68.1	62.3	60.3	54.9	-	8.7
Bs2	Loam	60-120	49	35	16	1.39	2.63	36	48.3	44.2	38.4	34.7	-	10.0
C	Sandy Loam	120-150	57	34	9	1.60	2.67	35	42.9	37.3	33.5	31.7	-	5.0

Appendix B – Full Soil Profile Descriptions and Hydraulic Properties (Chapter 3)

<b>Profile No. 7 - Slievecoiltia</b>														
<b>Horizon</b>	<b>Textural Class</b>	<b>Depth</b>	<b>Sand</b>	<b>Silt</b>	<b>Clay</b>	$\rho_b$	$\rho_s$	$n_e$	<b>Retained water</b>					
									<b>% volume</b>					
		<b>cm</b>	<b>%</b>	<b>%</b>	<b>%</b>	<b>g cm<sup>-3</sup></b>	<b>g cm<sup>-3</sup></b>	<b>%</b>	<b>0</b>	<b>-0.002</b>	<b>-0.059</b>	<b>-0.137</b>	<b>-1</b>	<b>-15</b>
									<b>bar</b>	<b>bar</b>	<b>bar</b>	<b>bar</b>	<b>bar</b>	<b>bar</b>
A1	Loam	0-10	45	28	27	0.98	2.36	43	61.9	58.4	57.7	57.5	-	15.4
A2	Loam	10-20	45	30	25	1.15	2.45	37	59.2	54.2	50.7	43.9	-	16.1
Bs	Loam	20-45	38	32	30	n/a	n/a	n/a			No SWCC data			
C1	Loam/Rock	45-46	29	34	37	n/a	n/a	n/a			No SWCC data			
C2	Shale Bedrock	46+	n/a	n/a	n/a	n/a	n/a	n/a			No SWCC data			

Appendix B – Full Soil Profile Descriptions and Hydraulic Properties (Chapter 3)

<b>Profile No. 8 – Suir</b>														
<b>Horizon</b>	<b>Textural Class</b>	<b>Depth</b>	<b>Sand</b>	<b>Silt</b>	<b>Clay</b>	$\rho_b$	$\rho_s$	$n_e$	<b>Retained water</b>					
									<b>% volume</b>					
									<b>cm</b>	<b>%</b>	<b>%</b>	<b>%</b>	<b>g cm<sup>-3</sup></b>	<b>g cm<sup>-3</sup></b>
A1	Clay Loam	0-10	20	42	38	1.05	2.41	28	54.9	53.3	50.2	49.3	45.4	28.1
A2	Clay Loam	Oct-20	19	43	38	1.13	2.53	28	52.5	49.8	44.5	43.2	38.6	27.2
A3.1	Clay Loam	20-30	18	44	38	1.18	2.57	26	51.2	49.7	43.0	41.6	37.2	28.1
A3.2	Clay Loam	30-40	18	44	38	1.16	2.57	27	54.6	52.6	43.8	42.3	37.5	27.6
Bw1.1	Clay Loam	40-55	28	29	43	1.00	2.57	30	59.7	55.6	49.0	47.4	45.7	30.9
Bw1.2	Clay Loam	55-70	28	29	43	1.19	2.57	29	57.4	47.1	42.3	41.0	37.6	25.0
Bw2	Loam	70-95	59	19	22	1.44	2.64	19	47.2	39.4	35.1	33.7	31.0	26.8
C1	Sand	95-110	86	6	8	n/a	n/a	n/a			No SWCC data			
C2	Sandstone	110-140	84	7	9	n/a	n/a	n/a			No SWCC data			

Appendix B – Full Soil Profile Descriptions and Hydraulic Properties (Chapter 3)

<b>Profile No. 9 - Tramore</b>														
<b>Horizon</b>	<b>Textural Class</b>	<b>Depth</b>	<b>Sand</b>	<b>Silt</b>	<b>Clay</b>	$\rho_b$	$\rho_s$	$n_e$	<b>Retained water</b>					
									<b>% volume</b>					
									<b>cm</b>	<b>%</b>	<b>%</b>	<b>%</b>	<b>g cm<sup>-3</sup></b>	<b>g cm<sup>-3</sup></b>
A1	Loam	0-10	43	38	19	0.87	2.38	52	69.9	61.1	60.0	59.5	-	11.9
A2	Loam	10-25	47	35	18	1.24	2.48	37	58.0	52.6	51.8	50.3	-	13.4
A3	Loam	25-40	48	35	17	1.35	2.56	37	54.1	47.2	44.9	43.8	-	10.2
Eg	Silt Loam	40-120	33	49	18	1.67	2.62	23	42.0	36.6	36.5	36.1	-	13.3
Bx	Silt Loam	45-120	23	65	12	1.76	2.62	22	38.6	34.8	33.9	33.6	-	22.2
Cg	Loam	>120	35	41	24	No data			No SWCC data					

Appendix B – Full Soil Profile Descriptions and Hydraulic Properties (Chapter 3)

<b>Non-Converging - Clashmore</b>														
<b>Horizon</b>	<b>Textural Class</b>	<b>Depth</b>	<b>Sand</b>	<b>Silt</b>	<b>Clay</b>	$\rho_b$	$\rho_s$	$n_e$	<b>Retained water</b>					
									<b>% volume</b>					
									<b>cm</b>	<b>%</b>	<b>%</b>	<b>%</b>	<b>g cm<sup>-3</sup></b>	<b>g cm<sup>-3</sup></b>
A1	Loam	0-10	51	31	18	1.41	2.41	23	49.7	48.8	45.3	44.3	38.9	18.4
A2	Loam	10-20	51	31	18	1.43	2.49	25	46.8	46.0	41.1	40.0	38.4	17.3
A3	Loam	20-32	50	31	19	1.47	2.59	27	46.6	45.8	40.0	37.7	30.1	15.9
E1	Loam	32-40	44	37	19	1.45	2.67	26	44.1	42.9	36.5	34.7	32.1	19.7
E2	Loam	40-50	44	37	19	1.52	2.67	23	42.8	40.7	34.5	32.6	29.2	20.2
Bw1	Loam	50-70	48	35	17	1.57	2.68	24	39.6	37.4	33.0	31.1	26.0	17.1
Bw2	Loam	70-90	48	35	17	1.79	2.68	18	33.6	30.8	28.5	27.4	24.8	15.6
C	Loam	>90	44	33	23	1.77	2.73	20	33.1	31.7	29.6	28.9	26.8	14.8

Appendix B – Full Soil Profile Descriptions and Hydraulic Properties (Chapter 3)

<b>Non-Converging - Dungarvan</b>															
<b>Horizon</b>	<b>Textural Class</b>	<b>Depth cm</b>	<b>Sand %</b>	<b>Silt %</b>	<b>Clay %</b>	<b><math>\rho_b</math> g cm<sup>-3</sup></b>	<b><math>\rho_s</math> g cm<sup>-3</sup></b>	<b><math>n_e</math> %</b>	<b>Retained water % volume</b>						
									<b>0 bar</b>	<b>-0.002 bar</b>	<b>-0.059 bar</b>	<b>-0.137 bar</b>	<b>-1 bar</b>	<b>-15 bar</b>	
									A1	Loam	0-10	54	28	18	1.42
A2	Loam	10-20	56	26	18	1.48	2.48	23	44.0	41.7	37.1	36.2	32.4	17.1	
A3.1	Loam	20-35	52	31	17	1.44	2.60	24	46.3	40.7	33.6	31.6	23.1	20.3	
A3.2	Loam	35-50	52	31	17	1.49	2.60	23	47.3	41.3	34.3	31.7	25.4	19.2	
E/B1.1	Sandy Loam	50-65	58	23	19	1.79	2.64	8	37.4	32.1	28.7	27.7	23.9	24.1	
E/B1.2	Sandy Loam	65-80	58	23	19	1.73	2.64	13	36.7	32.1	28.8	27.9	25.6	21.5	
Bt1.1	Loam	80-100	57	26	19	1.84	2.61	9	32.8	30.6	27.1	26.3	24.1	20.9	
Bt1.2	Loam	100-120	57	26	19	1.79	2.61	14	29.7	27.8	25.6	25.0	23.4	17.8	
Bt2	Loam	120-160	45	33	22	1.82	2.69	19	30.0	28.5	26.7	26.3	24.8	13.4	
C	Loam	160-200	53	28	19	n/a	n/a	n/a			No SWCC data				

Appendix B – Full Soil Profile Descriptions and Hydraulic Properties (Chapter 3)

<b>Non-Converging - Lickey</b>														
<b>Horizon</b>	<b>Textural Class</b>	<b>Depth</b>	<b>Sand</b>	<b>Silt</b>	<b>Clay</b>	$\rho_b$	$\rho_s$	$n_e$	<b>Retained water</b>					
									<b>% volume</b>					
									<b>cm</b>	<b>%</b>	<b>%</b>	<b>%</b>	<b>g cm<sup>-3</sup></b>	<b>g cm<sup>-3</sup></b>
A1	Loam	0-10	48	28	24	0.79	2.38	46	68.8	54.2	51.5	49.9	41.1	20.8
A2	Loam	10-18	45	30	25	1.27	2.52	25	50.4	45.2	43.7	42.7	38.2	24.6
Eg	Loam	18-30	61	24	15	1.71	2.69	17	35.8	31.5	30.5	29.7	26.7	19.6
Bg1	Loam	30-65	54	30	16	1.79	2.61	21	35.1	31.3	29.3	28.5	25.0	10.5
Bg2.1	Loam	65-80	50	30	20	1.81	2.73	20	30.0	28.1	26.2	25.7	23.5	13.7
Bg2.2	Loam	80-100	50	30	20	1.82	2.73	23	31.3	29.4	27.2	26.8	23.8	10.5
Bg3	Loam	100-110	50	32	18	n/a	n/a	n/a			No SWCC data			
Bg4	Loam	110-150	49	29	22	n/a	n/a	n/a			No SWCC data			
C	Sandy Loam	150-180	54	26	20	n/a	n/a	n/a			No SWCC data			

Appendix B – Full Soil Profile Descriptions and Hydraulic Properties (Chapter 3)

<b>Profile No. 1 - Ballymacart</b>												
Horizon	$\theta_r$	$\theta_s$	$\alpha$	$n$	$k_s$ (cm hr <sup>-1</sup> )	$R^2$	$\theta_r$	$\theta_s$	$\alpha$	$n$	$k_s$ (cm hr <sup>-1</sup> )	$R^2$
	<b>Textural Drop-down Menu</b>						<b>ROSETTA</b>					
A1	0.078	0.430	0.036	1.56	1.04	n/a	0.043	0.452	0.007	1.58	8.13	n/a
A2	0.078	0.430	0.036	1.56	1.04	n/a	0.045	0.436	0.007	1.58	5.21	n/a
A3.1	0.078	0.430	0.036	1.56	1.04	n/a	0.038	0.396	0.009	1.54	3.35	n/a
A3.2	0.078	0.430	0.036	1.56	1.04	n/a	0.038	0.394	0.009	1.54	3.22	n/a
Eg1	0.065	0.410	0.075	1.89	4.42	n/a	0.038	0.333	0.043	1.36	0.88	n/a
Eg2	0.065	0.410	0.075	1.89	4.42	n/a	0.042	0.374	0.033	1.45	1.67	n/a
Bg1	0.067	0.450	0.020	1.41	0.45	n/a	0.038	0.364	0.026	1.42	1.40	n/a
Bg2	0.067	0.450	0.020	1.41	0.45	n/a	0.035	0.337	0.033	1.36	0.91	n/a
Cg1	0.095	0.410	0.019	1.31	0.26	n/a	0.064	0.393	0.014	1.43	0.40	n/a

Appendix B – Full Soil Profile Descriptions and Hydraulic Properties (Chapter 3)

<b>Profile No. 1 - Ballymacart</b>												
Horizon	$\theta_r$	$\theta_s$	$\alpha$	$n$	$k_s$ (cm hr <sup>-1</sup> )	$R^2$	$\theta_r$	$\theta_s$	$\alpha$	$n$	$k_s$ (cm hr <sup>-1</sup> )	$R^2$
	<b>Full SWCC</b>						<b>Low pressure data - no -15 Bar point</b>					
A1	0.043	0.559	2.355	1.14	8.13	0.93	0.043	0.595	558.866	1.04	8.13	0.98
A2	0.045	0.554	0.123	1.36	5.21	0.96	0.045	0.598	106.655	1.04	5.21	0.98
A3.1	0.038	0.481	0.111	1.32	3.35	0.98	0.038	0.499	6.711	1.05	3.35	0.97
A3.2	0.038	0.474	0.098	1.34	3.22	0.98	0.038	0.490	4.678	1.05	3.22	0.96
Eg1	0.038	0.322	0.190	1.31	0.88	0.98	0.038	0.334	3.239	1.08	0.88	0.97
Eg2	0.042	0.374	0.033	1.45	1.67	0.95	0.042	0.397	200.822	1.04	1.67	0.96
Bg1	0.038	0.399	1.266	1.22	1.40	0.95	0.038	0.409	8.961	1.10	1.40	0.91
Bg2	0.035	0.352	0.155	1.39	0.91	0.95	0.035	0.387	196.354	1.04	0.91	0.95
Cg1	0.064	0.460	1.678	1.43	0.40	0.91	0.064	0.492	6928.070	1.02	0.40	0.97

Appendix B – Full Soil Profile Descriptions and Hydraulic Properties (Chapter 3)

<b>Profile No. 2 - Callaghane</b>												
<b>Horizon</b>	$\theta_r$	$\theta_s$	$\alpha$	$n$	$k_s$ (cm hr <sup>-1</sup> )	$R^2$	$\theta_r$	$\theta_s$	$\alpha$	$n$	$k_s$ (cm hr <sup>-1</sup> )	$R^2$
<b>Textural Menu</b>						<b>ROSETTA</b>						
A1	0.078	0.043	0.036	1.56	1.04	n/a	0.059	0.469	0.023	1.44	4.01	n/a
A2	0.078	0.043	0.036	1.56	1.04	n/a	0.060	0.495	0.024	1.43	5.46	n/a
Bs	No data						n/a					
C	No data						n/a					
<b>Full SWCC</b>						<b>Low pressure data - no -15 Bar point</b>						
A1	0.059	0.483	0.156	1.18	4.01	0.88	0.059	0.555	35520.1	1.03	4.01	0.93
A2	0.060	0.497	0.409	1.15	5.46	0.85	0.060	0.590	133820.9	1.04	5.46	0.95
Bs	No data						No data					
C	No data						No data					

Appendix B – Full Soil Profile Descriptions and Hydraulic Properties (Chapter 3)

<b>Profile No. 3 - Kill</b>												
<b>Horizon</b>	$\theta_r$	$\theta_s$	$\alpha$	$n$	$k_s$ (cm hr <sup>-1</sup> )	$R^2$	$\theta_r$	$\theta_s$	$\alpha$	$n$	$k_s$ (cm hr <sup>-1</sup> )	$R^2$
<b>Textural Menu</b>							<b>ROSETTA</b>					
A1	0.078	0.430	0.036	1.56	1.04	n/a	0.068	0.495	0.010	1.52	3.40	n/a
A2	0.078	0.430	0.036	1.56	1.04	n/a	0.068	0.461	0.012	1.49	1.69	n/a
A3	0.078	0.430	0.036	1.56	1.04	n/a	0.065	0.426	0.011	1.50	0.86	n/a
C1	No SWCC data						No SWCC data					
C2	No SWCC data						No SWCC data					
C3	No SWCC data						No SWCC data					
<b>Full SWCC</b>							<b>Low pressure data - no -15 Bar point</b>					
A1	0.069	0.578	0.069	1.31	3.40	0.981	0.068	0.618	68107.45	1.02	3.40	0.926
A2	0.068	0.579	0.060	1.35	1.69	0.991	Couldn't plot - not enough data					
A3	0.065	0.513	0.161	1.27	0.86	0.986	0.065	0.542	458.10	1.05	0.86	0.963
C1	No SWCC data						No SWCC data					
C2	No SWCC data						No SWCC data					
C3	No SWCC data						No SWCC data					

Appendix B – Full Soil Profile Descriptions and Hydraulic Properties (Chapter 3)

<b>Profile No. 4 - Kill II</b>												
<b>Horizon</b>	$\theta_r$	$\theta_s$	$\alpha$	$n$	$k_s$ (cm hr <sup>-1</sup> )	$R^2$	$\theta_r$	$\theta_s$	$\alpha$	$n$	$k_s$ (cm hr <sup>-1</sup> )	$R^2$
<b>Textural Menu</b>						<b>ROSETTA</b>						
A1	0.078	0.430	0.036	1.56	1.04	n/a	0.072	0.4604	0.007	1.58	1.61	n/a
A2	0.078	0.430	0.036	1.56	1.04	n/a	0.068	0.4289	0.007	1.60	0.95	n/a
A3	0.078	0.430	0.036	1.56	1.04	n/a	0.069	0.4435	0.006	1.61	1.31	n/a
A4	0.078	0.430	0.036	1.56	1.04	n/a	0.070	0.4484	0.006	1.61	1.45	n/a
Bs	0.078	0.430	0.036	1.56	1.04	n/a	0.070	0.4582	0.005	1.68	2.27	n/a
C1	0.078	0.430	0.036	1.56	1.04	n/a	0.045	0.3326	0.016	1.38	0.28	n/a
C2	0.067	0.450	0.020	1.41	0.45	n/a	0.036	0.2949	0.021	1.30	0.20	n/a
<b>Full SWCC</b>						<b>Low pressure data - no -15 Bar point</b>						
A1	0.072	0.559	0.074	1.27	1.61	0.980	0.072	0.604	186014.4	1.02	1.61	0.979
A2	0.068	0.558	0.106	1.23	0.95	0.976	Couldn't plot - not enough data					
A3	0.069	0.512	0.268	1.23	1.31	0.976	0.069	0.546	567.58	1.06	1.31	0.985
A4	0.070	0.535	0.331	1.25	1.45	0.980	0.070	0.567	247.09	1.08	1.45	0.993
Bs	0.070	0.547	0.206	1.30	2.27	0.959	0.070	0.600	2440.02	1.06	2.27	0.989
C1	0.045	0.386	0.096	1.28	0.28	0.966	0.045	0.453	5180049	1.02	0.28	0.986
C2	0.036	0.332	0.075	1.27	0.20	0.973	0.036	0.389	-	1.02	0.20	0.995

Appendix B – Full Soil Profile Descriptions and Hydraulic Properties (Chapter 3)

<b>Profile No. 5 - Newport</b>												
<b>Horizon</b>	$\theta_r$	$\theta_s$	$\alpha$	$n$	$k_s$ (cm hr <sup>-1</sup> )	$R^2$	$\theta_r$	$\theta_s$	$\alpha$	$n$	$k_s$ (cm hr <sup>-1</sup> )	$R^2$
<b>Textural Menu</b>						<b>ROSETTA</b>						
A1	0.078	0.430	0.036	1.56	1.04	n/a	0.067	0.533	0.012	1.48	6.63	n/a
A2	0.065	0.410	0.075	1.89	4.42	n/a	0.053	0.418	0.015	1.48	1.70	n/a
Eg1.1	0.078	0.430	0.036	1.56	1.04	n/a	0.042	0.337	0.022	1.36	0.45	n/a
Eg1.2	0.078	0.430	0.036	1.56	1.04	n/a	0.037	0.307	0.031	1.26	0.27	n/a
Eg2.1	0.065	0.410	0.075	1.89	4.42	n/a	0.040	0.297	0.047	1.25	0.33	n/a
Eg2.2	0.065	0.410	0.075	1.89	4.42	n/a	0.039	0.287	0.048	1.24	0.28	n/a
Bg	No data					No data						
C	No data					No data						
<b>Full SWCC</b>						<b>Low pressure data - no -15 Bar point</b>						
A1	0.067	0.582	0.021	1.34	6.63	0.968	0.067	0.607	3.638	1.09	6.63	0.944
A2	0.053	0.437	0.011	1.40	1.70	0.955	0.053	0.484	1725.969	1.03	1.70	0.930
Eg1.1	0.042	0.362	0.016	1.32	0.45	0.960	0.042	0.379	7.190	1.06	0.45	0.886
Eg1.2	0.037	0.324	0.012	1.28	0.27	0.973	0.037	0.334	4.156	1.05	0.27	0.882
Eg2.1	0.040	0.308	0.009	1.33	0.33	0.986	0.040	0.315	2.076	1.06	0.33	0.915
Eg2.2	0.039	0.288	0.036	1.37	0.28	0.995	0.039	0.289	0.425	1.33	0.28	0.979
Bg	No data					No data						
C	No data					No data						

Appendix B – Full Soil Profile Descriptions and Hydraulic Properties (Chapter 3)

<b>Profile No. 6 - Portlaw</b>												
<b>Horizon</b>	$\theta_r$	$\theta_s$	$\alpha$	$n$	$k_s$ (cm hr <sup>-1</sup> )	$R^2$	$\theta_r$	$\theta_s$	$\alpha$	$n$	$k_s$ (cm hr <sup>-1</sup> )	$R^2$
<b>Textural Menu</b>							<b>ROSETTA</b>					
Oa				No data						No data		
E	0.078	0.43	0.036	1.56	1.04	n/a	0.033	0.290	0.032	1.25	0.23	n/a
Bh				No data						No data		
Bs1	0.078	0.43	0.036	1.56	1.04	n/a	0.079	0.519	0.009	1.52	3.46	n/a
Bs2	0.078	0.43	0.036	1.56	1.04	n/a	0.054	0.399	0.013	1.49	0.99	n/a
C	0.065	0.41	0.075	1.89	4.42	n/a	0.036	0.342	0.029	1.38	0.95	n/a
<b>Full SWCC</b>							<b>Low pressure data - no -15 Bar point</b>					
Oa				No data						No data		
E	0.033	0.358	0.022	1.35	0.23	0.981				Insufficient data		
Bh				No data						Insufficient data		
Bs1	0.079	0.650	0.061	1.44	3.46	0.992	0.079	0.653	1.268	1.22	3.46	0.819
Bs2	0.054	0.463	0.213	1.25	0.99	0.989	0.054	0.483	169.320	1.06	0.99	0.980
C	0.036	0.397	0.103	1.39	0.95	0.975	0.036	0.429	1988.633	1.04	0.95	0.995

Appendix B – Full Soil Profile Descriptions and Hydraulic Properties (Chapter 3)

<b>Profile 7 - Slievecoiltia</b>												
<b>Horizon</b>	$\theta_r$	$\theta_s$	$\alpha$	$n$	$k_s$ (cm hr <sup>-1</sup> )	$R^2$	$\theta_r$	$\theta_s$	$\alpha$	$n$	$k_s$ (cm hr <sup>-1</sup> )	$R^2$
<b>Textural Menu</b>							<b>ROSETTA</b>					
A1	0.078	0.430	0.036	1.56	1.04	n/a	0.084	0.543	0.013	1.448	3.67	n/a
A2	0.078	0.430	0.036	1.56	1.04	n/a	0.076	0.486	0.011	1.479	1.75	n/a
Bs				No data						No data		
C1				No data						No data		
C2				No data						No data		
<b>Full SWCC</b>							<b>Low pressure data - no -15 Bar point</b>					
A1	0.084	0.596	0.019	1.40	3.67	0.994	Insufficient data					
A2	0.094	0.568	0.129	1.37	1.75	0.989	0.0763	0.56785	1.25183	1.36547	1.75	0.902
Bs				No data						No data		
C1				No data						No data		
C2				No data						No data		

Appendix B – Full Soil Profile Descriptions and Hydraulic Properties (Chapter 3)

<b>Profile No. 8 - Suir</b>												
<b>Horizon</b>	$\theta_r$	$\theta_s$	$\alpha$	$n$	$k_s$ (cm hr <sup>-1</sup> )	$R^2$	$\theta_r$	$\theta_s$	$\alpha$	$n$	$k_s$ (cm hr <sup>-1</sup> )	$R^2$
<b>Textural Menu</b>						<b>ROSETTA</b>						
A1	0.095	0.410	0.019	1.31	6.24	n/a	0.099	0.555	0.013	1.42	2.88	n/a
A2	0.095	0.410	0.019	1.31	6.24	n/a	0.097	0.531	0.012	1.44	1.84	n/a
A3.1	0.095	0.410	0.019	1.31	6.24	n/a	0.096	0.517	0.012	1.44	1.38	n/a
A3.2	0.095	0.410	0.019	1.31	6.24	n/a	0.096	0.523	0.012	1.44	1.54	n/a
Bw1.1	0.095	0.410	0.019	1.31	6.24	n/a	0.104	0.578	0.019	1.36	3.82	n/a
Bw1.2	0.095	0.410	0.019	1.31	6.24	n/a	0.098	0.519	0.016	1.37	1.49	n/a
Bw2	0.078	0.430	0.036	1.56	24.96	n/a	0.064	0.417	0.020	1.41	1.09	n/a
C1	No data						No data					
C2	No data						No data					
<b>Full SWCC</b>						<b>Low pressure data - no -15 Bar point</b>						
A1	0.099	0.526	0.017	1.19	2.88	0.970	0.099	0.544	14.478	1.04	2.88	0.983
A2	0.097	0.512	0.449	1.09	1.84	0.972	0.097	0.523	78.549	1.04	1.84	0.993
A3.1	0.096	0.507	1.033	1.08	1.38	0.988	0.096	0.512	41.800	1.05	1.38	0.999
A3.2	0.096	0.542	1.739	1.08	1.54	0.988	0.096	0.547	58.271	1.06	1.54	0.998
Bw1.1	0.104	0.580	0.913	1.08	3.82	0.927	0.104	0.597	491.674	1.03	3.82	0.991
Bw1.2	0.098	0.572	52.701	1.06	1.49	0.926	0.098	0.576	13344.12	1.03	1.49	0.998
Bw2	0.064	0.472	272.94	1.04	1.09	0.996	0.064	0.473	5436.946	1.04	1.09	0.999
C1	No data						No data					
C2	No data						No data					

Appendix B – Full Soil Profile Descriptions and Hydraulic Properties (Chapter 3)

<b>Profile No. 9 - Tramore</b>												
<b>Horizon</b>	$\theta_r$	$\theta_s$	$\alpha$	$n$	$k_s$ (cm hr <sup>-1</sup> )	$R^2$	$\theta_r$	$\theta_s$	$\alpha$	$n$	$k_s$ (cm hr <sup>-1</sup> )	$R^2$
<b>Textural Menu</b>						<b>ROSETTA</b>						
A1	0.078	0.430	0.036	1.56	1.04	n/a	0.074	0.546	0.008	1.54	7.46	n/a
A2	0.078	0.430	0.036	1.56	1.04	n/a	0.061	0.438	0.010	1.52	1.52	n/a
A3	0.078	0.430	0.036	1.56	1.04	n/a	0.057	0.410	0.012	1.50	1.06	n/a
Eg	0.067	0.450	0.020	1.41	0.45	n/a	0.050	0.336	0.011	1.43	0.22	n/a
Bx	0.067	0.450	0.020	1.41	0.45	n/a	0.042	0.317	0.011	1.43	0.27	n/a
Cg	No data					No data						
<b>Full SWCC</b>						<b>Low pressure data - no -15 Bar point</b>						
A1	0.074	0.645	0.036	1.42	7.46	0.976	Insufficient data					
A2	0.061	0.550	0.043	1.34	1.52	0.987	Insufficient data					
A3	0.057	0.502	0.068	1.34	1.06	0.975	0.050	0.574	2838495	1.02	1.06	0.998
Eg	0.050	0.390	0.048	1.25	0.22	0.967	Insufficient data					
Bx	0.042	0.364	0.047	1.28	0.27	0.981	0.042	0.397	1223786	1.01	0.27	0.988
Cg	No data					No data						

Appendix B – Full Soil Profile Descriptions and Hydraulic Properties (Chapter 3)

<b>Non-Converging - Clashmore</b>												
<b>Horizon</b>	$\theta_r$	$\theta_s$	$\alpha$	$n$	$k_s$ (cm hr <sup>-1</sup> )	$R^2$	$\theta_r$	$\theta_s$	$\alpha$	$n$	$k_s$ (cm hr <sup>-1</sup> )	$R^2$
	<b>Textural Menu</b>						<b>ROSETTA</b>					
A1	0.078	0.430	0.036	1.56	24.96	n/a	0.057	0.404	0.0146	1.47	0.92	n/a
A2	0.078	0.430	0.036	1.56	24.96	n/a	0.057	0.400	0.0149	1.46	0.85	n/a
A3	0.078	0.430	0.036	1.56	24.96	n/a	0.057	0.393	0.0152	1.44	0.67	n/a
E1	0.078	0.430	0.036	1.56	24.96	n/a	0.058	0.391	0.0115	1.49	0.55	n/a
E2	0.078	0.430	0.036	1.56	24.96	n/a	0.056	0.376	0.0127	1.46	0.42	n/a
Bw1	0.078	0.430	0.036	1.56	24.96	n/a	0.050	0.362	0.0163	1.41	0.46	n/a
Bw2	0.078	0.430	0.036	1.56	24.96	n/a	0.041	0.310	0.0282	1.25	0.20	n/a
C	0.078	0.430	0.036	1.56	24.96	n/a	0.051	0.326	0.0223	1.25	0.13	n/a
	<b>Full SWCC</b>						<b>Low pressure data - no -15 Bar point</b>					
A1	0.057	0.476	0.014	1.30	0.92	0.979	0.057	0.493	4.473	1.06	0.92	0.991
A2	0.057	0.438	0.008	1.36	0.85	0.947	0.057	0.470	86.273	1.03	0.85	0.987
A3	0.057	0.459	0.165	1.18	0.67	0.985	0.057	0.463	4.627	1.11	0.67	0.998
E1	0.058	0.435	0.520	1.10	0.55	0.955	0.058	0.443	62.424	1.05	0.55	0.995
E2	0.056	0.422	1.148	1.46	0.42	0.982	0.056	0.428	71.462	1.06	0.42	0.999
Bw1	0.050	0.386	0.394	1.12	0.46	0.986	0.050	0.389	11.244	1.08	0.46	0.987
Bw2	0.041	0.320	0.190	1.11	0.20	0.945	0.041	0.336	395.842	1.03	0.20	0.980
C	0.051	0.312	0.013	1.24	0.13	0.960	0.051	0.325	3.952	1.07	0.13	0.974

Appendix B – Full Soil Profile Descriptions and Hydraulic Properties (Chapter 3)

<b>Non-Converging - Dungarvan</b>												
<b>Horizon</b>	$\theta_r$	$\theta_s$	$\alpha$	$n$	$k_s$ (cm hr <sup>-1</sup> )	$R^2$	$\theta_r$	$\theta_s$	$\alpha$	$n$	$k_s$ (cm hr <sup>-1</sup> )	$R^2$
	<b>Textural Menu</b>						<b>ROSETTA</b>					
A1	0.078	0.430	0.036	1.56	1.04	n/a	0.057	0.406	0.017	1.45	1.02	n/a
A2	0.078	0.430	0.036	1.56	1.04	n/a	0.056	0.394	0.019	1.42	0.89	n/a
A3.1	0.078	0.430	0.036	1.56	1.04	n/a	0.055	0.395	0.016	1.46	0.90	n/a
A3.2	0.078	0.430	0.036	1.56	1.04	n/a	0.053	0.384	0.017	1.44	0.74	n/a
E/B1.1	0.065	0.410	0.075	1.89	4.42	n/a	0.045	0.318	0.035	1.22	0.24	n/a
E/B1.2	0.065	0.410	0.075	1.89	4.42	n/a	0.047	0.334	0.031	1.26	0.32	n/a
Bt1.1	0.078	0.430	0.036	1.56	1.04	n/a	0.042	0.305	0.037	1.20	0.17	n/a
Bt1.2	0.078	0.430	0.036	1.56	1.04	n/a	0.044	0.317	0.033	1.22	0.22	n/a
Bt2	0.078	0.430	0.036	1.56	1.04	n/a	0.047	0.312	0.026	1.22	0.12	n/a
C	No data						No data					
	<b>Full SWCC</b>						<b>Low pressure data - no -15 Bar point</b>					
A1	0.057	0.438	0.147	1.15	1.02	0.967	0.057	0.446	11.594	1.07	1.02	0.972
A2	0.056	0.419	0.091	1.16	0.89	0.941	0.056	0.439	94.112	1.04	0.89	0.994
A3.1	0.055	0.460	10.207	1.09	0.90	0.978	0.055	0.458	85.979	1.09	0.90	0.966
A3.2	0.053	0.468	9.268	1.09	0.74	0.986	0.053	0.472	181.060	1.08	0.74	0.985
E/B1.1	0.045	0.374	88.625	1.10	0.24	0.974	0.045	0.374	1116.878	1.04	0.24	0.983
E/B1.2	0.047	0.367	66.241	1.04	0.32	0.987	0.047	0.367	1879.178	1.04	0.32	0.998
Bt1.1	0.042	0.327	14.047	1.04	0.17	0.996	0.042	0.328	230.863	1.04	0.17	0.999
Bt1.2	0.044	0.288	0.596	1.06	0.22	0.951	0.044	0.297	428.446	1.03	0.22	0.997
Bt2	0.047	0.281	0.009	1.27	0.12	0.958	0.047	0.300	366.090	1.02	0.12	0.994
C	No data						No data					

Appendix B – Full Soil Profile Descriptions and Hydraulic Properties (Chapter 3)

<b>Non-Converging - Lickey</b>												
<b>Horizon</b>	$\theta_r$	$\theta_s$	$\alpha$	$n$	$k_s$ (cm hr <sup>-1</sup> )	$R^2$	$\theta_r$	$\theta_s$	$\alpha$	$n$	$k_s$ (cm hr <sup>-1</sup> )	$R^2$
<b>Textural Menu</b>						<b>ROSETTA</b>						
A1	0.078	0.43	0.036	1.56	1.04	n/a	0.084	0.600	0.013	1.43	7.90	n/a
A2	0.078	0.43	0.036	1.56	1.04	n/a	0.073	0.455	0.012	1.48	1.02	n/a
Eg	0.078	0.43	0.036	1.56	1.04	n/a	0.043	0.334	0.035	1.29	0.48	n/a
Bg1	0.078	0.43	0.036	1.56	1.04	n/a	0.040	0.312	0.035	1.24	0.26	n/a
Bg2.1	0.078	0.43	0.036	1.56	1.04	n/a	0.044	0.312	0.030	1.22	0.16	n/a
Bg2.2	0.078	0.43	0.036	1.56	1.04	n/a	0.044	0.310	0.031	1.22	0.15	n/a
Bg3				No data						No data		
Bg4				No data						No data		
C				No data						No data		
<b>Full SWCC</b>						<b>Low pressure data - no -15 Bar point</b>						
A1	0.085	0.612	0.219	1.16	7.90	0.891	0.085	0.691	15472.720	1.04	7.90	0.943
A2	0.073	0.470	0.059	1.14	1.02	0.940	0.073	0.504	2078.390	1.02	1.02	0.928
Eg	0.043	0.336	0.253	1.08	0.48	0.924	0.043	0.358	5382.435	1.02	0.48	0.941
Bg1	0.040	0.315	0.017	1.33	0.26	0.942	0.040	0.351	877.550	1.03	0.26	0.956
Bg2.1	0.044	0.280	0.023	1.20	0.16	0.948	0.044	0.300	298.287	1.03	0.16	0.979
Bg2.2	0.044	0.290	0.013	1.33	0.15	0.962	0.044	0.312	127.540	1.03	0.15	0.963
Bg3				No data						No data		
Bg4				No data						No data		
C				No data						No data		

## **Appendix D**

### **Effect of duration of centrifugation on soil hydraulic parameters, unsaturated zone time lag estimates and soil physical quality assessment**

#### **Introduction**

The statistical analysis (Chapter 5) indicated a significant effect of treatment (24, 48 or 72-hrs) on measured SWCCs, and identified the optimum time step (from those treatments) regarding the arable soil (further testing at prolonged time-steps would be required to do likewise for the grassland soil). Due to the time limitations constraining this study, it was not possible to test a greater number of experimental sites or soil textural classes, or to assess the optimum experimental duration for deeper soil horizons at these same sites. Consequently, only top-soils from the two catchment study sites were examined, as it is these sites which are of primary interest in this thesis. Chapter 5 should therefore indicate the methodology for experimental duration assessment, rather than being prescriptive of suitable time-steps on soils outside of those studied. As a result of the testing of the arable soil, a 48-hr duration was applied for both the arable and the grassland soils. Having acknowledged that this duration is likely insufficient for effective equilibrium to be reached at the grassland site, this appendix retrospectively considers the implications of this decision for  $t_u$  estimates described in Chapter 7. As the optimum time-step was satisfactorily ascertained for the arable soil using the statistical approach in Chapter 5, only the grassland site is discussed in this appendix.

#### **Materials and Methods**

SWCCs determined in Chapter 5, according to 24-, 48- and 72-hr treatments are used to derive soil hydraulic parameters. Due to the confounding effect of scatter at initial saturation (Šimůnek and Nimmo, 2005), it is misleading to directly compare hydraulic properties derived according to the various time-steps, hence, volumetric water contents were expressed on a relative basis (effective saturation) allowing comparison of the SWCCs across treatments (i.e. all soils start with an initial saturation of 100%). While this allows statistical comparison of the SWCCs themselves, hydraulic properties cannot be derived from such data using fitting equations, as a soil (which is implicitly a porous medium, having solid, liquid

Appendix C – Consequences of Centrifuge Duration on Hydraulic Parameters and  $t_u$  Estimates (Chapter 5)

and gaseous components) cannot in reality be 100% liquid. Effective saturation values were therefore, adjusted to ranges which are realistic for such mineral soil types. As it is common to encounter saturated volumetric water contents ranging between 33% and 50% total volume (Diamond and Sills, 2011), SWCCs were adjusted to these ranges (Fig. C1). Hydraulic properties for the grassland soil according to each of the temporal treatments (24-, 48- and 72-hours) were then derived using the VGM equation, within the RETC program (Schaap *et al.*, 2001). These parameters were used as inputs to the Hydrus 1D numerical model in accordance with the methodology outlined in Chapter 3 (50 cm deep soil profile, atmospheric upper boundary condition and free drainage lower boundary condition), for both wet (2004) and dry (2010) years, and IBT/Trend, Peak, COM and Exit were identified from resulting breakthrough curves.

**Table C1:** Effective saturation data for the grassland soil, according to treatment, expressed as relative to 100%, 50% and 33% VWC at saturation.

kPa	24 Hour			48 Hour			72 Hour		
	Relative	50%	33%	Relative	50%	33%	Relative	50%	33%
<b>0</b>	100	50	33	100	50	33	100	50	33
<b>50</b>	74	37	25	71	36	24	68	34	23
<b>100</b>	67	34	22	65	32	22	63	31	21
<b>150</b>	63	32	21	60	30	20	59	29	20
<b>200</b>	60	30	20	57	28	19	55	28	18
<b>1000</b>	45	22	15	41	20	14	39	20	13
<b>1,500</b>	40	20	13	36	18	12	34	17	11

## Results

### *Soil hydraulic parameters*

Hydraulic parameters for each treatment are displayed in Table C2. Differences in  $\theta_s$  between treatments, for both the high (50%) and low (33%) saturated VWC did not exceed 0.0004 and 0.0005, for the grassland and arable sites respectively. Differences in fitting parameters ( $\alpha$  and  $n$ ) were likewise minor.

**Table C2:** Hydraulic properties of the grassland soil according to treatment.

Treatment	Saturated VWC	$\theta_r$	$\theta_s$	$\alpha$	$n$	$k_s$ (cm hr <sup>-1</sup> )	$R^2$
24-hr	50%	0.1027	0.4994	0.0072	1.190	7.76	0.998
	33%	0.1027	0.3299	0.0070	1.191	7.76	0.997
48-hr	50%	0.1027	0.4997	0.0076	1.211	7.76	0.999
	33%	0.1027	0.3297	0.0071	1.206	7.76	0.997
72-hr	50%	0.1027	0.4995	0.0106	1.199	7.76	0.995
	33%	0.1027	0.3295	0.0076	1.218	7.76	0.994

*Time lag estimates*

Figure C1 indicates  $t_u$  estimates for each treatment, for the grassland site. Exit of the solute was not achieved, in any but the wet, low VWC simulations. Briefer  $t_u$  were observed in both the wet and dry years under this condition than at high saturated VWC, reflecting the lower water requirement to replace a deficit from field capacity. In other words, it requires the addition of less water to return these soils to field capacity, than on a higher porosity soil, and hence, the soil is typically wetter and hence, may transmit solutes over a greater period than those soils which are only intermittently saturated. There was no difference observed in any  $t_u$  marker under low saturated VWC conditions. Under high saturated VWC conditions, differences between treatments did not exceed 0.01 yrs for any marker.

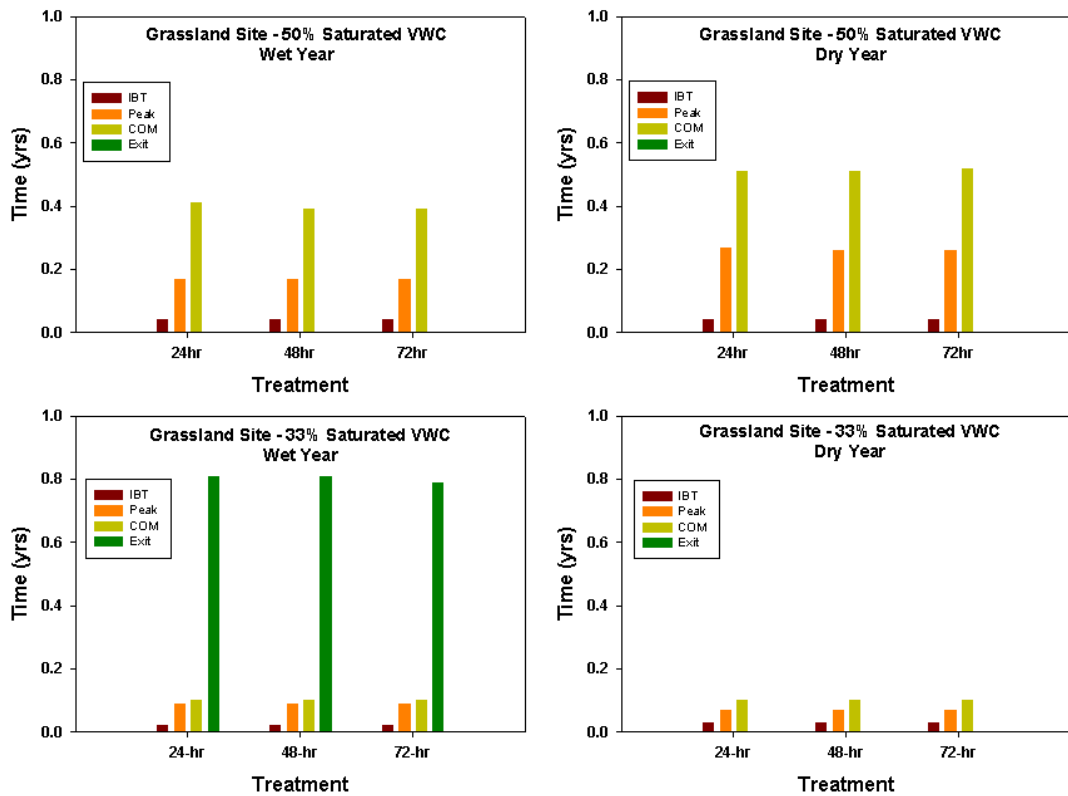


**Fig. C1:** Estimates of  $t_u$  (wet and dry years) for the grassland soil, under high (50%) and low (33%) saturated VWCs.

**Discussion**

*Soil hydraulic parameters*

Early implications of these results suggest that while differences in SWCCs arising as a result of various durations of centrifugation are statistically significant (as indicated in Chapter 5), the subsequent effect on hydraulic properties appear small. However, it remains difficult to ascertain the implications of these property differences without testing the results of these properties within the target numerical model application. In order to ascertain whether the differences in hydraulic parameters are important, they should be examined using numerical modelling, in this case;  $t_u$  estimation using Hydrus 1D.

#### *Time lag estimates*

Optimal time-steps determined according to the laboratory and statistical testing methodology described in Chapter 5 remain the most appropriate and should be considered the ‘gold-standard’ against which other SWCCs are compared. However, the analysis presented in this appendix indicates that the differences in  $t_u$  estimates at the grassland site, as a result of a briefer than optimum experimental durations are relatively small within the context of the six-year EU-WFD reporting periods. Further to Chapter 4, it is evident that the differences in  $t_u$  duration arising herein as a result of treatment duration (for example, differences in IBT/Trend not exceeding 0.01 yrs) were lesser than those differences arising as a result of heterogeneity of properties over a small area (differences in IBT/Trend between profiles A and B of 0.02-0.04 yrs (Chapter 4)). This suggests that when conducting a site-specific assessment of  $t_u$ , using either high- or low-complexity approaches, obtaining and testing a range of soil samples over the given area is to be preferred to a highly intensive analysis of fewer samples.

#### **Conclusions**

While the effects of the temporal treatments are statistically significant (Chapter 5) and an optimum duration of 48-hrs was identified for the arable soil, no such duration was identified for the grassland soil, and an identical duration was applied in  $t_u$  assessment at both sites (Chapter 7). For the grassland site, although the 48-hr duration applied in Chapter 7 was sub-optimal, the results indicate that the differences in the key IBT/Trend marker of  $t_u$ , are very small. From a policy perspective, the efficacies of POM are considered relative to the six year reporting

Appendix C – Consequences of Centrifuge Duration on Hydraulic Parameters and  $t_u$  Estimates (Chapter 5)

periods outlined by the EU-WFD. As the differences in IBT/Trend according to treatment did not exceed 0.01 yrs over the 50 cm deep soil profile, it seems unlikely that the application of the 48-hr experimental duration impaired the ability of the modelling exercise to ascertain POM efficacy relative to this timeframe. Other uncertainties, particularly the spatial variability of soil properties (Chapter 4), are likely of greater importance.

**Appendix E**

**Datasheets for the Modal Soil Profiles employed in Chapter 6.**

Appendix D – Full Datasheets for Modal Soil Profiles Employed in Chapter 6

**REPRESENTATIVE PROFILE DESCRIPTION**

**SERIES: BALLYLANDERS**

Reference profile: RPS62RC05  
 Status: ProfilePit  
 County: Kilkenny  
 Weather: Overcast  
 Elevation:

**LAND USE**  
 Land use: Grassland Improved  
 Human technologies: Fertilizer applications, Ploughing

**WATER TABLE** None

**ROCK OUTCROPS** None

**TOPOGRAPHY**  
 Position: Middle slope  
 Slope degree: 15  
 Slope Form: Straight  
 Aspect: NNE

**SURFACE STONE** Common

**IRISH CLASSIFICATION (2013)**  
 Soil subgroup: 11.0.0 Typical Brown Earth

**PARENT MATERIAL**  
 Substrate Type: Bedrock  
 Substrate Subgroup: Shale/slate

**National Soil Series:** Ballylanders  
 Fine loamy over shale bedrock

**TEXTURAL CRITERIA**

Textural Class: Fine loamy  
 Texturally contrasting:

**DESCRIPTION**

0 - 25 cm Ap  
 MATRIX COLOR: 10YR4.4. STONES (%): Common, 2-6 cm, Angular, Shale. TEXTURE: Loam. STRUCTURE: Moderate, Sub-angular blocky, Fine, Moderate. COMPACTION: Non-cemented and Non-compacted. CONSISTENCY: Friable. PLASTICITY: Slightly plastic. STICKINESS: Slightly sticky. ROOTS: Common, Fine. PACKING DENSITY: Low. BOUNDARY: Clear, Smooth.

25 - 45 cm Bw1  
 MATRIX COLOR: 7.5YR4.4. STONES (%): Many, 6-20 cm, Angular, Shale. TEXTURE: Loam. STRUCTURE: Moderate, Sub-angular blocky, Fine, Moderate. COMPACTION: Non-cemented and Non-compacted. CONSISTENCY: Friable. PLASTICITY: Slightly plastic. STICKINESS: Slightly sticky. ROOTS: Common, Fine. PACKING DENSITY: Low. BOUNDARY: Abrupt, Smooth.

45 - 75 cm Bw2  
 MATRIX COLOR: 5YR4.4. STONES (%): Many, 6-20 cm, Angular, Shale. TEXTURE: Loam. STRUCTURE: Moderate, Granular, Medium. PACKING DENSITY: Medium. BOUNDARY: Abrupt, Wavy.

75 - 85 cm Cr  
 MATRIX COLOR: 10YR4.4. STONES (%): Abundant, 20-60 cm, Shale. TEXTURE: Sandy loam. PACKING DENSITY: Medium. BOUNDARY: Abrupt, Irregular.



**LABORATORY ANALYSIS**

Horizon	pH	Total (%)		Organic Carbon (%)	Loss-on-ignition (%)
		Nitrogen	Carbon		
1(Ap)	5.8	0.45	3.99	2.81	
2(Bw1)	6.1	0.23	2.02	1.14	
3(Bw2)	6.1	0.17	1.80	0.89	
4(Cr)	6.2	0.15	1.41	0.48	

OXALATE EXTRACTABLE		CEC (cmol kg <sup>-1</sup> )	EXCHANGEABLE COMPLEX				Base Saturation (%)
Fe (g kg <sup>-1</sup> )	Al (g kg <sup>-1</sup> )		Exchangeable Base: (cmol kg <sup>-1</sup> )				
			Na <sup>+</sup>	K <sup>+</sup>	Mg <sup>2+</sup>	Ca <sup>2+</sup>	
10.31	3.52	11.86	0.08	0.14	0.68	8.62	80
10.95	3.26	6.31	0.08	0.05	0.63	4.55	84
14.35	5.44	7.19	0.08	0.03	0.45	2.92	49
8.82	4.93	4.34	0.08	0.02	0.24	1.89	51

PARTICLE SIZE (%)			Textural Class USDA	Bulk Density g/cm <sup>3</sup>	Standard Deviation
Sand 2000-60 μm	Silt 60-2 μm	Clay <2 μm			
40	34	26	Loam	0.89	0.11
43	36	21	Loam	0.85	0.15
49	34	17	Loam		
59	32	9	Sandy Loam		

Appendix D – Full Datasheets for Modal Soil Profiles Employed in Chapter 6

**REPRESENTATIVE PROFILE DESCRIPTION**

**SERIES: BALLYLANDERS**

Reference profile: RPS62RC05  
 Status: ProfilePit  
 County: Kilkenny  
 Weather: Overcast  
 Elevation:  
**LAND USE**  
 Land use: Grassland Improved  
 Human technologies: Fertilizer applications, Ploughing  
**WATER TABLE** None  
**ROCK OUTCROPS** None  
**SURFACE STONE** Common  
**IRISH CLASSIFICATION (2013)**  
 Soil subgroup: 11.0.0 Typical Brown Earth  
**PARENT MATERIAL**  
 Substrate Type: Bedrock  
 Substrate Subgroup: Shale/slate  
 National Soil Series: Ballylanders  
 Fine loamy over shale bedrock

**TEXTURAL CRITERIA**  
 Textural Class: Fine loamy  
 Texturally contrasting:

**DESCRIPTION**

**0 - 25 cm Ap**  
 MATRIX COLOR: 10YR4/4. STONES (%): Common, 2-6 cm, Angular, Shale. TEXTURE: Loam. STRUCTURE: Moderate, Sub-angular blocky, Fine, Moderate. COMPACTION: Non-cemented and Non-compacted. CONSISTENCY: Friable. PLASTICITY: Slightly plastic. STICKINESS: Slightly sticky. ROOTS: Common, Fine. PACKING DENSITY: Low. BOUNDARY: Clear, Smooth.

**25 - 45 cm Bw1**  
 MATRIX COLOR: 7.5YR4/4. STONES (%): Many, 6-20 cm, Angular, Shale. TEXTURE: Loam. STRUCTURE: Moderate, Sub-angular blocky, Fine, Moderate. COMPACTION: Non-cemented and Non-compacted. CONSISTENCY: Friable. PLASTICITY: Slightly plastic. STICKINESS: Slightly sticky. ROOTS: Common, Fine. PACKING DENSITY: Low. BOUNDARY: Abrupt, Smooth.

**45 - 75 cm Bw2**  
 MATRIX COLOR: 5YR4/4. STONES (%): Many, 6-20 cm, Angular, Shale. TEXTURE: Loam. STRUCTURE: Moderate, Granular, Medium. PACKING DENSITY: Medium. BOUNDARY: Abrupt, Wavy.

**75 - 85 cm Cr**  
 MATRIX COLOR: 10YR4/4. STONES (%): Abundant, 20-60 cm, Shale. TEXTURE: Sandy loam. PACKING DENSITY: Medium. BOUNDARY: Abrupt, Irregular.



**LABORATORY ANALYSIS**

Horizon	pH	Total (%)		Organic Carbon (%)	Loss-on-ignition (%)
		Nitrogen	Carbon		
1(Ap)	5.8	0.45	3.99	2.81	
2(Bw1)	6.1	0.23	2.02	1.14	
3(Bw2)	6.1	0.17	1.80	0.89	
4(Cr)	6.2	0.15	1.41	0.48	

OXALATE EXTRACTABLE		EXCHANGEABLE COMPLEX					
Fe (g kg <sup>-1</sup> )	Al (g kg <sup>-1</sup> )	CEC (cmol kg <sup>-1</sup> )	Exchangeable Bases (cmol kg <sup>-1</sup> )				Base Saturation (%)
			Na <sup>+</sup>	K <sup>+</sup>	Mg <sup>2+</sup>	Ca <sup>2+</sup>	
10.31	3.52	11.86	0.08	0.14	0.68	8.62	80
10.95	3.26	6.31	0.08	0.05	0.63	4.55	84
14.35	5.44	7.19	0.08	0.03	0.45	2.92	49
8.82	4.93	4.34	0.08	0.02	0.24	1.89	51

PARTICLE SIZE (%)			Textural Class USDA	Bulk Density g/cm <sup>3</sup>	Standard Deviation
Sand 2000-60 μm	Silt 60-2 μm	Clay <2 μm			
40	34	26	Loam	0.89	0.11
43	36	21	Loam	0.85	0.15
49	34	17	Loam		
59	32	9	Sandy Loam		

# Appendix D – Full Datasheets for Modal Soil Profiles Employed in Chapter 6

## REPRESENTATIVE PROFILE DESCRIPTION

### SERIES: CLONROCHE

Reference profile:	RPS62RC04	<b>LAND USE</b>	
County:	Kilkenny	Land use:	Grassland Improved
Weather:	Overcast	Human technologies:	Fertilizer applications, Ploughing
Elevation:	256		
<b>TOPOGRAPHY</b>		<b>WATER TABLE:</b>	None
Position:	Lower slope	<b>ROCK OUTCROPS</b>	None
Slope degree:	1	<b>SURFACE STONE</b>	None
Slope Form:	Straight		
Aspect:		<b>IRISH CLASSIFICATION (2013)</b>	
<b>PARENT MATERIAL</b>		Soil subgroup:	11.0.0 Typical Brown Earth
Substrate Type:	Drift	National Soil Series:	Clonroche
Substrate Subgroup:	Siliceous stones		Fine loamy drift with siliceous stones
<b>TEXTURAL CRITERIA</b>			
Textural Class:	Fine loamy		
Texturally contrasting:			

### DESCRIPTION

**0 - 21 cm Ap**  
**MATRIX COLOR:** 10YR4.3. **STONES (%)**: None. **TEXTURE:** Loam. **STRUCTURE:** Moderate, Sub-angular blocky, Medium. **COMPACTION:** Non-cemented and Non-compacted. **CONSISTENCY:** Friable. **PLASTICITY:** Plastic. **STICKINESS:** Slightly sticky. **ROOTS:** Common, Very fine. **PACKING DENSITY:** Low. **BOUNDARY:** Abrupt, Smooth.

**21 - 48 cm Bw1**  
**MATRIX COLOR:** 10YR4.4. **STONES (% TOTAL):** Common, Angular, Siliceous stones. **TEXTURE:** Loam. **STRUCTURE:** Moderate, Sub-angular blocky, Fine. **COMPACTION:** Non-cemented and Non-compacted. **CONSISTENCY:** Friable. **PLASTICITY:** Plastic. **STICKINESS:** Sticky. **ROOTS:** Common, Very fine. **PACKING DENSITY:** Low. **BOUNDARY:** Clear, Smooth.

**48 - 75 cm Bw2**  
**MATRIX COLOR:** 10YR4.4. **STONES (%)**: Many, 2-6 cm, Angular, Siliceous stones; 6-20 cm, Sub angular, Shale. **TEXTURE:** Loam. **STRUCTURE:** Moderate, Sub-angular blocky, Fine. **COMPACTION:** Non-cemented and Non-compacted. **CONSISTENCY:** Friable. **PLASTICITY:** Plastic. **STICKINESS:** Sticky. **ROOTS:** Very few, Very fine. **PACKING DENSITY:** Low. **BOUNDARY:** Abrupt, Wavy.

**75 - 100 cm BC**  
**MATRIX COLOR:** 2.5Y5.4. **MOTTLE:** 2.5Y6.6. **STONES (%)**: Many, 6mm - 2 cm, Flatplaty, Shale; 2-6 cm, Flatplaty, Shale. **TEXTURE:** Sandy loam. **STRUCTURE:** Weak, Angular blocky, Medium. **COMPACTION:** Cemented. **CONSISTENCY:** Firm. **PLASTICITY:** Plastic. **STICKINESS:** Sticky. **COATS:** Manganese. **PACKING DENSITY:** Medium.



### LABORATORY ANALYSIS

Horizon	pH	Total (%)		Organic Carbon (%)	Loss-on-ignition (%)
		Nitrogen	Carbon		
1(Ap)	6.6	0.48	4.27	3.57	
2(Bw1)	6.5	0.29	2.42	1.40	
3(Bw2)	6.5	0.18	1.23	0.80	
4(BC)	6.5	0.06	0.32	0.18	

OXALATE EXTRACTABLE		EXCHANGEABLE COMPLEX					Base Saturation (%)
Fe (g kg <sup>-1</sup> )	Al (g kg <sup>-1</sup> )	CEC (cmol kg <sup>-1</sup> )	Exchangeable Bases (cmol kg <sup>-1</sup> )				
			Na <sup>+</sup>	K <sup>+</sup>	Mg <sup>2+</sup>	Ca <sup>2+</sup>	
8.69	2.94	15.30	0.13	0.59	1.67	12.35	96
9.78	3.18	9.63	0.14	0.63	1.26	6.29	86
11.82	5.26	8.05	0.10	0.42	1.14	4.19	73
2.02	1.07	4.35	0.08	0.23	0.65	1.82	64

PARTICLE SIZE (%)			Textural Class USDA	Bulk Density g cm <sup>-3</sup>	Standard Deviation
Sand 2000-50 µm	Silt 50-2 µm	Clay <2 µm			
43	34	23	Loam	0.92	0.11
40	35	25	Loam	0.96	0.02
35	41	24	Loam		
53	33	14	Sandy Loam		

# Appendix D – Full Datasheets for Modal Soil Profiles Employed in Chapter 6

## REPRESENTATIVE PROFILE DESCRIPTION

### SERIES: DUARRIGLE

<b>Reference profile:</b>	RPR30BR03	<b>LAND USE</b>	
<b>County:</b>	Cork	<b>Land use:</b>	Grassland improved, Grassland improved
<b>Weather:</b>	Overcast	<b>Human technologies:</b>	Slurry applications, Fertilizer applications, Ditching
<b>Elevation:</b>	155	<b>Vegetation:</b>	Grassland,
<b>TOPOGRAPHY</b>		<b>Species:</b>	Dock, Meadow buttercup, Dandelion
<b>Position:</b>	Upper slope	<b>WATER TABLE</b>	None
<b>Slope degree:</b>	3	<b>ROCK OUTCROPS</b>	None
<b>Slope Form:</b>	Straight	<b>SURFACE STONE</b>	None
<b>Aspect:</b>	S	<b>IRISH CLASSIFICATION (2013)</b>	Soil subgroup: 1T.3.0 Stagnic Brown Earth
<b>PARENT MATERIAL</b>		<b>National Soil Series:</b>	Duarrigle
<b>Substrate Type:</b>	Bedrock		Fine loamy over shale bedrock
<b>Substrate Subgroup:</b>	Shale		
<b>TEXTURAL CRITERIA</b>			
<b>Textural Class:</b>	Fine Loamy		
<b>Texturally contrasting:</b>			

### DESCRIPTION

**0 - 28 cm Ap**  
**MATRIX COLOR:** 10YR3/4. **MOTTLE:** 5YR4/6, Common, Fine, Distinct, Sharp. **STONES (%)**: Common, 2-6 cm, Sub-angular, Siliceous stones; Few, 6 mm - 2 cm, Sub-angular, Siliceous stones. **TEXTURE:** Clay loam. **STRUCTURE:** Moderate, Sub-angular blocky, Fine. **COMPACTITY:** Non-cemented but compacted. **CONSISTENCY:** Friable. **PLASTICITY:** Non-plastic. **STICKINESS:** Non-sticky. **ROOTS:** Many, Fine. **PACKING DENSITY:** Medium. **POROSITY:** Medium. **MACROPORES:** Fine. **BOUNDARY:** Clear, Smooth.

**28 - 45 cm Bw1**  
**MATRIX COLOR:** 7.5YR4/6. **MOTTLE:** 7.5YR5/8, Few, Medium, Faint, Clear. **STONES (%)**: Many, 2-6 cm, Sub-angular, Siliceous stones; 6-20 cm, Sub-angular, Siliceous stones. **TEXTURE:** Clay loam. **STRUCTURE:** Moderate, Sub-angular blocky, Medium. **CONSISTENCY:** Friable. **PLASTICITY:** Non-plastic. **STICKINESS:** Non-sticky. **ROOTS:** Common, Fine. **COATS:** Clay, Common, Distinct, Continuous. **PACKING DENSITY:** Medium. **POROSITY:** Medium. **MACROPORES:** Fine. **BOUNDARY:** Clear, Broken.

**28 - 65 cm Bw2**  
**MATRIX COLOR:** 7.5YR5/8. **STONES (%)**: Many, 2-6 cm, Angular, Shale; Many, 6-20 cm, Sub-angular, Siliceous stones. **TEXTURE:** Sandy clay loam. **STRUCTURE:** Weak, Sub-angular blocky, Medium to Coarse. **CONSISTENCY:** Friable. **PLASTICITY:** Non-plastic. **STICKINESS:** Slightly sticky. **ROOTS:** Common, Fine. **COATS:** Clay, Many, Distinct, Continuous. **PACKING DENSITY:** Low. **POROSITY:** High. **MACROPORES:** Fine. **BOUNDARY:** Abrupt, Smooth.

**65 - 70 cm Cg**  
**MATRIX COLOR:** 10YR5/4. **MOTTLE:** 5YR5/8, Common, Medium, Prominent, Clear. **STONES (%)**: Abundant, 2-6 cm, Angular, Shale. **TEXTURE:** Clay loam. **STRUCTURE:** Massive. **CONSISTENCY:** Firm. **PLASTICITY:** Non-plastic. **STICKINESS:** Slightly sticky. **ROOTS:** Few, Fine. **COATS:** Clay, Few, Faint, Continuous. **PACKING DENSITY:** Medium. **POROSITY:** Medium. **BOUNDARY:** Abrupt, Smooth.

**70 cm + R**



### LABORATORY ANALYSIS

Horizon	pH	Total (%)		Organic Carbon (%)	Loss-on-ignition (%)
		Nitrogen	Carbon		
1(Ap)	5.4	0.16	3.38	2.70	
2(Bw1)	6.0	0.16	1.10	0.89	
3(Bw2)	6.0	0.15	1.23	0.73	
4(Cg)	5.9	0.13	0.61	0.31	

OXALATE EXTRACTABLE		EXCHANGEABLE COMPLEX					Base Saturation (%)
Fe (g kg <sup>-1</sup> )	Al (g kg <sup>-1</sup> )	CEC (cmol kg <sup>-1</sup> )	Exchangeable Bases (cmol kg <sup>-1</sup> )				
			Na <sup>+</sup>	K <sup>+</sup>	Mg <sup>2+</sup>	Ca <sup>2+</sup>	
11.11	2.46	8.87	0.08	0.11	0.60	6.11	78
7.56	2.15	6.97	0.08	0.03	0.30	6.28	96
9.20	3.63	4.51	0.08	0.05	0.24	3.95	96
4.70	2.46	5.34	0.08	0.04	0.45	4.44	94

PARTICLE SIZE (%)			Textural Class USDA	Bulk Density g/cm <sup>3</sup>	Standard Deviation
Sand 2000-60 μm	Silt 60-2 μm	Clay <2 μm			
29	37	34	Clay Loam	1.11	0.02
31	41	28	Clay Loam		
53	23	24	Sandy Clay Loam		
25	46	29	Clay Loam		

# Appendix D – Full Datasheets for Modal Soil Profiles Employed in Chapter 6

**REPRESENTATIVE PROFILE DESCRIPTION**

---

**SERIES: KILPIERCE**

<b>Reference profile:</b> 470	<b>LAND USE</b>	
<b>County:</b> Wexford	Land use: Unimproved pasture	
<b>Weather:</b>	Human technologies:	
<b>Elevation:</b>	Vegetation: Old pasture dominated by rush (Juncus)	

<b>TOPOGRAPHY</b>	<b>WATER TABLE</b>	
<b>Position:</b>		
<b>Slope Degree:</b>	<b>ROCK OUTCROPS</b>	
<b>Slope Form:</b>		
<b>Aspect:</b>	<b>SURFACE STONE</b>	

<b>PARENT MATERIAL</b>	<b>IRISH CLASSIFICATION (2013)</b>	
<b>Substrate Type:</b> Glacial drift	Soil subgroup: 00.0.0 Typical Groundwater Gley	
<b>Substrate Subgroup:</b> Ordovician shale		

<b>TEXTURAL CRITERIA</b>	<b>WRB CLASSIFICATION (2006)</b>	
<b>Textural Class:</b> Fine loamy	Definition: Fine loamy drift with siliceous stones	
<b>Texturally contrasting:</b>	Eutric Gleysol (Humic)	

---

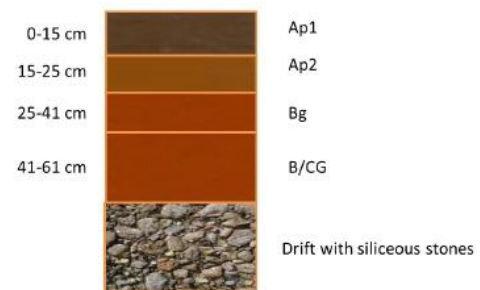
**DESCRIPTION**

0 - 15 cm **Ap1**  
**MATRIX COLOUR:** 10YR4/2. **TEXTURE:** Clay loam. **STRUCTURE:** Weak, Crumbly, Fine. **ROOTS:** Many. **BOUNDARY:** Gradual, Smooth.

15 - 25 cm **Ap2**  
**MATRIX COLOUR:** 10YR5/2. **TEXTURE:** Clay Loam. **STRUCTURE:** Weak, Crumbly, Fine. **CONSISTENCY:** Friable. **ROOTS:** Many. **BOUNDARY:** Clear, Smooth.

25 - 41 cm **Bg**  
**MATRIX COLOUR:** 10YR5/1. **MOTTLE:** 5YR4/6, Many, prominent. **TEXTURE:** Loam. **STRUCTURE:** Weak, Columnar, Fine to massive. **CONSISTENCY:** Friable. **ROOTS:** Few. **BOUNDARY:** Clear, Smooth.

41 - 61 cm **BCG**  
**MATRIX COLOUR:** 10YR5/1. **MOTTLE:** 5YR4/6, Many, Medium, Distinct. **TEXTURE:** Loam. **STRUCTURE:** Massive. **ROOTS:** No.



**LABORATORY ANALYSES**

Horizon	pH	Total (%)		C/N
		Nitrogen	Carbon	
Ap1	5.6	0.39	4.9	12.6
Ap2	5.6	0.23	2.7	11.3
Bg	5.9	0.08	0.8	8.9
BCG	6	0.06	0.2	3.3

EXCHANGEABLE COMPLEX				
CEC ( $\text{cmol kg}^{-1}$ )	TEB ( $\text{cmol kg}^{-1}$ )	Base Sat. (%)	Free Iron (%)	TNV (%)
15.6	5.3	34	2.0	
13.1	4.8	37	1.78	
6.6	3.8	58	1.78	
6.8	4.5	66	1.91	

PARTICLE SIZE (%)			Textural Class USDA	Bulk Density $\text{g/cm}^3$	Standard Deviation
Sand 2000-50 $\mu\text{m}$	Silt 50-2 $\mu\text{m}$	Clay <2 $\mu\text{m}$			
32.5	37.2	30.3	Clay loam		
36.3	35.3	28.3	Clay loam		
37.3	38.5	24.2	Loam		
34.2	38.8	27	Clay loam		

## Appendix D – Full Datasheets for Modal Soil Profiles Employed in Chapter 6

### REPRESENTATIVE PROFILE DESCRIPTION

#### SERIES: KILRUSH

<b>Reference profile:</b>	RPS24RC21	<b>LAND USE</b>	
<b>County:</b>	Tipperary South	<b>Land use:</b>	Grassland Improved
<b>Weather:</b>	Sunny/clear	<b>Human technologies:</b>	Ploughing, Fertilizer applications
<b>Elevation:</b>	191	<b>WATER TABLE</b>	None
<b>TOPOGRAPHY</b>		<b>ROCK OUTCROPS</b>	None
<b>Position:</b>	Middle slope	<b>SURFACE STONE</b>	None
<b>Slope degree:</b>	2	<b>IRISH CLASSIFICATION (2013)</b>	
<b>Slope Form:</b>	Straight	<b>Soil subgroup:</b>	07.0.0 Typical Surface-water Gley
<b>Aspect:</b>	S	<b>National Soil Series:</b>	Kilrush
<b>PARENT MATERIAL</b>			Fine loamy drift with siliceous stones
<b>Substrate Type:</b>	Drift		
<b>Substrate Subgroup:</b>	Siliceous stones		

**TEXTURAL CRITERIA**  
Textural Class: Fine loamy  
Texturally contrasting:

#### DESCRIPTION

**0 - 25 cm Apg**  
**MATRIX COLOR:** 10YR42. **MOTTLE:** 5YR46, Common, Fine, Distinct, Sharp. **STONES (%)**: Common, 2-6 cm, Sub angular, Sandstone. **TEXTURE:** Clay loam. **STRUCTURE:** Moderate, Sub-angular blocky, Fine. **PLASTICITY:** Slightly plastic. **STICKINESS:** Slightly sticky. **ROOTS:** Many, Fine. **PACKING DENSITY:** Medium. **BOUNDARY:** Abrupt, Smooth.

**25 - 55 cm Bg**  
**MATRIX COLOR:** 10YR53. **MOTTLE:** 5YR44, Many, Medium, Prominent, Sharp. **STONES (%)**: Common, 2-6 cm, Sub rounded, Sandstone. **TEXTURE:** Clay loam. **STRUCTURE:** Moderate, Sub-angular blocky, Fine to medium. **CONSISTENCY:** Very firm. **PLASTICITY:** Slightly plastic. **STICKINESS:** Slightly sticky. **ROOTS:** Common, Fine. **COATS:** Manganese, Many, Prominent. **PACKING DENSITY:** High. **BOUNDARY:** Clear, Smooth.

**55 - 80 cm BCg**  
**MATRIX COLOR:** 10YR53. **MOTTLE:** 10YR56, Many, Fine, Prominent, Sharp. **STONES (%)**: Many, 6mm -2 cm, Sub rounded, Sandstone; 6-20 cm, Angular, Shale. **TEXTURE:** Sandy clay loam. **STRUCTURE:** Moderate, Prismatic, Fine. **PLASTICITY:** Very plastic. **STICKINESS:** Very sticky. **COATS:** Clay, Common, Faint, Continuous. **Manganese, Few, Distinct. ACCUMULATIONS (Fe/Mn):** 2-5 %. **PACKING DENSITY:** High. **BOUNDARY:** Gradual, Wavy.

**80 - 110 cm Cg1**  
**MATRIX COLOR:** 10YR42. **MOTTLE:** 25Y43, Common, Medium, Distinct; 10YR46, Common, Fine, Prominent. **STONES (%)**: Many, 6mm -2 cm, Sub rounded, Sandstone. **TEXTURE:** Clay loam. **STRUCTURE:** Massive. **PLASTICITY:** Very plastic. **STICKINESS:** Very sticky. **COATS:** Manganese, Common, Distinct. **PACKING DENSITY:** High. **BOUNDARY:** Gradual, Smooth.

**110 - 140 cm Cg2**  
**MATRIX COLOR:** 25Y43. **MOTTLE:** 25Y51, Common, Medium, Prominent, Sharp; 10YR56, Common, Fine, Prominent, Sharp. **STONES (%)**: Many, 6-20 cm, Sub angular, Shale; Old Red sandstone. **TEXTURE:** Clay loam. **STRUCTURE:** Massive. **PLASTICITY:** Very plastic. **STICKINESS:** Very sticky. **COATS:** Manganese, Few. **PACKING DENSITY:** High.



#### LABORATORY ANALYSIS

Horizon	pH	Total (%)		Organic Carbon (%)	Loss-on-ignition (%)
		Nitrogen	Carbon		
1(Apg)	4.9	0.49	4.15	3.43	
2(Bg)	5.6	0.09	0.58	0.37	
3(BCg)	5.7	0.08	0.53	0.35	
4(Cg1)	6.1	0.08	0.29	0.28	
5(Cg2)	6.2	0.07	0.37	0.25	

CEC (cmol kg <sup>-1</sup> )	Exchangeable Bases (cmol kg <sup>-1</sup> )				Base Saturation (%)
	Na <sup>+</sup>	K <sup>+</sup>	Mg <sup>2+</sup>	Ca <sup>2+</sup>	
8.72	0.08	0.17	0.57	5.72	75
5.66	0.08	0.08	0.44	4.45	89
7.83	0.08	0.10	0.70	5.88	86
11.46	0.08	0.14	1.05	8.93	89
10.81	0.08	0.13	1.34	8.86	96

PARTICLE SIZE (%)			Textural Class USDA	Bulk Density g/cm <sup>3</sup>	Standard Deviation
Sand 2000-60 μm	Silt 50-2 μm	Clay <2 μm			
34	35	31	Clay Loam	1.04	0.05
39	34	27	Clay Loam/Loam	1.50	0.11
45	24	31	Sandy Clay Loam/Clay Loam	1.48	0.02
33	37	30	Clay Loam	1.58	0.04
34	37	29	Clay Loam		

Appendix D – Full Datasheets for Modal Soil Profiles Employed in Chapter 6

REPRESENTATIVE PROFILE DESCRIPTION

SERIES: ROSS CARBERY

Reference profile: RPW39BR01  
 County: Cork  
 Weather: Overcast  
 Elevation: 38

**LAND USE**  
 Land use: Grassland improved  
 Human technologies: Fertilizer applications, Slurry applications, Seeded/reseeded  
 Vegetation: Grassland, Grassland  
 Species: Bramble/Briars

**TOPOGRAPHY**  
 Position: Lower slope  
 Slope degree: 11  
 Slope Form: Concave  
 Aspect: SE

**PARENT MATERIAL**  
 Substrate Type: Drift  
 Substrate Subgroup: Siliceous stones

**TEXTURAL CRITERIA**  
 Textural Class: Coarse loamy  
 Texturally contrasting:

**WATER TABLE** None  
**ROCK OUTCROPS** None  
**SURFACE STONE** None

**IRISH CLASSIFICATION (2013)**  
 Soil subgroup: 09.0.0 Typical Brown Podzolic

**National Soil Series: Ross Carbery**  
 Coarse loamy compact drift with siliceous stones

DESCRIPTION

0 - 35 cm Ap  
 MATRIX COLOR: 10YR3.3. STONES (%): Few, 2-6 mm, Angular, Siliceous stones; Few, 2-6 cm, Angular, Siliceous stones. TEXTURE: Sandy loam. STRUCTURE: Weak, Crumb, Fine. CONSISTENCY: Very friable. PLASTICITY: Non-plastic. STICKINESS: Non-sticky. ROOTS: Many, Medium. PACKING DENSITY: Very Low POROSITY: Very High. MACROPORES: Medium. BOUNDARY: Clear, Smooth.

35 - 70 cm AB  
 MATRIX COLOR: 10YR4.3. STONES (%): Common, 2-6 mm, Angular, Shale; Common, 2-6 cm, Angular, Shale. TEXTURE: Coarse, Sandy loam. STRUCTURE: Moderate, Sub-angular blocky, Fine to Medium. CONSISTENCY: Friable. PLASTICITY: Non-plastic. STICKINESS: Non-sticky. ROOTS: Common, Fine. PACKING DENSITY: Medium. POROSITY: High. MACROPORES: Fine. BOUNDARY: Abrupt, Wavy.

70 - 100 cm Bs buried  
 MATRIX COLOR: 7.5YR4.6. STONES (%): Common, 2-6 mm, Angular, Shale; Common, 2-6 cm, Angular, Shale. TEXTURE: Sandy Loam. STRUCTURE: Weak, Sub-angular blocky, Fine. CONSISTENCY: Very friable. PLASTICITY: Non-plastic. STICKINESS: Non-sticky. ROOTS: Few, Fine. COATS: Clay, Few, Faint, Discontinuous. PACKING DENSITY: Medium. POROSITY: High. MACROPORES: Fine. BOUNDARY: Clear, Wavy.

100 - 150 cm 2C buried  
 MATRIX COLOR: 2.5Y6.2. VARIATION: 7.5YR4.6, Few, Fine, Distinct, Sharp. STONES (%): Many, 2-6 mm, Angular, Shale; Many, 2-6 cm, Angular, Shale. TEXTURE: Sandy Loam. STRUCTURE: Massive. COMPACTITY: Non-cemented but compacted. CONSISTENCY: Firm. PLASTICITY: Non-plastic. STICKINESS: Non-sticky. ROOTS: Very few, Fine. PACKING DENSITY: High. POROSITY: Low. MACROPORES: Fine.



LABORATORY ANALYSIS

Horizon	pH	Total (%)		Organic Carbon (%)	Loss-on-ignition (%)
		Nitrogen	Carbon		
1 (Ap)	8.3	0.31	4.26	2.78	
2 (AB)	8.5	0.12	2.62	0.94	
3 (Bs buried)	8.2	0.07	1.19	0.48	
4 (2C buried)	8.5	0.01	0.24	0.16	

OXALATE EXTRACTABLE		EXCHANGEABLE COMPLEX					Base Saturation (%)
Fe (g kg <sup>-1</sup> )	Al (g kg <sup>-1</sup> )	CEC (cmol kg <sup>-1</sup> )	Exchangeable Bases (cmol kg <sup>-1</sup> )				
			Na <sup>+</sup>	K <sup>+</sup>	Mg <sup>2+</sup>	Ca <sup>2+</sup>	
2.98	0.73	20.60	0.5	8.97	1.18	19.40	Sat.
4.47	0.83	12.20	0.35	5.00	0.39	11.9	Sat.
11.35	3.01	13.1	0.51	0.02	0.23	13.20	Sat.
0.93	0.73	1.82	0.26	0.14	0.209	2.27	Sat.

PARTICLE SIZE (%)			Textural Class USDA	Bulk Density g/cm <sup>3</sup>	Standard Deviation
Sand 2000-50 μm	Silt 50-2 μm	Clay <2 μm			
64	18	18	Sandy Loam	1.19	0.11
62	23	15	Sandy Loam	0.97	0.06
54	35	11	Sandy Loam		
57	37	6	Sandy Loam		